

Secondary resources directive

Characterisation of mining waste in central and southern Bergslagen, Sweden

Johan Camitz, Gunnar Rauséus, Johan Jönberger, Lena Persson,
Daniel Sopher, Mehrdad Bastani

January 2024

SGU-rapport 2024:03



Cover photo: Water filled mine pit, Haggruvan, Riddarhyttan.
Photographer: Gunnar Rauséus

Authors: Johan Camitz, Gunnar Rauséus, Johan Jönberger,
Lena Persson, Daniel Sopher, Mehrdad Bastani

Reviewed by: Patrick Casey

Head of unit: Ildikó Antal Lundin

Editor: Lina Rönnåsen

Geological Survey of Sweden

Box 670, 751 28 Uppsala

tel: 018-17 90 00

e-mail: sgu@sgu.se

www.sgu.se

CONTENTS

Abstract.....	6
Sammanfattning.....	7
Introduction	10
Geological setting.....	11
Methods and sampling.....	13
Sampling of tailings ponds.....	13
Geophysical methods for investigation of tailings.....	14
Sampling of waste rock	15
Lithogeochemical analysis	15
Scanning electron microscopy	16
Potential resources.....	16
Riddarhyttefältet	17
Existing and historical data.....	17
Drill cores and lithogeochemistry	17
Airborne geophysics	19
Ground geophysics	19
Exploration geophysics	24
Källfallsgruvan.....	25
Historical background	25
Tailings.....	25
Waste rock.....	33
Potential resources tailings and waste rock	37
Bäckegruvan.....	38
Historical background	38
Tailings.....	39
Potential resource tailings	47
Waste rock.....	48
Potential resource waste rock.....	54
Persgruvan	54
Historical background	54
Waste rock.....	54
Potential resource.....	58

Nya Bastnäs	59
Historical background	59
Waste rock	59
Kittelgruvan, Old Bastnäs.....	65
Historical background	65
Waste rock.....	66
Norberg area	72
Existing and historical data.....	72
Airborne geophysics	72
Ground geophysics	76
Malmkärragruvorna	77
Historical background	77
Waste rock.....	77
Åsgruvan	84
Historical background	84
Waste rock.....	84
Östanmossgruvan	88
Historical background	88
Waste rock.....	88
Vena ore field.....	93
Existing and historical data.....	93
Airborne geophysics	93
Ground geophysics	97
Waste rock	100
Results composite sampling.....	102
Potential resource	102
Tunaberg mine area.....	102
Existing and historical data.....	102
Historical drill cores and lithochemistry.....	104
Airborne geophysics	104
Ground geophysics	108
Waste rock	109

Baggetorp.....	114
Existing and historical data.....	114
Airborne geophysics	115
Ground-based electromagnetic and magnetic measurements	117
Ground-based gravity	118
Petrophysical data.....	119
Interpretation of newly acquired data	121
Waste rock	124
Results composite sampling.....	125
Results selective sampling	125
Potential resource	126
References	127
Appendix 1. Sample digestion and analytical methods.....	129

ABSTRACT

In 2021, the Geological Survey of Sweden (Sveriges geologiska undersökning, SGU) together with the Swedish Environmental Protection Agency received a governmental directive to work to increase the possibilities for sustainable extraction of metals and minerals from secondary resources (N2021/01038). The work is intended to contribute to the transition to a more circular and resource-efficient economy. The directive in its entirety was reported to the government in February 2023 (SGU RR 2023:01).

As part of the directive, SGU has documented, sampled, and characterised mining waste (waste rock and tailings) at closed Swedish mines to estimate the quantities of metals and minerals. Metallurgical slag and burnt alum shale were also investigated. Secondary resources from mining waste can possibly contribute to the supply of the critical raw materials needed in the ongoing energy transition.

A total of 70 locations was sampled by SGU during 2021 and 2022, with altogether 1,067 samples. A series of reports present background information and available data for each of these locations, as well as the results from the new investigations.

This report covers a subset of the investigated locations within the directive, from central-eastern and southern Bergslagen in Sweden. Sampling was conducted at 11 locations at the mine sites of Källfallsgruvan, Bäcke-gruvan, Persgruvan, Nya Bastnäs, Kittelgruvan (Old Bastnäs), Malmkär-gruvorna, Åsgruvan, Östanmossgruvan, Vena ore field, Baggetorp and Tunaberg mine area.

In eastern Bergslagen, the Riddarhyttan–Norberg area or the so called “REE-Line” was the focus of investigations. All waste rock samples from the Riddarhyttfältet and the Norberg area show elevated levels of rare earth elements (REE) and some of the mine sites show elevated values for Cu, Co and Mo, among other elements.

The results from the analysed tailings show anomalous concentrations of rare earth elements, particularly the light rare earth elements (LREE). The highest levels are noted at the tailings pond at Källfallsgruvan. At Bäcke-gruvan the highest concentrations of rare earth elements are noted in the oldest material, deposited before 1963, as well as elevated concentrations of Fe_2O_3 , Cu, Co and Ba.

In the southern part of Bergslagen, sampling was performed at Vena gruvor, Tunaberg and Baggetorp. At the Vena ore field, there are large quantities of waste rock material covering an area of approximately 40,000 square metres. Geochemical analysis of the waste rock material shows elevated levels of Cu, Zn, Co and Bi. In selective samples for Baggetorp, high levels of W, Mo and Re are seen. Notable at Tunaberg are high levels of Zn in the Skara mine, and elevated levels of Cu at several of the mines in the area.

SAMMANFATTNING

År 2021 fick Sveriges geologiska undersökning (SGU) tillsammans med Naturvårdsverket i regeringsuppdrag att arbeta för ökade möjligheter till hållbar utvinning av metaller och mineral ur sekundära resurser (N2021/01038). Arbetet är tänkt att bidra till omställningen till en mer cirkulär och resurseffektiv ekonomi. Uppdraget i sin helhet redovisades till regeringen i februari 2023 (SGU RR 2023:01).

Som en del av uppdraget har SGU dokumenterat, provtagit och karakteriserat gruvavfall (varphögar och sandmagasin) vid nedlagda svenska gruvor för att bedöma mängden metaller och mineral. Även metallurgiskt slagg samt rödfyr, som är en rest av bränd alunskiffer, har undersökts. Sekundära resurser från gruvavfall kan möjligen bidra till försörjningen av de kritiska råvaror som behövs i den pågående energiomställningen.

Inom uppdraget har totalt 70 platser provtagits under 2021 och 2022, med sammanlagt 1 067 prover. I en serie rapporter presenteras förutom resultaten från de nya undersökningarna även bakgrundsinformation och tillgängliga data för respektive undersökt plats.

Denna rapport tar upp en delmängd av de undersökta platserna inom uppdraget, från centrala och södra Bergslagen. Provtagningen utfördes på 11 platser vid gruvorna Källfallsgruvan, Bäcke-gruvan, Persgruvan, Nya Bastnäs, Kittelgruvan (Gamla Bastnäs), Malmkärragruvorna, Åsgruvan, Östanmossgruvan, Vena gruvor, Baggetorp och Tunabergs gruvfält.

Enligt Europeiska kommissionen klassas 34 råvaror som kritiska och strategiska för samhälle och industri. I dagsläget sker produktionen av dessa råvaror främst utanför EU. Till exempel är Kina den största producenten av bland annat sällsynta jordartsmetaller. Intentionen inom EU är att öka självförsörjningsgraden för dessa råvaror, och Sverige har en stor potential med kända förekomster av bland annat antimon, fluor, fosfor, grafit, kobolt, platina, sällsynta jordartsmetaller och volfram (SGU 2023). Gruvavfall i form av anrikningssand och gråbergsvarp från gruvdrift kan utgöra en källa för dessa kritiska råvaror. Dessa material utgör det som historiskt sett inte ansågs innehålla mineral av ekonomiskt intresse men som idag kan utgöra, en så kallad sekundär resurs.

I centrala Bergslagen har undersökningar utförts vid fem gruvor i Ridderhyttanområdet och tre i Norbergområdet. Alla dessa gruvor ligger längs den så kallade REE-linjen definierad av Jonsson & Högdahl (2013). I södra Bergslagen har undersökningar utförts vid tre gruvområden: Vena gruvor, Baggetorpsgruvan och i Tunaberg.

Varphögarna vid respektive gruva har provtagits enligt en metodik som möjliggör semi-kvantitativa uppskattningar av deras totala sammansättningar (Sädbom & Bäckström 2018). Sandmagasin har provtagits manuellt med ytprover och genom borrhning. Borrhningen utfördes med egen borrhvagn och provtagning gjordes i regel för varje meter ner till sandmagasinets botten. Samtliga prover skickades för analys av ALS i Piteå. Totalt omfattar analyserna 61 element (grundämnen).

Vid två sandmagasin, Bäcke-gruvan och Källfallsgruvan, har geofysiska undersökningar utförts för att kartlägga anrikningssandens utbredning, mäktighet och fysikaliska variationer. Olika elektromagnetiska och elektriska metoder har testats och utvärderats inom projektet, som elektrisk resistivitetstomografi (ERT), inducerad polarisation (IP), dragen transient elektromagnetisk metod (eng. *towed transient electromagnetic*, tTEM), radiometrotellurik (RMT) och georadar. Resultatet från mätningarna har använts för att lokalisera platser för borrhning samt för att beräkna volym och massa för magasinerna.

För att få en bättre förståelse för den sekundära resursen är det viktigt att också ha en bra karakterisering av den primära resurs från vilken gruvavfallet skapades. Som en del av det här projektet har därför undersökningar av berggrunden utförts i anslutning till flera områden med sekundära resurser. Syftet med dessa undersökningar var att skapa ett bättre geologiskt och geofysiskt underlag runt dessa objekt för att, där det är möjligt, skapa modeller av berggrunden eller uppdaterade geologiska kartor. Som en del av undersökningarna utfördes nya geologiska observationer samt provtagning av bergarter och gråberg. Fysikaliska egenskaper i form av magnetisk susceptibilitet och remanens samt densitet mättes vid SGU:s petrofysiska laboratorium i Uppsala. Markbaserade geofysiska mätningar utfördes också vid några objekt.

Potentiellt kvarvarande resurser har beräknats för de sandmagasin och varpområden där tonnaget av materialet har kunnat uppskattas och tolkats vara rimlig. Främst rör detta sandmagasinen där geofysiska fältmätningar och densitetsbestämningar utgör grund för tonnageberäkning. För varpmaterial är tonnagesiffror hämtade från historiska data.

Bäckegravans sandmagasin uppgår till 5,3 miljoner ton (Mt) med en uppskattad potentiell resurs av bland annat 665 000 ton järn, 6 300 ton koppar, 5 700 ton sällsynta jordartsmetaller och 1 700 ton kobolt. Medelhalten av barium i sandmagasinet uppgår till 6 568 ppm. Två varpområden norr om sandmagasinet, Östergruvan–Jacobsgruvan och Haggruvan, visar båda förhöjda halter av järn, vismut, koppar, kobolt och sällsynta jordartsmetaller. Även synligt guld har noterats i tunnslip av selektivt prov från varpmaterial från dessa gruvor.

Källfallsgruvan, som ligger några kilometer väster om Bäckegruvan, provtogs både i varp och sandmagasin och visar förhöjda halter av järn, molybden och sällsynta jordartsmetaller. Det uppskattade tonnaget av varpmaterial och anrikningssand uppgår till 1,87 Mt med en potentiell resurs av bland annat 250 000 ton järn, 460 ton molybden och 3 700 ton sällsynta jordartsmetaller inklusive yttrium.

Varpmaterial från Persgruvan visar anomala halter av bland annat koppar (0,75 %), sällsynta jordartsmetaller (750 ppm), vismut (17 ppm) och järn (17,5 %). Dokumenterat tonnage av varpmaterialet, som uppgår till 0,56 Mt, ger en potentiell resurs av omkring 68 500 ton järn, 488 ton sällsynta jordartsmetaller, 419 ton koppar och 10 ton vismut. SEM-EDS-analyser av ett selektivt bergartsprov visar att allanit-(Ce) är det dominerande värdmineralet för sällsynta jordartsmetaller.

Kittelgruvan i Bastnäsältet har en liten varphög på omkring 600 m³ som visar förhöjda halter av vismut (340 ppm), kobolt (370 ppm), koppar (1 800 ppm), gallium (45 ppm), molybden (2 850 ppm), nickel (43 ppm) och sällsynta jordartsmetaller rika på cerium, lantan och neodymium (8 000 ppm). Ett selektivt prov har höga halter av molybden (5,1 %) och rhenium (1,3 ppm) och ett annat prov innehåller ca 12 % sällsynta jordartsmetaller.

Analyser av varp vid Nya Bastnäs, som ligger strax norr om Kittelgruvan, visar förhöjda halter på koppar (0,18 %), molybden (0,28 %) och sällsynta jordartsmetaller (0,8 %). Även vismut, kobolt, gallium, nickel och guld visar förhöjda värden.

Selektiv provtagning i Malmkärragruvorna uppvisar höga halter av sällsynta jordartsmetaller med upp till 1,2 %.

Varpmaterial från Åsgruvan visar förhöjda halter av järn, molybden, koppar och sällsynta jordartsmetaller, om än i något lägre grad för de senare. Ett selektivt prov innehåller förutom 87,4 % järn, även 1,85 % molybden och 692 ppm koppar. Varpen i den närliggande Östanmossgruvan har förhöjda värden av järn (31,1 %) och sällsynta jordartsmetaller (1 442 ppm).

Vena gruvor i södra Bergslagen omges idag av stora varpområden med okänt tonnage. De bröts på koppar och kobolt. Analyser från varpmaterialet visar förhöjda halter av koppar (0,29 %), kobolt (155 ppm), antimon (35 ppm), vismut (130 ppm) och zink (1 700 ppm). Även lokalt höga halter av arsenik med över 850 ppm i enstaka prov.

Baggetorpsgruvan, ca 12 km sydväst om Finspång, har brutits på volfram fram till mitten av 1950-talet. Den totala mängden varp uppgår enligt bergverksstatistik till ca 90 000 ton, men i området finns även sandmagasin med okänt tonnage. Resultat från provtagning av varp visar på halter av 340 ppm volfram och 114 ppm molybden. Selektiva prover från varp visar ett prov med nära 0,9 % volfram samt ett prov rikt på molybden (5,5 %), koppar (0,15 %) och rhenium (nära 1 ppm).

Inom Tunabergs gruvfält, söder om Nyköping, provtogs varp från elva mindre gruvor av olika mineraliseringstyper; de har brutits på järn, koppar/kobolt, zink och mangan. Resultat av kemiska analyser av varp från fyra gruvor (Österbergsgruvan, Kabbelgruvan, Näsmansgruvan och Sjöbergsgruvan) i Koppartorps by visar förhöjda halter av upp till 0,3 % koppar och 148 ppm kobolt. De visar även 1 800 ppm bly, 71 ppm antimon och 844 ppm zink. Varp från Skaragruvan söder om Koppartorp visar halter om 6,6 % zink, 0,3 % bly, 13 ppm silver, 7 ppm antimon och 5 720 ppm barium. Tre gruvor brutna på järnoxid (Mormorsgruvan, Kärrgruvan och Blombergsgruvan) har förutom förhöjda halter järnoxid (mellan 16 och 23 %) även 0,13 % zink och 0,12 % bly. Mormorsgruvan har även 63 ppm nickel. Mangangruvan håller höga halter järnoxid (33 %), manganoxid (8,3 %) och zink (700 ppm).

INTRODUCTION

In 2021, the Geological Survey of Sweden (Sveriges geologiska undersökning, SGU) together with the Swedish Environmental Protection Agency received a governmental directive to work to increase the possibilities for sustainable extraction of metals and minerals from secondary resources (N2021/01038). The work is intended to contribute to the transition to a more circular and resource-efficient economy. The directive in its entirety was reported to the government in February 2023 (SGU RR 2023:01).

As part of the directive, SGU has documented, sampled, and characterised mining waste (waste rock and tailings) at closed Swedish mines to estimate the quantities of metals and minerals. Metallurgical slag and burnt alum shale were also investigated. Secondary resources from mining waste can possibly contribute to the supply of the critical raw materials needed in the ongoing energy transition.

The European Commission has classified 34 raw materials as critical and strategic for our society and industry (European Commission 2023), and the demand for these materials will increase in the future (Figure 1). A large part of the production of these materials occurs outside the EU where China is the largest producer of many critical raw materials such as the rare earth elements. The EU's intention is to increase the degree of self-sufficiency of the materials. There is a significant number of known deposits of critical material within the EU, in particular Sweden. Within Sweden there are known deposits of, antimony, fluorspar, phosphate rock, graphite, cobalt, PGE, REE, and tungsten (SGU 2023)

Global production of critical and strategic raw materials (CRM/SRM)

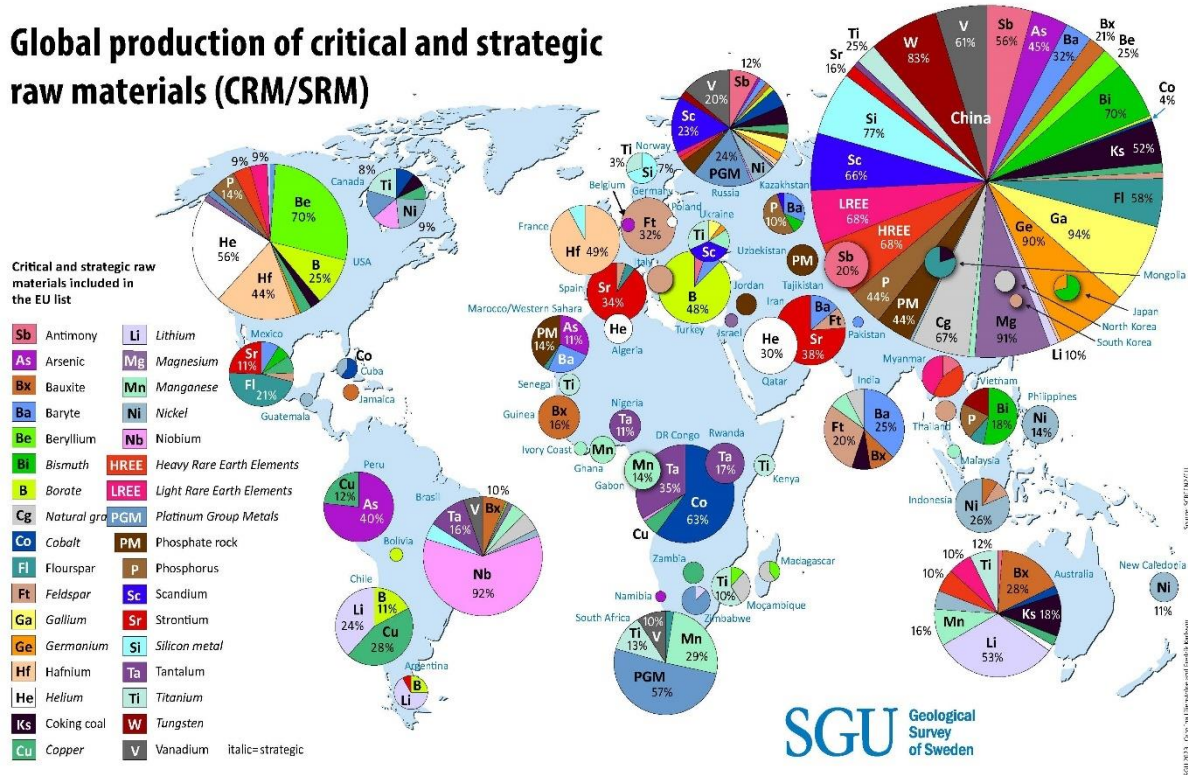


Figure 1. Global production of critical raw materials (CRM) according to the EU classification (European Commission 2023).

Sweden has a long mining history and holds many abandoned mines with remaining waste rock and tailings. Waste rock is the uneconomical fraction removed from a mine to access ore, as well as mineralised rock of lower grade that were uneconomical to process during the life of the mine. Tailings are a fine sand that is the residual product of ore after crushing, milling, and separating the economic fraction from the uneconomic fraction. As no recovery method is 100% effective, a fraction of the targeted minerals will remain in the tailings.

Within the directive, a total of 70 locations was sampled by SGU during 2021 and 2022, with altogether 1,067 samples. A series of reports present background information and available data for each of these locations, as well as the results from the new investigations.

This report includes objects sampled and investigated in central and southern Bergslagen at eleven mines. The coordinates in all figures and tables are given in the SWEREF 99 TM projection.

GEOLOGICAL SETTING

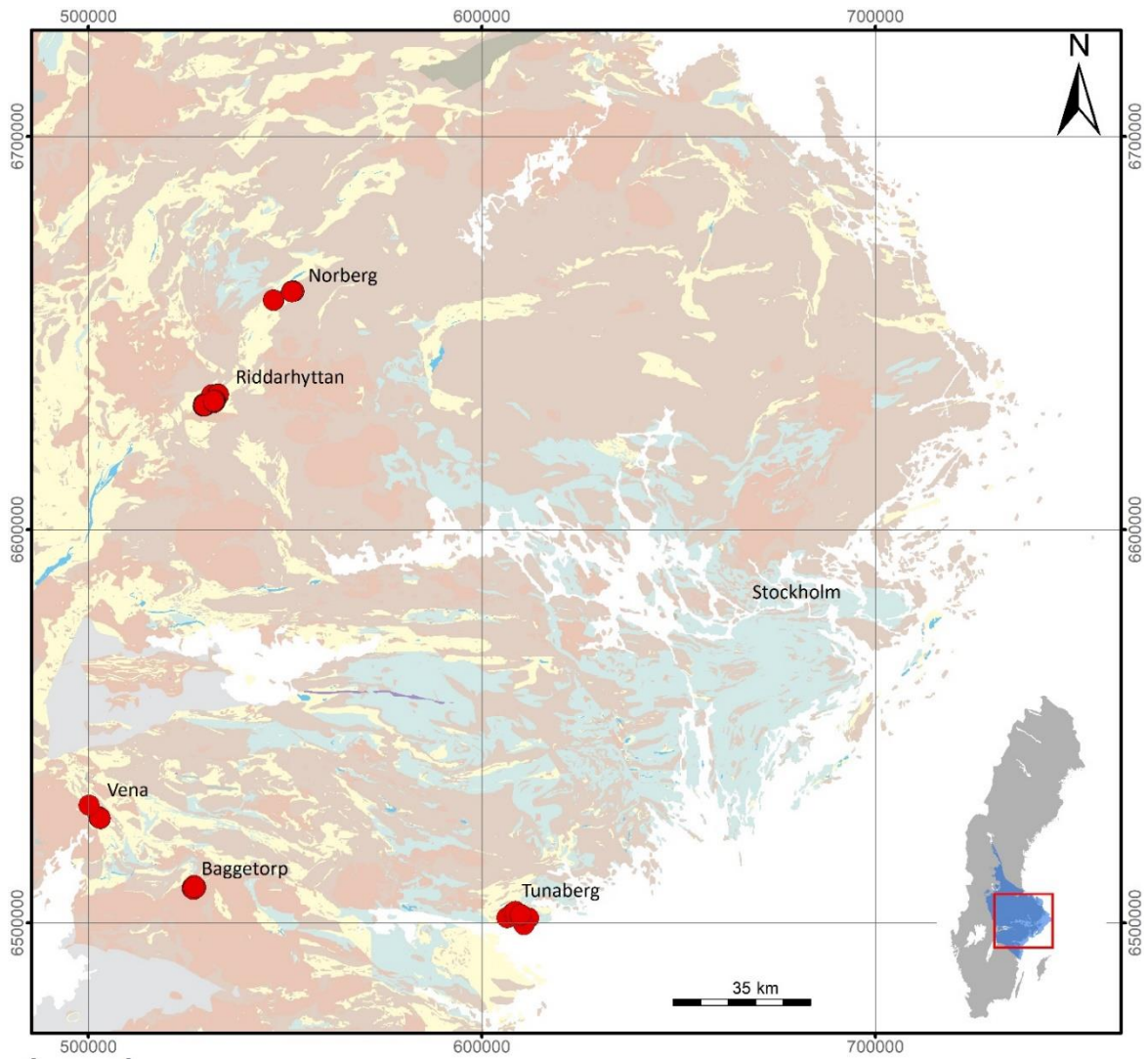
The Bergslagen region is a part of the Svecokarelian orogeny in the Fennoscandian Shield (Fig 2). Most of the metallic deposits of economic importance are hosted by 1.91–1.89 Ga hydrothermally altered, and subsequently metamorphosed, felsic volcanic rocks and associated skarn, calc-silicate or crystalline carbonate rocks (Stephens & Jansson 2020). The metavolcanic rocks are felsic to intermediate with dominating rhyolitic compositions (Stephens & Jansson 2020). The carbonate units are mainly dolomitic in composition and occur as strata in the volcanic sequences, and were deposited in shallow marine basins in periods of low volcanic activity.

The supracrustal rocks were intruded by several suites of igneous rocks. Three different plutonic suites have been identified, referred to as the 1.91–1.87 Ga Granitoid-dioritoid-gabbroid (GDG), the 1.9–1.8 Ga Granite-syenitoid-dioritoid-gabbroid (GSDG) and the 1.85–1.75 Ga Granite-pegmatite (GP) intrusive rock suites, respectively (Stephens et al. 2009). The GDG suite is volumetrically dominating the bedrock in the region. The metamorphic grade ranges from greenschist facies to granulite facies, but amphibolite facies is dominating (Stephens & Jansson 2020). The supracrustal rocks and parts of the GDG suite were affected by hydrothermal fluids resulting in Mg, Na, K and calc-silica (skarn) alterations.

Metamorphism in Bergslagen occurred shortly after the formation of the supracrustal rocks, ranging from greenschist facies through granulite facies. Amphibolite facies rock dominates throughout most of Bergslagen (Stephens & Jansson 2020).

Ore mineralisation in Bergslagen can be divided into three dominant types, each with subgroups. Most mineralisation was syn-volcanic with some exceptions. Fe mineralisation is the dominant ore in Bergslagen comprising 78% of deposits (Stephens et al. 2009), with magmatic, exhalative, and hydrothermal remineralisation (\pm Mn) the predominant modes of mineralisation. The largest Fe ore bodies in Bergslagen are magmatic Kiruna-type Fe-oxide-apatite deposits of Grängesberg. Other large Fe mineralisations such as Stråssa are exhalative banded Fe formations, or seafloor skarn carbonate replacement Fe ores associated with sulphide mineralisation such as Stållberg.

Sulphide mineralisation makes up 21% of other mineralisation and two modes of mineralisation occur the sedimentary-ash-siltstone deposits (SAS), such as Zinkgruvan. These ores are stratiform exhalative ores formed on the seafloor by venting of metal and sulphide rich fluids into dense seafloor brines. These ores typically have a large, continuous extent in sheet-like bodies and are dominated by Zn and Pb with subordinate Cu.



Legend

- Neoproterozoic and Lower Palaeozoic sedimentary rocks
- Clastic sedimentary rock (1.5 - 0.9 Ga)
- Dolerite or grabbroid (1.5 - 0.9 Ga)
- Intrusive or meta-intrusive rock suite and associated supracrustal rock (1.7 Ga)
- Intrusive rock suite and associated supracrustal rock (1.87 - 1.75 Ga)
- Meta-intrusive rock suites (1.92 - 1.87 Ga)
- Crystalline carbonate rock (1.92 - 1.87 Ga)
- Metavolcanic rock (1.92 - 1.87 Ga)
- Metasedimentary rock (1.96 - 1.87 Ga)

Figure 2. Map showing the bedrock in Bergslagen. Sampled mining areas are marked by red dots.

The second type of mineralisation is stratabound-volcanic-associated-limestone-skarn deposits (SVALS), such as Garpenberg and Falun. These mineralisations occur as massive to disseminated ore bodies lacking in the continuous extent of the SAS type deposits, occurring instead as lenses of strongly altered carbonate bodies showing skarn type alteration.

The remaining 1% of ore mineralisation types are skarn replacement ores related to the emplacement of the 1.80–1.77 Ga GP suite. These ores include Mo, Bi, and W mineralisations, with the largest found near Yxsjöberg, where the W mineralisation formed in relation to fluid flow from the emplacement of a GP suite body interacting with silicate and carbonate bodies.

The Riddarhyttan–Norberg area in central Bergslagen belongs to an approximately 80 km long, north–east to south–west trending lens of supracrustal rocks, surrounded by intrusive rocks to the east and intrusive and supracrustal rocks to the west (Fig. 2). The Riddarhyttan–Norberg area is situated along the so called REE-line, as proposed by Jonsson & Högdahl (2013).

The southern Bergslagen region is largely a continuation of central Bergslagen to the south (Fig. 2). The main geological units are Svecokarelian subvolcanic and extrusive volcanic rocks, metasedimentary rocks and coeval granodioritic to tonalitic metaplutonic rocks (Wikström & Karis 1991). In addition, synorogenic alkali granites (Lewerentz et al. 2020) and subordinate amphibolite occur. These rocks were formed 1.91–1.87 billion years ago. A more detailed account of the geology can be found in e.g. Stephens et al. (2009). Tunaberg, Vena and Baggetorp are located in southern Bergslagen (Fig. 2).

METHODS AND SAMPLING

Sampling of tailings ponds

Sampling of the tailings ponds was carried out by handheld Edelman auger drill in hand-dug holes (Fig. 3). For each sample, ca. 2 kg material was collected at approximately 50–120 cm depth, with the aim to sample material only from below the weathered horizon. Colour, grain size, and other characteristics of the sample material were described on site. For some of the sampled tailings ponds, additional data are available from previous SGU sampling campaigns (e.g., Hallberg & Reginiussen 2020).

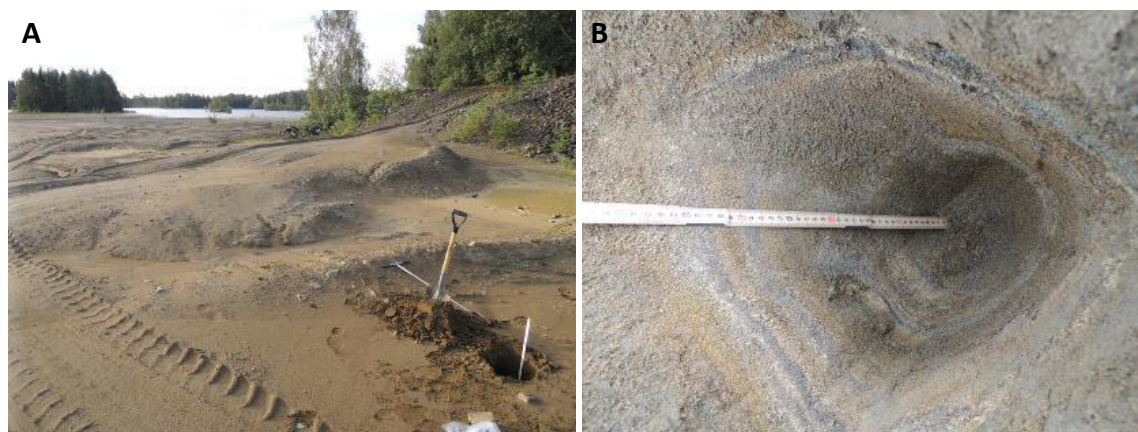


Figure 3. A. Sampling of tailings at Bäckegruvan with spade and Edelman auger drill. B. Hand-dug sampling pit to reach sampling depth. Photos: Gunnar Rauséus.

Drilling was carried out at the Bäckegruvan and Källfallet tailings repositories. In both areas, two drilling sites were chosen based on evaluation of results from surface sampling, geophysical measurements, and field observations. Drill cores were collected using a 40 mm diameter sampler equipped with a core cutter and catcher, allowing to identify structures within the sediment. Below the ground water surface, the sediment was more fluid and a 100 cm long by 10 cm wide screw was used to clean the borehole and to collect a sample. Some sections were collected using a plastic sampling tube in order to obtain material possible to split into one archival “half core” and another half for analysis. Regardless of sampling method, drill samples were generally collected as one-metre sections and sent for analysis using the same methods as described for the surface samples.

Bulk density measurements were performed for both surface and drill samples from tailings; 100 or 200 ml of dry material was weighed, and the results recalculated to tonnes per cubic metre.

Geophysical methods for investigation of tailings

Geophysical ground measurements were performed on two tailings ponds in the Ridderhyttan ore field, Källfallet and Bäckegruvan. The main purpose of the geophysical investigation was to determine the thickness of the tailings and to identify variations within the tailings that could be related to variation in their composition.

Several geophysical methods that measure the electrical properties of the ground were tested and evaluated. A more detailed description of the methods, survey design and results will be presented in a separate publication (Bastani et al., in preparation). The methods used in Källfallet and Bäckegruvan were electrical resistivity tomography (ERT), time-domain induced polarisation (IP), radiomagnetotelluric (RMT), towed transient electromagnetics (tTEM) and ground penetrating radar (GPR).

The ERT method is a direct measurement of the ground’s resistance to conduct electrical current. An array of electrodes is inserted into the ground along a profile and an electrical current is transmitted. Different electrodes act as current and potential during a predesigned measurement scheme, giving information along the profile and at depth. IP measurements is done simultaneously as the ERT measurement but with somewhat adjusted acquisition parameters. IP measurements are based on the fact that different material induce different IP effects, put simply to act as a capacitor. This effect results in a time lag for charges to build up (and decrease) when the current is switched on (or off).

TEM is a geophysical technique by which electric and magnetic fields are induced by transient pulses of electric current, from which the response is measured. As a result, the electrical resistivity distribution of the ground can be determined. The tTEM (towed transient electromagnetic) system (Auken et al. 2018) consists of a transmitter and receiver coil, which are towed by a vehicle.

The RMT method makes use of the signal in the frequency range 10–250 kHz from long-distance radio transmitters. The ratio between the horizontal electric and magnetic field components for each frequency is directly related to the electrical resistivity distribution of the ground. The signal at the lower frequencies penetrates deeper into the ground and the variation of resistivity with depth can then be determined. In this project, the EnviroMT system, developed at Uppsala University (Bastani 2001) was used.

GPR uses high frequency electromagnetic waves (in this investigation 70 and 300 MHz) that may be reflected at boundaries where the electrical properties change. The result is presented as a radargram where different layers can be identified.

At each tailings pond several profiles were measured with the aim to cover as large an area as possible. Different methods also have different ease of access and thereby different distributions within each area.

Sampling of waste rock

Waste rock sampling was carried out according to the sampling methods described by Sädbom & Bäckström (2018), by which each waste rock sampling area is divided into 15–20 subareas following visual criteria. A composite sample is collected from each subarea, and contains 25–50 randomly collected, 2–7 cm long waste rock chips. The composite samples are thereby considered to represent the average composition of the waste rock material in their respective subareas. Each collected chip is then documented in terms of rock and mineralogy.

The appearance of the waste rock sampling areas varies from well-exposed to excessively overgrown by forest and moss. The sampling was mainly carried out in well-exposed parts, which constitutes a possible sampling bias since waste rock material in an area may have partly different mineralogy in different places, and richly mineralised parts could hence be overgrown and therefore not sampled.

In addition to the composite samples, certain samples were selectively collected to represent the mineralisation types found at each locality. In general, two to three representative samples were selected per locality and sent for geochemical analysis. Thin sections were made of these samples for petrographic and mineralogical analyses.

Lithochemical analysis

Geochemical analysis of all samples was conducted by ALS laboratories. Sample preparation including weighing and crushing took place at ALS Piteå, Sweden. Samples were initially crushed to approximately 2 mm, and the samples were subsequently split and pulverized to <75 µm fractions for analysis at ALS Galway, Ireland. Three SGU internal standards were analysed with each batch of samples to ensure the accuracy and consistency of the results.

A total of 61 major and trace elements were analysed. Major elements were analysed using ICP-AES after acid digestion. Trace elements were analysed using lithium borate fusion prior to acid digestion and ICP-MS. Aqua regia and 4 acid digestion with ICP-MS analysis were used for trace elements with low concentrations. Ore minerals that exceed detection limit of standard analyses (typically at 10,000 ppm) were analysed again using ore-grade methods with higher detection limits.

Many elements are analysed multiple times using several analysis methodologies, and data in this report are presented using SGU's preferred analysis methodology. For a complete list of elements analysed and their preferred analytical methodology, see appendix 1: Sample Digestion and Analytical Methods.

Results in this report are given in oxide form for major elements presented in weight percent (i.e. Fe concentration is presented as Fe₂O₃). Elements such as zinc, lead, copper and molybdenum are given in weight percent or ppm depending on concentrations. REE is presented as the sum of all rare earth elements including yttrium.

Scanning electron microscopy

A selection of thin sections from waste rock localities were analysed using scanning electron microscopy (SEM). The main target was to obtain semi-quantitative chemical analysis of critical raw material (CRM)-bearing minerals. The work was conducted at the Swedish Museum of Natural History in Stockholm using a FEI Quanta650 Scanning Electron Microscope. Chemical analysis was done using an Oxford Instruments electron dispersal spectrometer (EDS) with an 80 mm² detector and a 25 second analysis time. Spectra were analysed and compositions calculated with the Aztec software. Detection limits for trace elements were typically around 0.5 wt %.

Potential resources

Based on tonnage of the material type in the tailings pond and waste rock material and the average values for some of the elements of economic interest, a simplified estimate of potential resource, including tonnage and grade, can be made. This should not be seen as a formal mineral estimate in the strict form used by for example the mining industry, which requires an approval of a qualified person, QP.

For the two tailings repositories included in this report, geophysical investigations by SGU, drilling and inhouse bulk density measurements has resulted in an estimated tonnage, which correspond quite well to documented historical numbers for tonnage. A potential resource is estimated for the elements with elevated concentrations and the estimated tonnage of the tailings. The technical possibility of recovery for any element has not been considered.

Estimation of potential resources for waste rock piles have been made on tonnage provided from SGU database and average grades for elements of interest sampled within this project. This estimation assumes all material is fully accessible and not removed for use as aggregates or ballast or backfilled into the mines.

Further evaluation of data presented herein by competent persons as defined by the UNFC (UNFC 2019) is needed to provide any qualified resource estimations, and as such the resource potential herein should be considered as only a framework for guiding future studies.

RIDDARHYTTFÄLTET

Riddarhyttfältet, the Riddarhyttan ore field, was active for several hundred years and consists of hundreds of abandoned mines which were mined mainly for iron oxide and copper (Fig. 4). They include variously sized open pits, as well as underground mines. A total of 20.2 million tonnes (Mt) of ore and gangue material was mined between 1731 and 1980, resulting in 4.6 Mt of waste rock and 7.2 Mt of tailings pond material (Bergquist 1985). In total, 207 samples were collected from tailings and waste rock at several sites in the area (Table 1).

Table 1. Compilation of sample type and number of samples for mines in the Riddarhyttan ore field.

Mine	Waste rock	Tailings surface	Tailings drilling
Källfallsgruvan	17	23	21
Östergruvan–Jacobsgruvan	15	-	-
Haggruvan	15	-	-
Bäckegruvan	15	23	49
Kittelgruvan	15	-	-
Nya Bästnäs	16	-	-
Persgruvan	15	-	-
Total number of samples	93	23	70

Existing and historical data

Drill cores and lithogeochemistry

According to the SGU drill core database, ca. 460 drill cores have been drilled in the Riddarhyttan area, of which remaining material from 132 drill cores are stored in the SGU drill core archive in Malå, Sweden. Logging protocols, assay results and other information is stored digitally and in physical archives. The cores were mainly drilled at the Bäckegruvan, Bjursjön, Bastnäs and Persgruvan mine sites on behalf of Nämnden för statens gruvegendom (NSG) and Bäckegruve AB during the period 1979–1986 (Ihre 1985; Ihre & Sädbom 1986).

Some of the drill cores have been reanalysed by Dannemora Mineral AB in two campaigns, 2010 and 2013, resulting in 485 chemical analyses. In 2019, SGU analysed 43 one-meter sections of drill core from different mineralisations and mines in the area, including Bastnäsorten, Persgruvan, Riddarhyttan Skärsjön, Lerklockan and Östergruvan (Hallberg & Reginiussen 2020). Four drill cores from the Bastnäs area have been scanned using IR-technic within the framework of a SGU-project during the years 2014–2016. The results from the scanning is presented in SGU drill core database. Furthermore, the SGU database Lithochemstry comprises over 150 whole rock analyses predominantly from mineralised waste rock and outcrop samples from the Riddarhyttan area.

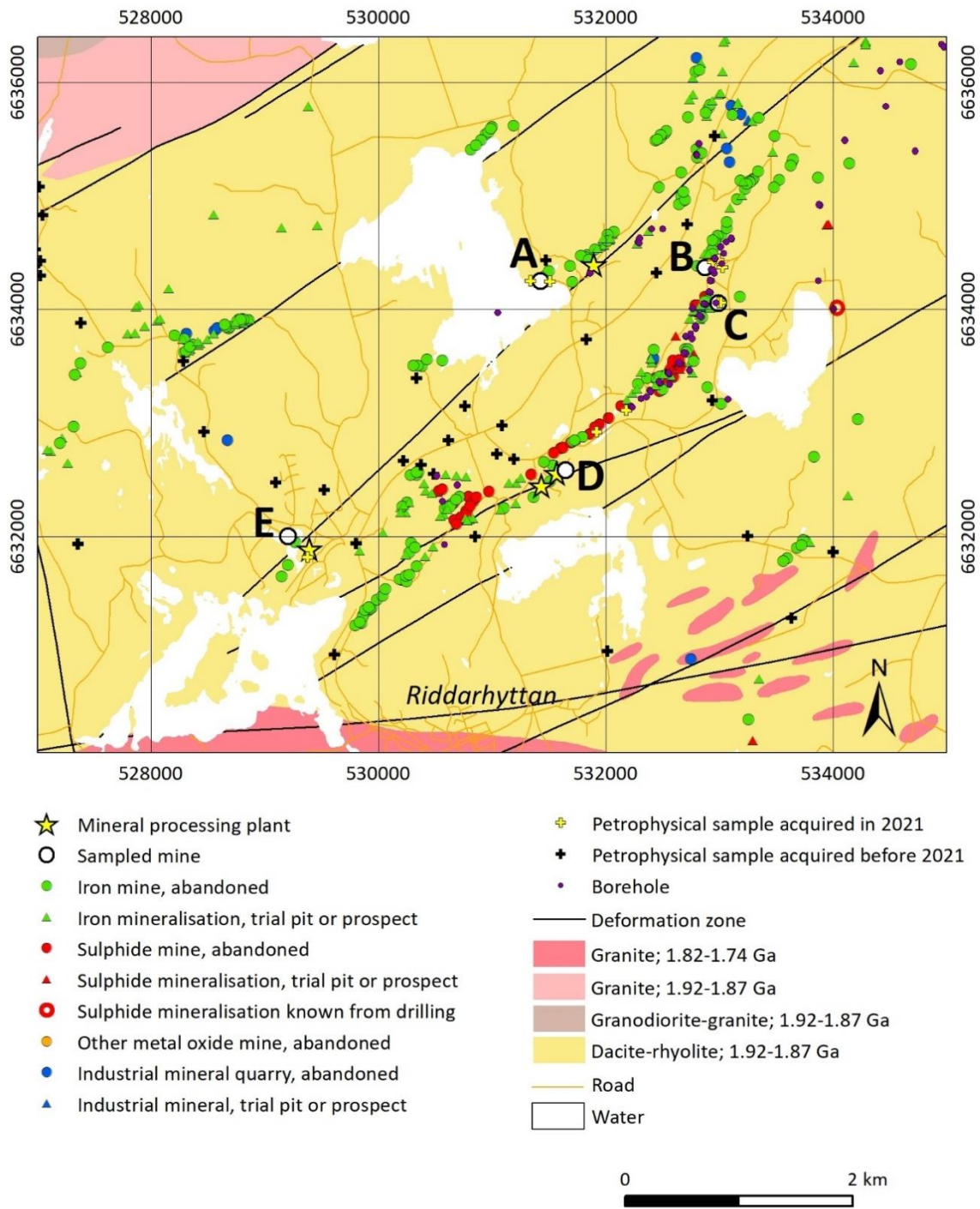


Figure 4. Simplified bedrock map over the Riddarhyttan area (SGU 2022). A = Persgruvan, B = Nya Bastnäs, C = Kittelgruvan, (Old Bastnäs) D = Bäcke-gruvan, Hagggruvan and Östergruvan–Jacobsgruvan, E = Källfallsgruvan.

Airborne geophysics

Two airborne geophysical surveys have been carried out by SGU in the Riddarhyttan area and its surroundings (Figs. 4–6, Table 2). The flight direction of the most recent one was approximately northwest–southeast. This direction of flight lines is more favourable in the Riddarhyttan area as it is almost perpendicular to the general strike of the main bedrock structures. The VLF measurements from two transmitters make it possible to derive apparent resistivity and current density maps of the ground. Also, the electrical conductors in the bedrock can be identified independent of their direction with respect to the VLF transmitters.

Table 2. Previously made airborne geophysical surveys by SGU over the area around Riddarhyttan.

Year	Organisation	Geophysical methods used	Flight direction	Flight line separation (m)	Flight altitude (m)
1969	SGU	Magnetics, gamma spectrometry	East–west	200	30
2017	SGU	Magnetics, gamma spectrometry, VLF (2-transmitters)	Approximately northwest–southeast	200	60

Ground geophysics

The north-eastern part of the investigated area has been covered with extensive ground-based magnetic measurements (Fig. 5, Table 3). Within one of these areas, ground slingram data were also acquired (Fig. 6, Table 3). Both magnetic and slingram data were collected along pre-defined, parallel profiles with 80 m line spacing. Along these profiles, data were collected every 20 m. Data from one of these areas are shown in Figure 7. Additional measurements, along profiles where both magnetic and VLF data were acquired, were made by SGU in 2020 (Figs. 5 and 6).

Gravity measurements have been conducted around Riddarhyttan in 1975, 1978, 2018, and 2020. From these data the residual gravity field is calculated (Fig. 8). The general data coverage has a spacing of approximately 1–1.5 km between sites of measurement. Along two profiles, stretching northwest–southeast across large parts of the mineralized sequence, more closely spaced measurements at 100 to 250 m intervals have been made.

Table 3. Previously acquired ground magnetic and slingram data in the Riddarhyttan area. Polygon numbers correspond to Figure 5. The area that was subject for slingram measurements is shown in Figure 6.

Polygon nr	Name of investigated area	Geophysical data	Responsible	Year acquired
1	Bjursjön	Magnetic Z-anomaly	NSG	1987
2	Bjursjön	Magnetic anomaly	SGAB	1984
3	Bjursjön	Magnetic total field, slingram	NSG	1986

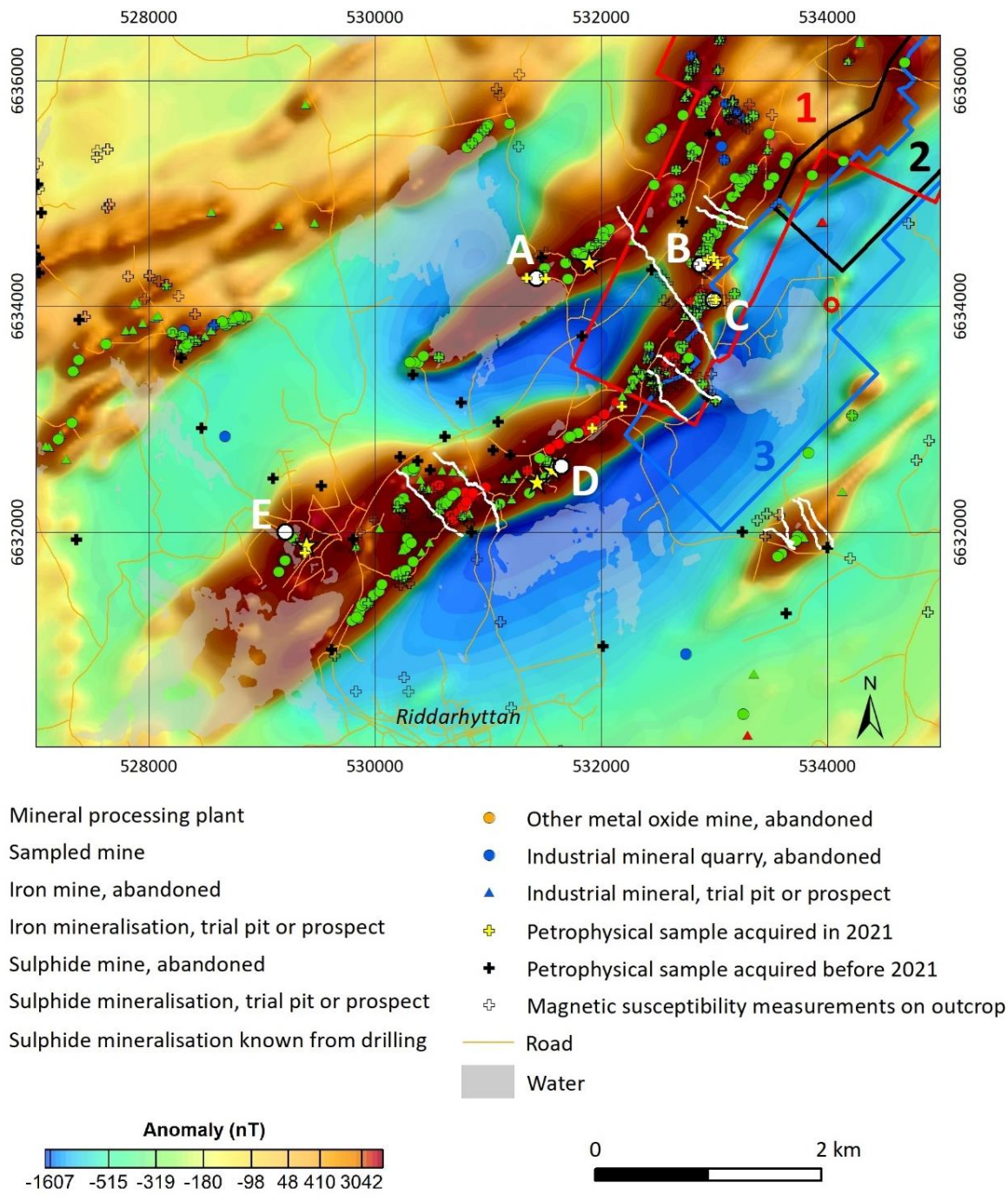


Figure 5. Map over the magnetic anomaly field for the area around Riddarhyttan. The magnetic data is based on the measurements made during the airborne survey in 2017. White lines correspond to profiles where ground magnetic data previously have been acquired. The polygons 1–3 delineate areas in which SGU previously have been acquiring extensive ground magnetic data (Table 3). A = Persgruvan, B = Nya Bastnäs, C = Kittelgruvan, D = Bäcke-gruvan, Haggruvan and Östergruvan–Jacobsgruvan, E = Källfallsgruvan.

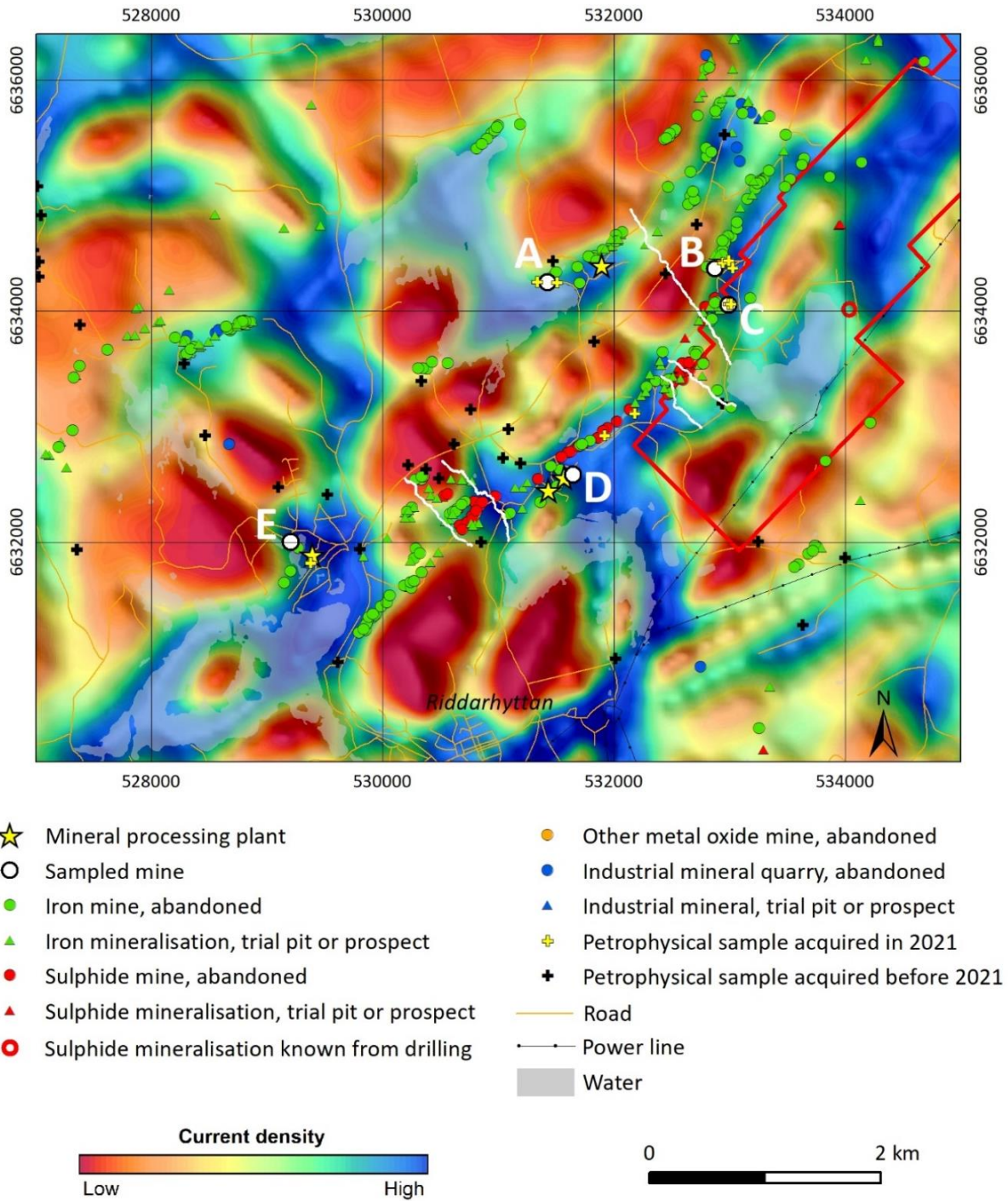


Figure 6. Map over the current density in the ground for the area around Riddarhyttan. The data is based on airborne VLF measurements from two transmitters in 2017. White lines correspond to profiles where ground VLF data previously have been acquired. The red polygon encompasses an area of slingram ground measurements previously carried out by SGU. A = Persgruvan, B = Nya Bastnäs, C = Kittelgruvan, D = Bäcke-gruvan, Haggruvan and Östergruvan–Jacobsgruvan, E = Källfallsgruvan.

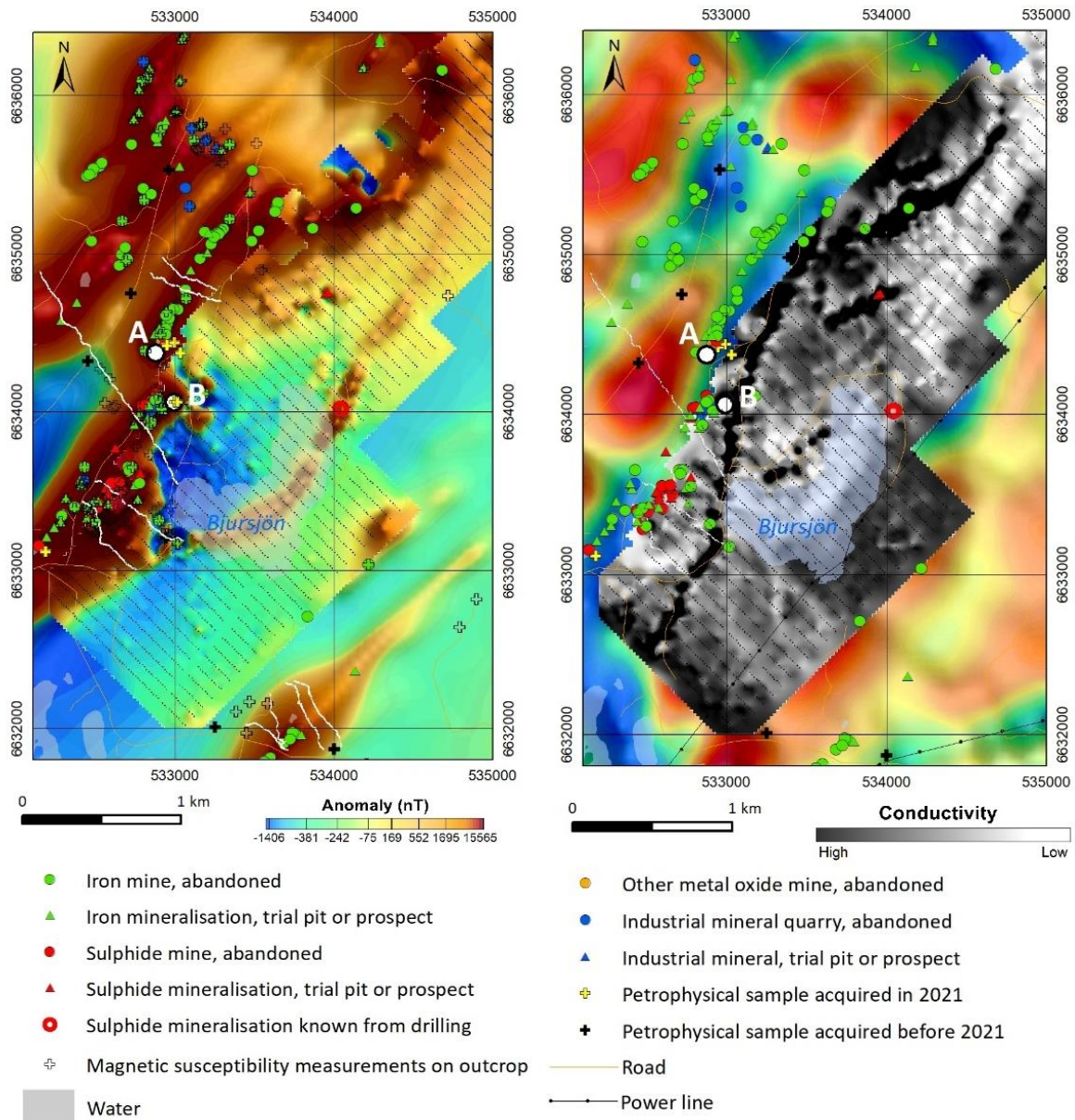


Figure 7. Maps showing the magnetic anomalies (left) and the real-part of the slingram data (right) for the ground geophysical surveys at Bjursjön. Small black dots in the maps are locations for measurements during these surveys. White lines in the maps are profiles where ground magnetic data (left) and VLF data (right) previously have been acquired. A = Nya Bastnäs, B = Kittelgruvan. The backdrop images in the Figures are the magnetic anomalies (left) and the current density (right) from SGU's airborne survey in 2017.

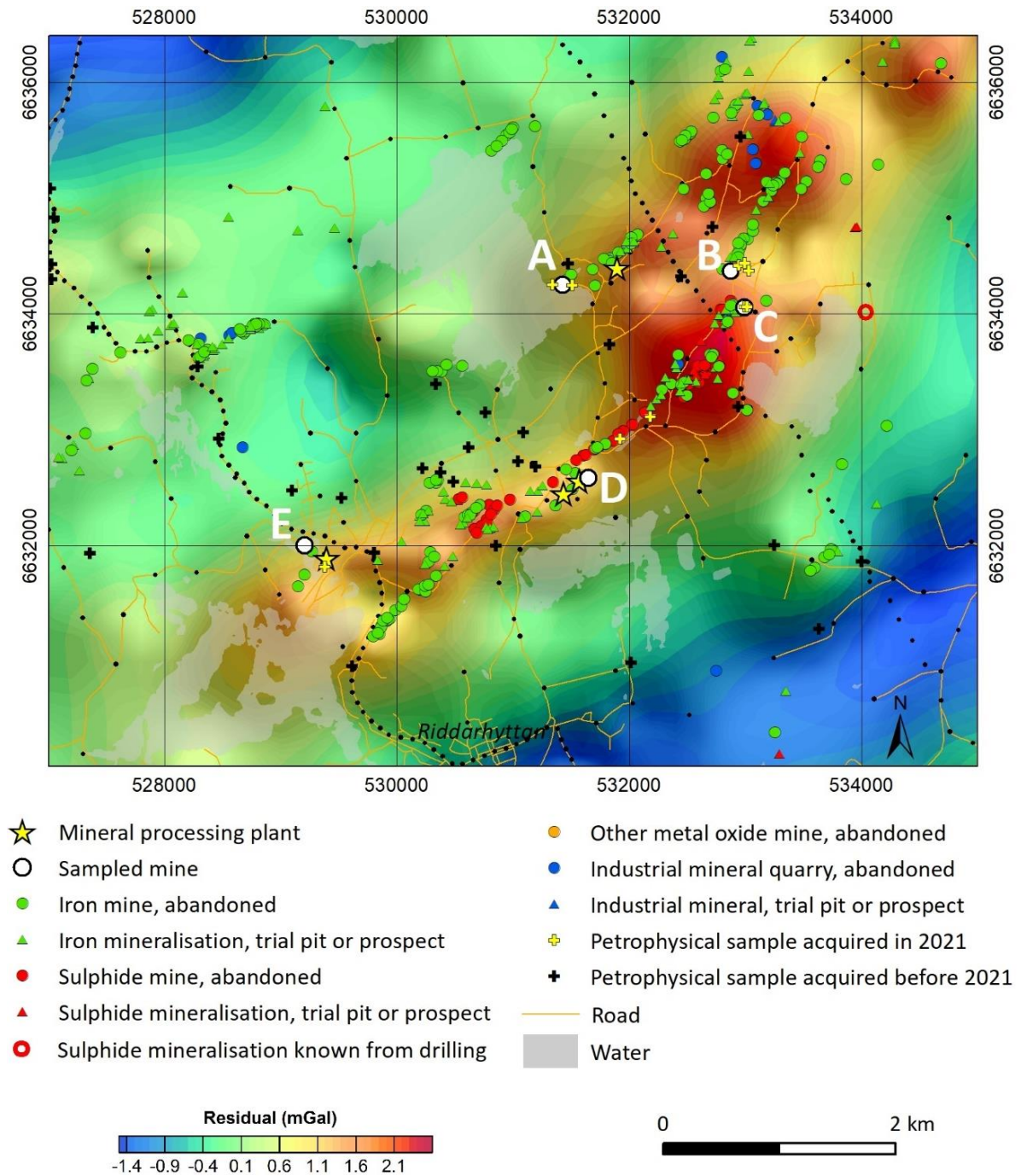


Figure 8. Map of the residual gravity field for the area around Riddarhyttan, expressed as the difference between the Bouguer anomaly and an analytical continuation upwards to 3 km. Black dots show the location of gravity measurements. A = Persgruvan, B = Nya Bastnäs, C = Kittelgruvan, D = Bäcke-gruvan, Haggruvan and Östergruvan–Jacobsgruvan, E = Källfallsgruvan.

Exploration geophysics

Several geophysical exploration surveys have been conducted in the area (Fig. 9, Table 4). These data are available in SGU's databases.

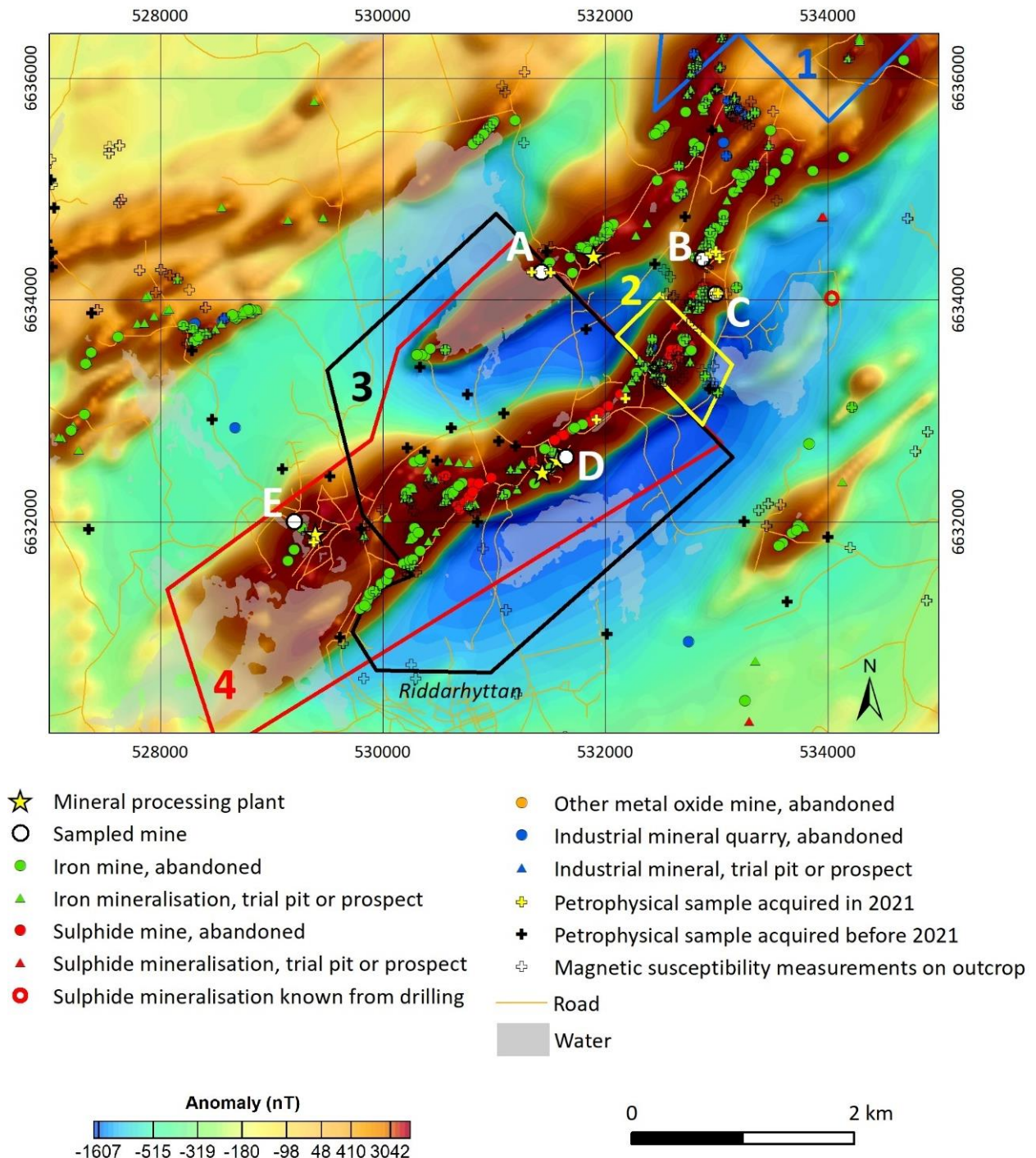


Figure 9. Map over the magnetic anomaly field for the area around Riddarhyttan. The magnetic data are based on the measurements made during the airborne survey in 2017. The polygons 1–4 delineate areas in which geophysical exploration surveys previously have been carried out. Data from these surveys are now available in SGU's databases (Table 4). A = Persgruvan, B = Nya Bastnäs, C = Kittelgruvan, D = Bäckegruvan, Haggruvan and Östergruvan–Jacobsgruvan, E = Källfallsgruvan.

Table 4. Previously made geophysical exploration surveys at Riddarhyttan, from which data now are available in SGU's databases. The polygon numbers correspond to those found in Figure 9.

Polygon nr	Name of exploration area	Geophysical methods used	Responsible	Year of permit
1	Riddarhyttan nr 2	Magnetics	Dannemora Mineral AB	2009–2015
2	Riddarhyttan nr 3	Magnetics	Dannemora Mineral AB	2009–2015
3	Riddarhyttan nr 1001	Magnetics, VTEM	Boliden Mineral AB	2005–2008
4	Riddarhyttan nr 1	Magnetics	Dannemora Mineral AB	2008–2014

Källfallsgruvan

Historical background

Källfallsgruvan is situated in the north-eastern part of lake Lien and about 10 kilometres west of Skinnskatteberg (Fig. 4). The mine started to produce iron ore in 1897. From 1943, ore from Persgruvan was processed at the Källfallsgruvan processing plant, which ran until closure in the summer of 1963. The mining continued until 1967, and for four years material from both Källfallsgruvan and Persgruvan was transported to the processing plant in Bäckegruvan (Bergquist 1985). From 1897 to 1963, about 3.5 Mt was processed in the dressing plant, resulting in nearly 1.5 Mt of iron concentrate as well as 2.0 Mt of tailings and waste rock (Hallberg & Reginiussen 2020). A total of 0.93 Mt of waste rock was deposited from production between 1903 and 1967 (SGU 2023)

Tailings

The tailings were deposited in the northeast part of lake Lien and are now found in two separate ponds separated by a pine forest (Figs. 10–11), hereafter referred to as the west and east ponds, respectively. Sampling of the bottom sediments in the northern part of lake Lien has shown that they are composed of mine tailings (SGI 2014, de Campos Pereira 2014). The two tailings ponds comprise an area on land of ca 50,000 m², as measured from aerial photographs.

During a sampling campaign in 2019, SGU collected surface samples from the tailings ponds which together with the present sampling campaign make a total of 31 surface samples available for geochemical evaluation. Two boreholes were drilled in the tailings ponds, one in each part (Fig. 10). The borehole in the western pond measured seven metres depth and the borehole in the eastern pond eight metres, resulting in a total of 21 samples.

During the years of 1979–1980, after the mine was closed, attempts were made to extract molybdenum from the tailings. In total, 92,600 tonnes of tailings were processed, resulting in 22,100 tonnes of Mo-rich concentrate.

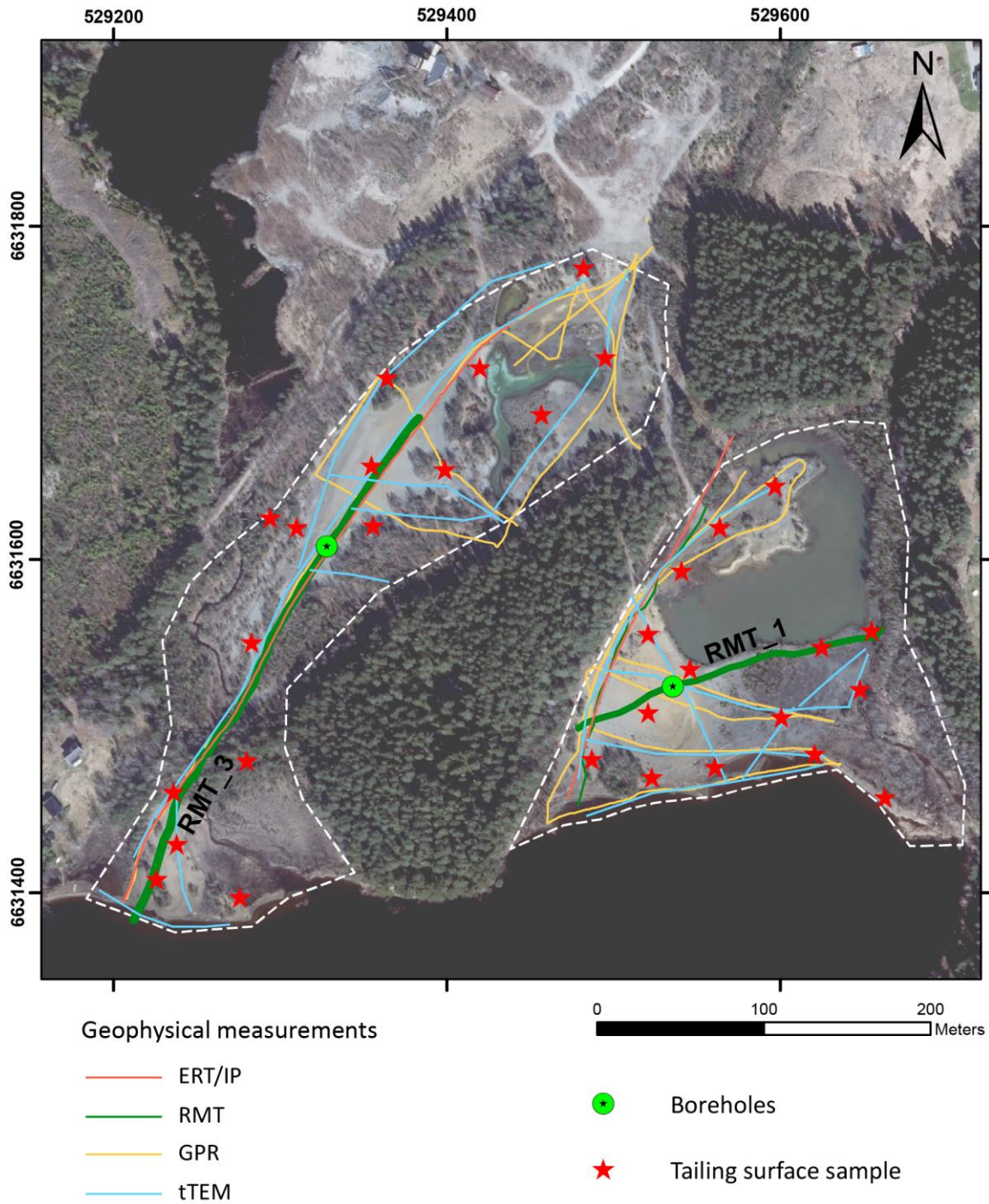


Figure 10. Orthophoto (Lantmäteriet) shows tailings ponds at Källfallsgruvan. The dashed white lines outline the two areas, west and east. The thicker green lines show the location of the profiles shown in Figures 12 and 13 (RMT_3 and RMT_1).



Figure 11. Tailings at Källfallsgruvan. **A.** Wider area of the west pond. **B.** Part of the east tailings pond, partly below groundwater surface, and in the background the pine forest separating the two ponds. Photos: Gunnar Rauséus.

Results from geophysical measurements

The location of the geophysical measurements acquired at Källfallet are shown in Figure 10. The IP data collected at Källfallet show low quality and that may be caused by cultural noise. Consequently, no IP results could be used at this site. The electric resistivity models obtained from the ERT, RMT and t TEM have all been used to determine the thickness of the tailings. They generally show quite similar results; however, ERT and RMT have higher resolution and depth of investigation compared to t TEM. The site conditions were quite favourable for GPR, especially over the glaciofluvial deposits, and the radargrams offered a good complement to the resistivity profiles.

Profile RMT3 (Figs. 10 and 12A) was measured in the western tailings pond. The resistivity model shows a high resistivity layer at the top corresponding to dry sand, followed by a low resistivity layer corresponding to water-saturated sand. The water-saturated sand shows resistivities around 30 to 50 ohmm. The tailings are underlain by till and bedrock with higher resistivity. The maximum thickness of the tailings along this profile is about 7 to 8 m, which is also confirmed by the drilling site at distance 240 m. At distances 65 to 130 m along the profile the resistivities are considerably higher in the uppermost 10 m (around 200 to 600 ohmm). This structure is interpreted as glaciofluvial deposits, and the tailings are probably very thin here. In Figure 12B, the ground-penetrating radargram along the same profile shows significantly different reflection patterns inside the structure interpreted as glaciofluvial deposits, compared to the reflection patterns on the sides where the signal is rapidly attenuated under the tailings.

Profile RMT1 (Figs. 10 and 13) was measured in the eastern tailings pond. Like profile RMT3, the resistivity model shows three layers. A high resistive layer at the top corresponding to dry sand followed by a low resistive layer corresponding to water-saturated sand and at the bottom a high resistive layer corresponding to till and bedrock. The second low resistive layer, show resistivities between 20 to 50 ohmm. The drilling at distance 60 m along the profile shows 8 m of sand, which correlates well with the resistivity model. At distance 120 to 140 m along the profile, the resistivity model shows lower resistivities at greater depth which may be caused by either a fracture zone in the bedrock or larger soil depth, or a combination of both.

The bottom of the tailings has been interpreted along all profiles and then interpolated to a surface that covers both the western and eastern tailings ponds, which together with the boreholes allow for the estimation of the tailings thickness (Fig. 14). The thickness varies generally between 6 and 9 m, with somewhat larger depths in the eastern tailings pond.

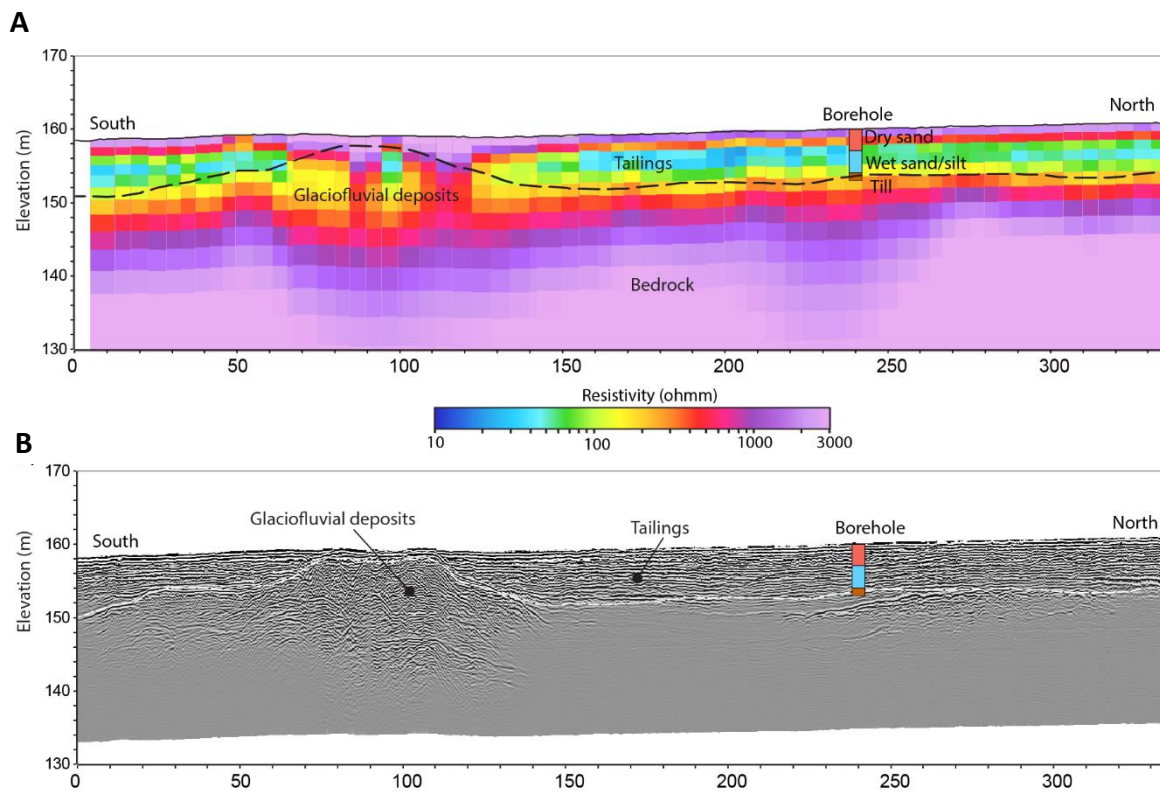


Figure 12. Profile RMT 3 located in the western tailings pond (Fig. 10). **A.** Resistivity model with interpretation and location of the borehole with simplified lithological description. The black dashed lines represent the bottom of the tailings. **B.** Ground penetrating radargram (70 MHz source signal). The location of the borehole is shown. The white dashed lines represent the interpreted bottom of the tailings.

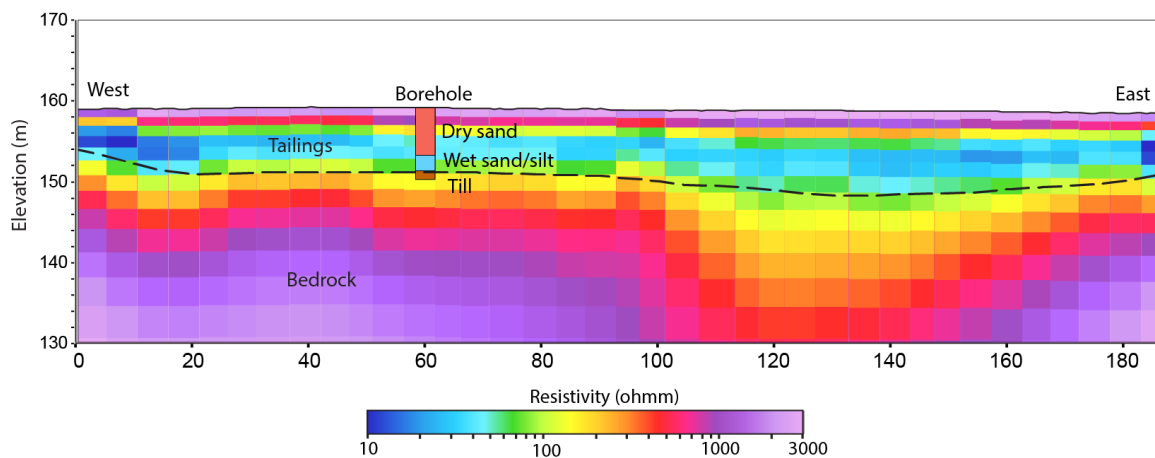


Figure 13. Profile RMT 1 located in the eastern tailings pond (Fig. 10). Resistivity model with interpretation and location of the borehole with simplified stratigraphical description. The black dashed lines represent the bottom of the tailings.

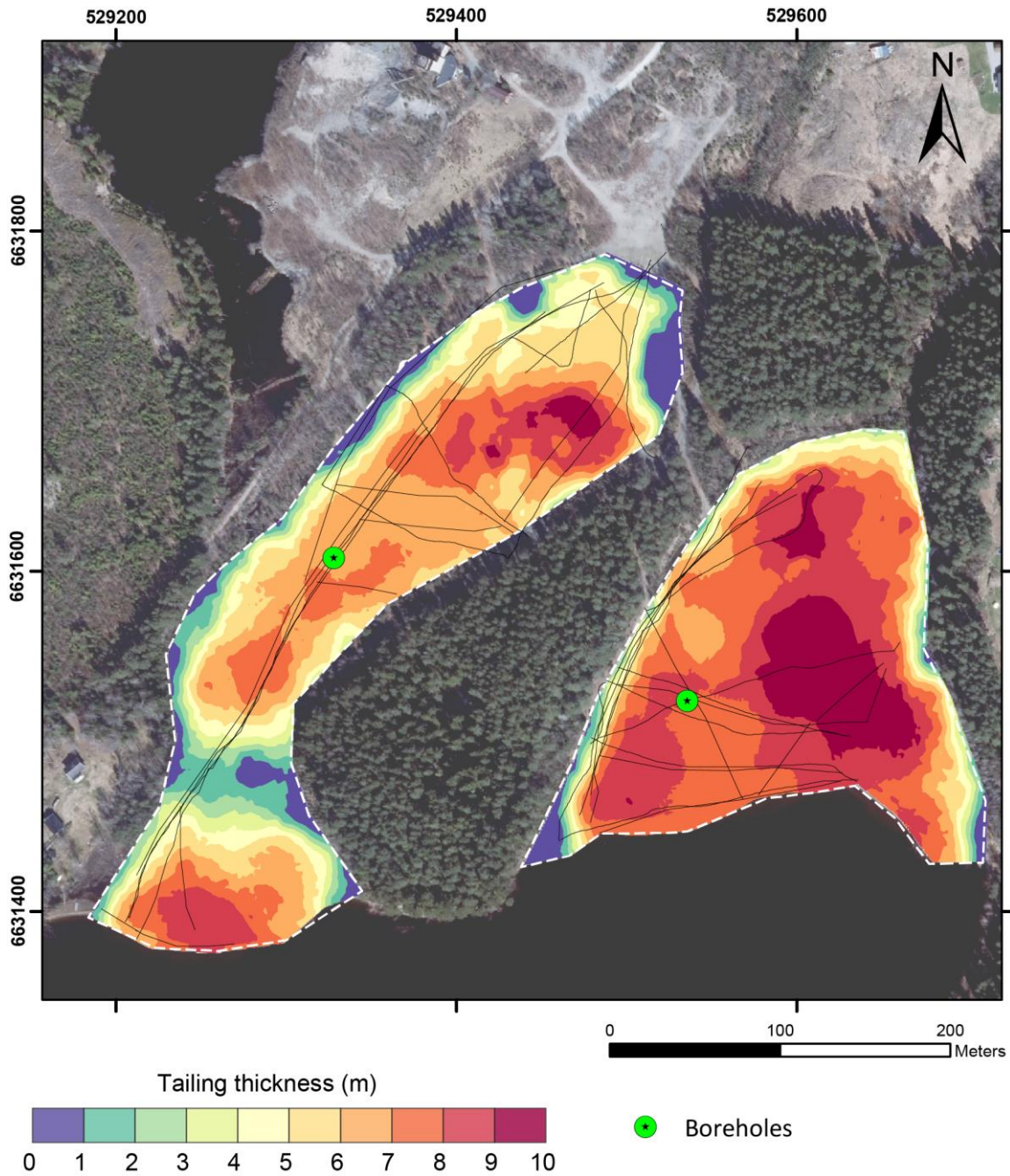


Figure 14. Modelled thickness of the tailings at Källfallsgruvan based on geophysical measurements (thin black lines) and boreholes.

Results from chemical analyses of surface and drilling samples

Analyses of surface samples show elevated concentrations for Fe_2O_3 , Bi, Ga, Mo, Y and REE (Table 5). The REE content ranges from 1,121 to 5,989 ppm, with an average of 2,668 ppm (Table 5). Concentration of REE shows a slight enrichment in the western part of the eastern pond and in the southern part of the western pond (Fig. 15). A similar trend is also seen for Fe_2O_3 . The REEs are dominated by LREE and constitute ca. 94% of the average total REE content.

Geochemical analyses from drilling samples show elevated concentrations for Fe_2O_3 , Bi, Ga, Mo, Y and REE as in the surface samples (Table 6). REE concentration from the drilling samples are higher near the surface in the eastern pond, but below three metres depth, both boreholes show

similar concentrations around 2,000 ppm (Fig. 16). The concentration of Fe_2O_3 is generally lower in the western pond which can be seen in Figure 18A, showing correlation between iron content and density. All samples from both surface and drilling show negative Eu anomalies when normalised against Boynton (1984) (Fig. 17). However, surface samples show a wider spread in REE concentrations than the drill samples.

Bulk density

Bulk density was measured for 20 surface samples and 17 drill core samples and resulted in an average of 1.66 tonnes/ m^3 . It shows relatively positive correlation with Fe_2O_3 (Fig. 18B). Average bulk density is higher in samples from the eastern pond (1.75 tonnes/ m^3) than in the western (1.54 tonnes/ m^3). Bulk density of tailings western pond is not only is lower in general but also decreasing with depth (Fig. 18B).

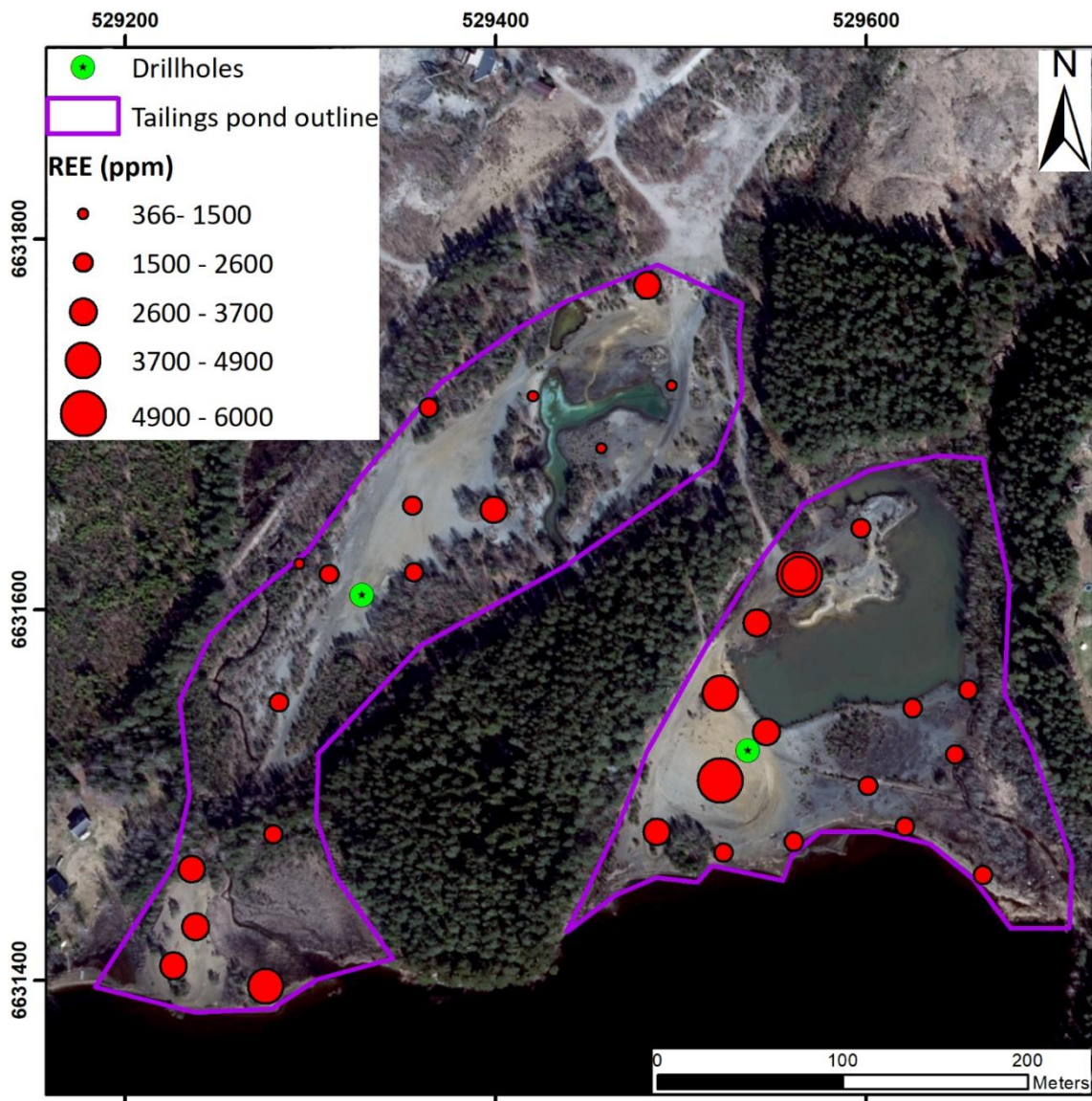


Figure 15. Show graduated values of total REE from Surface samples (red dots) at Källfallsgruvan tailings pond. Green dots show location of boreholes.

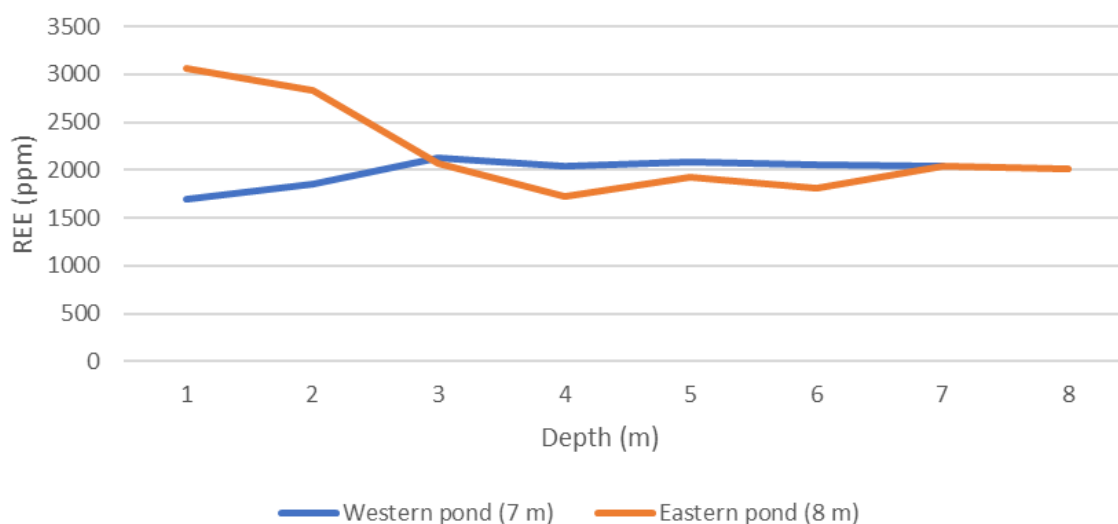


Figure 16. Figure shows REE concentration along the boreholes from tailings ponds at Källfallsgruvan.

Table 5. Selected geochemical data for surface samples from tailings at Källfallsgruvan (n =31). Of these 8 samples are from a sampling campaign 2019 (Hallberg & Reginiussen 2020)

Element	Fe ₂ O ₃ %	Bi ppm	Ga ppm	Mo ppm	Y ppm	LREE ppm	HREE ppm	REE ppm
Average	21	25	32.6	312	233	2,515	173	2,688
Min	9	4.2	20.3	157	151	1,025	96	1,121
Max	47	166	45.3	512	403	5,722	300	5,989
Median	16	17	32.4	300	212	2,294	161	2,472

Table 6. Selected geochemical data for drilling samples from tailings at Källfallsgruvan (n =21).

Element	Fe ₂ O ₃ %	Bi ppm	Ga ppm	Mo ppm	Y ppm	LREE ppm	HREE ppm	REE ppm
Average	16.8	16.2	31.1	379	232	1,952	163	2,088
Min	9.8	2.2	26.5	209	158	2,879	203	1,691
Max	28.8	43.2	36.5	774	299	1,550	117	3,057
Median	14.6	14.7	30.9	330	239	1,873	174	2,034

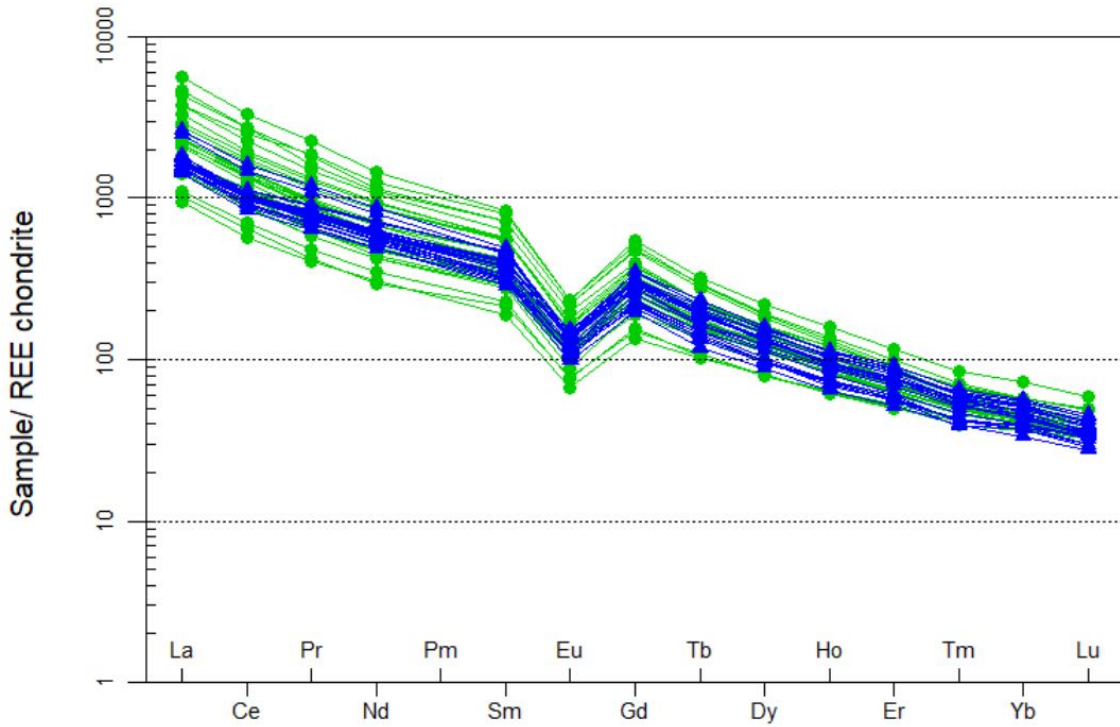


Figure 17. Chondrite-normalised (Boynton 1984) REE diagram from surface samples (green, n=31), and drilling samples (blue, n=21).

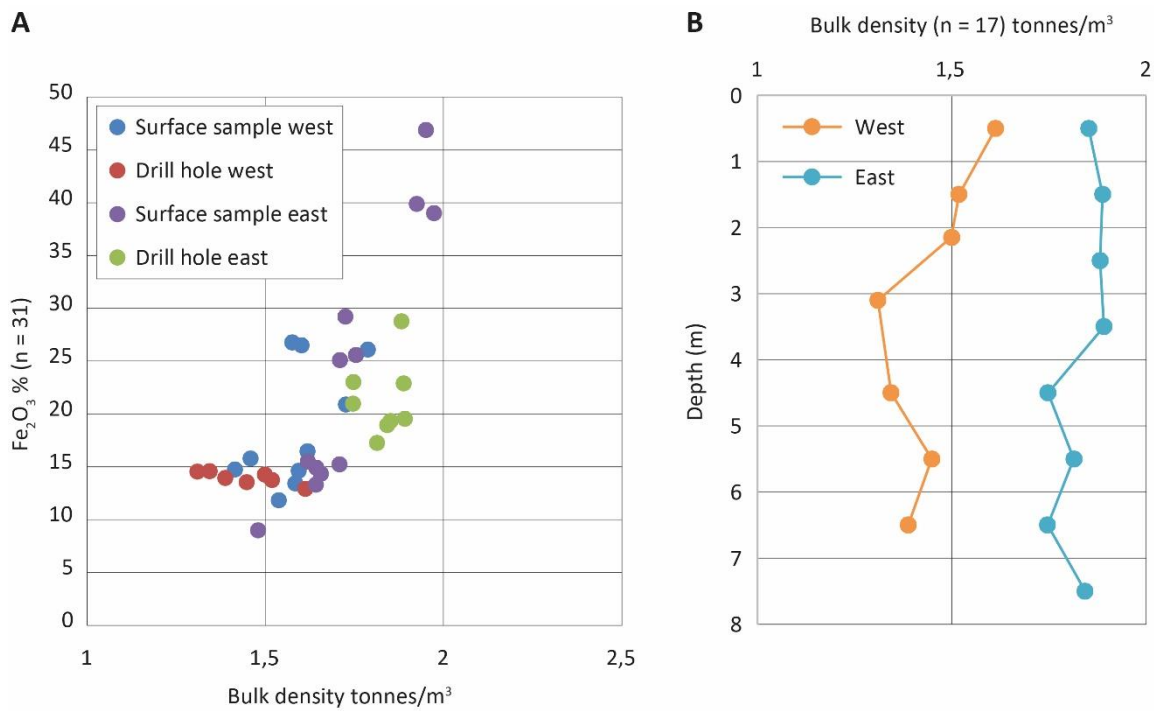


Figure 18. A. Plot showing correlation between density and iron oxide content in surface and drilling samples from the western and eastern tailings pond, respectively. **B.** Density vs depth plot for borehole samples in the western (orange) and eastern (blue) tailings pond (n=17).

Waste rock

Waste rock piles at Källfallsgruvan vary from well-exposed slopes to more overgrown areas with young forest and moss. Sampling was carried out in areas with well exposed waste rock, around the waterfilled open pit and the mineshaft (Fig. 19). The sampled material varies in size between 5 and 30 cm and shows partial red oxidization on the surface. The present amount of waste rock is difficult to estimate as part of the southern area appears to be reworked after deposition, with waste rock being removed in the southern part of the area. This can be seen when comparing old aerial photos with present day LiDAR data (Fig. 20). The sampling consists of 15 samples and the material is dominated by metavolcanic rocks, amphibole skarn and pieces with iron oxide mineralisation. Distribution of rocks is compiled in Figure 21. Two mineralised selective samples were collected for chemical characterisation and thin sections studies.

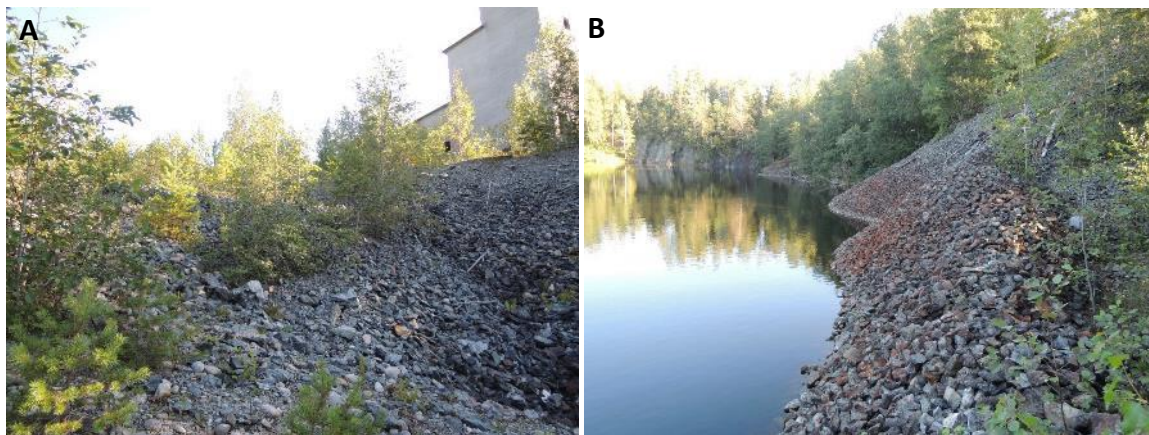


Figure 19. A. Waste rock area at Källfallsgruvan with mineshaft visible in the background. B. Waste rock with oxidized surface at the edge of the waterfilled open pit at Källfallsgruvan. Photos: Gunnar Rauséus.

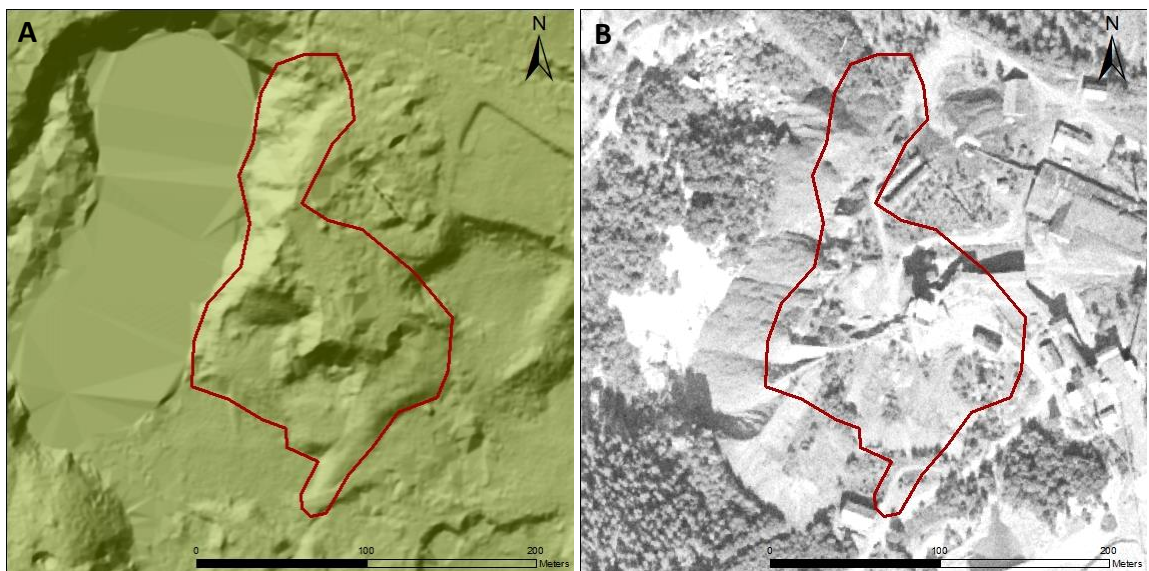


Figure 20. A. LiDAR data with red polygon for interpreted extents of waste rock at Källfallsgruvan. B. Aerial photo from 1959 for the same area (eight years prior to shutdown).

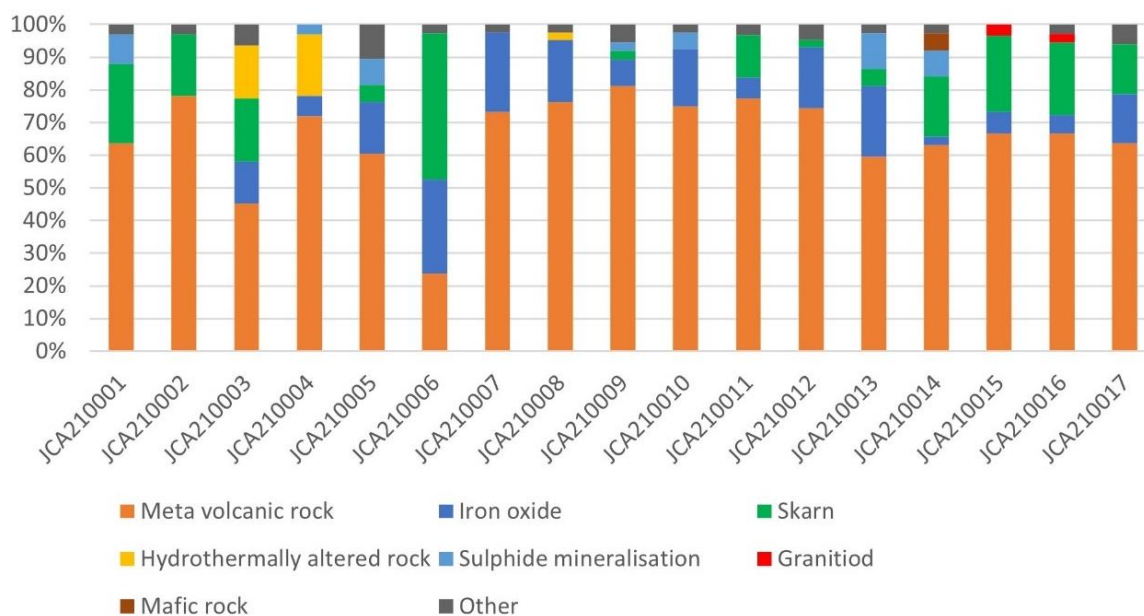


Figure 21. Distribution of rocks for each composite sample from Källfallsgruvan.

Results composite sampling

Geochemical analyses of composite samples show elevated values of Fe_2O_3 , Ga, Mo, Te, Y, and REE (Table 7). The REEs are dominated by LREE. The average concentration of REE in the waste rock is roughly half the average concentration observed for tailings at Källfallsgruvan. All samples show negative Eu anomalies (Fig. 22). It can be noted that one composite sample exhibits strong depletion in LREE compared to the rest of the samples.

Table 7. Selected geochemical data for waste rock composite samples from Källfallsgruvan (n = 17).

Element	Fe_2O_3 %	Ga ppm	Mo ppm	S %	Te ppm	Y ppm	LREE ppm	HREE ppm	REE ppm
Average	19.1	33	153	1.0	3.3	143	980	104	1,083
Min	6.6	22	18	0.0	0.1	63	261	42	302
Max	31.5	44	474	3.7	33.7	314	2,284	232	2,410
Median	19.6	3	120	0.9	0.9	130	793	10	892

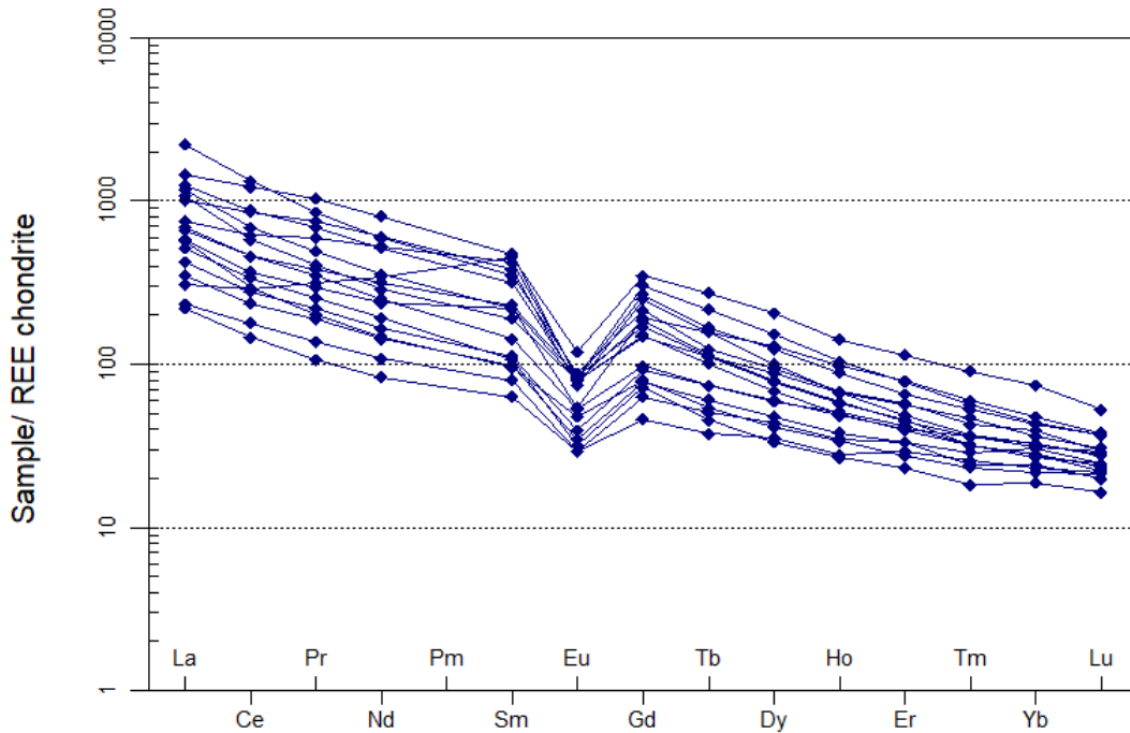


Figure 22. Chondrite normalised (Boyton, 1984) REE diagram for waste rock samples from Källfallsgruvan (n=17).

Results selective sampling

Two mineralized samples were collected from Källfallsgruvan for mineralogical and chemical characterization of the mineralisation types present in the waste pile, JCA210003C and JCA210015B.

JCA210003C is a fine-grained, foliated magnetite skarn, rich in quartz and amphiboles (mainly anthophyllite), with patches of massive magnetite and disseminated sulphides such as molybdenite and chalcopyrite (Fig. 23). SEM analyses identified the dominant REE-bearing minerals as monazite-(Ce) and xenotime-(Y). In JCA210003C, up to 200 μm sized grains of allanite-(Ce) are found together with quartz, magnetite and molybdenite, as well as minor grains of uranyl carbonate containing Y and HREE. Geochemical analysis of both samples shows total REE contents of ca. 450 ppm with notable LREE dominance. In JCA210003C, the Fe_2O_3 content is 63.4%, REE (462 ppm) and Mo (99 ppm) (Table 8).

JCA210015B can be characterised as an amphibole skarn, mainly composed of anthophyllite, biotite, and some magnetite (Fig. 24). Sulphides, such as chalcopyrite and pyrrhotite, are present in small quantities. In JCA210015B zircon is abundant, often enclosed in overgrowths of xenotime. This sample also contains a mixture of Y-, Nb-, and Ti-bearing minerals, whose chemical formulae mostly resemble fergusonite (YNbO_4) and euxinite (YTINbO_6). Geochemical analysis of sample JCA210015B show elevated concentrations of REE (448 ppm), Nb (17 ppm) and Zr (289 ppm) (Table 8).

For both samples, LREE is dominant and constitute ca. 93% of total REE (Table 8).

A chondrite-normalised plot (Fig. 25) of REE distribution shows a similar pattern as the waste rock samples except for a slight increase in the HREE for sample JCA210015B which may be related to the large amounts of xenotime (Y+HREE PO_4).

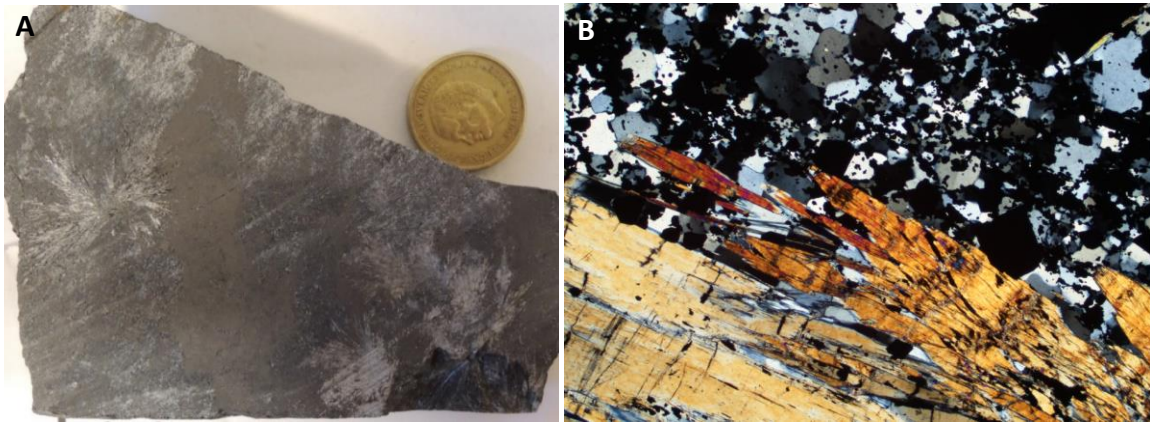


Figure 23. A. Sample JCA210003C magnetite in amphibole skarn. B. Thin section (XPL) with fine-grained, foliated magnetite skarn, rich in quartz and amphibole (anthophyllite), with patches of massive magnetite and disseminated sulphides such as molybdenite and chalcopyrite (opaques). Photos: Gunnar Rauséus.

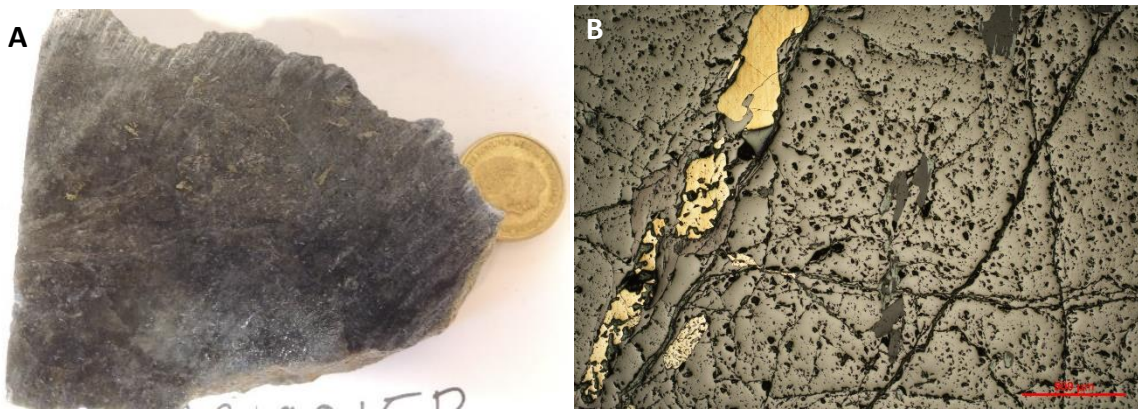


Figure 24. A. Sample JCA210015B consisting of amphibole skarn. B. Thin section (reflecting light) with abundant magnetite (grey) and chalcopyrite (yellow). Photos: Gunnar Rauséus.

Table 8. Selected geochemical data for selective samples from Källfallsgruvan.

	Fe ₂ O ₃ %	Mo ppm	Nb ppm	Zr ppm	Y ppm	LREE ppm	HREE ppm	REE ppm
JCA210003C	63.4	99	2	12	62	430	32	462
JCA210015B	15.0	2	17	289	38	419	29	448

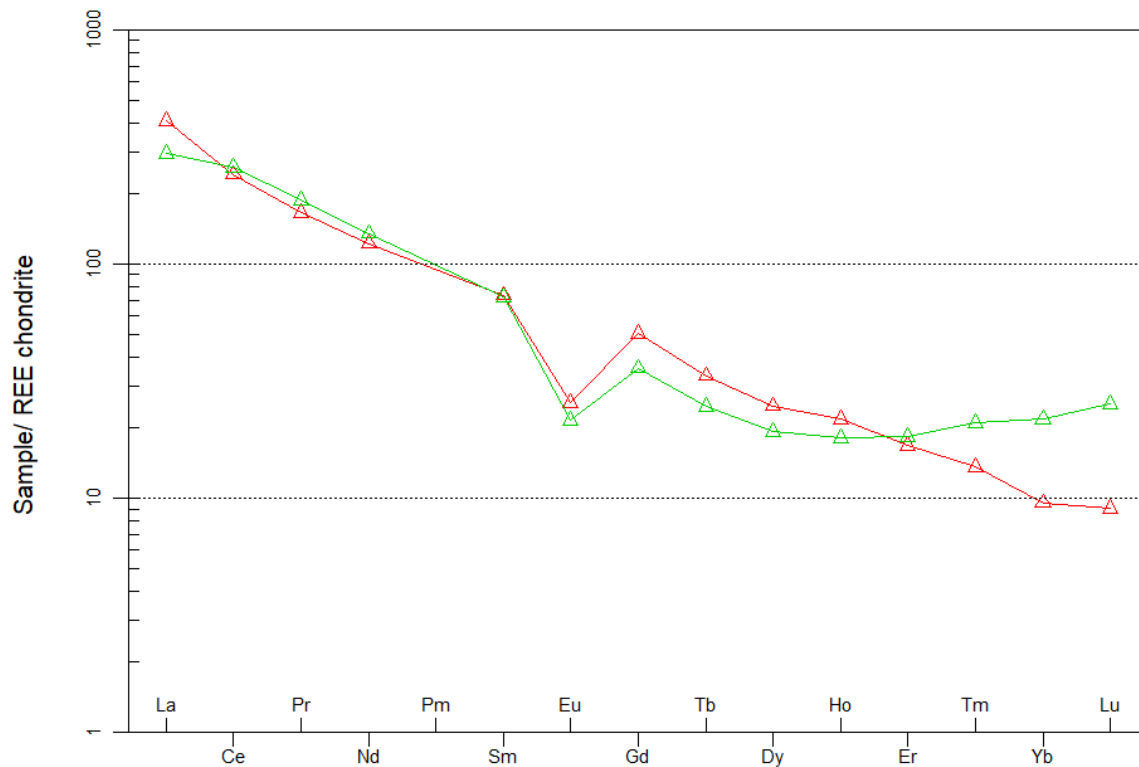


Figure 25. Chondrite normalised (Boyton, 1984) REE diagram for selective samples from Källfallsgruvan, JCA210003C (red) and JCA210015B (green).

Potential resources tailings and waste rock

Based on the depth model deduced from the geophysical data (Fig. 14), the estimated total volume of the tailings in Källfallsgruvan is approximately 553,000 m³. Using the average density of 1.7 ton/m³, a total tonnage of 0.94 Mt of tailings is calculated. This is less than half of the expected amount based on the processing data from Källfallsgruvan (SGU 2023) This indicates that a majority of the tailings may be deposited on the bottom of lake Lien, which is also indicated by analyses of lake sediments (SGI 2014, de Campos Pereira 2014).

Based on the chemical analyses, bulk density measurements, and the volume estimated by geophysical data, the potential resource in the tailings is estimated to 130,000 tonnes Fe, 310 tonnes of Mo, 320 tonnes of Cu and 2,560 tonnes of REE + Y.

The tonnage of waste rock is documented to be 0.93 Mt (SGU 2023). Assuming that no material has been removed (which LiDAR data indicates), potential resources are estimated at 124,240 tonnes of Fe, 1,140 tonnes of REE including Y and 140 tonnes of Mo.

Bäckegruvan

Historical background

The Bäckegruvan area is historically included in the Myrbacksfältet ore field (Tegengren 1924) and consists of several mines that have been mined since at least the 16th century, including both open-pit and underground mining. The magnetite mineralisation in Bäckegruvan mine is hosted by an even-grained potassium rich volcanic rock and ore quartzite where skarn-altered, locally baryte-bearing dolomitic layers occur (Ambros 1983).

In modern times, the iron and copper ores were processed in the Bäckegruvan dressing plant, which was in operation until 1982. Waste material from the plant was deposited in the vicinity of the nearby lake Skärsjön.

Between 1960 and 1963, the dressing plant was modified to improve the yield. This also enabled combined extraction of an Fe-concentrate with low sulphide content and a Cu-concentrate with approximately 25% Cu, 3 ppm Au and 50–60 ppm Ag (Bergquist 1985). The copper concentrate was transported and processed at Rönnskärsverket. Hereafter, the tailings from before 1963 are named “pre-1963” and tailings produced after 1963 “post-1963” due to the introduction of the new dressing plant. Between 1963 and 1967, the processing plant also received material from Persgruvan and Källfallsgruvan. The distribution of the material in the tailings pond over the years can be seen in old aerial photos. Prior to 1963, the material was discharged from the western side of the present-day extent of the tailings (Fig. 26A). After implementation of the new ore processing method in 1963, tailings were discharged from the northern side (Fig. 26B) and partly overlie the older material. Pre-1963 tailings are therefore found mainly in the southwestern parts of the area, whereas post-1963 tailings are found to the northeast.

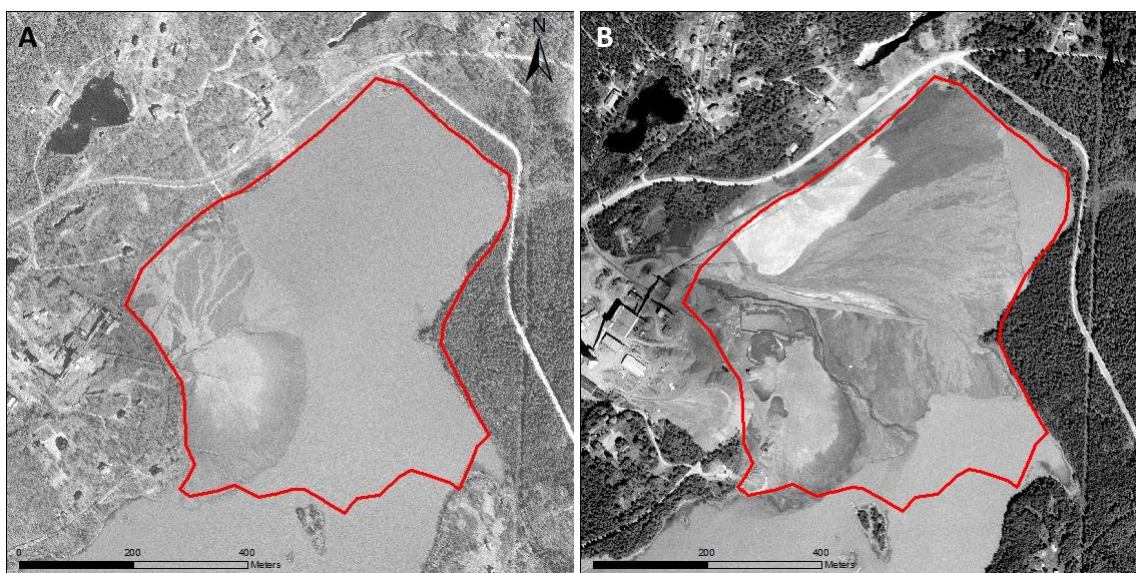


Figure 26. Aerial photos of the Bäckegruvan, red polygon represent present extension of tailings pond. **A.** Tailings deposit in 1960 with of entirely pre-1963 material. **B.** Tailings deposit 1975 with pre-1963 material in the southern part and post-1963 material in the northern part.

Tailings

The pre-1963 material is exposed in the southern part of the tailings pond at the border of lake Skärsjön and is stratigraphically underlying the post-1963 material, which is found in the topographically higher northern part. The pre-1963 material is mainly greyish black, dominated by silt and sand, and water saturated. The post-1963 material is sandier and drier as it overlies the groundwater surface. The northern area of the pond is covered with pine forest, while the southern area is mostly open terrain (Fig. 27).

The tailings ponds at Bäckegruvan have previously been sampled by Hallberg & Reginiussen (2020), which together with the 22 samples collected in this study makes a total of 65 surface samples, 33 samples of pre-1963 material and 32 samples of post-1963 material.

Two boreholes were drilled in the tailings ponds, one in the pre-1963 area and one in the post-1963 area (Fig. 28). Sampling for geochemical analysis was generally made every metre, however, sometimes in smaller sections due to sampling difficulties. The pre-1963 pond was drilled down to 13 metres depth (22 samples) and the post-1963 pond to 20.5 metres depth (27 samples). The second borehole unveiled a transition from post- to pre-1963 material at 15 metres depth from surface. The transition is also clearly seen in the geochemical data, in particular the cobalt content is considerably higher in the pre-1963 material.



Figure 27. Pre-1963 tailings in the older part of the Bäckegruvan tailings pond, with the processing plant in the background. Photo taken towards west. Photo: Gunnar Rauséus.

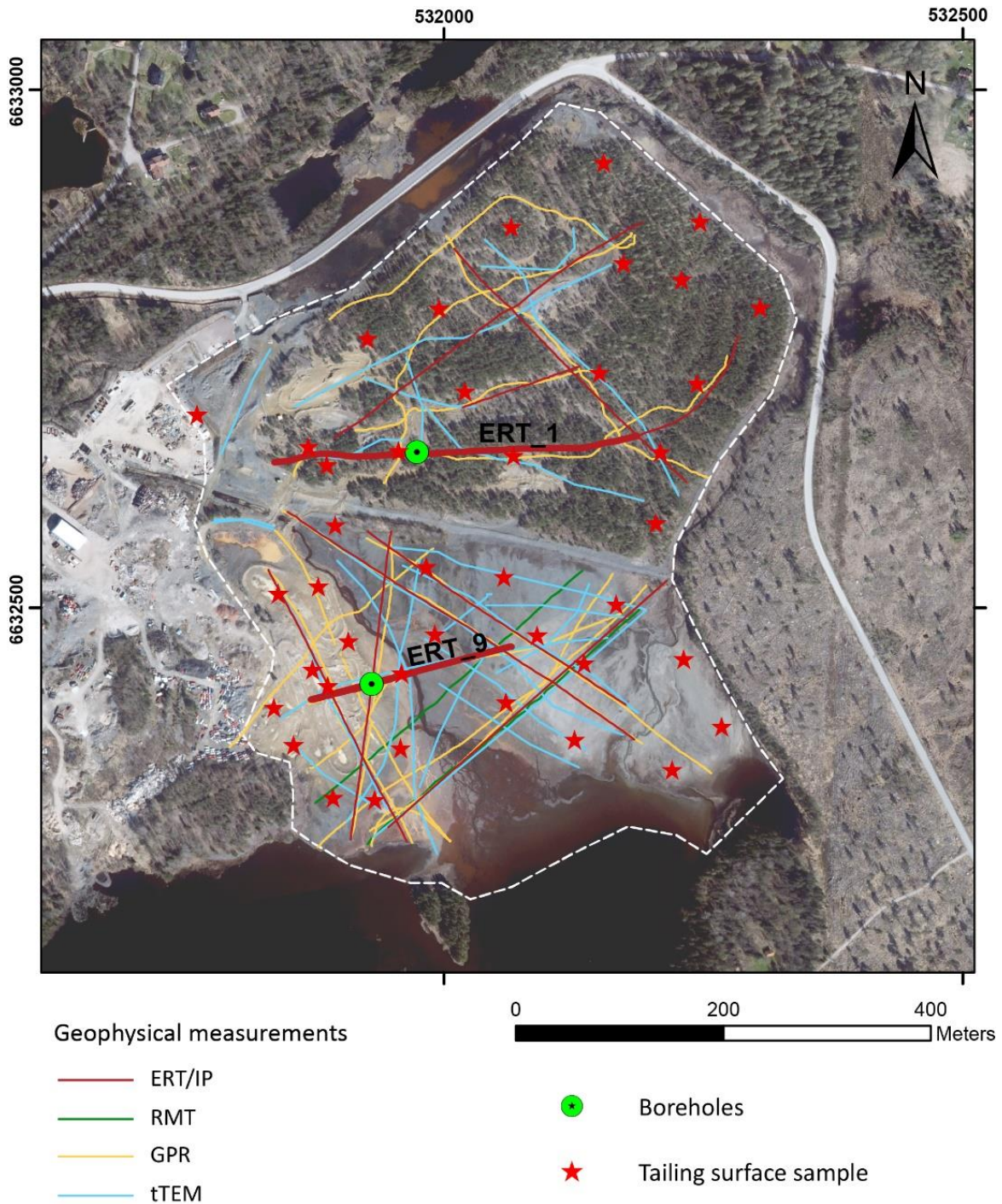


Figure 28. Orthophoto of the Bäckegruvan tailings dam. The dashed white lines mark the lateral extent of the tailings, with pre-1963 material in the south and post-1963 material in the north (overgrown by pine trees). The thicker dark red lines show the location of profiles ERT_1 and ERT_9 (Figs. 29 and 30).

Results from geophysical measurements

The location of where the geophysical data were acquired at Bäckegruvan is shown in Figure 28. The resistivity models from the ERT, RMT and tTEM were used to determine the thickness of the tailings. They generally show quite similar results, but ERT and RMT show both higher resolution and larger depth of investigation compared to tTEM. The tailings at Bäckegruvan show in some parts very low resistivity (<10 ohmm), especially in the old tailings area. The very

low resistivities results in poor IP and GPR data quality and very limited depth penetration. Therefore, the results from the IP and GPR measurements are not shown here but discussed in more details in Bastani et al. (in preparation).

The resistivity model along profile ERT1 (Figs. 28 and 29) shows high resistivities up to 1000 ohmm at the topmost layer, corresponding to dry sand. It is followed by a low resistivity layer corresponding to water-saturated sand and silt with resistivities around 20 to 40 ohmm. The tailings are underlain by lake sediments and bedrock with higher resistivities. The thickness of the tailings is largest in the western part of the profile (up to 25 m) and decreases towards the east. The drilling at 140 m distance along the profile shows 21 m tailings, which correlates well with the resistivity model (Fig. 29).

Profile ERT9 (Figs. 28 and 30A) was measured in the southern tailings pond, located on ca. 10 m lower elevation than to the northern pond and adjacent to the lake Nedre Skärsjön. Here the groundwater table is close to the ground surface and consequently the high resistive layer at the top corresponding to dry sand is absent. The resistivity of the tailings is very low in the western part of the profile (5–10 ohmm) and increases towards the east (40–50 ohmm). The interpreted thickness of the tailings varies between 11 and 17 m along the profile. The drilling at 60 m distance along the profile showed 15 m of tailings and this result correlates well with the interpretation from the resistivity model.

The resistivities modelled from tTEM measurements are comparable with the ERT model in the upper low resistivity layer, although some details are missing (Figs. 30A and 30B). At greater depth, the tTEM method does not resolve the high resistive bedrock. Despite the lower resolution it is still possible to delineate the bottom of the tailings in the resistivity model (Fig. 30B).

The tTEM data has a good coverage in the tailings pond. Figure 31 shows the interpolated resistivity calculated from the resistivity sections at elevation 170–175 m. This level corresponds to the wet tailings in both the northern and southern pond (see also Figs. 29 and 30). There is a clear resistivity contrast between the southwestern and northeastern areas. Comparison with the historical aerial photos from 1960 and 1975 (Fig. 26), shows the area of very low resistivities in the southwestern part corresponds to the location of pre-1963 deposition of tailings. Conversely, the higher resistivities in the northeastern part correspond to post-1963 deposition of tailings.

The bottom of the tailings has been interpreted along all profiles (ERT, RMT and tTEM) and then interpolated to a surface that covers both the northern and the southern tailings pond. Figure 32 shows the depth model of the tailings based on the resistivity models and the two drillings. The depth varies generally between 6 and 22 m with the largest depth found in the northern tailings pond.

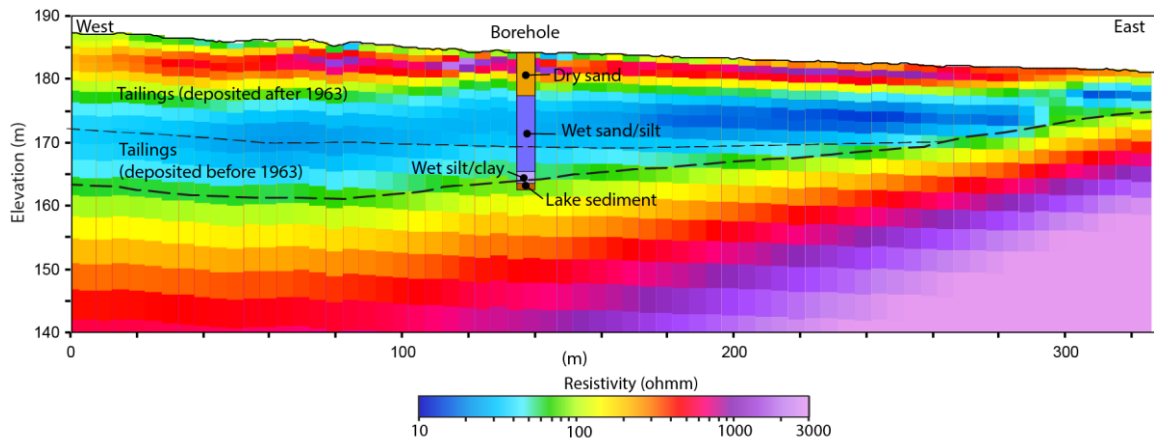


Figure 29. Profile ERT 1 located in the northern part of the tailings pond (Fig. 28). Resistivity model with interpretation and location of the borehole with simplified stratigraphical description. The thicker black dashed line represents the bottom of the tailings, and the thinner dotted line marks the interpreted boundary between younger material on top and older material at the bottom.

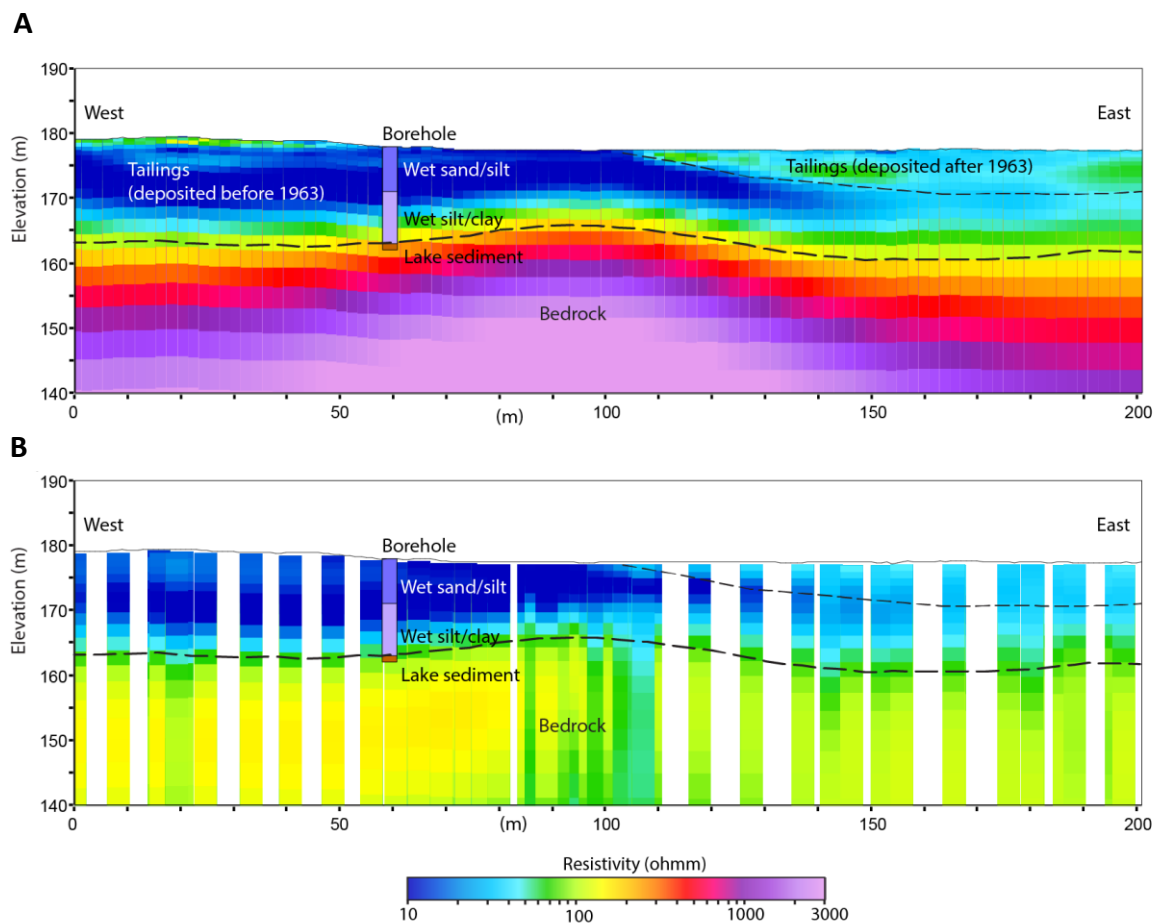


Figure 30. Resistivity models from **A.** ERT data and **B.** tTEM data along profile ERT 9 (Fig. 28). Interpretation and location of the borehole with simplified stratigraphical description. The thicker black dashed line represents the bottom of the tailings, and the thinner dotted line marks the interpreted boundary between younger material on top and older material at the bottom.

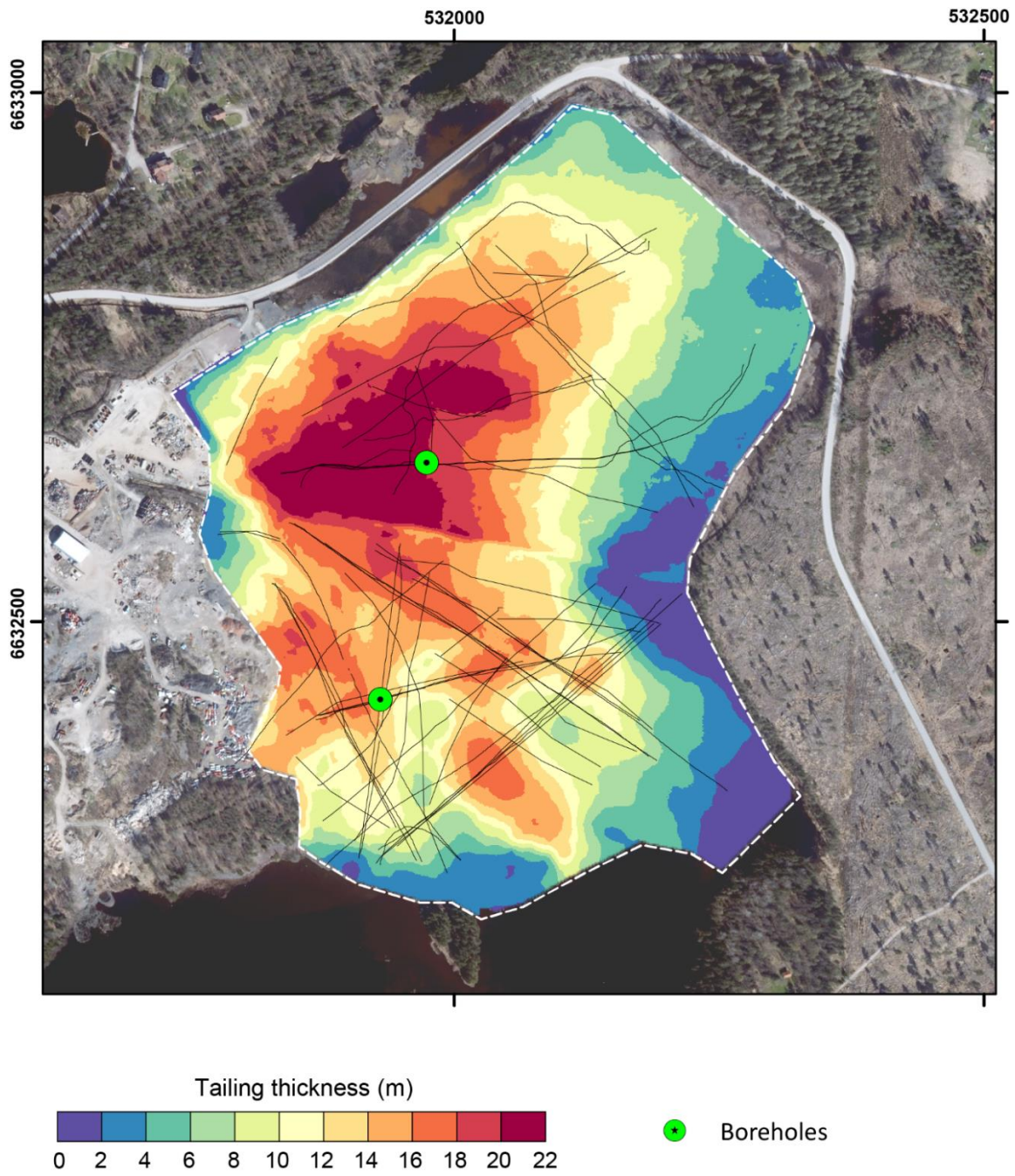


Figure 32. Modelled thickness of the tailings in Bäckegruvan based on geophysical measurements (thin black lines) and boreholes.

Results from chemical analyses of surface and drilling samples

The chemical analyses from the Bäckegruvan tailings consist of a total of 92 samples, 43 surface samples and 49 drilled samples. It was not possible to achieve meter section samples in all parts of the boreholes. For this sections samples have been weighted to represent one-meter sections. The samples have been divided according to whether they belong to the pre- or post-1963 material; 53 samples are included in the pre-1963 material and 39 samples are included in the post-1963 material.

The tailings show elevated values for Fe₂O₃, Ba, Bi, Co, Cu, W, and REE (Tables 9 and 10). The REE contents range from 276 to 2,719 ppm with an average of 1,063 ppm and is dominated by Ce, La and Nd which together constitute more than 90% of the average total REE content.

The highest REE concentrations are found in the pre-1963 material in the southwestern part of the area (Fig. 36). In general, the average contents of selected elements are higher in the tailings discharged before 1963 compared to the younger material (Tables 9 and 10). The difference in grades between the two areas is probably due to the improvement made in the processing plant in 1963. The only exception is Ba, which is found in higher concentrations in the post-1963 material, possibly indicating that the improved processing during resulted in relative enrichment of Ba in the tailings.

Figure 34 shows the chondrite normalised plot (Boynnton 1984), for the tailings samples, which mostly display a negative Eu anomaly for both the pre- and post-1963 material, but in the pre-1963 material some Eu anomalies are slightly positive or absent. There is a weak positive correlation between iron oxide content and REE for the tailings (Fig. 33).

Table 9. Selected geochemical data for tailings pre-1963. Including surface samples (n=23) and drillcore samples (n=30).

Element	Fe ₂ O ₃ %	Ba ppm	Bi ppm	Co ppm	Cu ppm	W ppm	Zr ppm	LREE ppm	HREE ppm	REE ppm
Average	21.3	5,036	100	610	1,571	87	133	1,394	85	1,479
Min	10.9	1,455	17	46	326	18	97	492	45	537
Max	37.4	11,173	268	1,720	7,450	302	190	2,586	134	2,719

Table 10. Selected geochemical data for tailings post-1963. Including surface samples (n=20) and drillcore samples (n=19).

Element	Fe ₂ O ₃ %	Ba ppm	Bi ppm	Co ppm	Cu ppm	W ppm	Zr ppm	LREE ppm	HREE ppm	REE ppm
Average	15.7	7,656	21	116	922	28	107	597	52	648
Min	11.5	4,640	7	31	454	8	78	247	29	276
Max	26.5	10,270	64	260	2,230	52	138	1,161	97	1,257

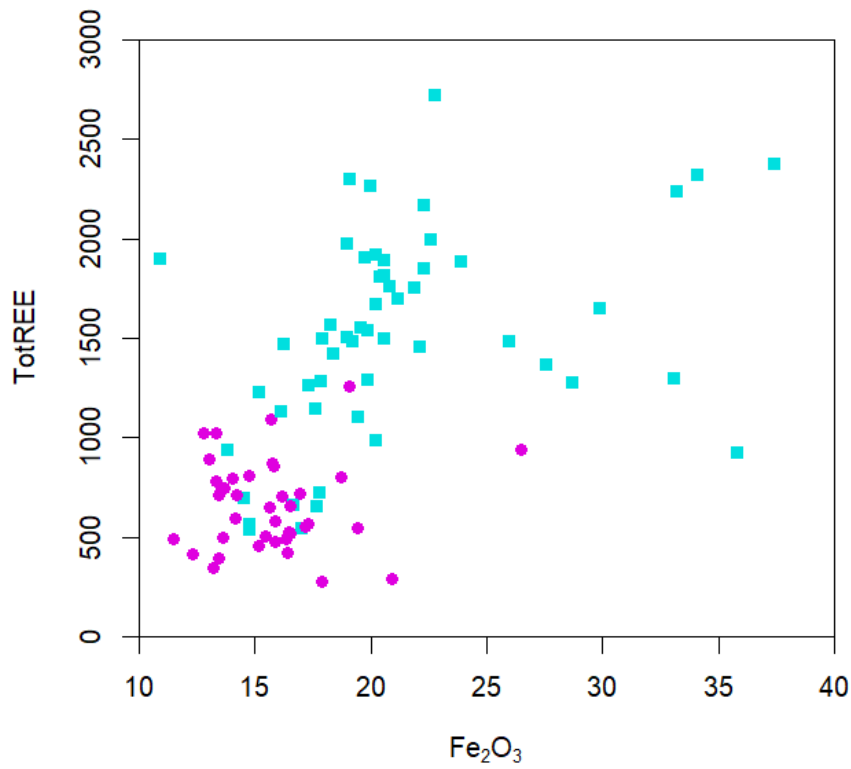


Figure 33. Ratio between REE vs Fe_2O_3 (n=92). Light blue squares represent samples from the pre-1963 tailings, purple dots represent post-1963 samples.

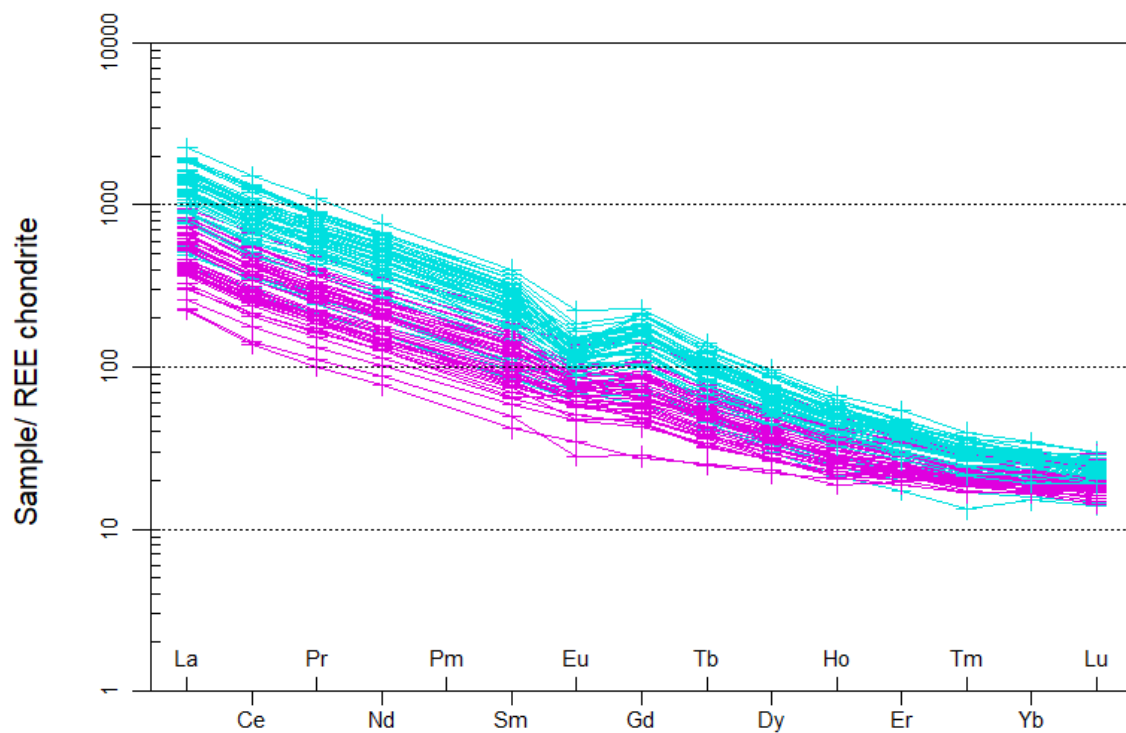


Figure 34. Chondrite normalised (Boynnton 1984) REE diagram for all samples in the Bäckegruvan tailings pond (n=92). Light blue line represents pre-1963 samples. Purple line represents post-1963 samples.

Bulk Density

Bulk density was measured for a total of 71 samples, 22 surface and 49 drilled. The average density for all samples is 1.6 tonnes/m³. There are no significant differences in average bulk density between the two material types though the average concentration for iron oxide is slightly higher in the pre-1963 tailings. There is no significant correlation seen between density and iron content, except for a slight positive trend for pre-1963 samples. (Fig. 35).

Potential resource tailings

Based on the modelled thickness (Fig. 32) from the geophysical survey, the total volume of the tailings in Bäckegruvan is estimated to 3,300,000 m³. Using the average density of 1.6 ton/m³, the mass of the tailings is calculated at 5.3 Mt (table 11) which is close to the historical production data of 5.44 Mt (Hallberg & Reginiussen 2020).

Models were made to differentiate pre-1963 from post-1963 tailings (Fig. 36). The older tailings are mainly deposited in the southern pond, but the aerial photo from 1960 shows that older material is also deposited on the northern side (Fig. 26A). Likewise, the aerial photo from 1975 shows that younger material can be found in the southern pond (Fig. 26B).

Modelled volumes of the two generations of tailings are 1,350,000 m³ and 1,950,000 m³ for the pre-1963 and post-1963 materials, respectively. Using the same average density of 1.6 ton/m³ yields a total weight of 2.2 Mt for the pre-1963 tailings and 3.1 Mt for the post-1963 tailings which is also in agreement with the historical production data (Table 11). The potential resource is based on the estimated tonnage for each type of tailings and using the average concentrations for elements of interest. Grades and tonnage are compiled in Table 11.

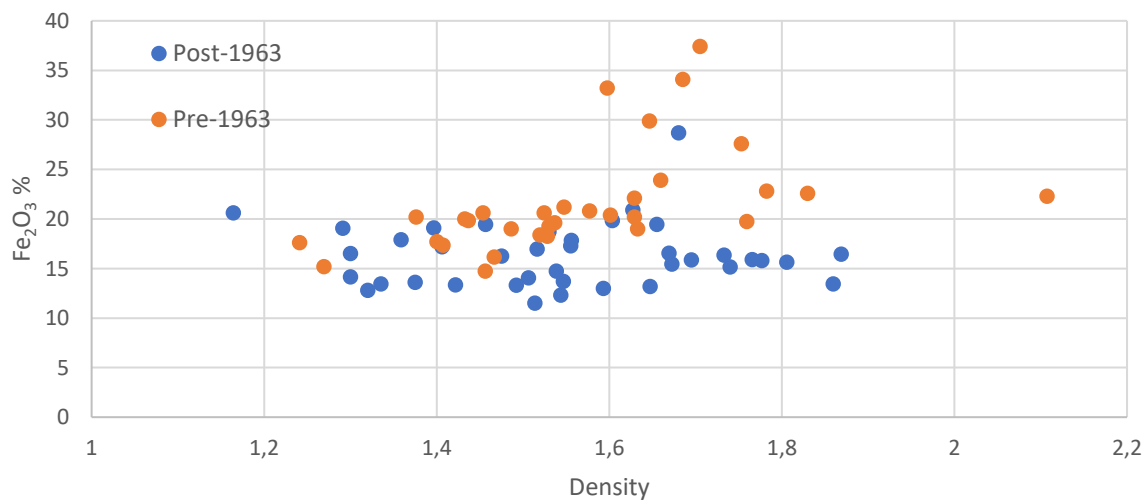


Figure 35. Bulk density versus iron oxide grade for the Bäckegruvan tailings pond materials (n=71).

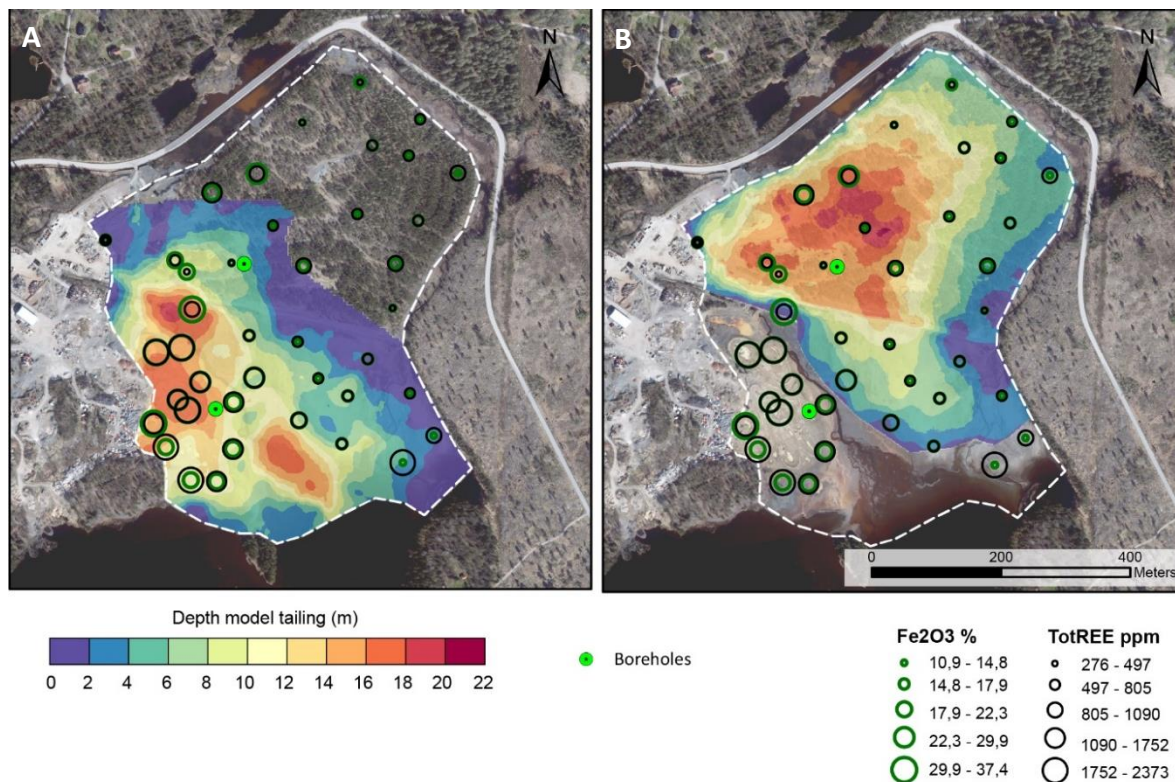


Figure 36. Modelled thickness of the tailings at Bäckegruvan based on geophysical measurements and boreholes. **A.** Material deposited before 1963. **B.** Material deposited after 1963. Graded symbols show levels of Fe₂O₃ and REE from surface samples.

Table 11. Potential resource and average grades for elements of economic interest in the Bäckegruvan tailings.

		Fe %	Ba ppm	Cu ppm	Co ppm	Mo ppm	REE+Y ppm
Pre-1963 tailings	grades	15	5,035	1,571	610	64	1,581
2.2 Mt	tonnes	330,000	11,000	3,500	1,300	140	3,500
Post-1963 tailings	grades	11	7,655	922	116	35	719
3.1 Mt	tonnes	338,000	23,700	2,900	350	110	2,200
Total tailings	grades	13	6,568	1,191	321	47	1,077
5.3 Mt	tonnes	668,000	34,700	6,400	1,650	250	5,700

Waste rock

The sampled waste rock areas are located to the northeast of the Bäckegruvan processing plant. Waste rock was sampled from an approximately 400 metres long waste dump along the side of two water filled pits, Östergruvan–Jacobsgruvan and Haggruvan (Fig. 37). For each area, 15 composite samples were collected. Based on interpretation of orthophotos, the size of the sampling areas is estimated to ca. 8,300 m² and 5,900 m², respectively. The depth of the waste rock dumps is unknown, but locally it exceeds several metres (Fig. 38).

The waste rock material varies in size between 5 and 30 cm and is to a large extent oxidised, showing a red surface colour. The sampled material is dominated by fine-grained magnetite-rich rock and metavolcanic rock. Distribution of rocks are presented in Figure 39. Sulphides, such as chalcopyrite, pyrite and pyrrhotite, were observed within the sampled waste rock. Locally, malachite and baryte were also observed.

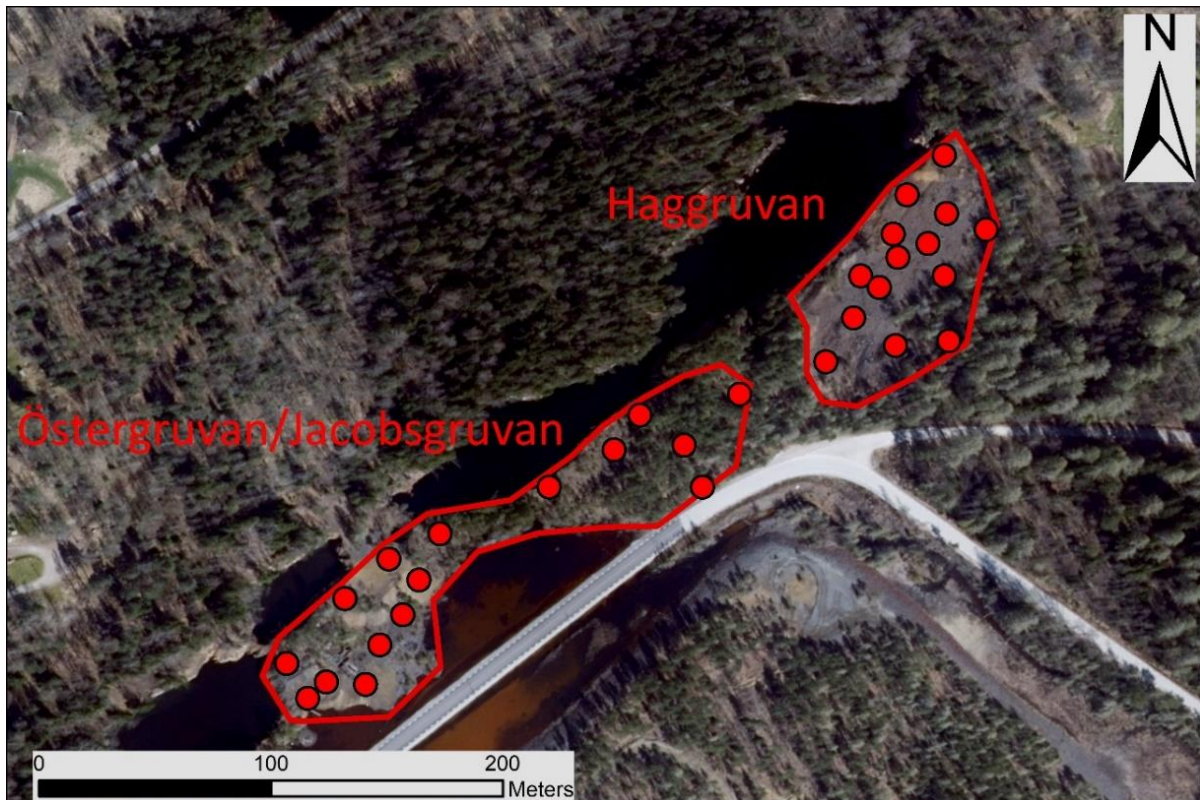


Figure 37. Orthophoto showing areas (red polygon) for sampled waste rock at Östergruvan–Jacobsgruvan (n = 15) and Haggruvan (n = 15). Red dots mark the locations for composite samples.

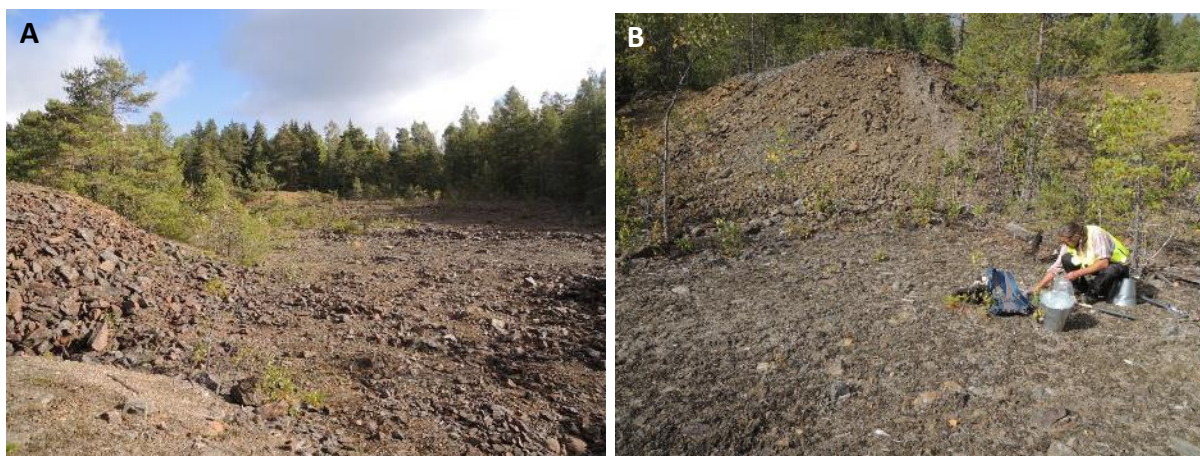


Figure 38. Photos of sampled waste rock area at Haggruvan. Photos: Gunnar Rauséus.

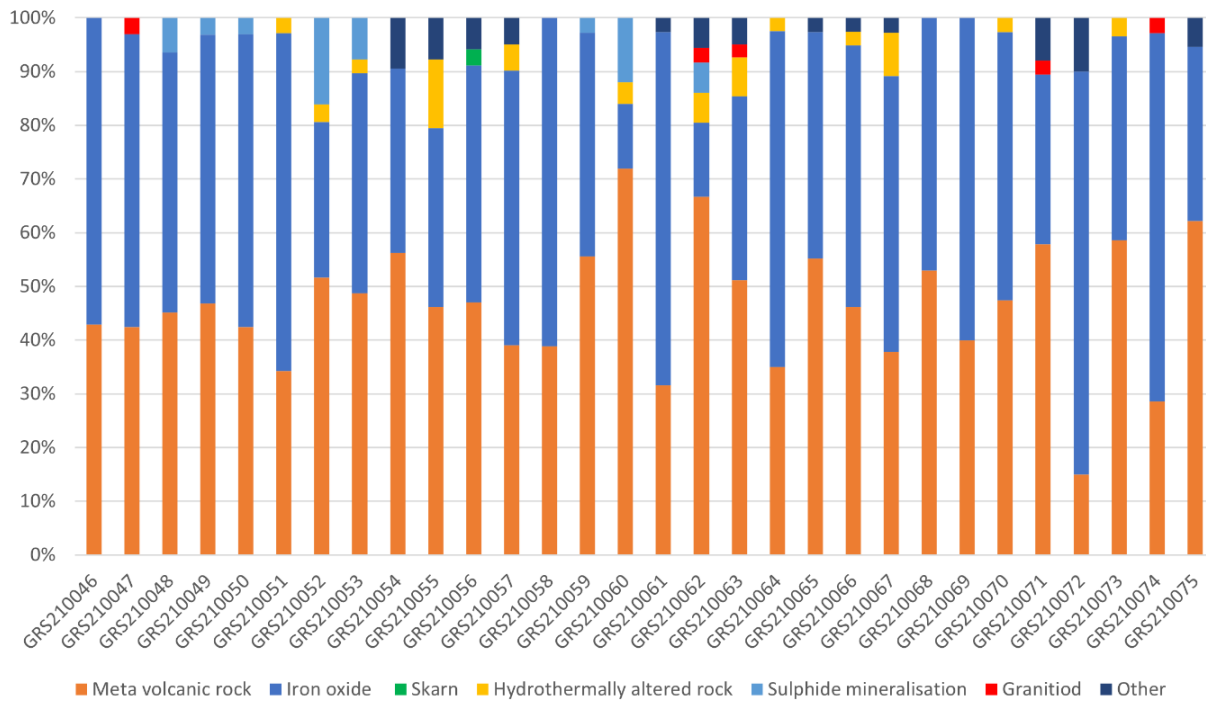


Figure 39. Distribution of rocks in composite samples. Samples GRS210046–60 were collected at Östergruvan–Jacobsgruvan, and samples GRS210061–75 at Haggruvan.

Results composite sampling

Sampling and analysing of waste rock in the Östergruvan–Jacobsgruvan and Haggruvan areas show elevated levels of Fe_2O_3 , Ba, Co, Cu and REE (Tables 12 and 13). The average concentration for Fe_2O_3 exceeds 30% and for copper ca. 0.4–0.5% in both areas. The REEs are dominantly represented by Ce, La, and Nd. LREE constitutes ca. 95% of the total REE in both areas. The sampled material from both mines has elevated content of S, but the Östergruvan–Jacobsgruvan differs from Haggruvan with higher grades of arsenic up to 723 ppm. Östergruvan–Jacobsgruvan shows higher concentrations of Co, Ba, and REE than Haggruvan. In the chondrite normalised REE diagram (Fig. 40) it is shown that the composite samples display both positive and negative Eu anomalies for the Östergruvan–Jacobsgruvan samples and only rather smooth or negative Eu anomalies for the Haggruvan samples.

Table 12. Selected geochemical data for waste rock composite samples from Östergruvan–Jacobsgruvan (n=15).

Element	Fe_2O_3 %	As ppm	Ba ppm	Bi ppm	Co ppm	Cu ppm	S ppm	LREE ppm	HREE ppm	REE ppm
Average	37.2	139	2,690	138	427	4,471	1.5	950	42	992
Min	23.1	6	935	26	123	1,560	0.6	371	25	396
Max	53.7	723	7,670	414	922	7,100	3.1	2,152	69	2,221
Median	39.0	67	2,030	87	425	4,520	1.4	637	40	673

Table 13. Selected geochemical data for waste rock composite samples from Haggruvan (n=15).

Element	Fe ₂ O ₃ %	Ba ppm	Bi ppm	Co ppm	Cu ppm	S ppm	LREE ppm	HREE ppm	REE ppm
Average	33.5	1,090	71	146	4,939	0.9	434	28	462
Min	14.9	468	8	51	788	0.1	145	16	161
Max	50.1	3,870	185	244	9,660	1.9	657	40	692
Median	31.9	877	71	159	5,500	1.0	443	27	471

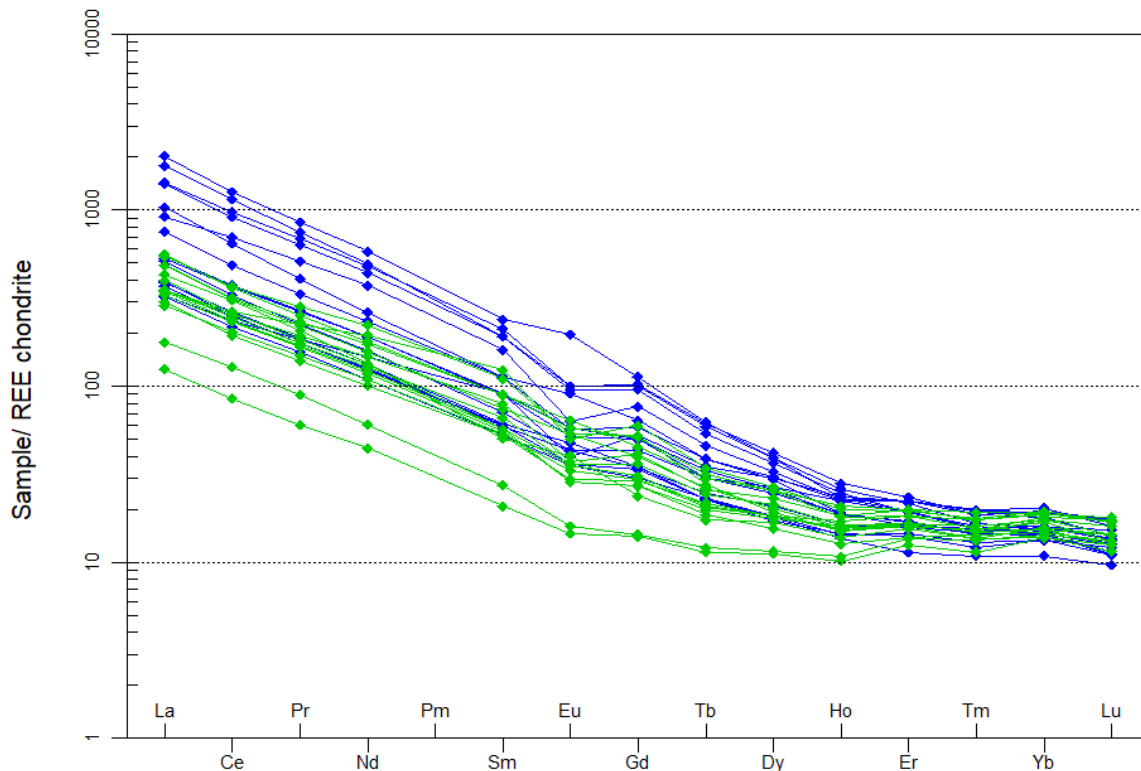


Figure 40. Chondrite normalised (Boynnton 1984) REE diagram from Östergruvan–Jacobsgruvan (blue) and Haggruvan (green) (n = 30).

Results selective sampling

Three richly mineralized samples were selectively collected from Haggruvan and Östergruvan–Jacobsgruvan for mineralogical and chemical characterization of the mineralisation types present in the waste piles, GRS210053B, GRS 210069B, and GRS210070B.

GRS210053B was sampled at Östergruvan–Jacobsgruvan and is described as a quartz banded metavolcanic rock with additional bands of tremolite skarn and an abundant magnetite dissemination and some sulphides (Figs. 41A and B). SEM analyses identify Ba-rich feldspar as the predominant Ba-bearing mineral. This sample shows high concentrations of Fe₂O₃, and Ba. (Table 14).

GRS210069B is rich in fine-grained magnetite dissemination in a groundmass of quartz and biotite (Fig. 41C). Sulphide mineralisation such as chalcopyrite, pyrite is identified in thin section (Fig. 41D). SEM analysis confirms several REE-bearing minerals adjacent to magnetite and chalcopyrite and vary in size from 5 to 100 microns. Two types of REE-bearing minerals are found. REE-fluorocarbonates such as parisite and bastnäsité dominated by Ce, and phosphates such as monazite-(Ce). Minor grains of the Co-mineral linnaeite is identified in thin section and are typically associated with chalcopyrite. Geochemical analyses show high concentrations of Fe₂O₃ and elevated grades of REE in this sample (Table 14).

GRS210070B represent the magnetite mineralisation and is rich in sulphide minerals, dominantly chalcopyrite, covellite, pyrite and Co-bearing minerals (Figs. 41E and F). The Co mineral was identified as euhedral linnaeite in thin section, typically associated with chalcopyrite and pyrite, and confirmed with SEM-SED analyses.

Small grains (<10 µm) of native gold within grains of magnetite and in contact with chalcopyrite were identified using SEM-EDS, as well as small quantities of scheelite and fluorite and minor grains with Bi-Te-bearing sulphides. In addition, fergusonite (YNbO₄) occurs as inclusions within chalcopyrite. Some small grains with REE-bearing minerals such as fluorocarbonates rich in Ce, La, Nd and gadolinite-(Ce) are confirmed with SEM-EDS. Elevated element concentrations include Cu, Co, Fe₂O₃, REE, as well as anomalous levels of Au (Table 14).

Figure 42 shows the chondrite normalised REE diagram for the selective samples. In two of the samples there is a positive anomaly concerning Eu, GRS210053B and GRS210069B, and for the third sample, GRS210070B, there is a weak negative Eu anomaly. It can be noted that the sample with the highest positive Eu anomaly is a banded metavolcanic rock with alternating bands of quartz and tremolite skarn.

Table 14. Selected geochemical data for selective samples from Bäckegruvan.

Element	Fe ₂ O ₃ %	Au ppm	Ba ppm	Co ppm	Cu ppm	Sr ppm	Y ppm	LREE ppm	HREE ppm	REE ppm
GRS210053B	57.4	0.02	6,930	12	358	16,6	18	59	14	73
GRS210069B	71.4	0.01	480	161	441	1,6	34	610	28	638
GRS210070B	83.2	1.17	416	845	13,300	0,5	6	117	6	123

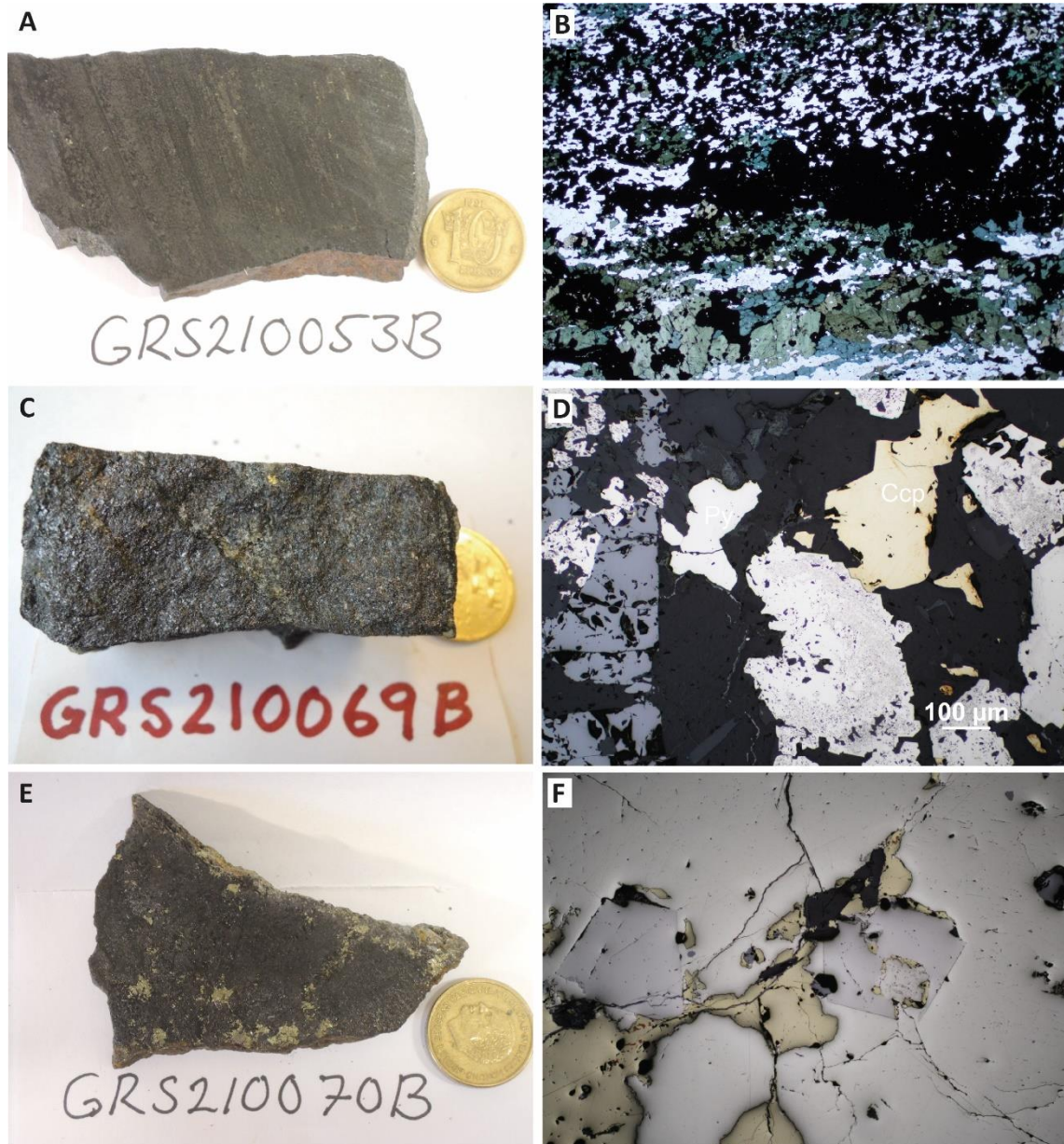


Figure 41. Photos and microphotos from selective samples. **A.** Sample GRS210053B with quartz banded metavolcanic rock with bands of tremolite skarn and abundant magnetite impregnation. **B.** Thin section of GRS210053B: banded quartz (light transparent), tremolite (greenish blue) with abundant magnetite dissemination (opaque). **C.** Sample GRS210069B with magnetite mineralisation. **D.** Thin section of GRS210069B with magnetite (grey), chalcopyrite (light yellow) and pyrite (white). **E.** Sample GRS210070B magnetite mineralisation rich in chalcopyrite. **F.** Thin section of GRS210070B with chalcopyrite (light yellow), pyrite (white) and euhedral linneaite (slightly blueish). Photos: Gunnar Rauséus.

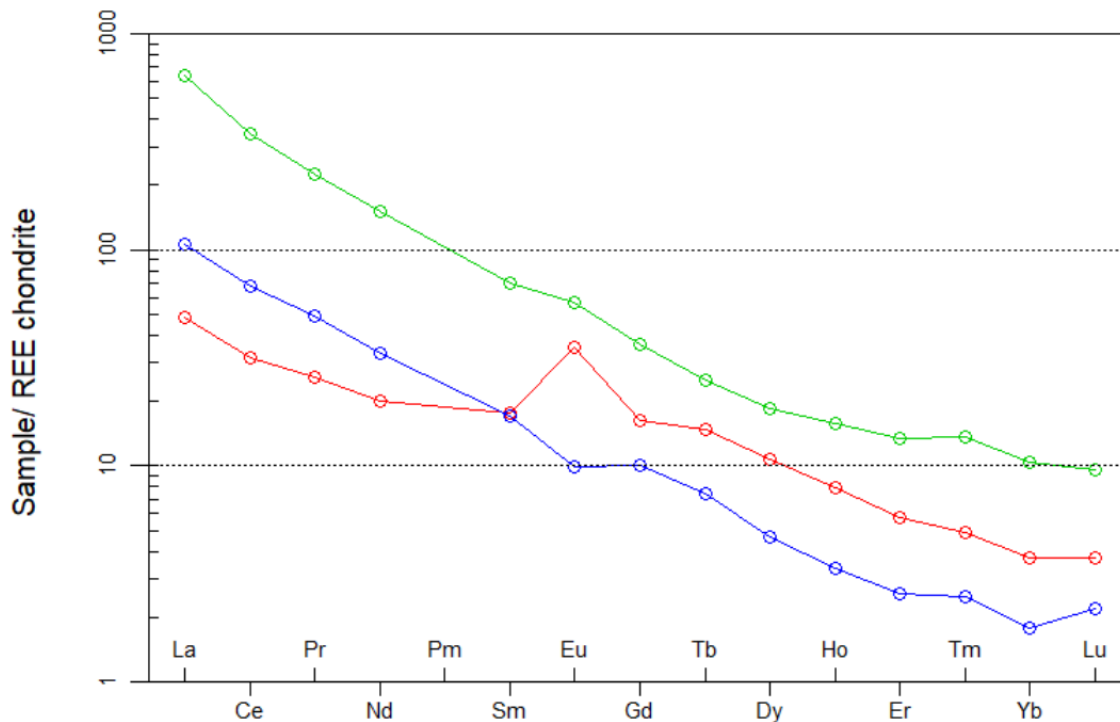


Figure 42. Chondrite normalised (Boynnton 1984) REE diagram from the three whole rock samples from Haggruvan GRS210069B (green) and GRS210070B (blue) and GRS210053B (red) from the Östergruvan–Jacobsgruvan.

Potential resource waste rock

Documentation from mine operators (Bergquist 1985) indicates that a total of 4.5 Mt of waste rock was produced (not including tailings) in the Riddarhytte ore field. The sampled area is about 1,400 square metres but constitutes only a minor part of the total amount of waste rock found in the area around Bäckegruvan. Therefore it is not possible to estimate a potential resource for the sampled waste rock pile.

Persgruvan

Historical background

Persgruvan is situated on the east shore of lake Övre Skärsjön, around 3.5 kilometres north of Källfallsgruvan (Fig. 4). Mining started in 1903 and was in operation until 1967. From 1943, the raw ore was transported by cableway to Källfallsgruvan and processed. When the processing plant in Källfallsgruvan was closed in 1963, the ore was transported to Bäckegruvan for processing. A total amount of 0.56 Mt waste rock is documented as produced and deposited in the Persgruvan area (SGU 2023). The remaining unmined resource is estimated to 2.76 Mt of ore with a grade of 37.2% Fe (Bergquist 1985).

Waste rock

In the mining area, a waterfilled open pit occurs along with a mineshaft. The sampled area extends from the lake to the southern part of the open pit situated north of the lake. The waste rock material is generally well-exposed and only sparsely overgrown by small pine trees (Fig. 43).

Along the shore, the waste rock material is 5 to 20 cm in size, showing abundant oxidized surfaces and includes magnetite-rich material with minor chalcopyrite, bornite, and pyrite. A few

metres inland, this material is overlain by coarser waste rock dominated by a light grey, felsic, fine-grained metavolcanic rock. The volcanic rock is rich in mica, poor in iron oxide minerals, and partially Mg-altered with anthophyllite and cordierite. The different appearance between the two types of waste rock material is shown in Figure 44. Distribution of the rocks in the sampled material is compiled in Figure 45.



Figure 43. Orthophoto of sampled area at Persgruvan (red polygon). Red dots show location of samples.



Figure 44. Photo of waste rock piles at Persgruvan, facing away from the shore of lake Övre Skärsjön. Oxidised waste rock material is exposed adjacent to the shore (lower part of photo). The oxidised material is overlain by coarser, grey-coloured waste rock material (upper part of photo). Photo: Gunnar Rauséus.

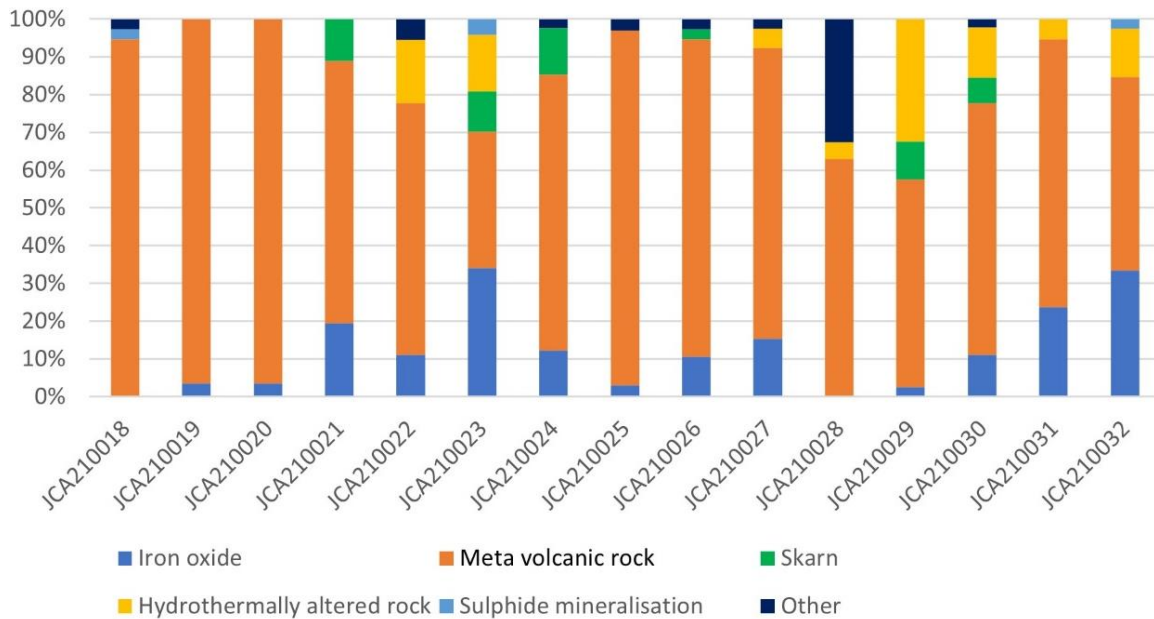


Figure 45. Distribution of rocks in composite samples from Persgruvan.

Results composite sampling

Composite samples show elevated concentrations of Fe₂O₃, Bi, Cu, Y, and REE, (Table 15). LREE is dominant and constitute 89% of the total REE. All of the composite samples from Persgruvan show a negative Eu anomaly. A few samples show a more even distribution of the LREE, La to Sm, than the majority, which could imply that two different mineralisation types for REE minerals are present (Fig. 46).

Those parts of the waste rock pile material which represent oxidised magnetite mineralisation (along the lake) show higher grades of Fe₂O₃, REE, and Cu than the material rich in metavolcanic rock. This difference in the waste rock material may be explained by that after closure of the Persgruvan processing plant in 1963, the crude ore was instead transported to the processing plant at Källfallsgruvan. Most of the waste rock material deposited at Persgruvan after 1963 is therefore poorly mineralised or entirely barren country rock likely derived from tunnelling in the mine.

Table 15. Selected geochemical data for waste rock composite samples from Persgruvan. (n = 15).

Element	Fe ₂ O ₃ %	Bi ppm	Cu ppm	Y ppm	LREE ppm	HREE ppm	REE ppm
Average	17.5	17	749	120	668	84	751
Min	3.1	-	1	40	161	31	212
Max	36.7	163	3,910	554	2,413	328	2,741
Median	16.7	5	92	59	337	50	375

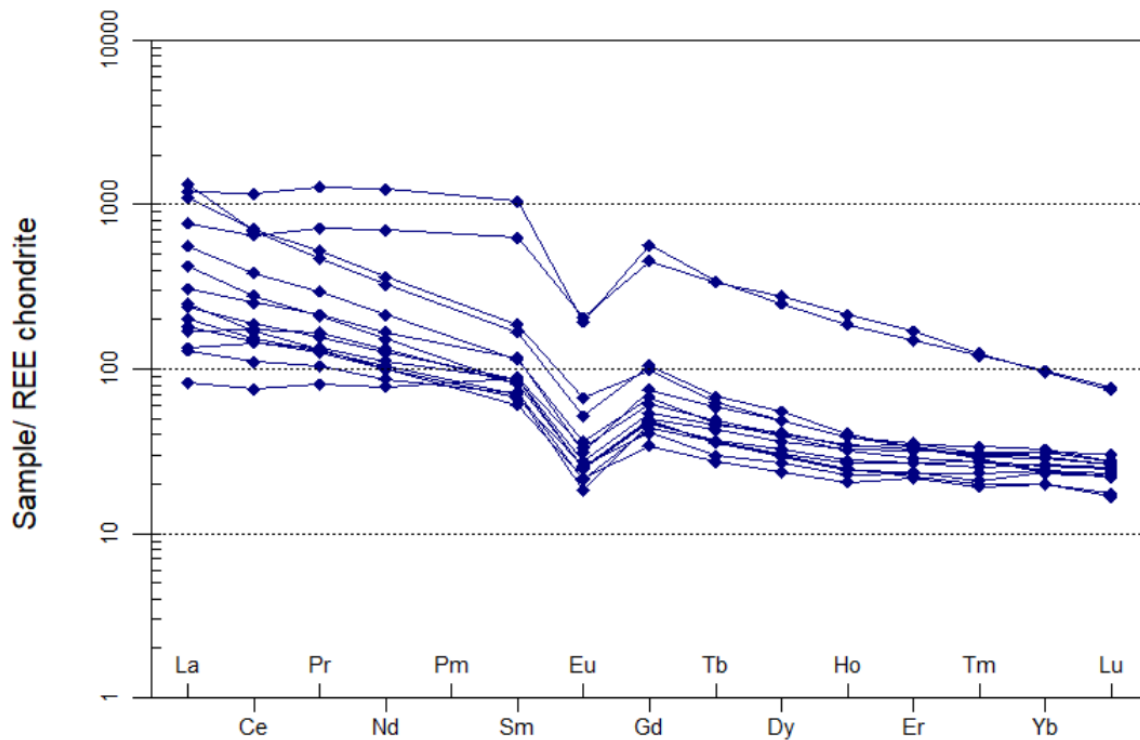


Figure 46. Chondrite normalised (Boynnton 1984) REE diagram from the composite samples from Persgruvan. Note that the two samples with even distribution of La-Sm (LREE) also are enriched in HREE compared to the other composite samples (n = 15).

Results selective sampling

Two mineralised samples were selectively collected for mineralogical and chemical characterisation of the mineralisations present in the waste piles, JCA210021B and JCA210029B.

JCA210021B consists of massive fine-grained magnetite mineralisation with sparse amphibole and quartz (Fig. 47A). Using SEM-EDS, REE-bearing minerals were shown to be allanite-(Ce), which occurs as up to 250 µm sized crystals intergrown with magnetite and parisite-(Ce). Additionally, minor grains of LREE-bearing monazite were identified by SEM-EDS. Geochemical analysis show high Fe₂O₃ content and elevated REE, dominated by LREEs (Table 16).

JCA210029B is dominated by radiant amphibole, biotite and phlogopite with fine-grained disseminated magnetite (Fig. 47B). In thin section, small grains identified as allanite occur as small inclusions within the biotite. Geochemical analyses show elevated concentration of Fe₂O₃, REE and Rb (276 ppm) (Table 16).

Figure 48 shows the chondrite normalised plot for the two selective samples. Both samples exhibit negative Eu anomalies.

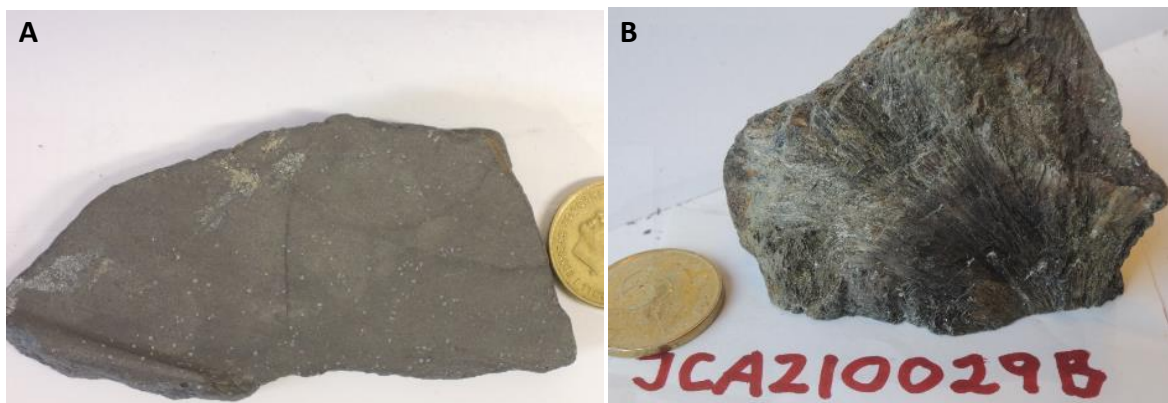


Figure 47. A. Sample JCA210021B with massive fine-grained magnetite mineralisation. B. Sample JCA210029B with radiant amphibole. Photos: Gunnar Rauséus.

Table 16. Selected geochemical data for selective samples from Persgruvan.

Sample	Fe ₂ O ₃ %	Rb ppm	Y ppm	LREE ppm	HREE ppm	REE ppm
JCA210021B	97	1	26	507	22	529
JCA210029B	39	276	62	546	40	586

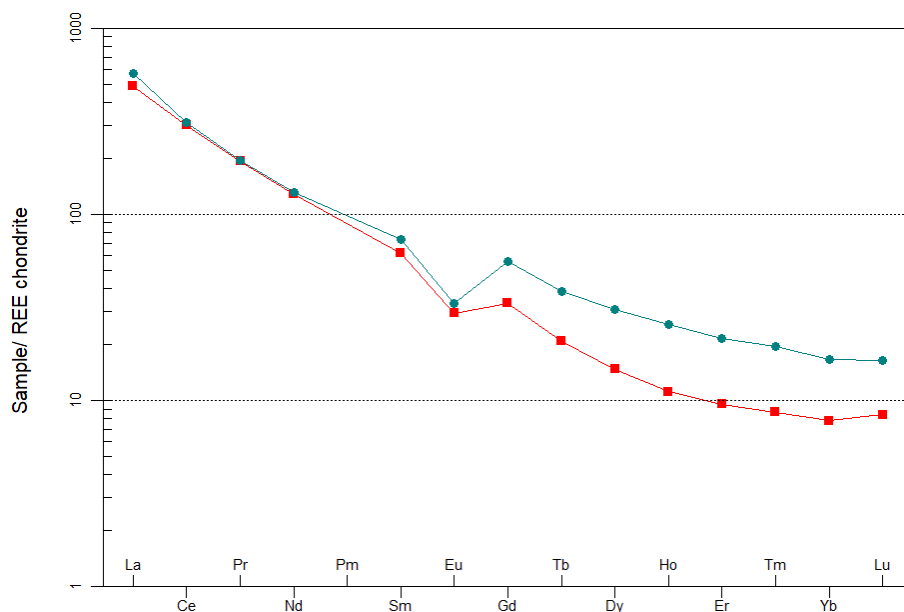


Figure 48. Chondrite normalised (Boynnton 1984) REE diagram from the two whole rock samples from Persgruvan. JCA210021B (red), JCA210029B (green).

Potential resource

The potential resource is estimated on the historical tonnage for waste rock of 0.56 Mt at Persgruvan, and assuming that no material has been removed. Using the average concentrations for elements with elevated gives a potential resource of 68,500 tonnes of Fe, 490 tonnes of REE including Y, 420 tonnes of Cu and 10 tonnes of Bi to remain within the waste rock.

Nya Bastnäs

Historical background

Nya Bastnäs is located about 2 km northwest of Bäckegruvan mine (Fig. 4). The Bastnäs area is one of the most mineral rich areas in the world. The area has been mined for iron oxides and copper but is most famous for the discovery of the element cerium (Ce), discovered in samples from the mines in 1803 by Jöns Jacob Berzelius and Wilhelm Hisinger. Between 1875 and 1888, the so called Ceritgruvan yielded around 4,500 tons of cerite ore. The Nya Bastnäs area is type locality for numerous minerals, including bastnäsite-(Ce), cerite-(CeCa), lanthanite-(Ce), törnebohmite-(Ce), and linnaeite, as well as the discovery of the rare earth elements Ce and La.

Waste rock

Waste rock at Nya Bastnäs originates from several mines: Ceritgruvan (Ce), Göransgruvan (Cu) and Bastnäsfältet (Fe). The material within the waste rock piles is spread over approximately 6,000 m² and is highly variable in its character. The piles are locally reworked. The size of the waste rock material varies from a few centimetres to several decimetres. Partially the material shows a red oxidized surface (Fig. 49A). It is dominated by iron oxide mineralised rock, predominantly magnetite but hematite occurs in some samples together with an amphibole-dominated skarn assemblage. Lesser amounts of felsic volcanic rocks are partially skarn-altered with amphibole. Locally, the material is mineralised by sulphides, predominantly chalcopyrite. In the southern part of the sampled area, the waste rock shows a distinctly different appearance with greyish and coarser material (Fig. 49B). Here, the material is rich in quartz-mica schist with low contents of iron oxides and sulphides. Four mineralised selective samples were collected for chemical characterisation and thin sections studies.



Figure 49. A. Overviews of waste rock pile material at Nya Bastnäs with partly oxidised material. B. Coarse rock material rich in quartz-mica and low in iron oxides. Photos: Gunnar Rauséus.

Results composite sampling

Numerous elements are elevated within the composite samples collected from Nya Bastnäs (Table 17), including Bi, Co, REE, as well as base metals such as Cu and Fe₂O₃. LREE dominate, with approximately 94% of total REE. All samples except one show negative Eu anomaly (Fig. 50). The odd sample instead shows a slightly positive Eu anomaly. The material in the southern waste rock heap, dominated by quartz-mica schist, contains lower grades of Fe₂O₃, REE and Cu, than the northern part of the sampled area. Higher concentrations of Ba are noted in a few samples, but generally they are low in barium. Barium was observed as occurring in feldspar, however, and occasional baryte crystals were also observed. Bismuth content is generally low with some exceptions.

Tabell 17. Selected geochemical data for waste rock composite samples from Nya Bastnäs. (n=16).

Element	Fe ₂ O ₃ %	Ba ppm	Be ppm	Bi ppm	Co ppm	Cu ppm	Ni ppm	Y ppm	LREE ppm	HREE ppm	REE ppm
Average	34.6	1,453	9	101	202	1,181	35	256	7,633	218	7,851
Min	14.8	137	1	1	12	3	1	50	382	34	416
Max	48	8,320	27	783	421	3,190	76	529	17,666	496	18,162
Median	35.3	393	7	25	214	1,210	33	238	5,818	197	6,013

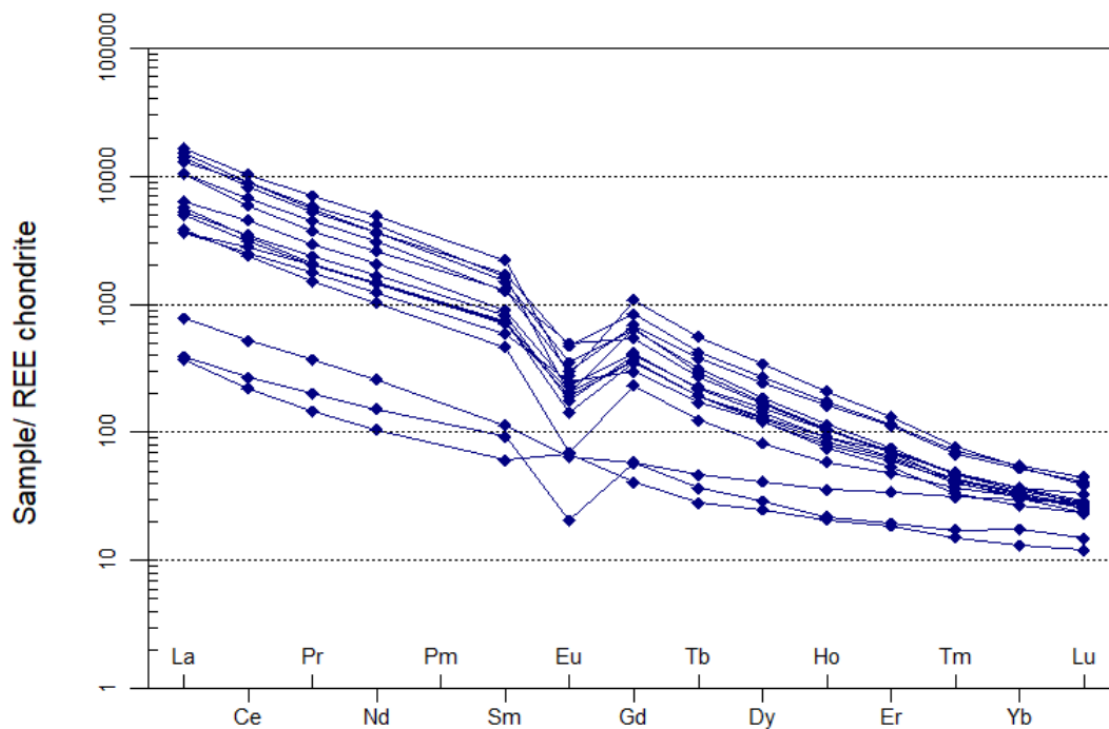


Figure 50. Chondrite normalised (Boynton 1984) REE diagram from the composite samples at Nya Bastnäs (n= 16).

Results selective sampling

At Nya Bastnäs, four richly mineralised samples were collected for whole rock analysis, representing different types of mineralisation observed in the waste rock piles, JCA210049D, JCA210049E, JCA210049G and JCA210054B.

JCA210049D is dominated by iron oxide mineralisation with fine-grained magnetite associated with green amphibole skarn (Fig. 51A). The amphiboles are identified in thin sections as anthophyllite and actinolite. The opaque minerals are dominated by magnetite and small amounts of chalcopyrite and locally chalcocite. Allanite is present and associated with both magnetite and the skarn. Allanite occur as fine-grained, brown-pleochroic aggregates with high interference colours (Fig. 51B). SEM-EDS analyses show allanite-(Ce) as the dominant REE-bearing mineral. Apart from this, SEM-EDS analysis confirms the presence of the following minerals: bornite, wolframite, galena, apatite, gadolinite-(Y), törnebohmitte, bastnäsite, monazite, xenotime, ferriallanite, gadolinite-(Nd), bismuthinite, scheelite, and pyrite–catterite with ca. 2% cobalt. Also, Bi-Cu mineral wittichenite, Bi-Te-Cu sulphosalts, Bi-Te mineral tetradymite. Whole rock analysis shows high grades of REE (> 4.5%), dominated by LREE. The sample is also rich in Cu, S and Fe₂O₃ (Table 18).

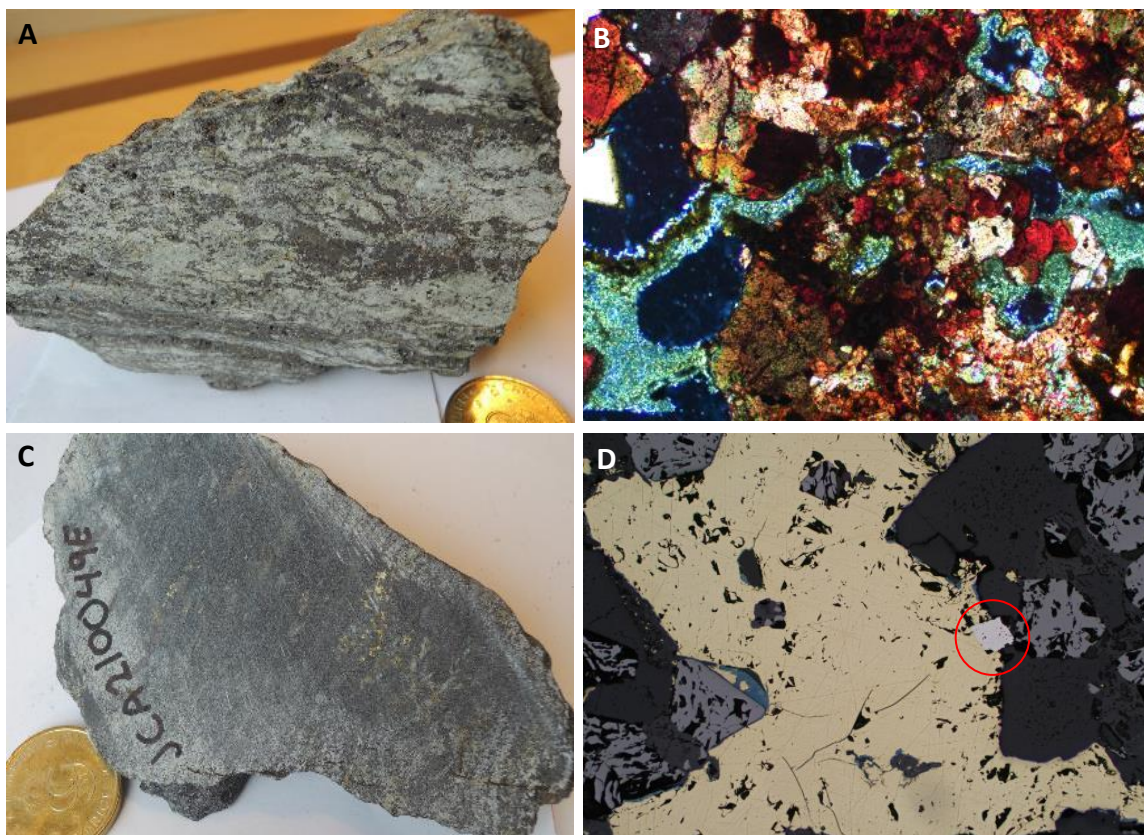


Figure 51. Photos and microphotos from selectiv samples **A.** Sample JCA210049D with fine-grained magnetite mineralisation in a mass of green amphibole skarn. **B.** Thin section of JCA210049D with fine-grained REE minerals dominated by allanite (high interference colours). **C.** Sample JCA210049E with grey, fine-grained, banded magnetite rich volcanic rock, containing amphiboles. **D.** Thin section of JCA210049E with chalcopyrite (yellow), magnetite (light grey), covellite (blue), and linnaeite (silver grey rhomb in red circle). Photos: Gunnar Rauséus.

JCA210049E can be characterised as a grey, fine-grained, foliated volcanic rock, rich in magnetite and some amphibole. Visible sulphides within the sample are chalcopyrite and pyrite (Fig. 51C). In thin section, the sample is dominated by quartz and anthophyllite and possibly serpentine alteration. Opaque phases are dominated by magnetite and occasionally chalcopyrite and covellite. Co-bearing linnaeite and carrolite is seen as inclusions within the chalcopyrite (Fig. 51D). Back-scattered electron (BSE) image in Figure 52 shows allanite with darker rims and patchy dark zonation of epidote. The dark rims of the allanite crystals show lower concentrations of REE and may point to loss of REE. Whole rock analysis shows elevated values for Cu (1,055 ppm), Co (402 ppm), Bi (145 ppm), Fe₂O₃ (41.4%), REE (1,619 ppm), where LREE constitute ca. 91% of the total REE (Table 18).

JCA210049G is a dark coloured to green, fine-grained banded amphibole skarn, mineralised with magnetite and hematite (Fig. 53A). In thin section, opaque phases are seen as bands, rich in magnetite and elongated hematite crystals within the amphibole skarn, dominated by actinolite (Fig. 53B). REE-bearing minerals seen in thin section are dominated by fine-grained allanite-(Ce) (Fig. 53C) SEM-EDS analyses show minor grains of monazite-(Ce) within the allanite as well as apatite with grains size up to 100 µm. Baryte is observed as fracture fill in magnetite. Geochemical analyses show elevated concentrations for Fe₂O₃ and REE, where LREE constitute ca. 93% of total REE (Table 18).

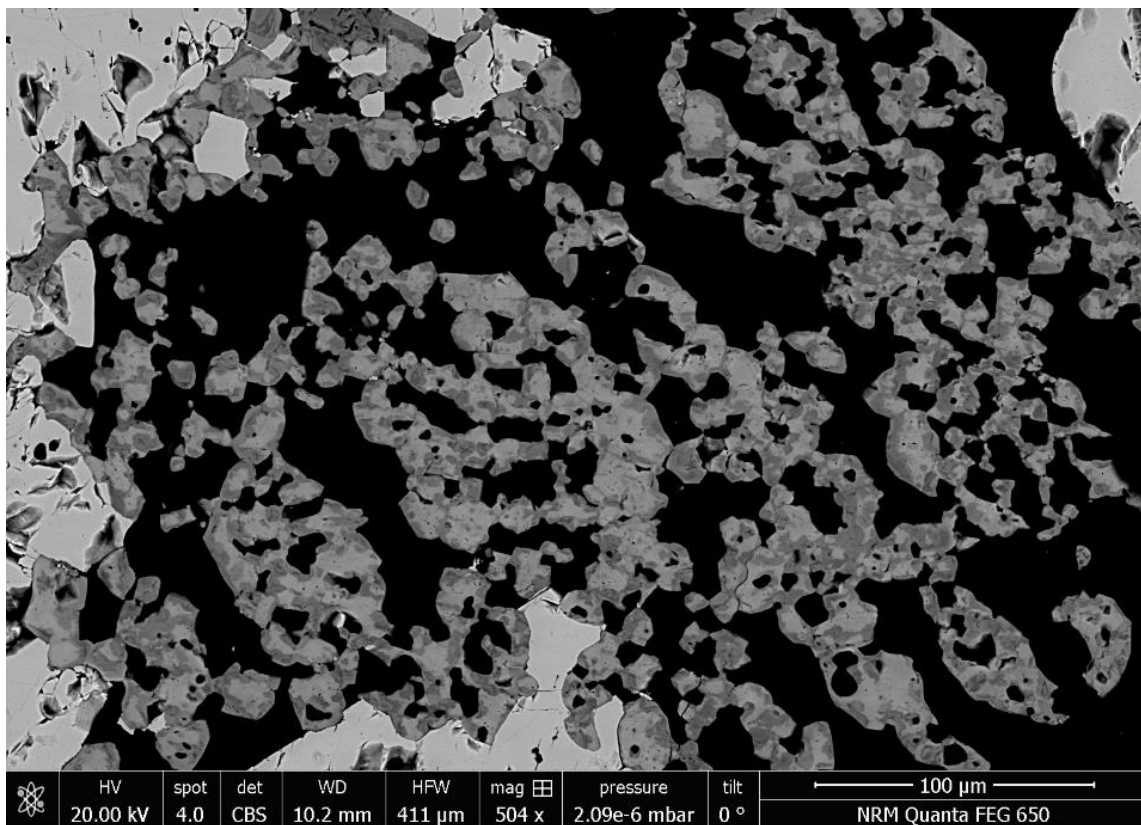


Figure 52. BSE image from sample JCA210049E showing allanite with darker rims and patches being poorer in Ce and closer to epidote in composition, magnetite (light grey, pitted), light silicates (black). Photo: Patrick Casey.

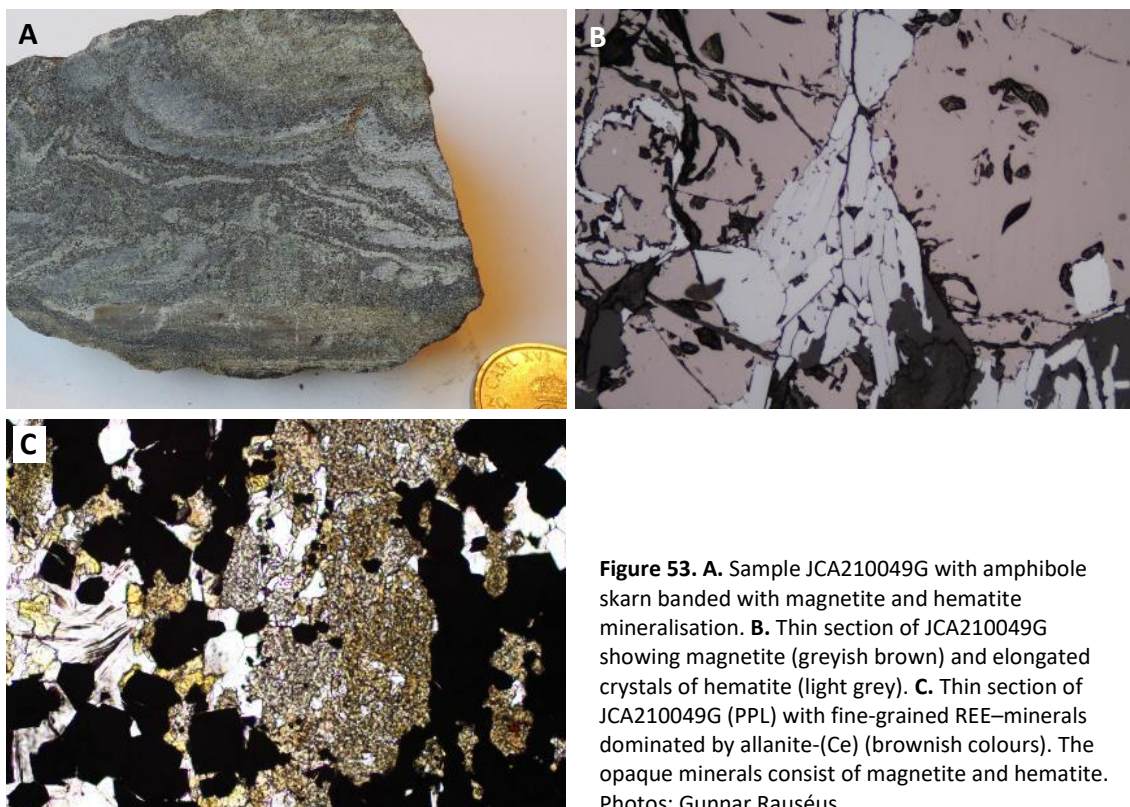


Figure 53. A. Sample JCA210049G with amphibole skarn banded with magnetite and hematite mineralisation. B. Thin section of JCA210049G showing magnetite (greyish brown) and elongated crystals of hematite (light grey). C. Thin section of JCA210049G (PPL) with fine-grained REE-minerals dominated by allanite-(Ce) (brownish colours). The opaque minerals consist of magnetite and hematite. Photos: Gunnar Rauséus.

Table 18. Selected geochemical data for selective samples from Nya Bastnäs.

Sample	Fe ₂ O ₃ %	Ba ppm	Bi ppm	Co ppm	Cu ppm	Ga ppm	Mo ppm	Y ppm	LREE ppm	HREE ppm	REE ppm
JCA210049D	30.8	95	18	194	4,040	120	104	900	44,174	988	45,162
JCA210049E	41.4	160	146	402	1,055	16	14	89	1,469	61	1,530
JCA210049G	54.7	345	3	28	338	21	3	138	3,560	129	3,689
JCA210054B	76.6	760	7	13	238	8	3	147	839	94	933

JCA210054B is characterised as a fine-grained quartz-banded iron oxide formation with bands of hematite (Figs. 54A and B). In thin section hematite is observed both as bands and as small inclusions in parts of the quartz rich areas, appearing as reddish–pink coloured minerals (Fig. 54D). Skarn minerals such as garnet, and small amounts of amphiboles and magnetite were observed in thin section. (Fig. 54C). SEM-EDS analysis identifies crystals of baryte within the hematite rich bands. Geochemical analyses show elevated concentrations for Fe₂O₃ (76.6%) Ba (760 ppm), REE (933 ppm) where LREE constitutes ca. 90% of total REE (Table 18).

Figure 55 shows the chondrite normalised plot (Boynton 1984) for the samples. All samples show small negative Eu anomalies.

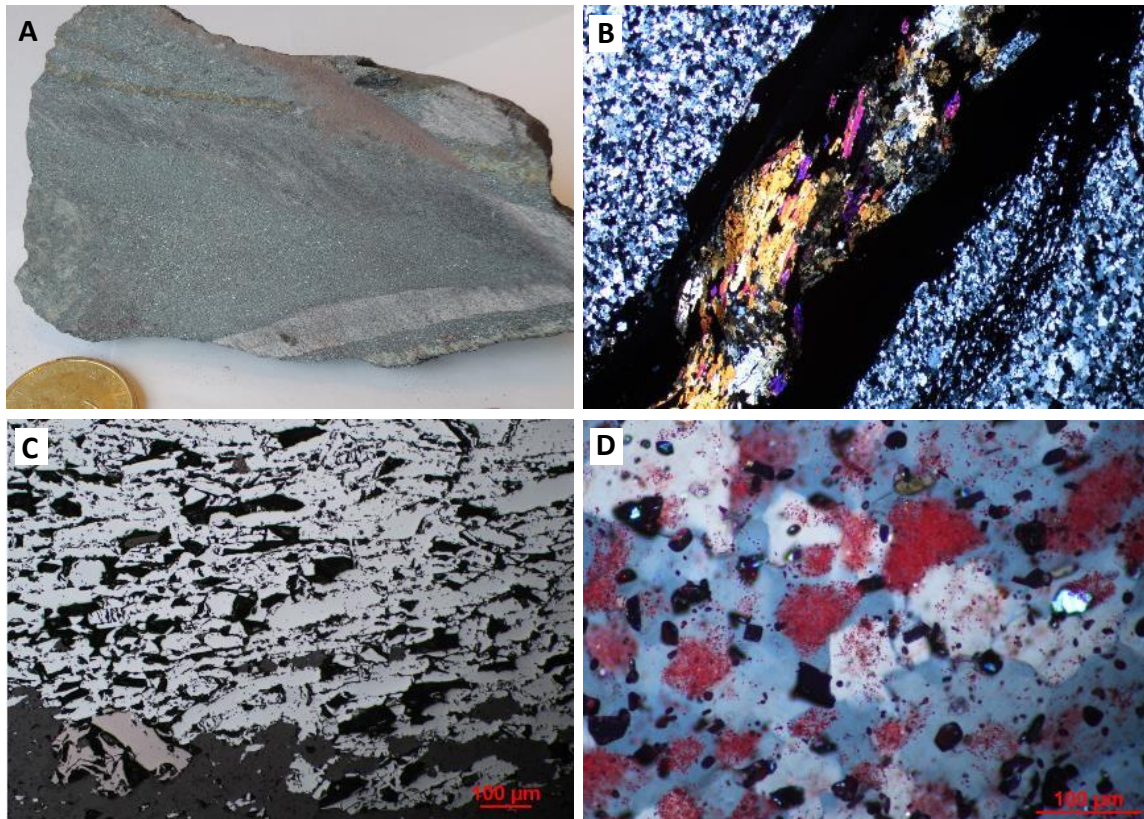


Figure 54. A. Sample JCA210054B with iron oxide mineralisation with banded quartz and hematite. B. Thin section (XPL) showing banded fine-grained quartz, hematite (opaque) and amphibole (low to mid second order interference colours). C. Thin section (reflected light) of JCA210054B with elongated crystal of hematite (light grey) and grains of magnetite (light brown). D. Thin section (XPL) JCA210054B with hematite (red) inclusions in quartz (white- grey). Photos: Gunnar Rauséus.

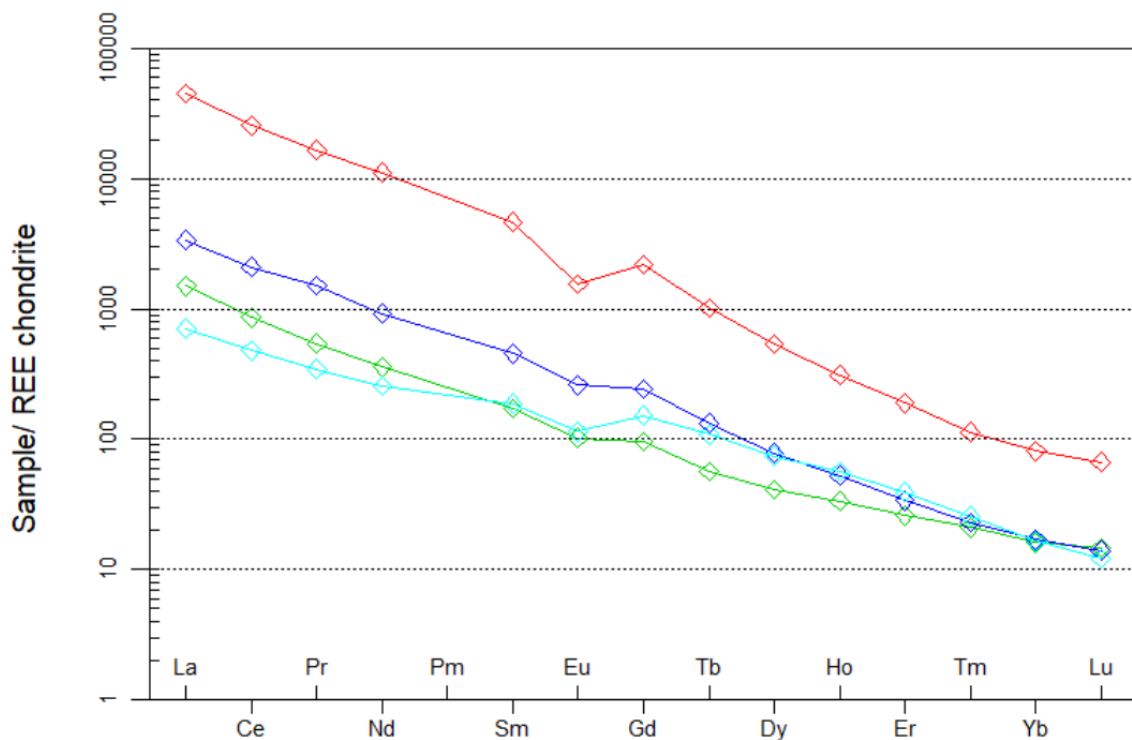


Figure 55. Chondrite normalised (Boynnton 1984) REE diagram from the four whole rock samples from Nya Bastnäs. JCA210049D (red), JCA210049E (green), JCA210049G (dark blue) and JCA210054B (light blue).

Kittelgruvan, Old Bastnäs

Historical background

Kittelgruvan is located 2 km northwest of Bäckegruvan and a few hundred metres south of Nya Bastnäs. The Kittelgruvan mine is part of the Old Bastnäs ore field and is a sulphide deposit mined for copper, cobalt and molybdenum. The Old Bastnäs ore field includes several mines mined for iron oxides, sulphides (Cu, Co), and dolomite and marble (Fig. 56). The mines at Bastnäs are first mentioned 1692. Kittelgruvan was accessed by a few hundred metres long tunnel (stoll) in the country rock. The stoll is still possible to access. The waste material from the mine is deposited near the entrance to the stoll.

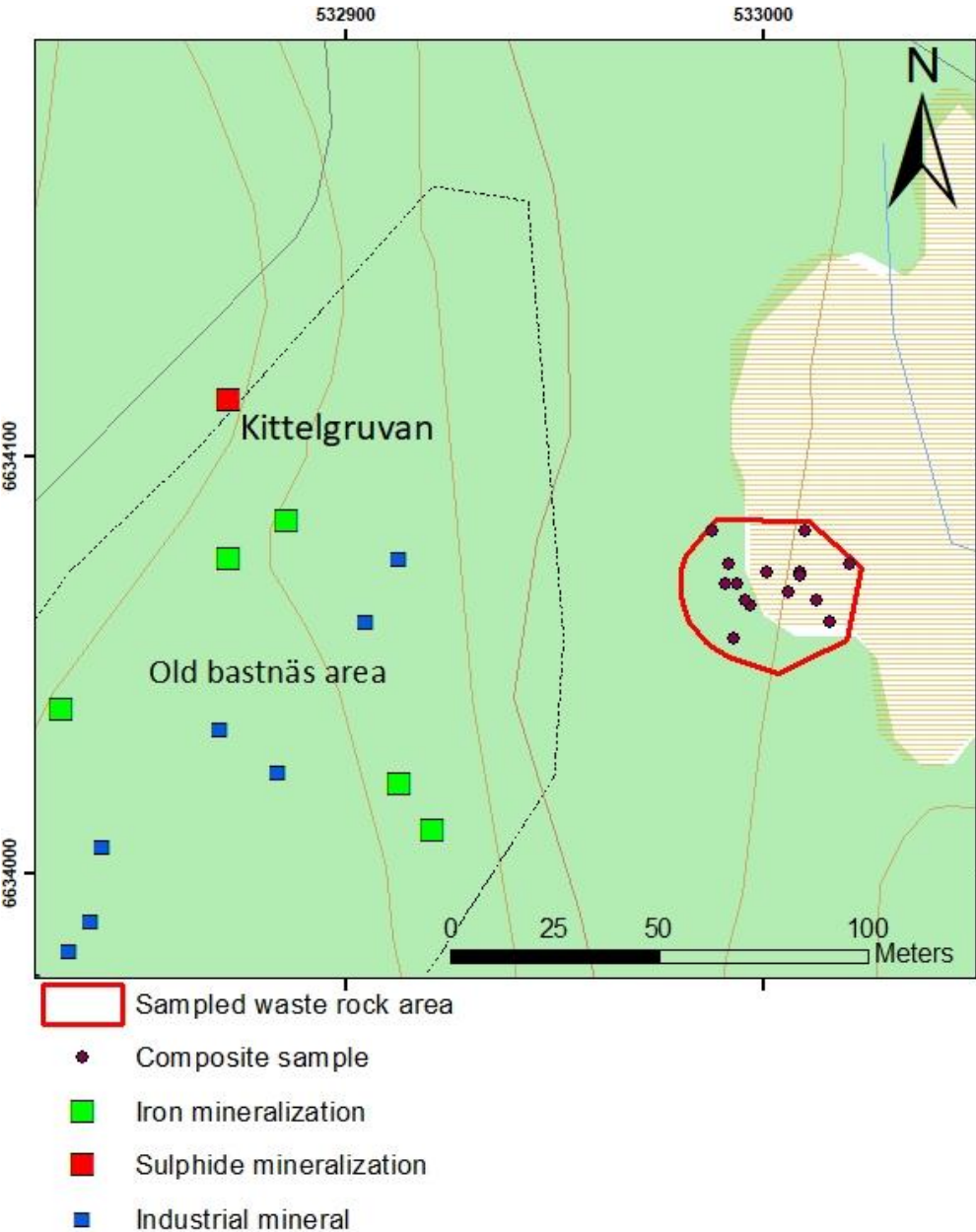


Figure 56. Location of sampled waste rock area in relation to Kittelgruvan (red square).

Waste rock

Waste rock was sampled from two small waste rock piles with a total area of ca. 600 m², situated east of the stoll entrance. The height of the piles is just over one meter. The material size varies from ca. 5 to 30 cm, with an overrepresentation of coarser material. Parts of it show oxidized surfaces (Fig. 57). The waste material is dominated by metavolcanic rock, amphibole skarn and hydrothermally altered rocks. Both iron oxide and sulphide mineralised rocks are found, and several samples are rich in chalcopyrite and molybdenite. The distribution of the different rocks for each of the 15 samples can be seen in Figure 58.

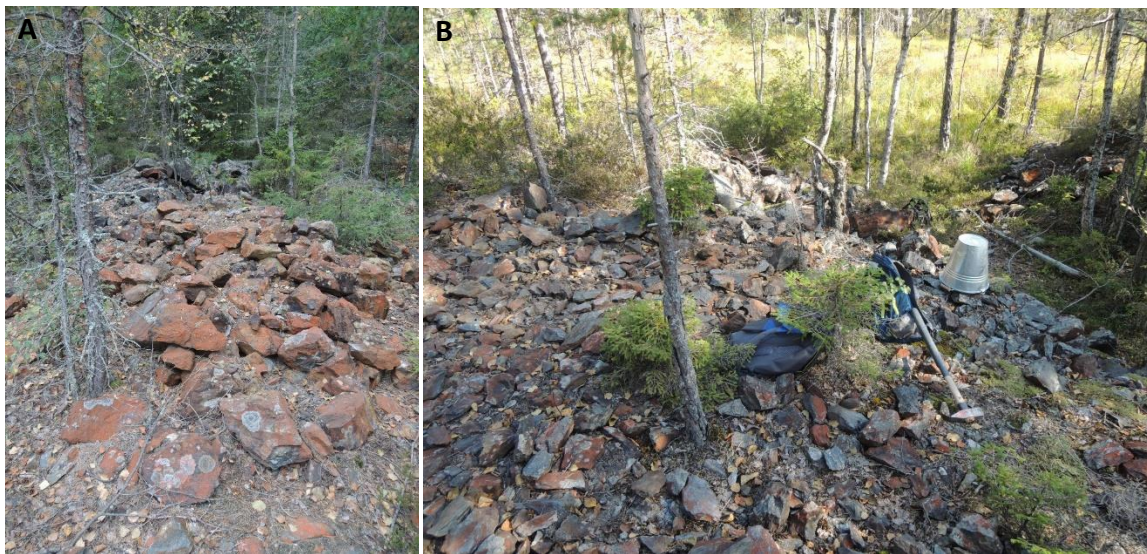


Figure 57. Photos from sampled waste rock at Kittelgruvan. **A.** Waste rock at Kittelgruvan showing surfaces with strong oxidation. **B.** Waste rock with partly oxidised surfaces. Photos: Gunnar Rauséus.

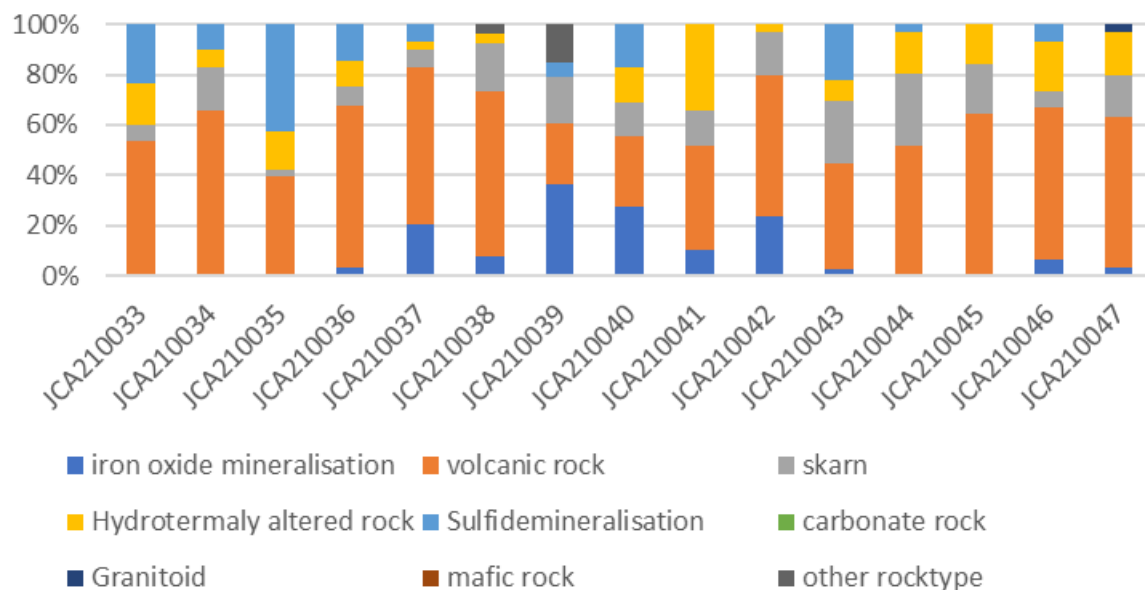


Figure 58. Distribution of rocks in composite samples from Kittelgruvan (n = 15).

Results composite samples

Geochemical analyses show elevated concentration of Fe₂O₃, Bi, Co, Cu, Ga, Mo, Ni, Te, Y and REE (Table 19). The REEs are dominated by LREE, which contributes with 96% of the total REE. Figure 59 shows the chondrite normalised REE diagram where all samples show negative Eu anomalies.

Table 19. Selected geochemical data for waste rock composite samples from Kittelgruvan. (n=15).

Element	Fe ₂ O ₃ %	Bi ppm	Co ppm	Cu ppm	Ga ppm	Mo ppm	Ni ppm	Te ppm	Y ppm	LREE ppm	HREE ppm	REE ppm
Average	17.8	340	371	1,807	45	2,864	43	2.7	141	7,881	179	8,059
Min	9.5	18	36	86	25	14	8	0.5	52	410	45	455
Max	34.5	1,125	1,200	5,120	94	21,500	141	9.7	392	26,921	512	27,433
Median	15.3	316	268	1,620	35	1,515	31	1.5	115	5,163	136	5,299

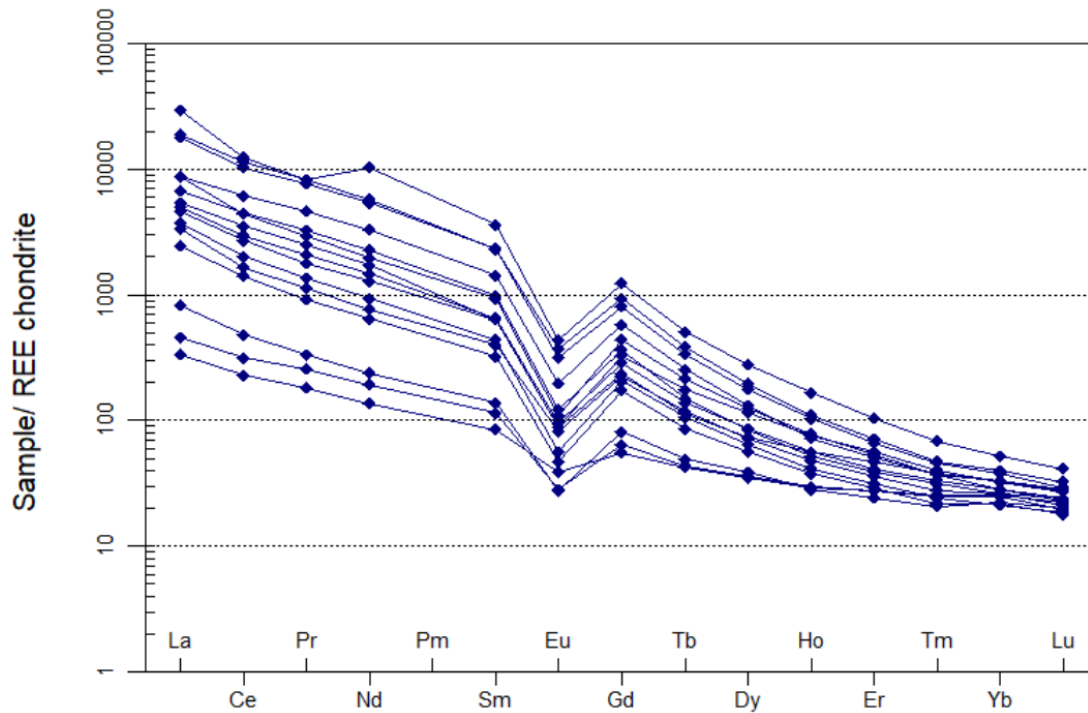


Figure 59. Chondrite normalised (Boynnton 1984) REE diagram from the composite samples from Kittelgruvan (n=15).

Results selective sampling

Four samples were taken for whole rock analysis from Kittelgruvan, JCA210036B, JCA210037B, JCA210041B and JCA210047C.

JCA210036B can be described as dark, fine-grained amphibole skarn, rich in chalcopyrite and some pyrrhotite. The sample is rich in REE, dominated by allanite-(Ce), which appears as dark areas in hand specimen (Fig. 60A). The thin section shows areas rich in of chalcopyrite, pyrrhotite and cobalt-bearing minerals such as euhedral shaped crystals of linnaeite (Fig. 60B). Other parts of the thin section are rich in fine-grained allanite together with sulphides (Fig. 60C). Small amounts of molybdenite, and cobalt minerals such as catterite, and carrolite is present.

SEM-EDS identified allanite-(Ce) as the dominant REE-bearing mineral comprising most of the thin section, as well as minor amounts of bastnäsite. Small crystals of native bismuth and Bi-Se-minerals occurs in association with chalcopyrite. This sample is the richest in terms of REE found during this study, with concentration totalling over 12% REE. However, the total concentration of REE is unknown as the Ce and Pr content exceeded the maximum detection limits (50,000 and 5,000 ppm respectively) even in the ore grade analysis. Other elements enriched in the sample are (Cu 2.3%), Bi (287 ppm), Co (1,415 ppm), Fe₂O₃ (30%), Mo (564 ppm), Re (28 ppm), and Zr (170 ppm) (Table 20).

JCA210037B is characterised as a green-coloured amphibole skarn comprised of radially grown tremolite, with varying amounts of chalcopyrite mineralisation (Fig. 60D). Thin sections identify tremolite, muscovite, sericite and areas with fine-grained REE mineralisation (Fig. 60E). Sulphide mineralisation consists of chalcopyrite together with pyrite and euhedral crystals of linnaeite. Covellite appears as replacement along edges and within pyrite (Fig. 60F). Minor amount of molybdenite is present. SEM-EDS identifies allanite-(Ce) and gadolinite-(Y) as the dominating REE minerals in the sample. Fluorapatite occurs as small grains less than 20 µm as well as small amounts of native bismuth, bismuthinite, galena together with chalcopyrite and also gustavite with Ag-Pb-Bi. Whole-rock geochemistry shows elevated concentrations for Co (109 ppm), Cu (2,130 ppm), Mo (324 ppm), REE (5,720 ppm), where LREE constitute ca. 75% of total REE (Table 20).

JCA210041B is characterised as an iron oxide mineralisation with magnetite in an amphibole skarn. Dark coloured fine-to medium-grained, partly with chalcopyrite (Fig. 61A). The thin section is dominated by a ground mass of fine-grained quartz, amphiboles, mainly tremolite and anthophyllite, and fine-grained, partly euhedral magnetite (Fig. 61B). Locally patches of disseminated chalcopyrite, molybdenite and pyrrhotite.

SEM-EDS analysis identifies small amounts of monazite-(Ce), fluorite, apatite, REE-fluorocarbonates such as bastnäsite-(Nd) and bismuthinite is also present. SEM-EDS analysis showed that pyrrhotite contains up 3% of cobalt. Whole rock analysis shows elevated concentrations for Fe₂O₃ (64.3%), Cu (467 ppm), Co (189 ppm), and REE (268 ppm), dominated by LREE (Table 20).

JCA210047C is characterised as a fine- to fine medium-grained biotite schist, partly with green actinolite and rich in molybdenite mineralisation. Thin section is dominated by amphibole, biotite and areas with abundant molybdenite with sparse grains of chalcopyrite (Fig. 61C). The molybdenite mineralisation is interpreted as two generation where the first consist of elongated grains effected by folding while the second generation overprint the first and with generally larger crystals (Fig. 61D).

SEM-analysis identifies local areas up to 500 µm with REE minerals dominated by allanite-(Ce) and small amount of gadolinite-(Ce) and Ce-bearing fluorocarbonates such as bastnäsite and parisite/synchysite. Allanite often show inclusion of molybdenite, chalcopyrite and small grains of bismuthinite. A metamict Y-bearing uranium oxide is seen as inclusion in allanite as well as small grains of REE-bearing apatite.

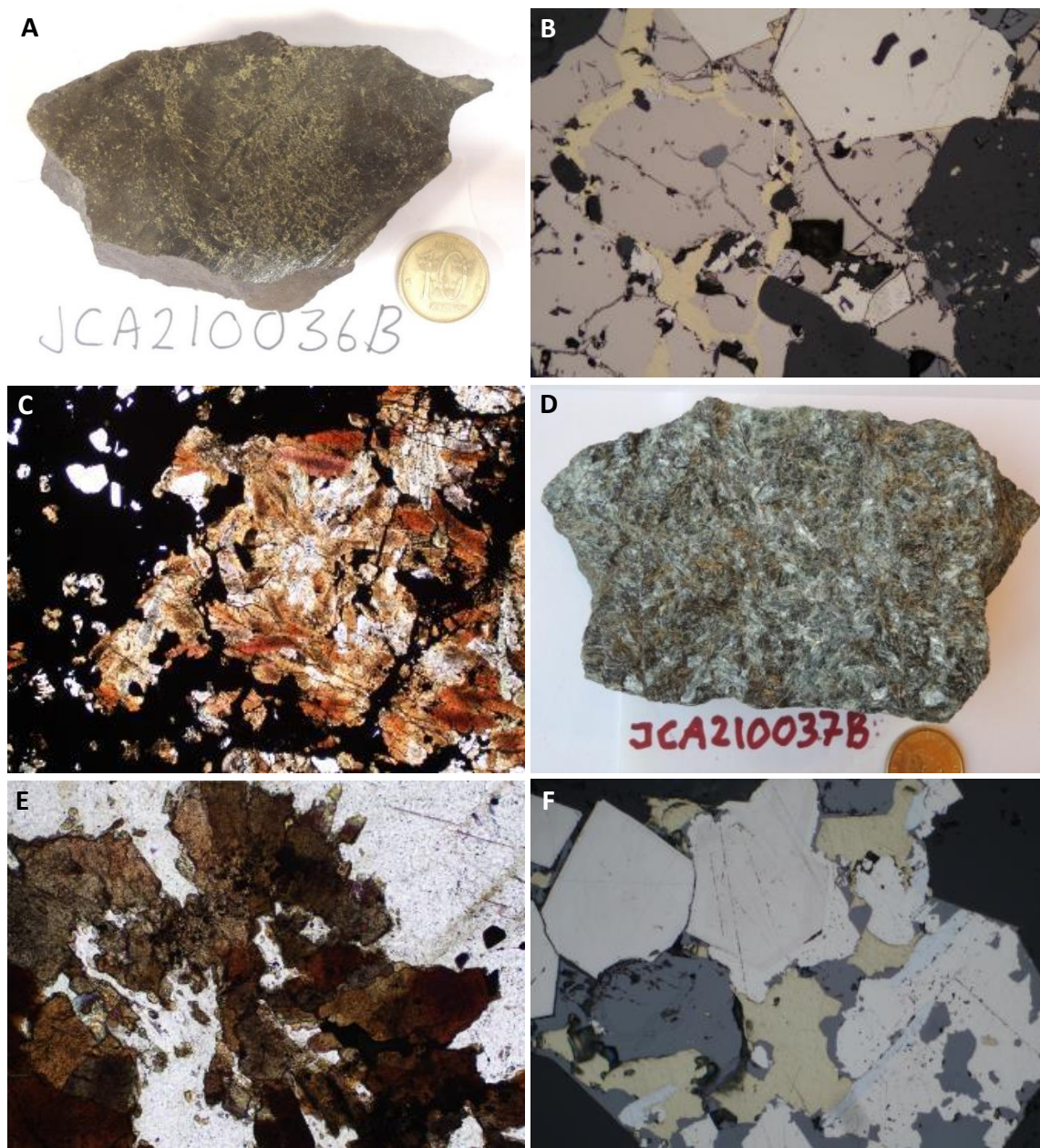


Figure 60. Photos and microphotos from selective samples. **A.** Sample JCA210036B fine-grained amphibole skarn, rich in chalcopyrite and some pyrrhotite. **B.** Thin sections of JCA210036B under reflected light with pyrrhotite (brown), chalcopyrite (yellow) and euhedral crystals of linnaeite (greyish white). **C.** Thin section of JCA210036B (PPL) with magnetite (opaque) and REE-minerals dominated by allanite-(Ce). **D.** Amphibole skarn rock, containing dissemination of chalcopyrite and pyrrhotite. **E.** Thin section from JCA210037B (PPL) showing allanite-(Ce) (brownish). **F.** Thin section of JCA210037B (reflected light) with pyrite, chalcopyrite and Co-bearing mineral. Photos: Gunnar Rauséus.

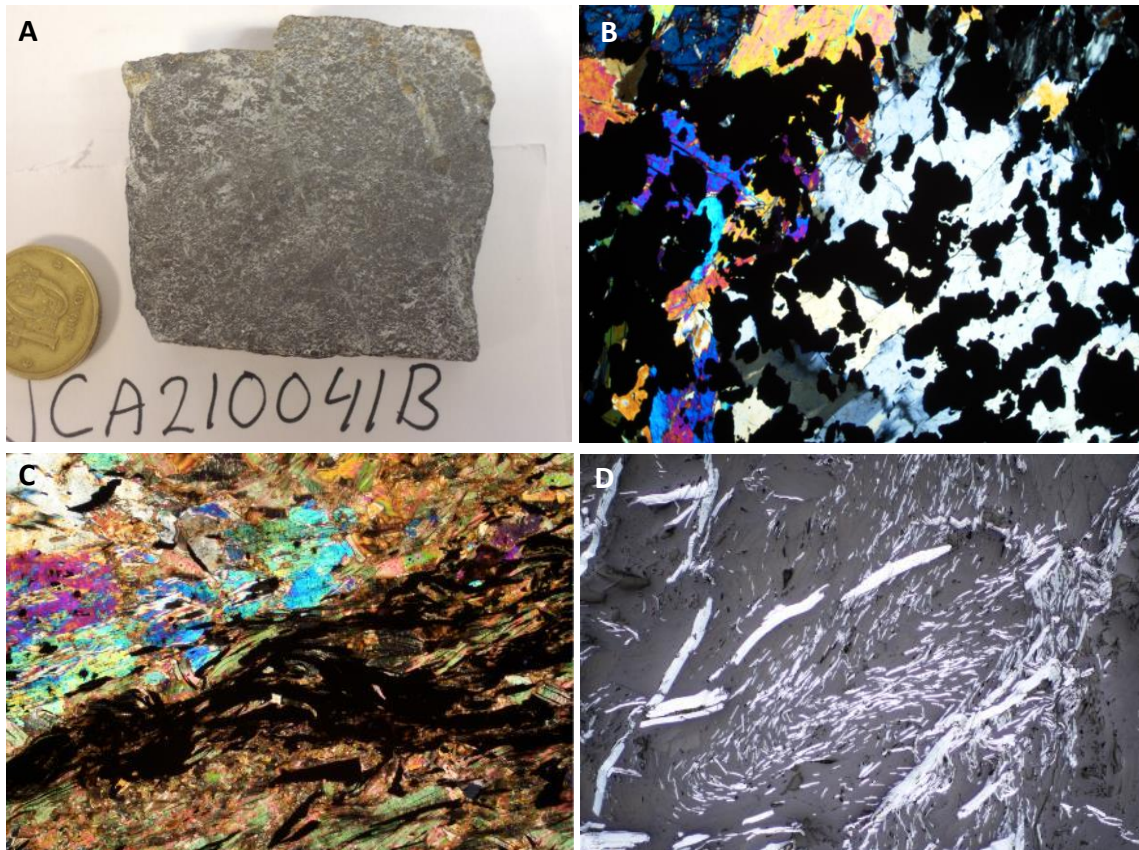


Figure 61. Photos and microphotos from selective samples. **A.** Sample JCA210041B with iron oxide mineralisation dominated by magnetite amphibole skarn. Dark coloured fine- to medium-grained, partly with chalcopyrite. **B.** Thin section of JCA210041B (XPL) with fine-grained groundmass of quartz and amphibole with disseminated magnetite (opaque). **C.** Thin section image from JCA210047C (XPL) with biotite schist with actinolite and rich in molybdenite (opaque). **D.** Thin section image from JCA210047C (reflected light) with two generations of molybdenite. First generation with smaller elongated grains which have been folded and a second generation of molybdenite that overprint previous structures. Photos: Johan Camitz.

At Kittelgruvan strongly altered REE minerals were observed, demonstrating a later alteration event. Figure 62 shows an example of a crystal of gadolinite that has been altered, with loss of REE in the centre of the crystal, as evidenced by the darker areas, and a uranium-REE-hydroxylcarbonate has been formed. Molybdenite also shows evidence of later formation, following the foliation of the silicate minerals, as well as forming inclusions within the gadolinite crystal (bright lathe like crystal in the lower right side of the gadolinite crystal).

Whole rock geochemistry shows elevated Mo concentration of more than 5% (51,100 ppm), Re (1.28 ppm) and REE (892 ppm). The REEs are dominated by LREE (Table 20). The Rhenium grades is due to enrichment in molybdenite.

Analytical results for selected elements can be seen in Tables 20. Figure 63 shows the chondrite normalised REE plot for the selective samples. All samples display a negative Eu anomaly.

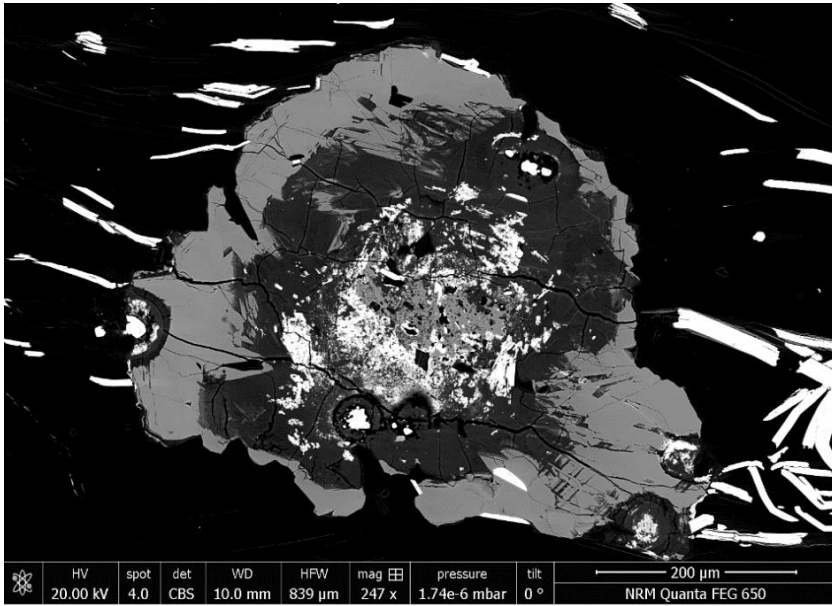


Figure 62. BSE image of gadolinite with uranyl-carbonate (bright white round crystals) and molybdenite. Note the radiation halos surrounding the uranium minerals. Photo: Patrick Casey.

Table 20. Selected geochemical data for selective samples from Kittelgruvan.

SAMPLE	Fe ₂ O ₃ %	Bi ppm	Co ppm	Cu ppm	Mo ppm	Rb ppm	Re ppm	U ppm	Y ppm	LREE ppm	HREE ppm	REE ppm
JCA210036B	30.3	287	1,415	22,800	564	28	0.07	36.1	1550	120,030	2452	122,482
JCA210037B	7.8	21	109	2,130	324	0.5	0.04	34.2	850	4,277	593	4,870
JCA210041B	64.3	16	189	467	4.26	0.6	0	0.9	33	245	23	268
JCA210047C	9.1	52	233	383	51,100	229	1.28	173	59	829	63	892

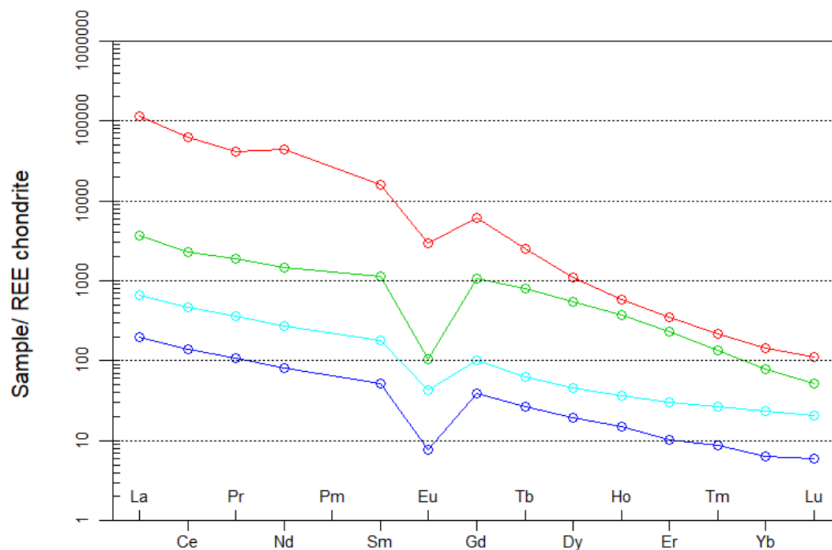


Figure 63. Chondrite normalised REE diagram (Boynnton 1984) from the four whole rock samples from Kittelgruvan. JCA210036B (red), JCA210037B (green), JCA210041B (dark blue) and JCA210047C (light blue).

NORBERG AREA

The Norberg ore field was active for several hundred years and includes hundreds of abandoned mines which were mined mainly for iron oxide. These include variously sized open pits, as well as underground mines. Most of these are included in the SGU mineral resources database. A total of 45 composite samples were collected from waste rock at three mine sites in the area, 15 samples each at Åsgruvan, Östanmossgruvan and Malmkärragravorna (Fig. 64).

Existing and historical data

Airborne geophysics

SGU has made two airborne geophysical surveys over the Norberg area (Figs. 64–66, Table 21). The flight direction of the most recent one was approximately northwest–southeast. This direction of the flight lines is more favourable in the Norberg area as they go almost perpendicular to the general strike of the main bedrock structures. The VLF measurements from two transmitters make it possible to derive apparent resistivity and current density maps of the ground. Also, the electrical conductors in the bedrock can be identified independent of their direction with respect to the VLF transmitters.

Table 21. Previously made airborne geophysical surveys by SGU over the area around Norberg.

Year	Geophysical methods used	Flight direction	Flight line separation (m)	Flight altitude (m)
1978	Magnetics, gamma spectrometry	North–south	200	30
2016	Magnetics, gamma spectrometry, VLF (2-transmitters)	Approximately northwest–southeast	200	60

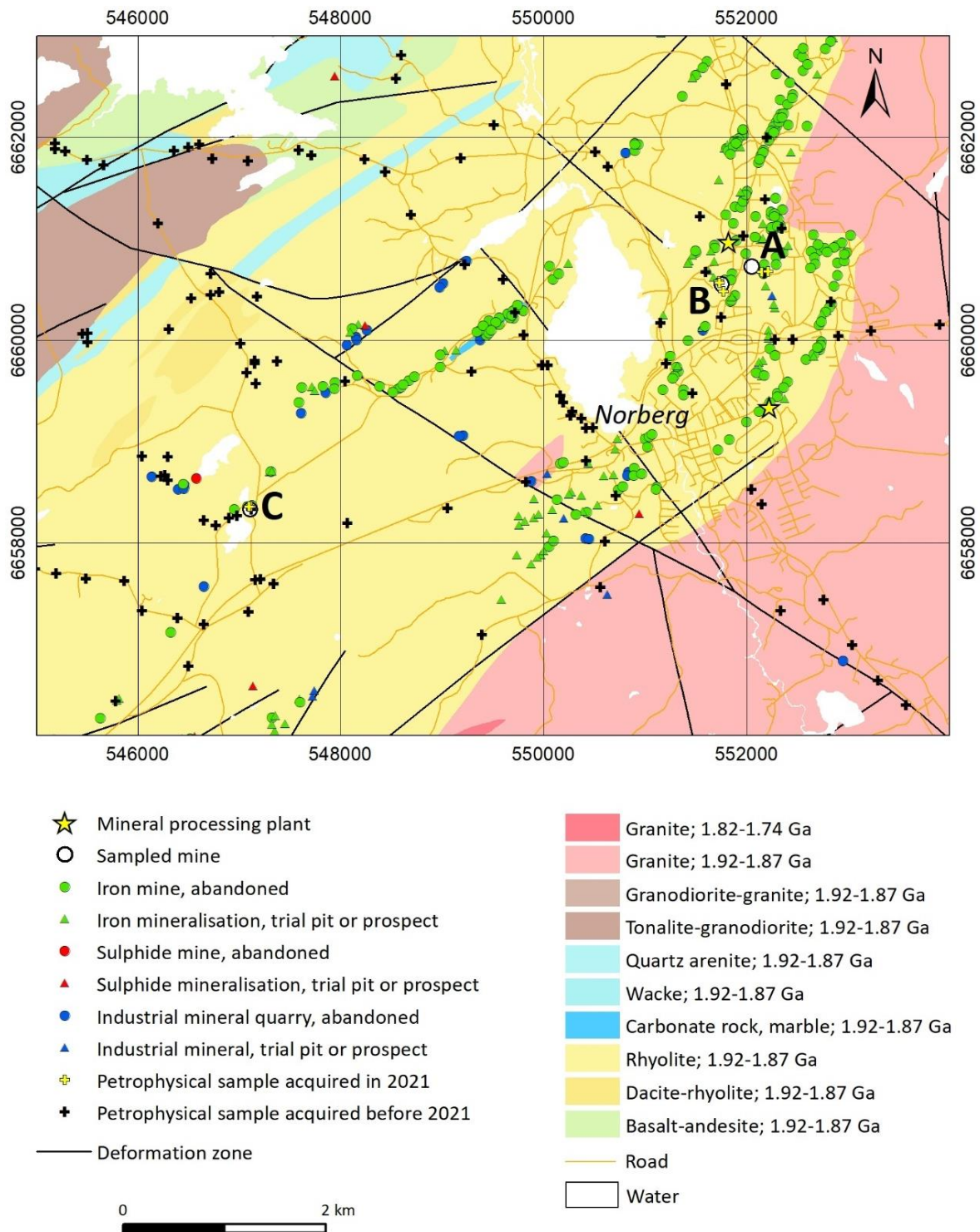


Figure 64. Simplified bedrock map over the Norberg area (SGU 2022). The investigated mine sites in this study are Åsgruvan (A), Östanmossgruvan (B), and Malmkärragruvorna (C).

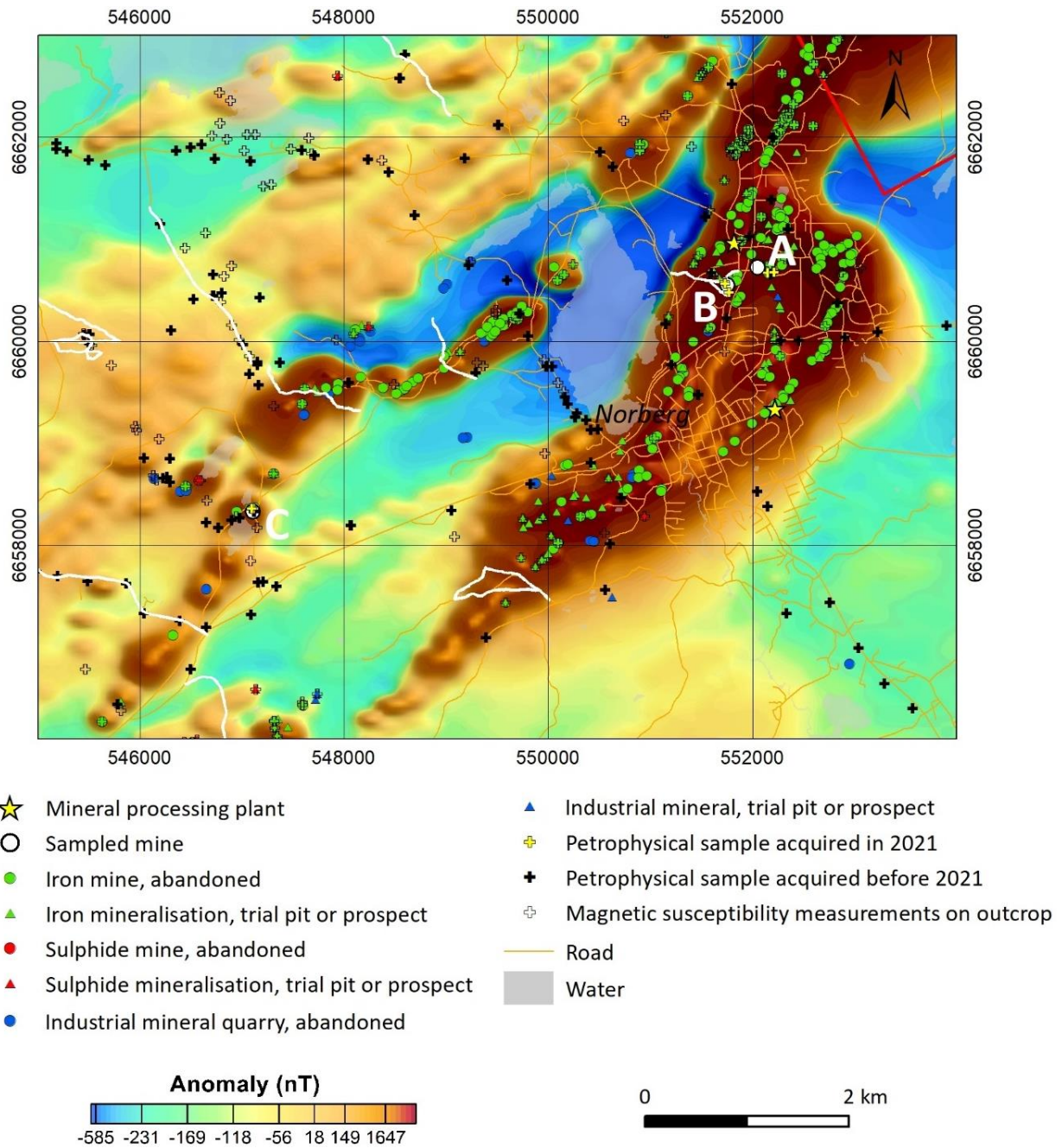


Figure 65. Map showing the magnetic anomalies, derived from SGU's airborne measurements done in 2016, at the investigated mines of this study and their surroundings. The investigated mine sites in this study are Åsgruvan (A), Östanmossgruvan (B), and Malmkärgruvorna (C). White lines represent profiles along which previous acquisition of ground magnetic data have been made. A previous geophysical exploration survey has been made within the red polygon in the upper right corner. Data from this survey are now available in SGU's databases (Table 22).

Table 22. Previously acquired geophysical exploration data in the area around Norberg, from which data now are available in SGU's databases. The geographical extension of these measurements is shown in figure 65.

Name of exploration area	Geophysical methods used	Responsible	Year of permit
Norberg nr 1001	Magnetics, VTEM	Boliden Mineral AB	2005–2008

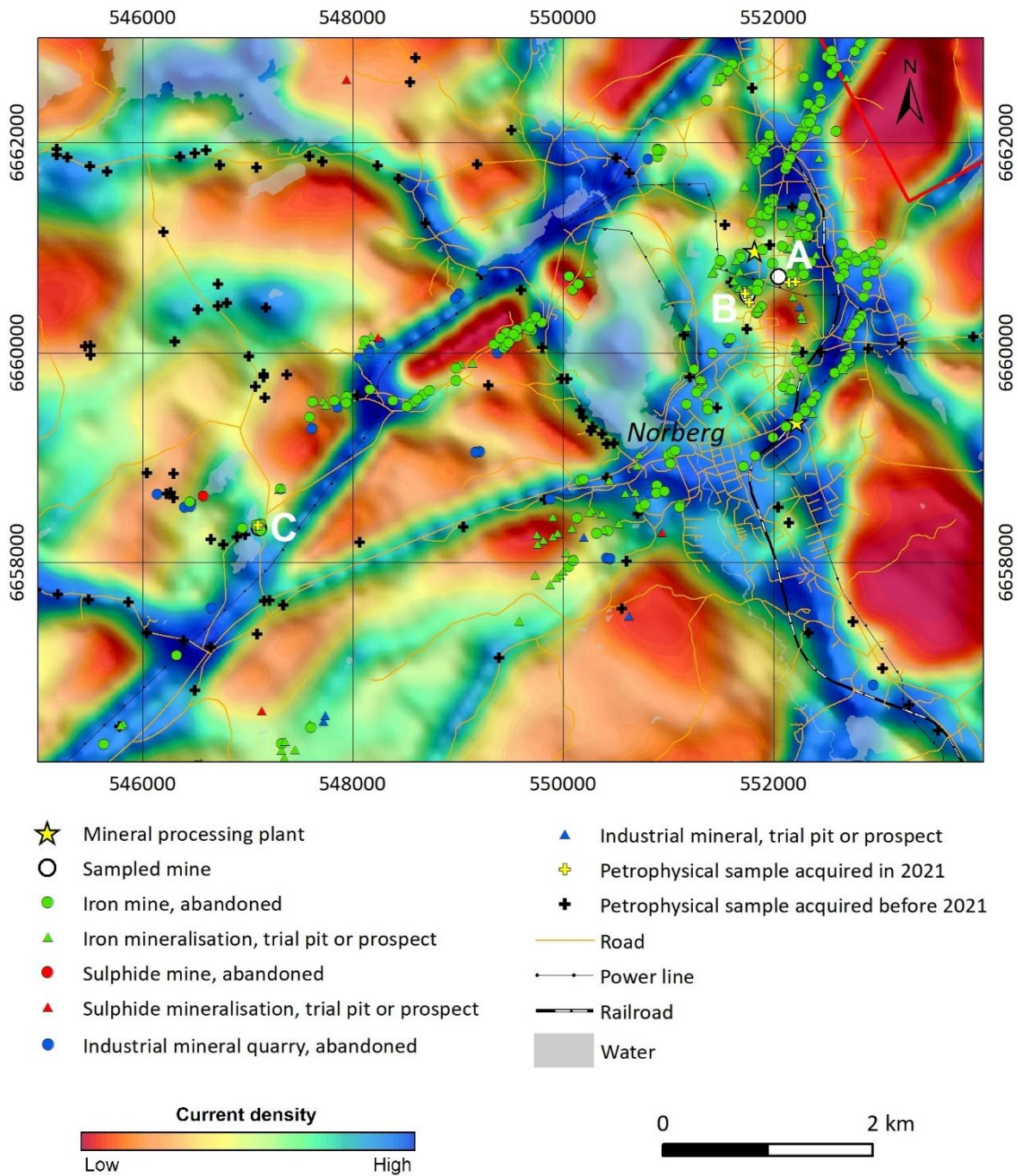


Figure 66. Map showing the current density in the ground at the investigated mines in this study along with their surroundings. The current density is derived from airborne VLF measurements from two transmitters, acquired by SGU in 2016. The investigated mine sites in this study are Åsgruvan (A), Östanmossgruvan (B), and Malmkärragruvorna (C). A previous geophysical exploration survey has been made within the red polygon in the upper right corner. Data from this survey are now available in SGU's databases (Table 22).

Ground geophysics

During previous bedrock mapping activities by SGU in the area around Norberg, magnetic data were collected along certain profiles (Fig. 65). The gravity data around Norberg have been acquired during the years 1975, 1976, 1992, and 2017. One of the aims during the most recent survey was to achieve a more closely spaced net of gravity measurements in the area, with approximately 1–1.5 km station spacing (Fig. 67). A profile with more tightly spaced gravity measurements, with approximately 100 m station spacing, has been achieved across the mineralised sequence.

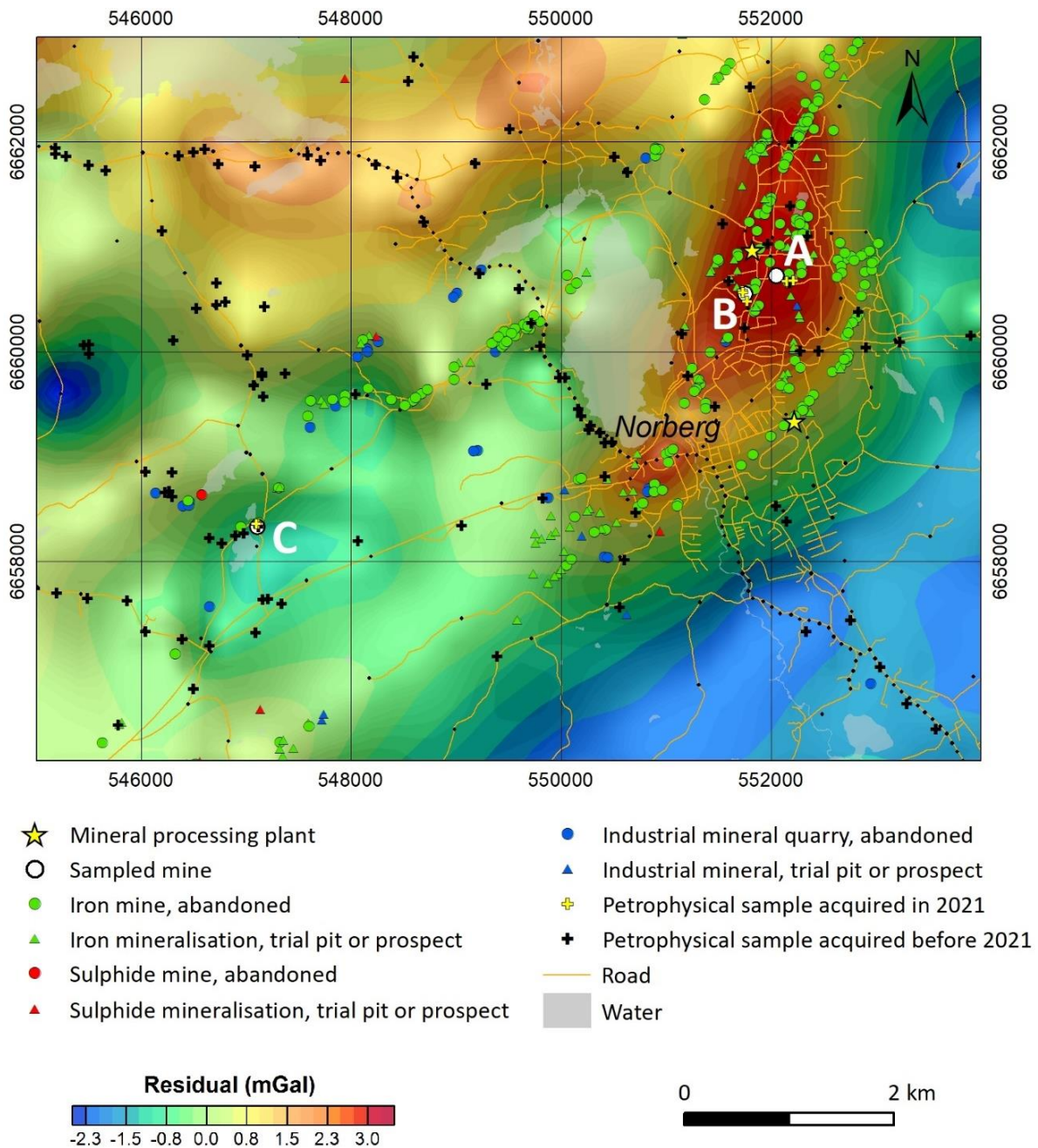


Figure 67. Map showing the residual gravity field at the investigated mines in this study along with their surroundings. The residual gravity field is expressed as the difference between the Bouguer anomaly and an analytical continuation upwards to 3 km. The small black dots represent localities for gravity measurements. The investigated mine sites in this study are Äsgruvan (A), Östanmossgruvan (B), and Malmkärragruvorna (C).

Malmkärragruvorna

Historical background

Malmkärragruvorna is located ca 5 km west of Norberg (Fig. 64). The Malmkärragruvorna mines include four small open pits and underground mines in the area between the lakes Lilla and Stora Malmkärnen. (Hellström et. al. 2022). The ore consists of magnetite occurring alongside skarn metamorphosed dolomite in contact with chlorite mica schist. The skarn consists of tremolite and actinolite and humite minerals (containing F) and phlogopite mica. The magnetite ore is rich in allanite. Locally, up to half a metre thick layers of solely cerium minerals occur (Geijer & Magnusson 1944). Magnetite mineralisation contains varying amounts of sulphides such as pyrite, chalcopyrite and molybdenite (Geijer & Magnusson 1944). Ophicalcite is also present where metamorphic conditions formed serpentine and humite-group minerals. Malmkärragruvorna are included in the so called “REE-line” as defined by Jonsson and Högdal (2013). The Malmkärragruvorna are type locality for the REE minerals gadolinite-(Nd), ulfanderssonite-(Ce) and västmanlandite-(Ce) (Holstam et. al 2005).

In the 1908 ore estimates by Tegengren et al. (1924) the ore tonnage was estimated to 106,000 tons. Mining in the period 1910–1934 (1931), resulted in 106,715 tons produced ore at Malmkärragruvorna. In the SGU database Litho geochemistry, previous analyses from the Malmkärragruvorna includes a total of 19 samples. 16 of these were sampled by Tasman Metals during 2010 within their exploration permit in the area where one samples containing ca. 15% REE.

Waste rock

The waste rock pile area at Malmkärragruvorna is to a large extent overgrown by moss and trees (Fig. 68A). The waste rock pile is occasionally exposed where moss cover is thin. The area includes three waterfilled open pits which are oriented in a line striking approximately north-south (Figs. 68B and 69). The sampled area is presented in Figure 69. The sampled waste rock material is dominated by a fine-grained meta volcanic rock partly foliated, iron oxide mineralisation dissemination in greenish amphibole skarn, strongly foliated biotite schist classified as hydrothermally altered rock and rock material dominated by green amphibole skarn. A small number of samples are characterised as sulphide-bearing, mainly with chalcopyrite, pyrrhotite and pyrite. Distribution of the different rocks in composite samples is compiled in Figure 70. Four mineralised selective samples were collected for chemical characterisation and thin section studies.



Figure 68. A. An overgrown waste rock pile area at Malmkärragruvorna. B. Waterfilled open pit at Malmkärragruvorna. Photos: Gunnar Rauséus.



Figure 69. Red polygon indicates area of sampling at Malmkärrgruvorna. Yellow dots show sampling locations. Green dots are locations of mines (open pits) with labels.

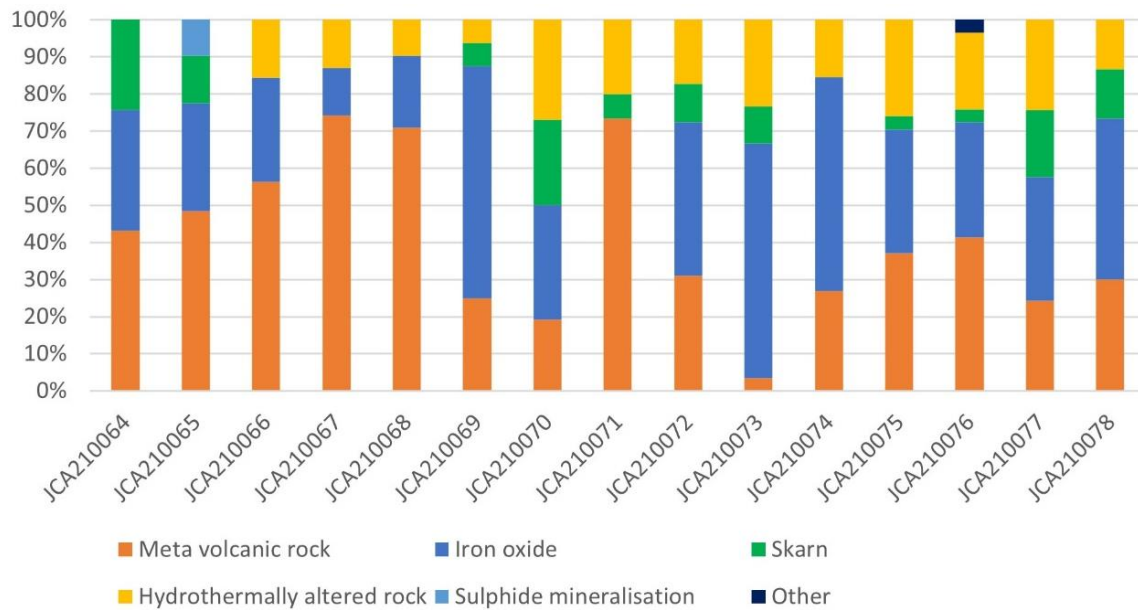


Figure 70. Distribution of rocks in composite sample at Malmkärrgruvorna.

Results composite sampling

The 15 composite samples from Malmkärragruvorna show a wide spread in concentrations of Fe₂O₃, Be, Ga, W, Y and REE, dominated by LREE, constituting ca. 94% of the total REE (Table 23). A chondrite normalised REE diagram is seen in Figure 71, where all samples show negative Eu anomaly.

It should be noted within samples from Malmkärragruvorna that the analytical results for Ga may be overestimated. Mass spectrometry analysis of Ga in samples with high levels of REE may lead to the over counting of gallium due to certain REE isotopes (particularly Nd) being counted as 2 gallium atoms. This trend is particularly apparent at Malmkärragruvorna, where a strong linear correlation between Ga and REE ($r^2 = 0.6521$) is observed (Fig. 72).

Table 23. Selected geochemical data for waste rock composite samples from Malmkärragruvorna. (n = 15).

Element	Fe ₂ O ₃ %	Be ppm	Ga ppm	U ppm	W ppm	Y ppm	LREE ppm	HREE ppm	REE ppm
Average	32.1	20	104	58	200	270	4,923	294	5,217
Min	4.3	2	52	13	7	79	584	78	694
Max	52.4	62	180	159	589	572	20,212	713	20,925
Median	34.5	13	98	56	148	273	2,667	297	2,996

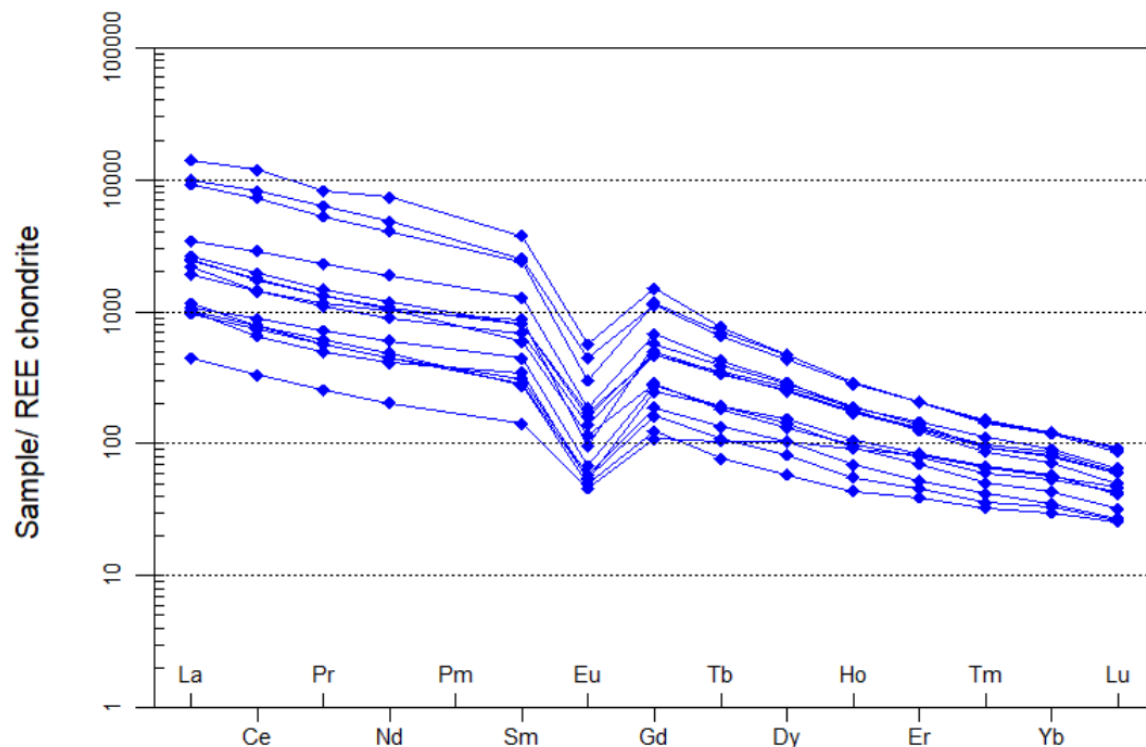


Figure 71. Chondrite normalised (Boynton 1984) REE diagram for composite samples from Malmkärragruvorna (n = 15).

Ga vs REE at Malmkärragruvorna

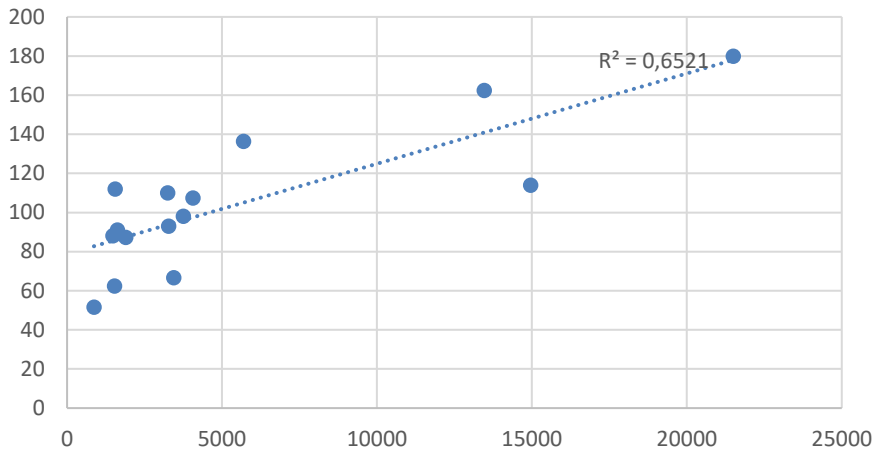


Figure 72. Scatter plot of gallium (x-axis) and REE (y-axis) in composite samples at Malmkärragruvorna showing the strong correlation.

Results selective sampling

Four richly mineralised samples were selected from Malmkärragruvorna for whole rock analysis, JCA210065B, JCA210065C, JCA210076B and JCA210076C.

JCA210065B is characterised as iron oxide mineralisation of fine-grained massive magnetite, partly with green skarn and chalcopyrite (Fig. 73A). Amphiboles and garnet are observed as fracture filling. SEM-EDS analysis show needle like crystals of REE mineral parisite associated with magnetite and silicates (Fig. 73B). An unidentified Bi-Te mineral is observed with SEM-EDS as small grains within the skarn. Geochemical analysis showed elevated concentrations of Fe₂O₃ (78.7%), Ga (144 ppm), REE (880 ppm). LREE comprises 91% of the total REE content (Table 24).

JCA210065C can be characterised as a fine-grained iron oxide mineralisation with magnetite in a ground mass of amphibole skarn, mainly actinolite (Fig. 73C). Thin section shows small amount of pyrite and chalcopyrite associated with magnetite in a ground mass of amphibole skarn (Fig. 73D). Geochemical analysis showed elevated concentrations Fe₂O₃ (40.1%), gallium (91 ppm), REE (321 ppm) (Table 24).

JCA210076B can be characterised as a fine-grained ophicalcite dominated by Mg-rich dolomite with porphyroblasts of serpentine, disseminated magnetite and dark coloured REE-minerals (Fig. 73E). Thin sections can be described as ophicalcite (calcite/dolomite) occurring alongside with opaques, e.g., magnetite and large areas with REE-rich allanite-group minerals (Fig. 73F). SEM-EDS analysis show a wide range of REE-minerals in this sample with an abundance of Nd-dominated minerals such as gadolinite-(Nd) and fluorocarbonates parisite-synchysite, which occurred as both the -Ce and -Nd analogues. Furthermore, allanite-(Ce) and fluorbritholite and britholite (Ce, Y) are observed. Titanium-REE minerals such as titanite-Y was observed, with a high Nd content, as well as aeschynite-(Nd). BSE image (Fig. 74) show "mélange" of REE-silicates with inclusions of xenotime. Preliminary observations of Nd-dominant fluorbritholite and britholite may confirm prior observations made by Holtstam et al. (2007), which speculated on the presence of an Nd fluorbritholite analogue at Malmkärragruvorna. Geochemical analysis showed elevated concentrations of REE (11,908 ppm), Y (682 ppm), U (111 ppm) and Sr (32 ppm) (Table 24).

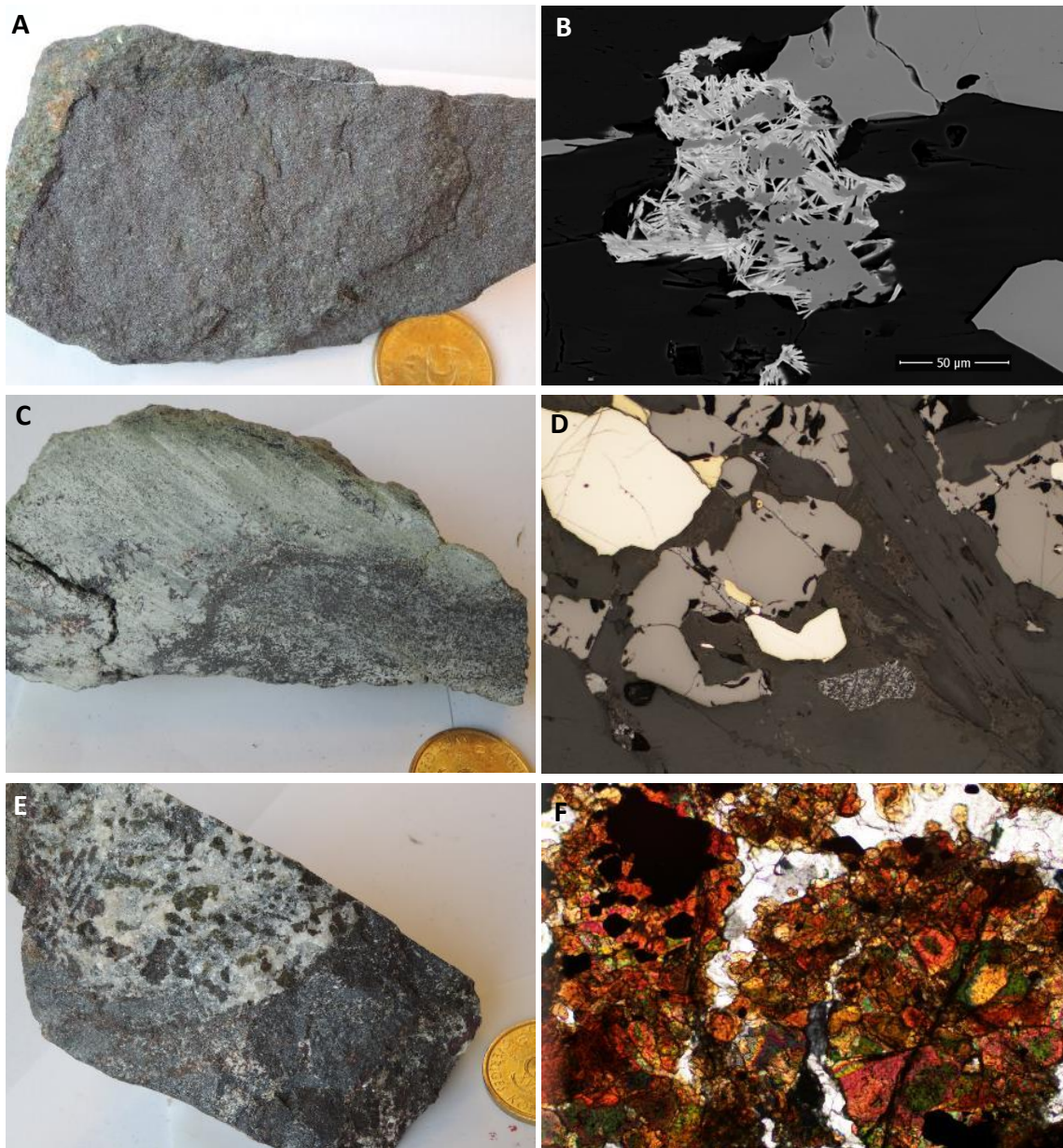


Figure 73 **A.** Whole rock sample JCA210065B with fine-grained magnetite, partly with green skarn. Photo: Gunnar Rauséus. **B.** BSE image from JCA210065B showing parisite (light needle like crystals) in magnetite (grey) and silicates (black). Photo: Patrick Casey. **C.** Sample JCA210065C with fine-grained iron oxide mineralisation with magnetite and amphiboles, mainly actinolite. Photo: Gunnar Rauséus. **D.** Thin section of JCA220065B (reflected light) shows magnetite (grey), chalcopyrite (yellow), pyrite (white) and amphiboles (dark grey). Photo: Gunnar Rauséus. **E.** Sample JCA210076B with opicalcite dominated by Mg-rich dolomite and porphyroblasts of serpentine and magnetite dissemination. Photo: Gunnar Rauséus. **F.** Thin section from JCA210076B (ppl) rich in REE minerals showing high interference colours in a ground mas of calcite/dolomite (white) and magnetite (opaque). Photo: Gunnar Rauséus.

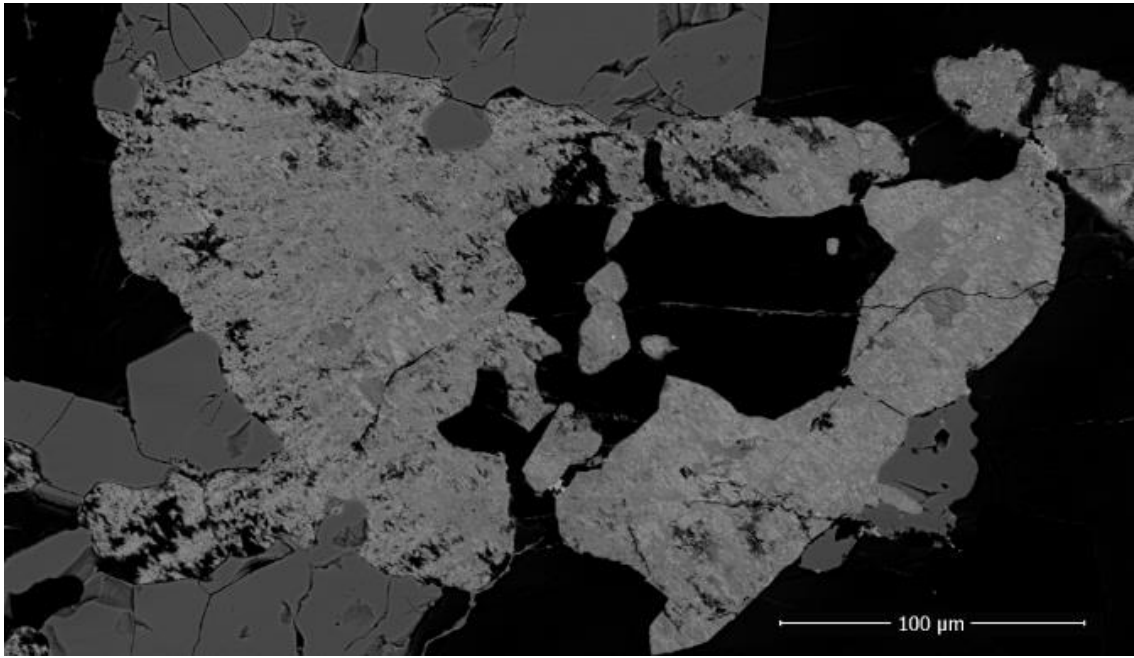


Figure 74. BSE image from sample JCA210076B with a "mélange" of REE-silicates (medium grey) with inclusions of xenotime (light grey). Photo: Patrick Casey.

JCA210076C is characterised as an amphibole skarn, rich in sulphides, mainly chalcopyrite, and up to centimetre-sized crystals of red-brown REE-minerals (Fig. 75A). Small grains of scheelite are observed with UV-light in the hand specimen.

SEM-EDS analysis shows presence of REE-minerals such as parisite, synchysite, fluorbritholite and gadolinite. Analysis also confirms, fluorbritholite appearing in chlorite, and common were "melanges" of REE minerals in single grains, typically parisite/synchysite and gadolinite (Fig. 75B). Gadolinite and magnetite often had inclusions of a uranium carboxyl mineral. Somewhat abundant scheelite explains the elevated W content in the sample. The analytical results for the whole rock show elevated values for Cu (5,900 ppm), W (3,170 ppm), Fe₂O₃ (46.2%), U (235 ppm) and REE (1,498 ppm) (Table 23). Notable for this sample is a depletion of LREE elements such as La, Ce, Pr and Nd relative to other selective samples from Malmkärragruvorna (Fig. 76).

A chondrite normalised REE diagram is seen in Figure 76. All selective samples show negative Eu anomaly. In sample JCA210076C a depletion in the lightest REEs is seen, with an enrichment towards the middle REEs. Sample JCA210076B shows a depletion of LREE relative to the MREE, which can also be seen in the results from the composite samples. Neodymium was enriched in this sample, and the sample hosts a varied Nd-rich mineralogy.

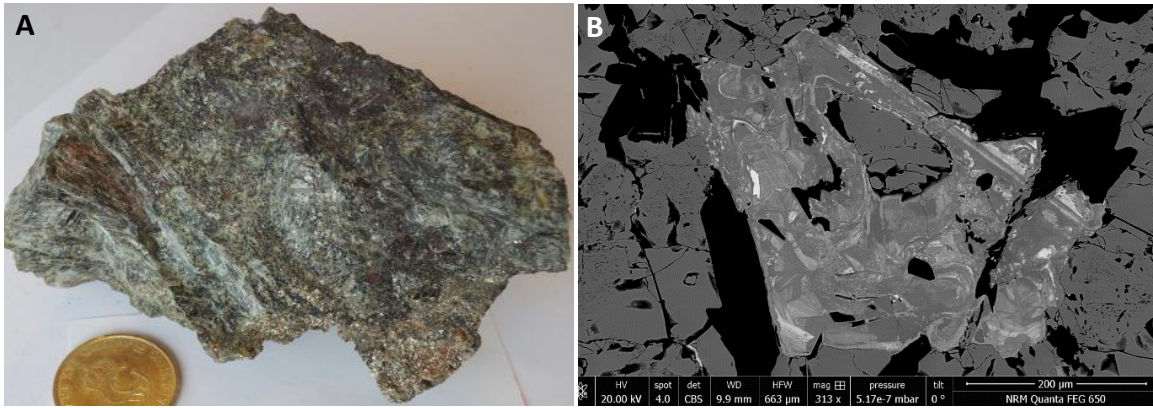


Figure 75. A. Sample JCA210076C amphibole skarn, rich in sulphide (mainly chalcopyrite) and dark REE minerals. Photo: Gunnar Rauséus. **B.** BSE image of sample JCA210076C show mixture of parisite (light grey to white) and gadolinite (medium grey) surrounded by magnetite (grey) and silicates (black). Photo: Patrick Casey.

Table 24. Selected geochemical data for selective samples from Malmkärragruvorna.

Sample	Fe ₂ O ₃ %	Cu ppm	Ga ppm	Rb ppm	Sr ppm	U ppm	Y ppm	W ppm	LREE ppm	HREE ppm	REE ppm
JCA210065B	78.7	19	144	2	1	2	42	20	800	38	838
JCA210065C	40.1	42	91	66	2	6	56	273	281	40	321
JCA210076B	35	9	114	2	32	111	682	28	11,012	896	11,908
JCA210076C	16.2	5,900	47	66	3	235	357	3,170	773	368	1,141

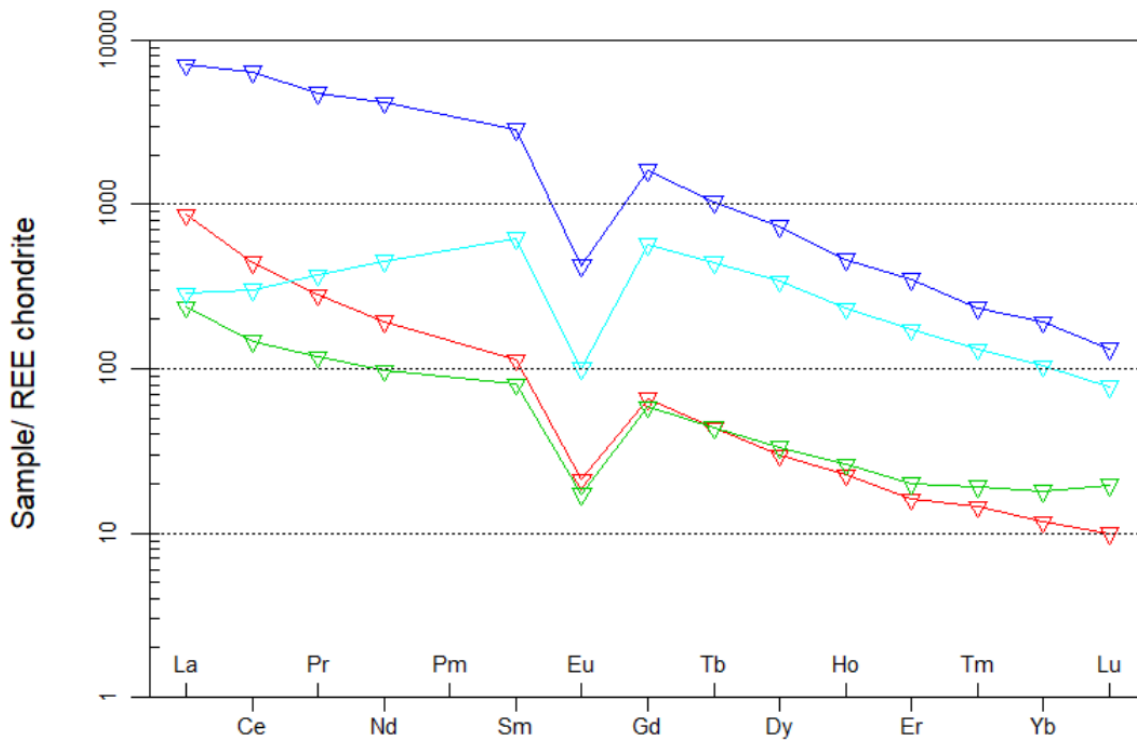


Figure 76. Chondrite normalised (Boynnton 1984) REE diagram from the four whole rock samples from the Malmkärragruvorna JCA210065B (red), JCA210065C (green), JCA210076B (dark blue) and JCA210076C (light blue).

Åsgruvan

Historical background

Åsgruvan is situated in the northern part of Norberg (Fig. 64) and belongs to the mining area Getbacksfältet (Geijer 1936). Mining at Åsgruvan was initiated around 1860 and was in production until 1963. Mine production statistics from the area includes several mines with a total production of 2.69 million tons of processed iron oxide, resulting in 0.573 million tons of waste rock (SGU 2023).

The magnetite ore occurs within carbonate rocks, both limestone and dolomitic marble. The skarn which coexists with the iron oxide mineralisation is composed of diopside, actinolite and garnet. The diopside being whitish green indicates that the iron content is low (Geijer 1936).

Waste rock

The sampled area around Åsgruvan is located to the southwest of the open pit as well as in the vicinity of the mineshaft. It is to a great extent overgrown by moss and trees (Fig. 77A) which made it hard to estimate the extension of the waste rock area. The sampling was conducted in an area of ca. 7,500 square metres, Figure 77B. The size of the sampled boulders varies between 5–30 centimetres. The material is dominated by iron oxide mineralised rock followed by metavolcanic rocks and greenish diopside skarn with garnet. A small number of samples are characterised as sulphide bearing, mainly with chalcopyrite and pyrite. A few samples show hydrothermal alteration, containing mica minerals such as biotite. Distribution of rocks in composite sample is compiled in Figure 78. Three mineralised selective samples were collected for chemical characterisation and thin sections studies.

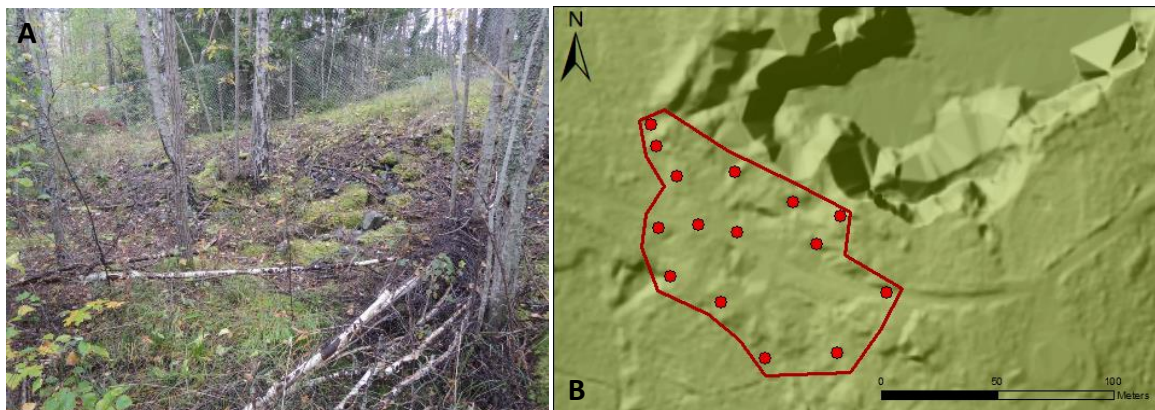


Figure 77. A. Part of sampling area with sporadic waste rock material visible. Photo: Gunnar Rauséus. B. Lidar picture with red polygon showing the sampled area and the red dots the distribution of composite sampling.

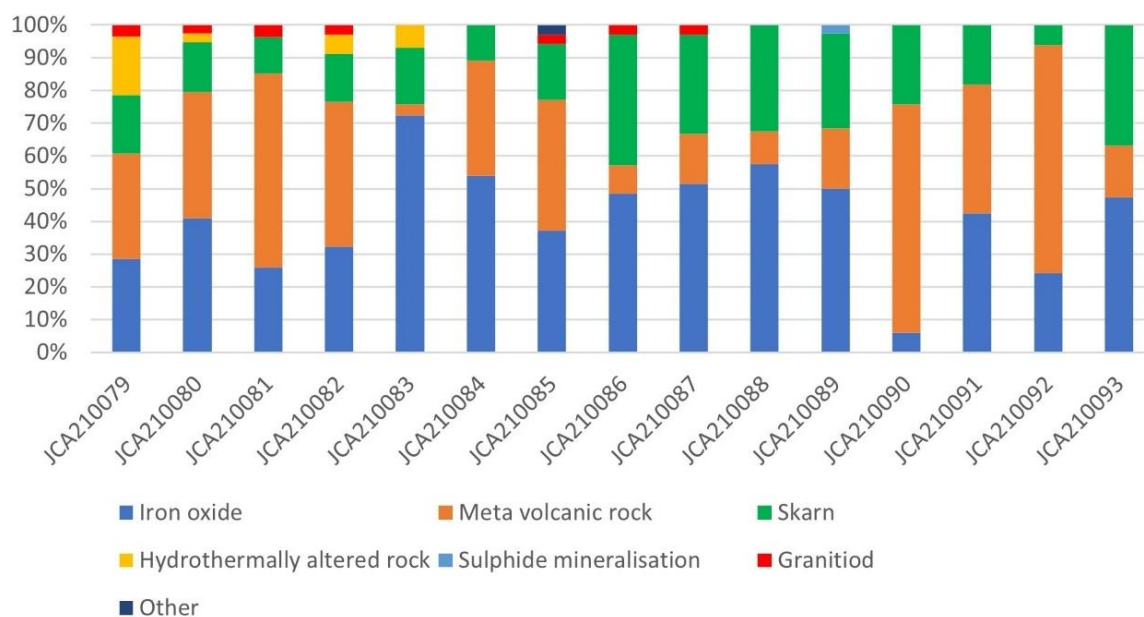


Figure 78. Distribution of rocks in composite samples from Åsgruvan (n= 15).

Results composite sampling

The analytical results from the composite samples from Åsgruvan show elevated values for Fe₂O₃, Ba, Mo and REE (Table 25). LREE is dominating and constitutes ca. 90% of total REE content. In Figure 79 most of the samples show a strong negative Eu anomaly; however, a few samples have a more moderate depletion in Eu and with one composite sample shows depletion in Ce and La.

Table 25. Selected geochemical data for waste rock composite samples from Åsgruvan (n=15).

Element	Fe ₂ O ₃ %	Ba ppm	Mo ppm	LREE ppm	HREE ppm	REE ppm
Average	28.6	297	142	359	39	398
Min	7.7	22	2	112	17	129
Max	45.5	955	1,760	1,138	76	1,214
Median	30.2	209	21	297	36	340

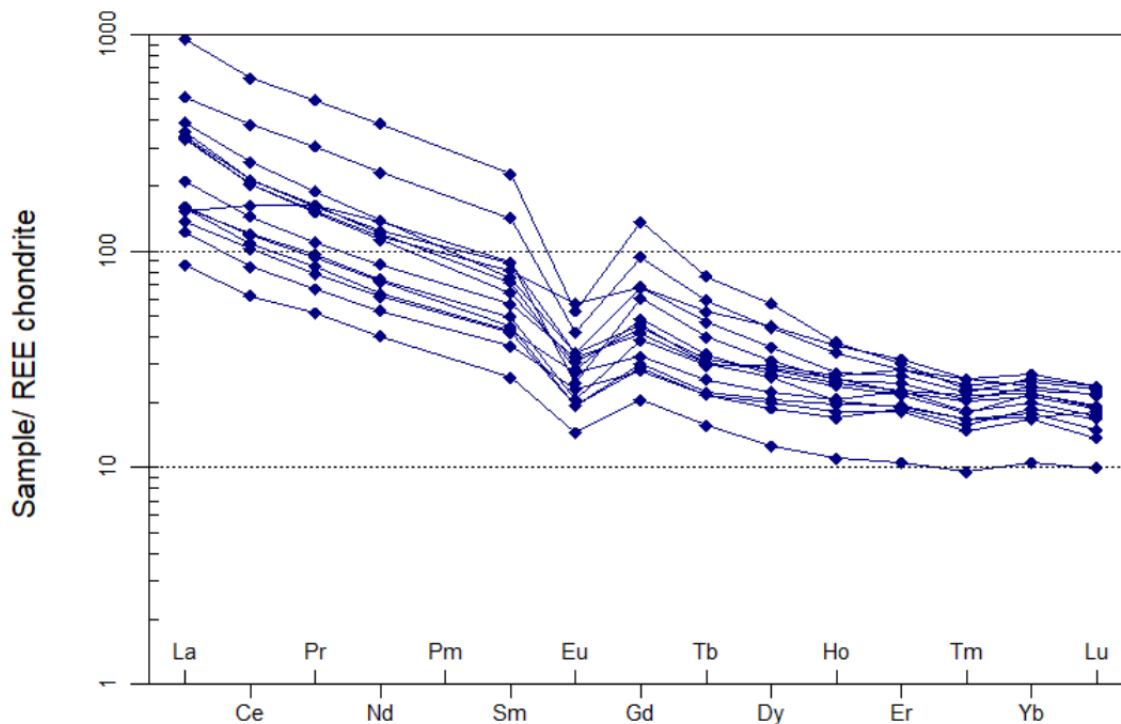


Figure 79. Chondrite normalised (Boynnton, 1984) REE diagram from the composite samples from Åsgruvan (n =15).

Results selective sampling

Three richly mineralised samples were chosen for whole rock analysis JCA210083B, JCA210086B and JCA210093B.

JCA210083B is characterised as fine-grained magnetite mineralisation in green amphibole skarn (Fig. 80A). Thin section observations showed abundant magnetite with occasional molybdenite, pyrite and chalcopyrite. The amphibole is dominated by tremolite and actinolite. REE-bearing allanite occurs along with magnetite in some areas (Fig. 80B).

SEM-EDS analyses identified the REE-bearing minerals as dominated by allanite-(Ce) and fluorocarbonate such as parisite-synchysite-(Ce). Part of the pyrite show inclusion of Bi- and Te-sulphide minerals and also small sized crystals of sulfosalt with Bi and Pb. Small amounts of scheelite and fluorite are present. Geochemical analysis shows elevated concentrations for Fe_2O_3 (52.2%) and REE (306 ppm) (Table 26).

JCA210086B is characterised as a green, banded quartz-epidote white magnetite dissemination (Fig. 80C). Thin section shows banded fine-grained quartz and epidote with diffuse magnetite crystals (Fig. 80D). Notable elements with elevated grades are Fe_2O_3 (24.7%) and REE (148 ppm) (Table 26).

JCA210093B is a dark coloured, fine to medium-grained amphibole skarn with abundant magnetite mineralisation (Fig. 80E). In addition to magnetite, areas rich in elongated crystals of molybdenite, chalcopyrite and pyrite are seen in thin section (Fig. 80F). Notable elements with elevated concentrations are Fe_2O_3 (87.4%), Mo (1.85%) and Cu (692 ppm) (Table 26).

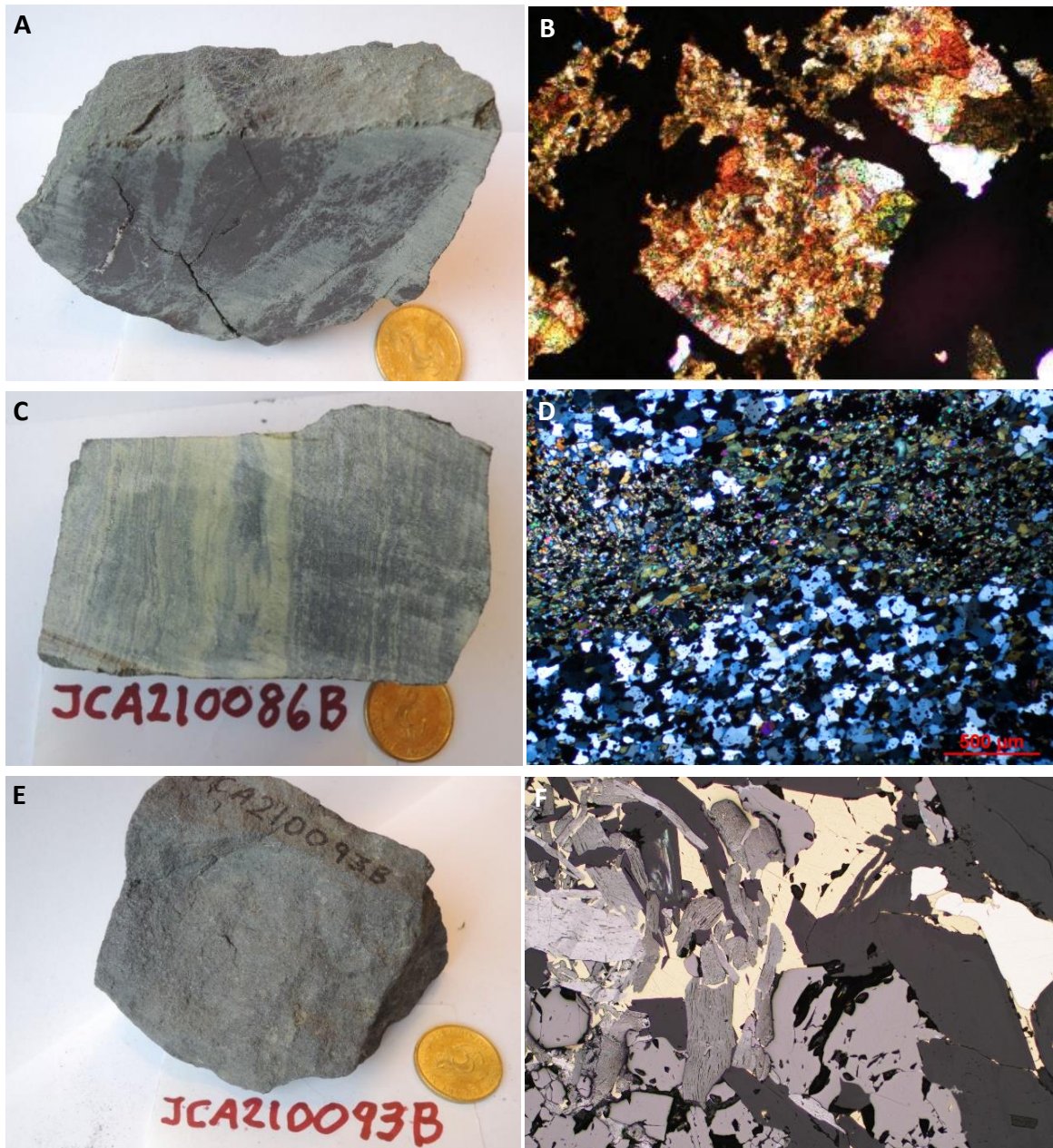


Figure 80. A. Sample from JCA210083B magnetite in amphibole skarn. B. Thin section of sample JCA210083B (PPL) with allanite (high interference colours) within magnetite (opaque). C. Sample JCA210086B with banded epidote-quartz skarn. D. Thin section of JCA210086B (XPL) showing banded fine-grained epidote (green-brownish) – quartz (light to blue) skarn with magnetite dissemination (opaques). E. Mineralised sample JCA210093B of skarn with abundant magnetite mineralisation. F. Thin section of JCA210093B (reflected light) with magnetite (brownish-grey), molybdenite (elongated light to dark grey minerals), chalcocopyrite (yellow) and pyrite (creamy-white). Photos: Gunnar Rauséus.

Table 26. Selected geochemical data for selective samples from Åsgruvan.

Sample	Fe ₂ O ₃ %	Cu ppm	Mo ppm	Y ppm	LREE ppm	HREE ppm	REE ppm
JCA210083B	52.2	124	5	36	282	24	306
JCA210086B	24.7	2	1	29	129	20	148
JCA210093B	87.4	692	18,500	2	4	1	5

Östanmossgruvan

Historical background

Östanmossgruvan is situated in the northern part of the Norberg mine field (Fig. 64) and belongs to the Röbergfältet. Östanmossgruvan produced iron ore from a skarn iron oxide ore in the period from 1859 to 1934. The mine was worked underground to a depth of 115 metres. During the years 1908 to 1931 the production of iron ore products was 232,000 tonnes (Geijer 1936). There is no data available for amount of waste rock produced and the mine was waterfilled in 1931.

The mineralisation constitutes of magnetite impregnated skarn dominated by actinolite and dolomitic to calcitic marble (Hellström 2022). The mineralisation includes areas enriched with Ce-minerals and is regarded as a Bastnäs-type REE deposit, belonging to the subtype 2 (Norberg type) in that it is enriched in heavy REE (Jonsson et al. 2019). The REE deposits are hosted in skarns associated with marble horizons in a strongly Na/K and/or Mg-altered meta volcanic succession. The Östanmossgruvan deposit is type locality for dollaseite-(Ce), arrheniusite-(Ce), and norbergite.

Waste rock

Sampling of waste rock was restricted to areas around the waterfilled open pit and Filips's shaft (Fig. 81). The waste rock material is found at east and southeast side of the open pit. The deposit area is to a large extent overgrown by moss and trees with some larger piles rising up, exposing waste rock material with coarse material (Fig. 82A and B). The sampled boulders size varies between 5–30 cm. The sampled material is dominated by iron oxide mineralisation, skarn, carbonate rock, metavolcanic rock, and occasional sulphide mineralisation. The distribution of rocks is presented in Figure 83. Three mineralised selective samples were collected for chemical characterisation and thin sections studies.



Figure 81. Red polygon outlines the sampled area at Östanmossgruvan. Yellow dots represent the sampling point.



Figure 82. A. Picture of well exposed waste rock pile with large boulders. B. Picture of overgrown waste rock areas at Östanmossgruvan. Photos: Gunnar Rauséus.

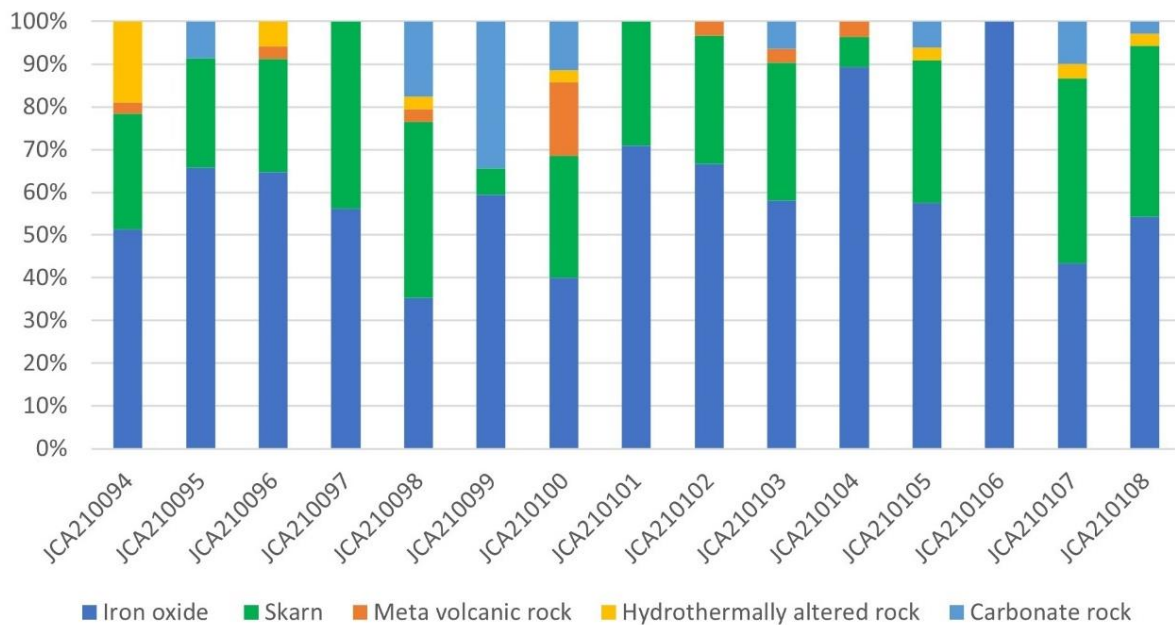


Figure 83. Distribution of rocks in composite samples from Östanmossgruvan.

Results composite sampling

The analytical result from the composite samples shows elevated average concentration for Fe₂O₃ (31.1%), Be (10 ppm) and REE (1,444 ppm) (Table 27). LREE constitute ca. 85% of total REE. All the samples show a negative Eu anomaly (Fig. 84).

Table 27. Selected geochemical data for waste rock composite samples from Östanmossgruvan (n=15).

Element	Fe ₂ O ₃ %	Be ppm	Cu ppm	W ppm	LREE ppm	HREE ppm	REE ppm
Average	31.1	10.3	194	84	1,225	217	1,442
Min	17.7	3.7	4	36	475	102	636
Max	40.4	16.9	607	161	1,880	302	2,182
Median	29.5	9.9	176	77	1,244	212	1,512

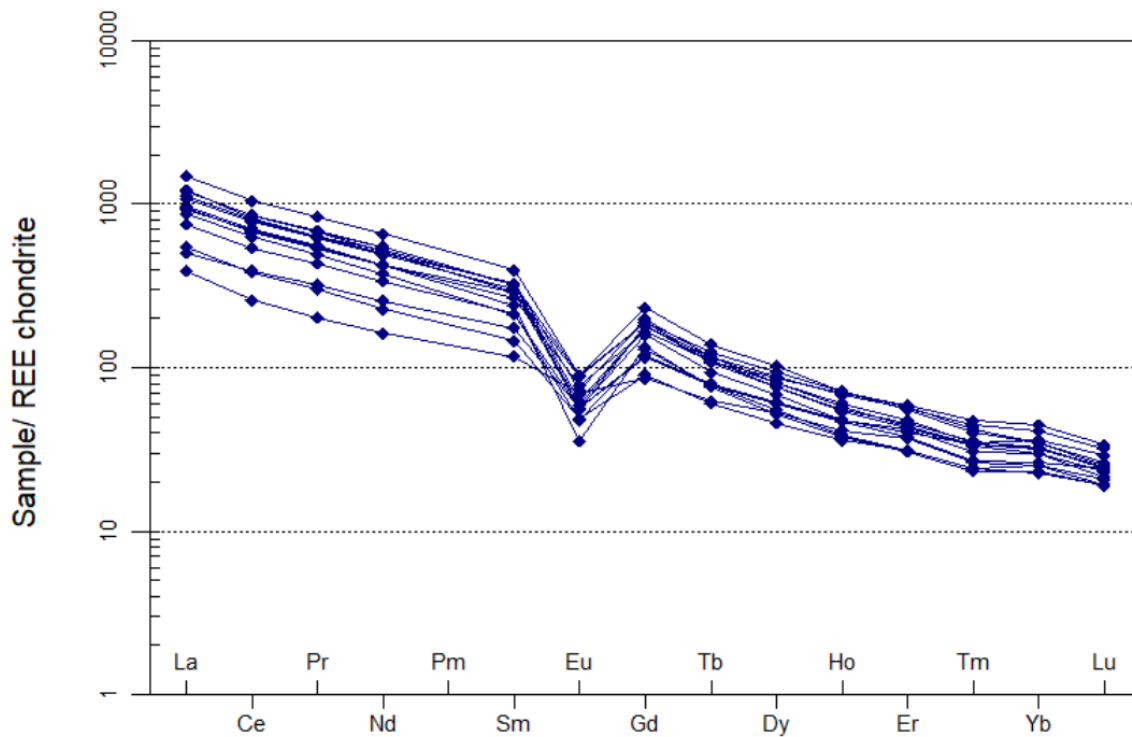


Figure 84. Chondrite normalised (Boynton 1984) REE diagram from the composite samples from Östanmossgruvan.

Results selective sampling

Three richly mineralised samples were selected for whole rock analysis, JCA210098B, JCA210099C and JCA210106B.

JCA210098B is characterised as a fine-grained, light grey to dark volcanic rock (Fig. 85A), partly rich in disseminated fine-grained magnetite and sulphide mineralisation with predominantly chalcopyrite. SEM-EDS analyses identified small grains of monazite-(Ce), allanite-(Ce) and minerals belonging to the gadolinite-group enriched in Y, Nd and Ce. Minor inclusions of bismuthinite were observed within chalcopyrite. Whole rock analysis shows elevated grades for Fe_2O_3 , Cu, Bi, Sr and REE (Table 28).

JCA210099C constitutes of a fine-grained amphibole skarn rich in patches of fine-grained magnetite mineralisation (Figs. 85B and C). Scheelite is detected with UV light as small grains in the rock and confirmed with SEM-EDS analysis in thin section. Scheelite occurs as inclusions in magnetite, often with grain size less than 50 micrometres. The whole rock analysis shows elevated grades for Fe_2O_3 and W (Table 29).

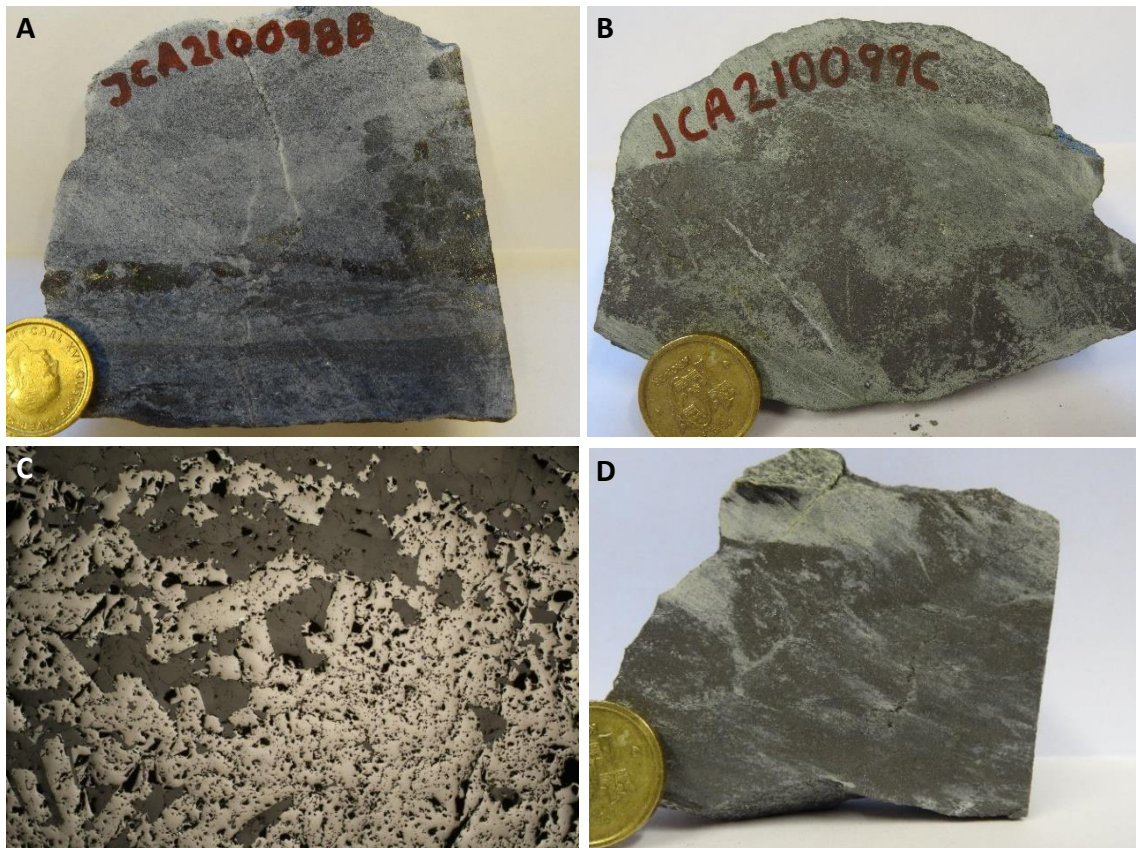


Figure 85. A. Whole rock sample JCA210098B with volcanic rock partly with magnetite mineralisation. B. Whole rock sample JCA210099C with amphibole skarn rich in patches of fine-grained magnetite mineralisation. C. Thin section of JCA210099C (reflected light) with magnetite (light grey) in a groundmass of amphibole (dark grey) D. Whole rock sample JCA210106B with amphibole skarn rich in iron oxide mineralisation of magnetite. Photos: Gunnar Rauséus.

JCA210106B is characterised as fine-grained amphibole skarn rich in iron oxide mineralisation of magnetite (Fig. 85D). REE-bearing minerals were observed as grains and fracture fillings with a mix of different fluorocarbonates such as parisite and synchysite enriched in Nd, Ce and La, and minerals belonging to the britholite-group enriched in Y. Small grains of scheelite and bismuthinite occurs as inclusions within the magnetite. Whole rock analysis shows elevated grades for Fe₂O₃ and REE (Table 29).

A chondrite normalised REE diagram according to Boynton (1984) for the composite samples can be seen in Figure 86. All samples show a strong negative Eu anomaly. Sample JCA210099C (green) shows a flat curve while sample JCA210106B (blue) shows strong depletion in the HREE.

Table 28. Selected geochemical data for selective samples from Östanmossgruvan.

Sample	Fe ₂ O ₃ %	Bi ppm	Cu ppm	Sr ppm	Y ppm	LREE ppm	HREE ppm	REE ppm
JCA210098B	30.9	55	3,750	17	61	211	35	246

Table 29. Selected geochemical data for selective samples from Östanmossgruvan.

Sample	Fe ₂ O ₃ %	W ppm	Y ppm	LREE ppm	HREE ppm	REE ppm
JCA210099C	48.6	237	17	20	9	29
JCA210106B	56.9	101	62	1866	73	1,939

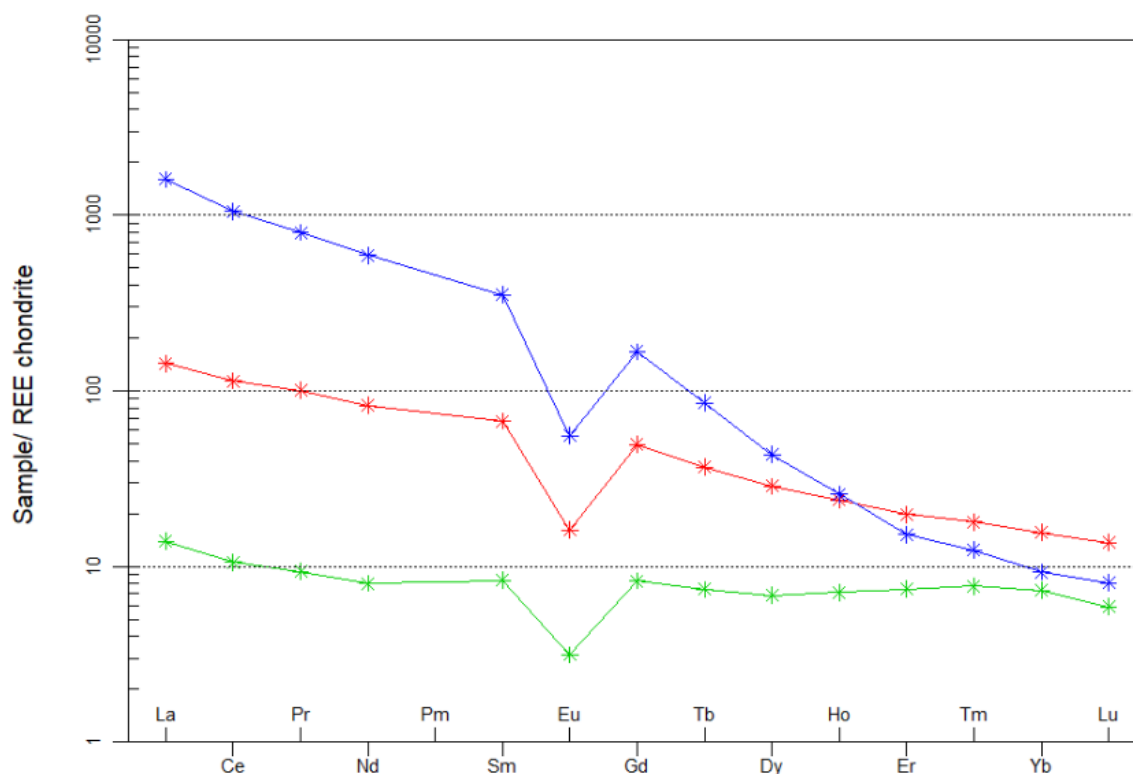


Figure 86. Chondrite normalised (Boynton 1984) REE diagram from the three whole rock samples from Östanmossgruvan, JCA210098B (red), JCA210099C (green) and JCA210106B (blue).

VENA ORE FIELD

Existing and historical data

The Vena iron, copper and cobalt mines are situated approximately 3 km northeast of the town of Ämmeberg in Örebro county (Fig. 87). Mining has taken place in hundreds of small iron oxide deposits since the 18th century. The copper and cobalt operations at Vena were active intermittently between the years of 1770 and 1880, and in the beginning focused on copper production. In the beginning of the 19th century cobalt production started, and from 1812 onwards cobalt was the main economic mineral. This resulted in a production of in total ca. 416 metric tons of ore with an average grade of 0.1–0.5% Co (c). In 1852, the mining ended due to a diminishing market for cobalt.

Descriptions of the mineralisations at Vena and surroundings can be found in Wikström & Karis (1991), Blomberg & Holm (1902), Tegengren et al. (1924), Geijer & Magnusson (1944), Henriques (1964), Sundblad (1994) and Lewerentz et al. (2020). Vena orefield constitutes type locality for the Pb-Cu-Sb-Bi-sulphosalt minerals kobellite (Setterberg 1839), izoklakeite (Zakrzewski & Makovicky 1986) and jaskolskiit (Zakrzewski 1984). Sulphide mineralisations containing chalcopyrite, cobaltite and kobellite occurs in a felsic metavolcanic rock with rhyolitic to andesitic composition (Lewerentz et al. 2020). At Skuru Gruvor about 8 km to the north of Vena ore field a recent investigation shows anomalous grades of REE (0.71% total REE; Lewerentz et al. 2020)

Earlier lithochemical analysis from Vena ore field are included in the SGU database Lithochemistry. The existing geochemical data derives from field studies by SGU in 2018 and sampling of waste rock by Bäckström (2005). These analyses are made on both rock samples and mineralised samples and waste rock.

Airborne geophysics

Both LKAB and SGU have made airborne geophysical surveys over the Vena area; LKAB has made one while SGU has made two. These surveys cover the entire area displayed in Figures 87–91 and more information can be found in Table 30. The most recent airborne survey by SGU was carried out along northeast–southwest striking flight lines, which is more advantageous compared to the previous surveys since it is roughly perpendicular to the strike of the distribution of various rocks. Also, by acquiring information from two VLF transmitters, it is possible to derive datasets which identify electrically conductive zones in the ground independent of their strike with regards to the transmitters.

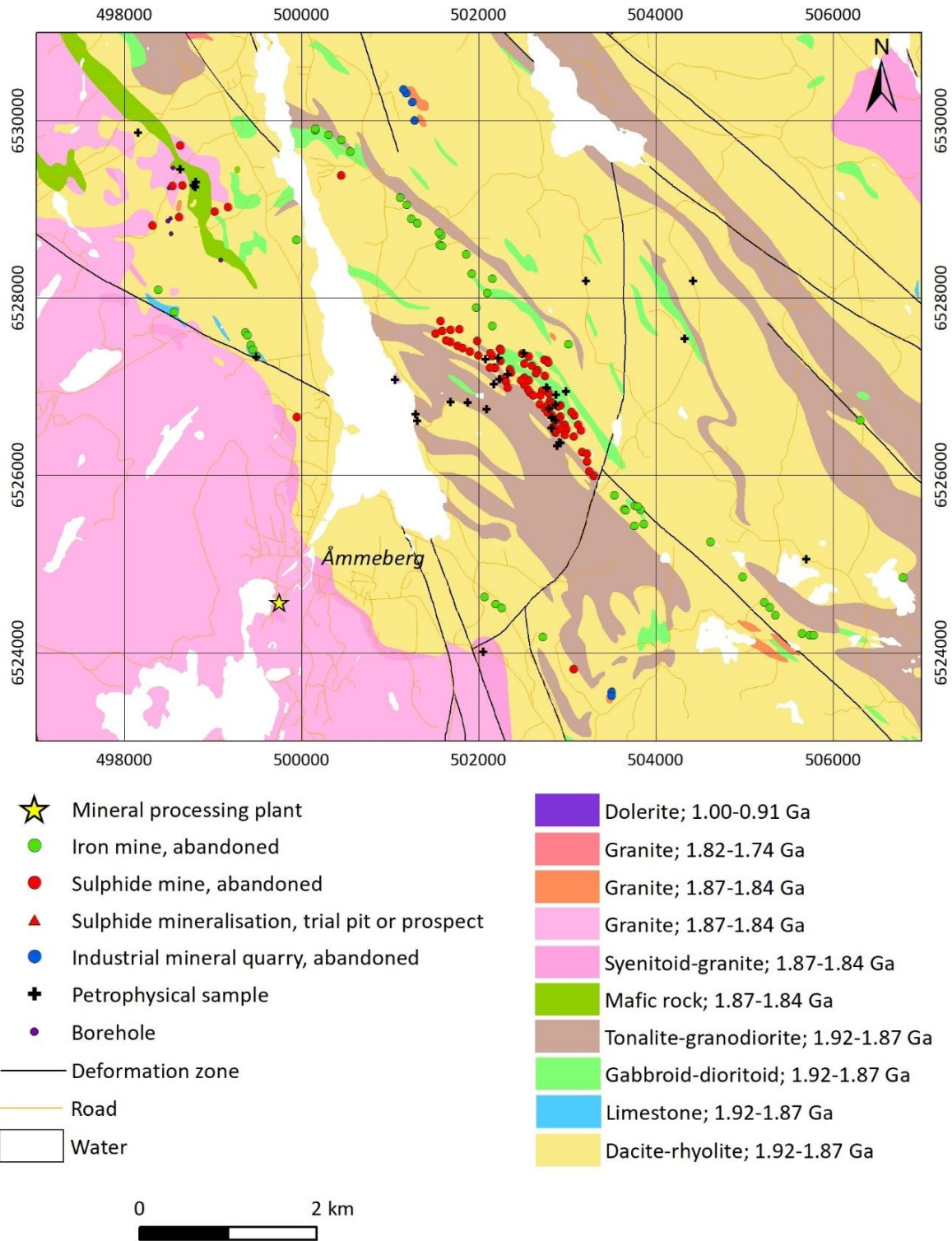


Figure 87. Simplified bedrock map over the Vena area (SGU 2022).

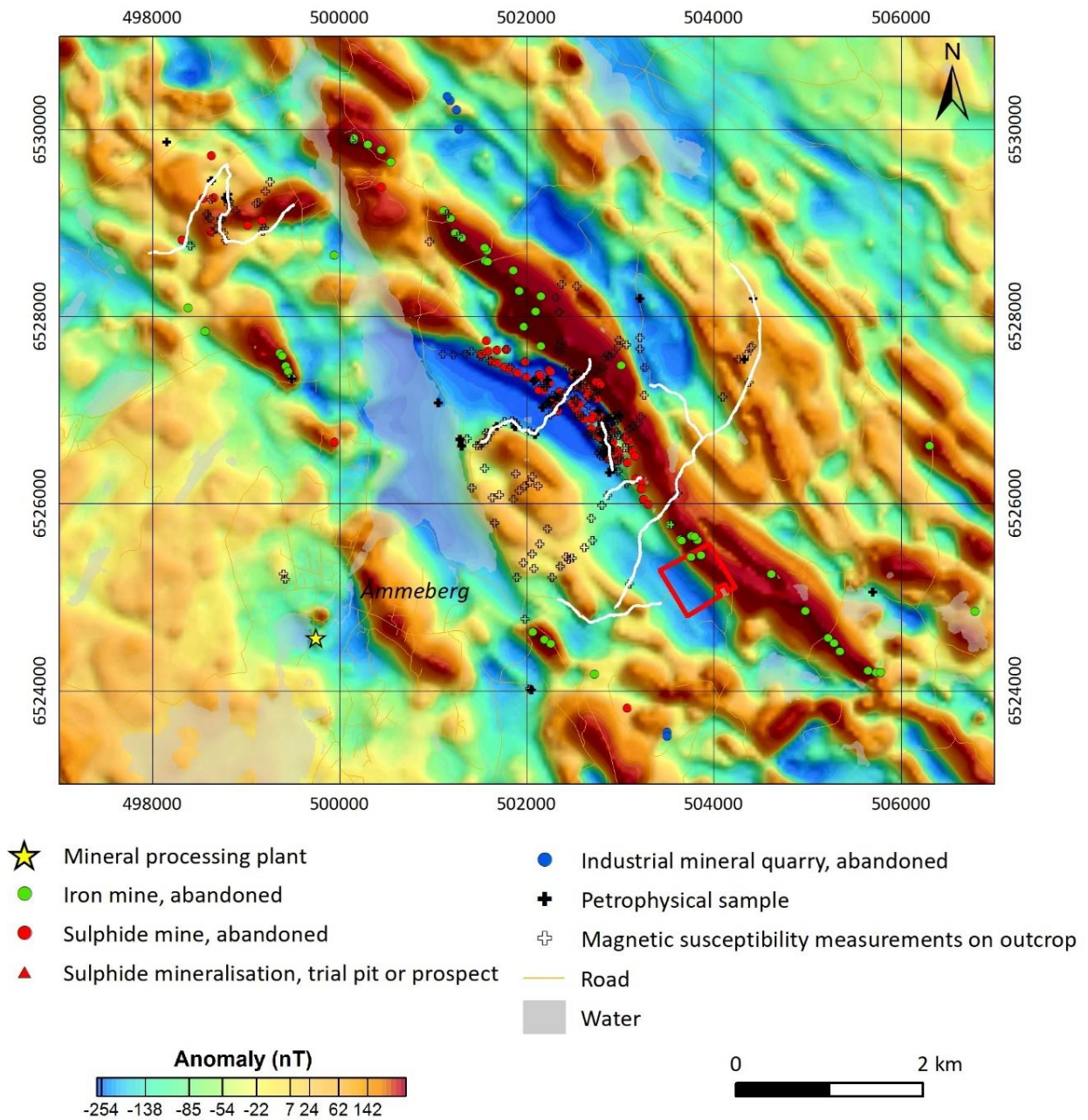


Figure 88. Map showing the magnetic anomalies, derived from SGU’s airborne measurements in 2018, at the investigated area in this study along with its surroundings. White lines show profiles along which ground magnetic data previously have been acquired. The red polygon in the lower part of the figure delineates an area where previously dense ground magnetic measurements have been carried out (Fig. 90).

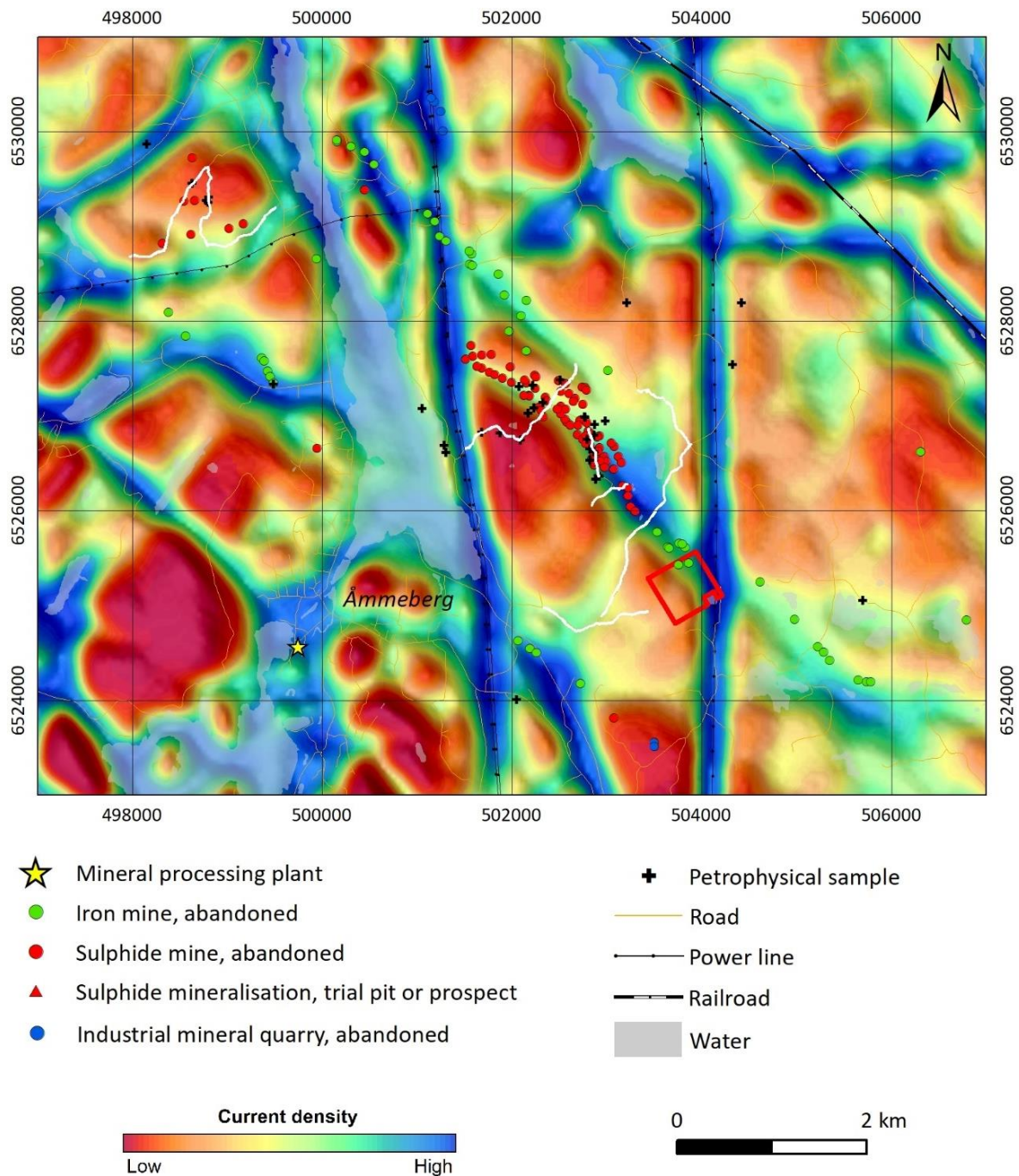


Figure 89. Map showing the current density in the ground at the investigated area in this study along with its surroundings. The current density is derived from airborne VLF measurements from two transmitters, acquired by SGU in 2018. White lines show profiles where ground VLF data previously have been acquired. The red polygon in the lower part of the figure delineates the area where previous dense ground IP, SP, and resistivity measurements have been carried out.

Table 30. Previously acquired airborne geophysical data by SGU or LKAB over the area around Vena.

Year	Organisation	Geophysical methods used	Flight direction	Flight line separation (m)	Flight altitude (m)
1979	LKAB	Magnetics, gamma spectrometry, VLF (1-transmitter)	North–south	200	30
1980	SGU	Magnetics, gamma spectrometry, VLF (1-transmitter)	North–south	200	30
2018	SGU	Magnetics, gamma spectrometry, VLF (2-transmitters)	Northeast–southwest	200	60

Ground geophysics

During previous bedrock mapping projects at SGU, ground magnetic and VLF data have been acquired along certain profiles in the area around the Vena mine district (Figs. 88 and 89). These measurements have been carried out to serve as information for modelling the various rocks with respect to their geometry and depth extent, also in conjunction with other geophysical methods like gravity data, and together with information from analysed petrophysical samples. In addition to this, LKAB has previously carried out dense ground magnetic, SP, IP, and resistivity measurements in the southeastern part of the Vena mine area. These ground geophysical measurements were carried out in 1982, along eight semi-parallel profiles. The length of each profile is around 600 m and the distance between them varies from 40 to 150 m. Along the profiles, measurements were made with just a few metres spacing. Data from the ground magnetic survey are presented in Figure 90.

In the area around Vena, three gravity surveys have been carried out from which data are stored in SGU's gravity database. These surveys have been carried out by LKAB, Zinkgruvan AB, and SGU. During the gravity survey conducted by LKAB, in 1979, a regional net of gravity stations with approximately 1–3 km station spacing was established over the Vena area. During LKAB's survey, gravity data was also acquired primarily further south and east compared to what is visible in Figure 91. The gravity measurements by Zinkgruvan AB were primarily made at Zinkgruvan mine, which is located further south of the Vena area, but surrounding areas were also covered. Their measurements were done in the southern part of the area shown in Figure 91, up to north coordinate 6525500, and have a station spacing of approximately 1–2 km. SGU's gravity survey in 2018 was carried out with the aims of improving the regional net of gravity data and to achieve still closer spacing between the measurements along profiles at or near the mineralisations at Vena. The result of this approach results in a regional net of gravity data with approximately 1–1.5 km, or less, station spacing for the area shown in Figure 91. In addition to this, several northeast–southwest trending measurement profiles were made across a big part of the mineralised northwest–southeast striking sequence at Vena. Along these profiles, gravity measurements were made approximately every 200 m.

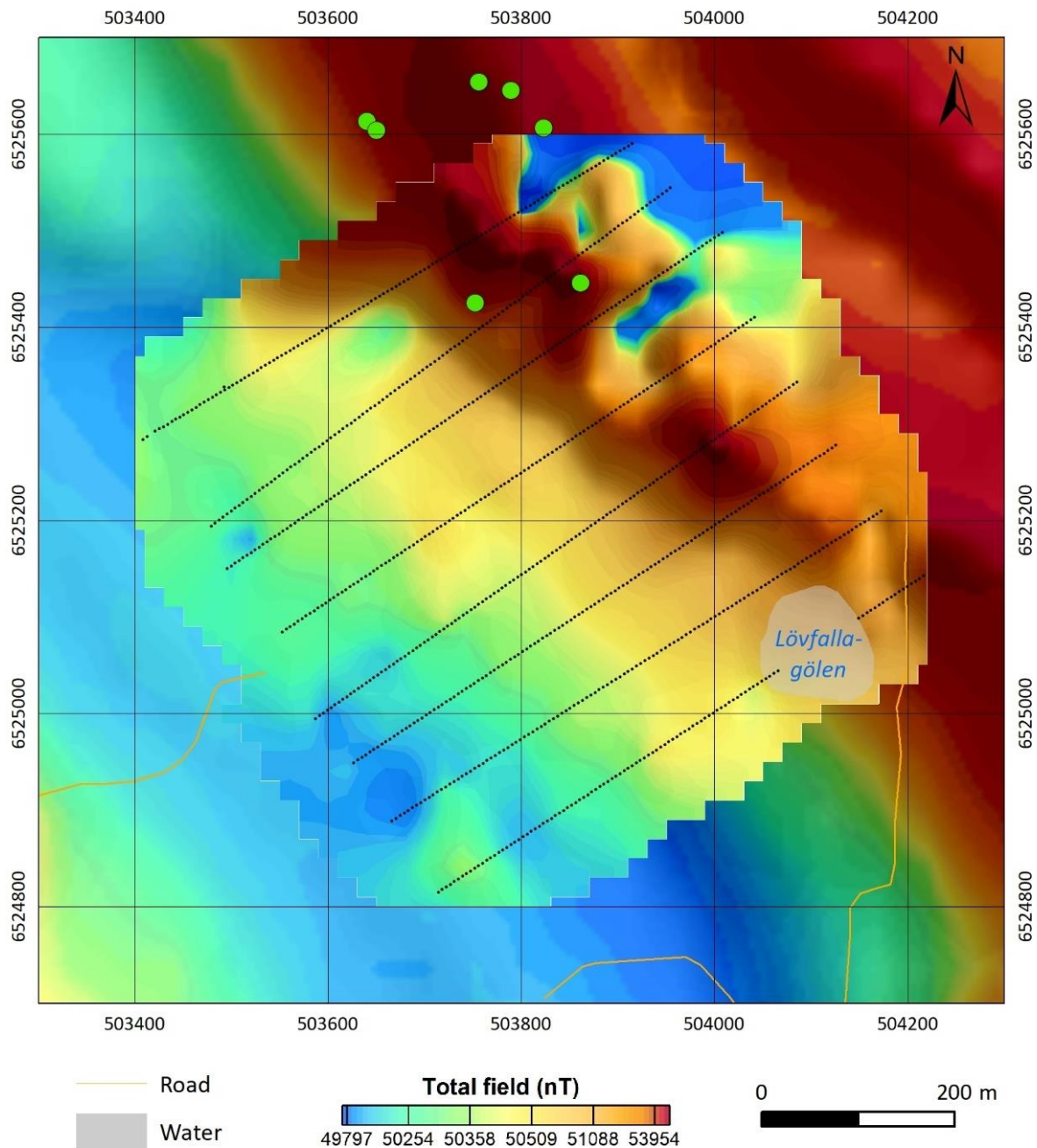


Figure 90. Map showing the total magnetic field, based on the ground magnetic measurements acquired in 1982 along the marked profiles where black dots represent measurement sites. Green dots in the upper part of the figure show the locations of abandoned iron mines. The magnetic anomalies from SGU's airborne survey in 2018 is shown as the backdrop image.

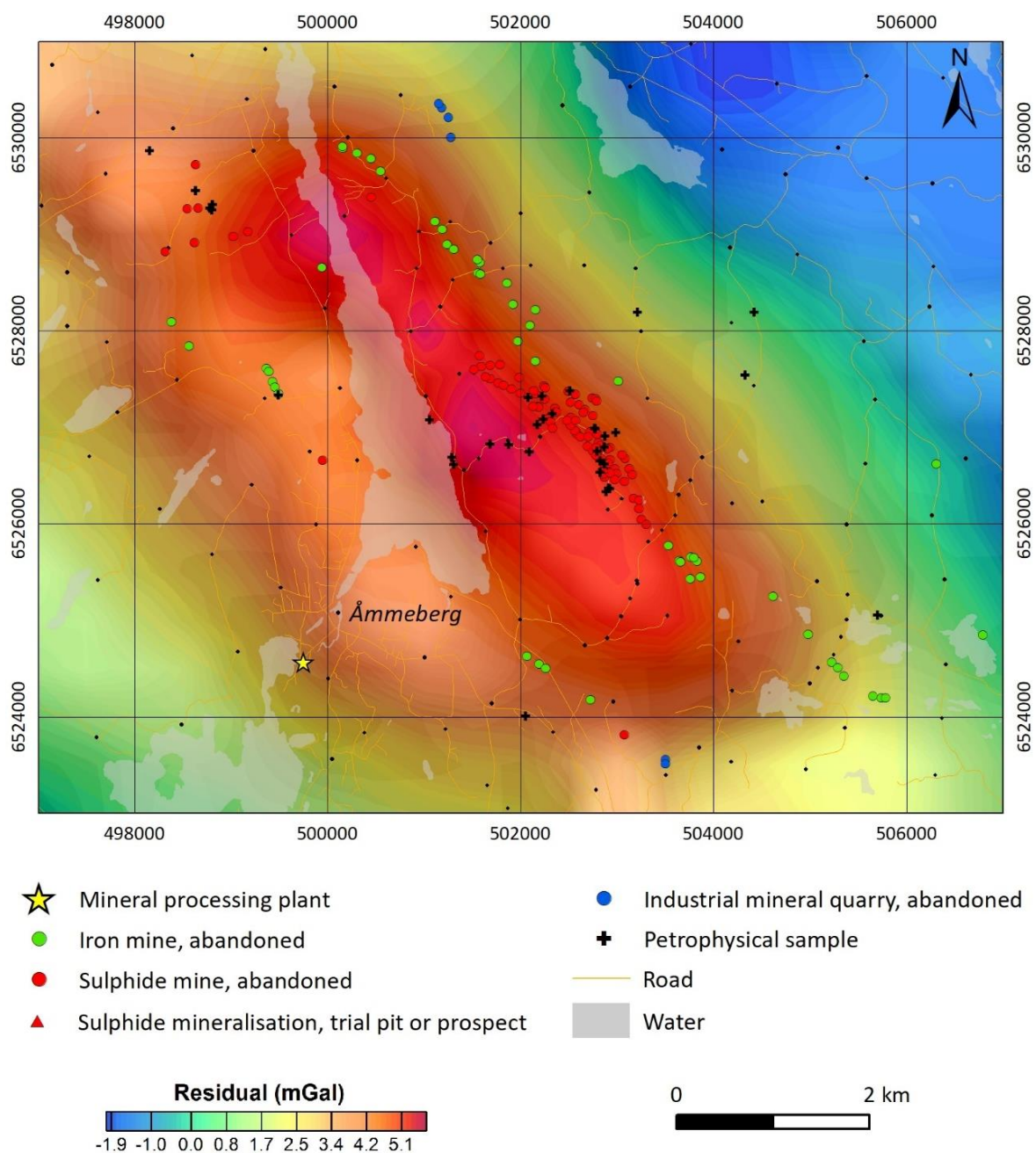


Figure 91. Map showing the residual gravity field at the investigated area in this study along with its surroundings. The residual gravity field is expressed as the difference between the Bouguer anomaly and an analytical continuation upwards to 3 km. Black dots represent localities for gravity measurements.

Waste rock

The Vena ore field consists of several water filled open pits and underground mines with large areas of waste rock material located between the mine sites (Fig. 92). The total sampled area is estimated to cover 40,000 m² with an unknown thickness, but the height of the waste rock piles varies by several metres. The whole area is well exposed and only sparsely overgrown by small pine trees (Fig. 93). The size of the material in the waste rock piles varies between 5 and 50 cm. The waste material often has a red weathered surface and consists almost exclusively of a fine-grained grey metavolcanic rock with some sulphide dissemination of visible chalcopyrite, pyrite and pyrrhotite. Some of the observed waste rock is strongly oxidised and mica altered, which makes it brittle. Three major waste rock areas were sampled with a total of 45 composite sample.

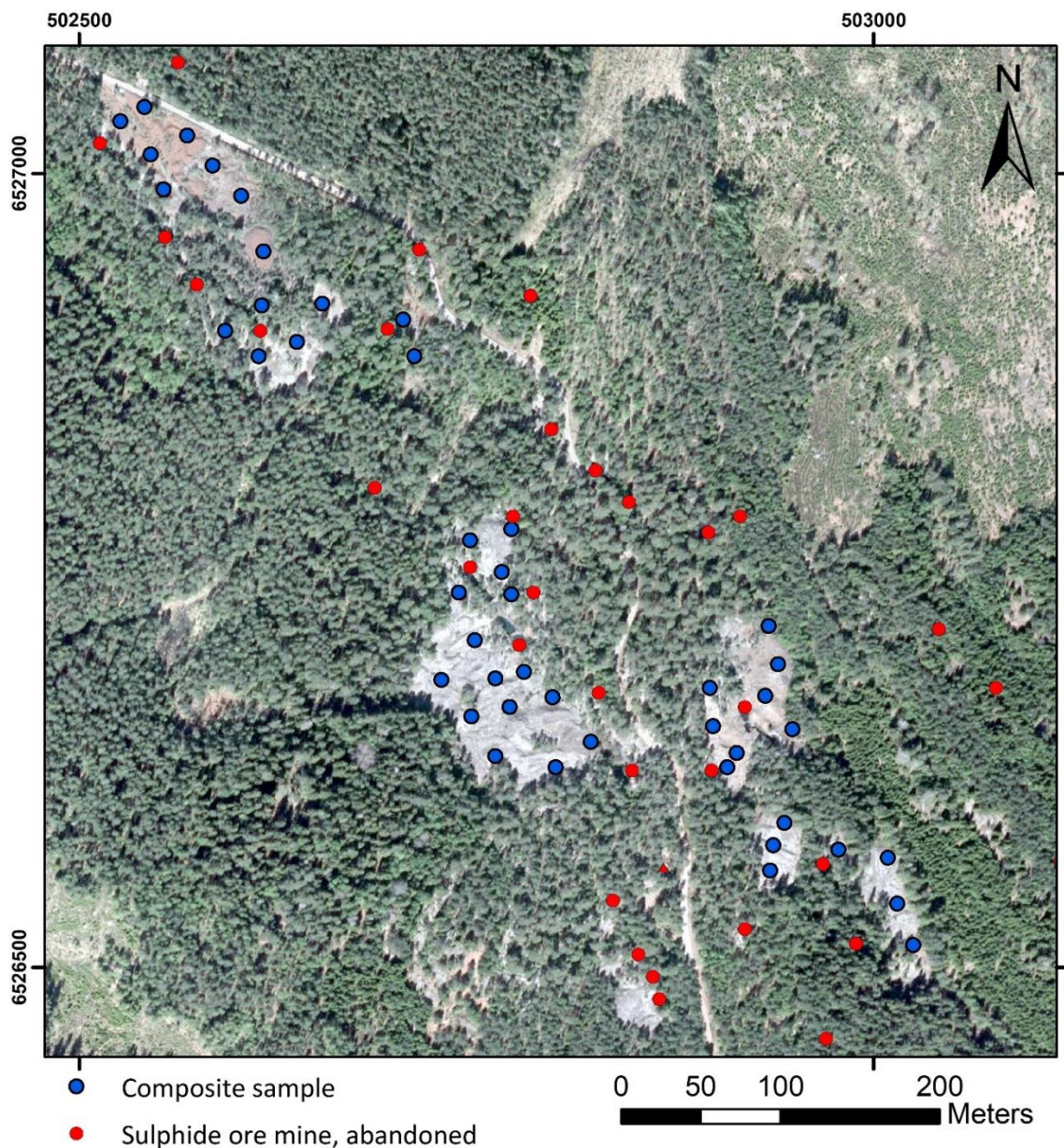


Figure 92. Orthophoto showing an overview of the sampled area. Red dots are historical mine sites (often open pits) and blue dots show locations of the composite samples.



Figure 93. Examples of the appearance of the waste rock piles at Vena ore field. Photos: Gunnar Rauséus.

Results composite sampling

The geochemical analysis of the waste rock samples shows elevated concentrations of Cu (0.29%), Zn (0.17%), Co (156 ppm) and Bi (130 ppm) (Table 31).

Table 31. Selected geochemical data for waste rock composite samples from Vena orefield (n = 45).

	Ba ppm	Bi ppm	Sb ppm	As ppm	Co ppm	Cu ppm	Zn ppm
Average (n=45)	651	129.8	34.54	857.9	155.6	2,896	1,695
Max	391	961	154	9,730	1,140	6,810	3,800
Min	1,100	1.66	2.04	120.5	16	484	282
Median	654	76.3	22.8	428	109	2,630	1,450

Potential resource

The SGU database (SGU 2023) provides a waste rock tonnage of 1,384 tonnes for the production period between 1807 and 1908. This is not realistically the total tonnage of waste produced since the sampled area is estimated to ca. 40,000 square metres and believed to contain a significantly larger tonnage, and therefore a probable potential resource calculation cannot be made for this location.

TUNABERG MINE AREA

Existing and historical data

Tunaberg mining area is located in the southern part of Bergslagen, about 15 km southwest of the town of Nyköping in Södermanland county. The mining history in the Tunaberg mining field dates back to the Middle Ages. The mining area was considered as a separate “Bergslag” and was privileged in the year 1420 by king Eric of Pomerania.

The most favourable period for the mining in the area was in the late 18th century, and with time the operations decreased until 1890 when it ended. However, one mine in the area (Mangruvan) was opened in 1920 and mined until 1956 for manganese and iron oxide.

Three main types of mineralisations are defined in the Tunaberg area. Marble- and skarn-hosted copper-cobalt mineralisation, volcanic- or supracrustal- and skarn-hosted zinc-lead mineralisations and skarn-hosted iron oxide deposits (Lewerentz et al. 2020). The geology in the Tunaberg area is described in Lundström (1974).

Historic production data is limited with a few exceptions. Skaragruvan was mined for zinc and copper between 1914 and 1916 resulting in 1,341 tonnes waste rock. Mangruvan (Mn, Fe) had a total production of 39,400 tonnes of ore resulting in 4,500 tonnes of waste rock (SGU 2023). The Tunaberg ore field near Koppartorp includes several smaller mines for copper and cobalt. Sampling at Tunaberg ore field was conducted at Sjöbergsgruvan, Österbergsgruvan, Näsmanngruvan and Kabbelgruven. The documented production between 1847 to 1895 in this area was 25,600 tonnes (SGU 2023).

Figure 94 show simplified bedrock map over the Tunaberg area and the location of the investigated mine sites.

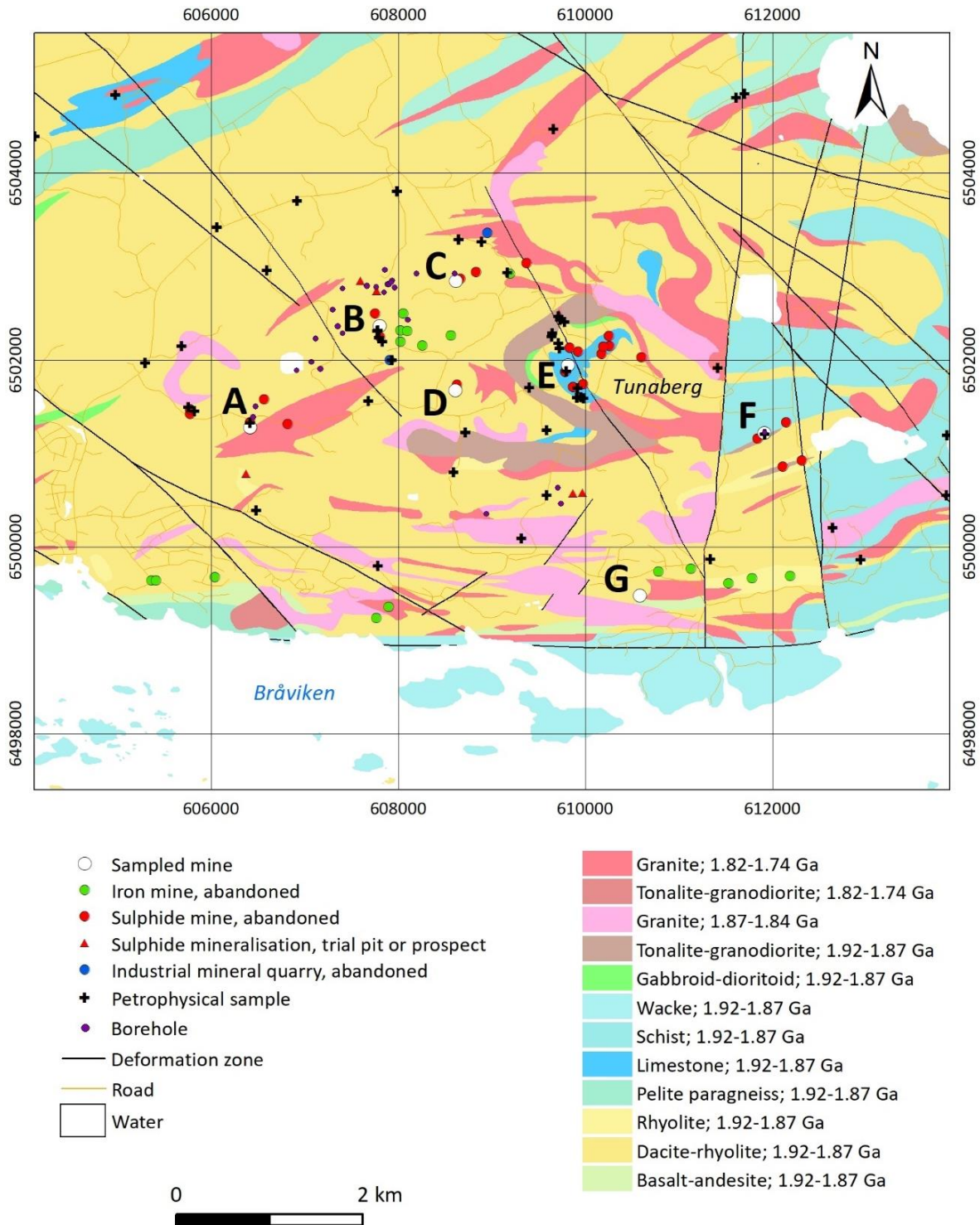


Figure 94. Simplified bedrock map over the Tunaberg area (SGU 2022). The investigated mine sites in this study are Mormorsgruvan (A), Kärngruvan/Blombergstorp (B), Hultebrogruvan (C), Strömbergsgruvan (D), Tunaberg ore field (E), Skaragruvan (F), Mangruvan (G).

Historical drill cores and lithochemistry

According to the SGU drill core database, 26 drill cores have been drilled in the Tunaberg mine area. The preserved drill cores are stored in the SGU drill core archive in Malå, Sweden. Logging protocols, assay results and other information is stored digitally and in physical archives. The cores were drilled by Boliden in the 1950s and BHP in the late 1990. Four of the more recent drill cores has been scanned using IR-technic within the framework of a SGU-project during the years 2014–2016. The result from the scanning is presented in SGU drill core database. Also, several lithochemical analysis from Tunaberg are included in the SGU database Lithochemistry.

Airborne geophysics

SGU has made three airborne geophysical surveys over the Tunaberg area. The first was conducted in 1970 when the Earth's magnetic field and naturally occurring gamma radiation from the ground were measured. The survey covered most of the area displayed in Figures 94–98. The second airborne survey was made in 1999 and it was made south of the previous one. During the survey in 1999, the instrumentation had been added with an EM instrument, capable of measuring VLF signals from two independent transmitters, which makes it possible to derive datasets that identify electrically conductive zones in the ground independent of their strike with regards to the transmitter. In 2020, the third survey was carried out which remeasured the area covered by the first survey in 1970. The updated magnetometer, gamma spectrometer, and navigation/positioning technique in the 2020 survey resulted in more accurate data, and, combined with an EM instrument which was not present in the 1970 survey, makes it possible to achieve a consistent dataset all over the area with regards to the electrical conductivity in the ground. A compilation of these surveys and data acquisition methods is shown in Table 32.

Table 32. Previously acquired airborne geophysical data by SGU over the area around Tunaberg.

Year	Geophysical methods used	Flight direction	Flight line separation (m)	Flight altitude (m)
1970	Magnetics, gamma spectrometry	North–south	200	30
1999	Magnetics, gamma spectrometry, VLF (2-transmitters)	North–south	200	60
2020	Magnetics, gamma spectrometry, VLF (2-transmitters)	North–south	200	60

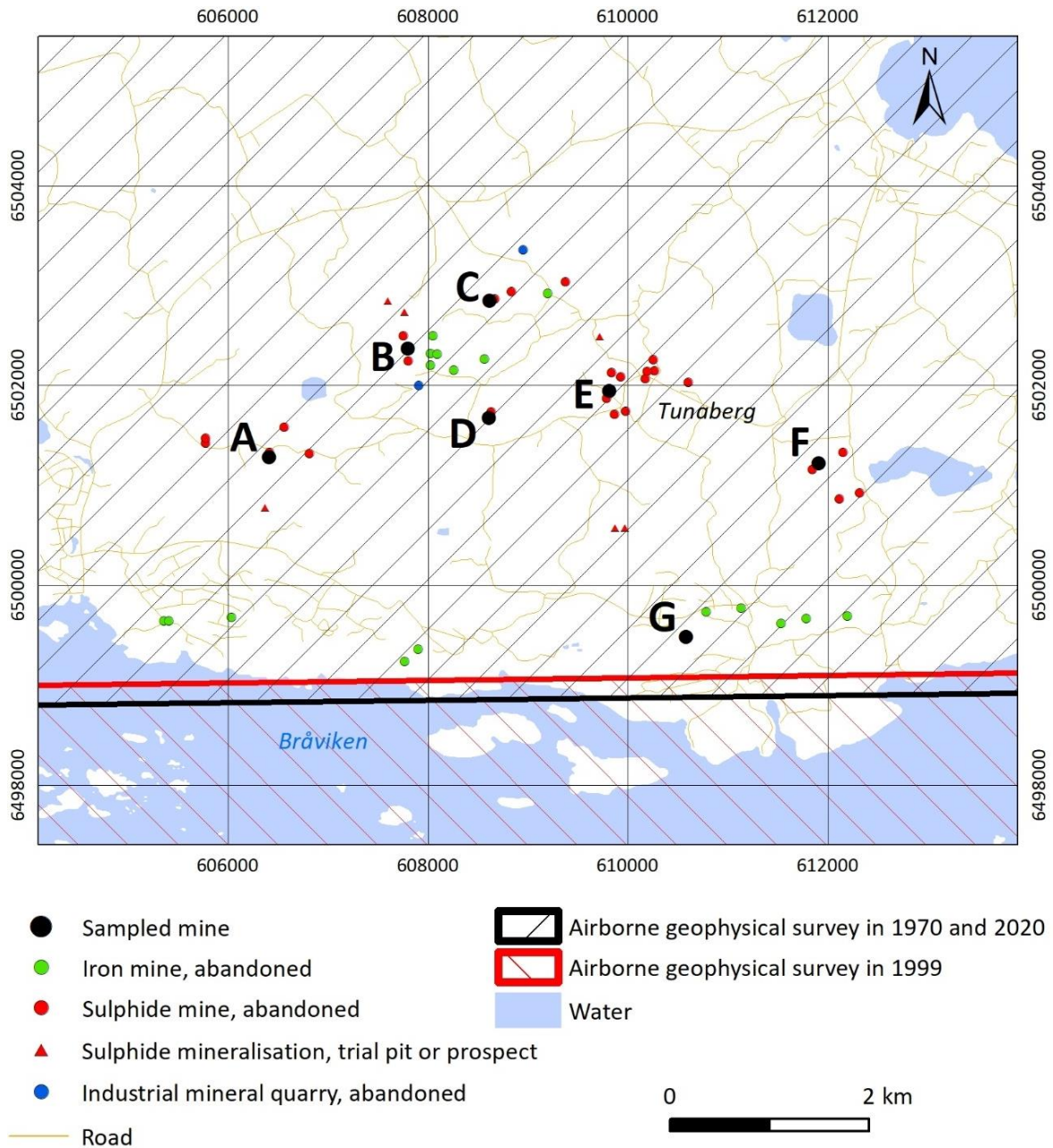


Figure 95. Map showing the extent of the previously conducted airborne geophysical surveys by SGU over the Tunaberg area. The investigated mine sites in this study are Mormorsgruvan (A), Kärrgruvan/Blombergstorp (B), Hultebrogruvan (C), Strömbergsgruvan (D), Tunaberg ore field (E), Skaragruvan (F), Mangruvan (G).

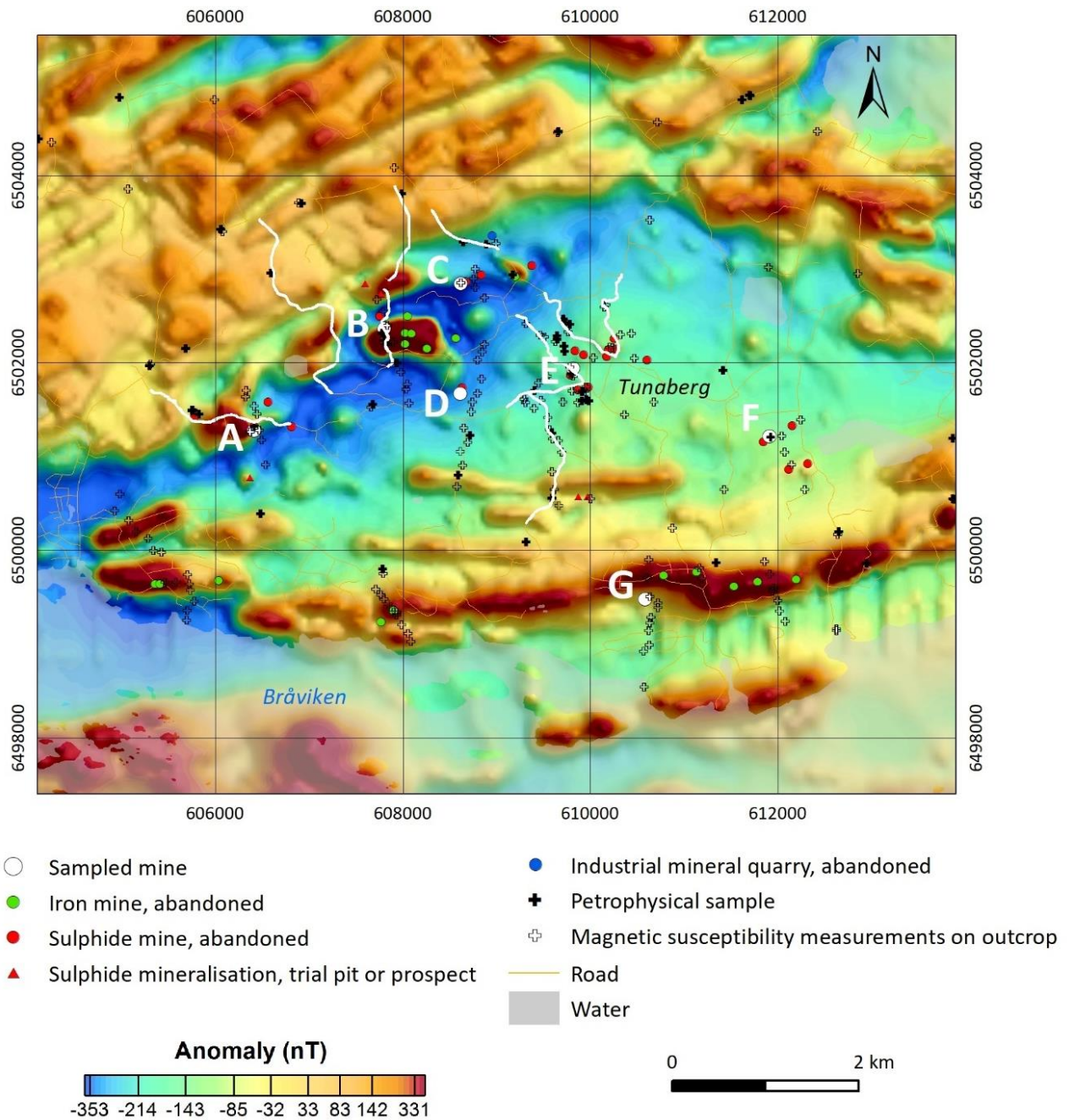


Figure 96. Map showing the magnetic anomalies, derived from airborne measurements in 1999 and 2020, at the investigated mines in this study along with their surroundings. White lines show profiles along which ground magnetic data previously have been acquired. The investigated mine sites in this study are Mormorsgruvan (A), Kärngruvan/Blombergstorp (B), Hultebrogruvan (C), Strömbergsgruvan (D), Tunaberg ore field (E), Skaragruvan (F), Mangruvan (G).

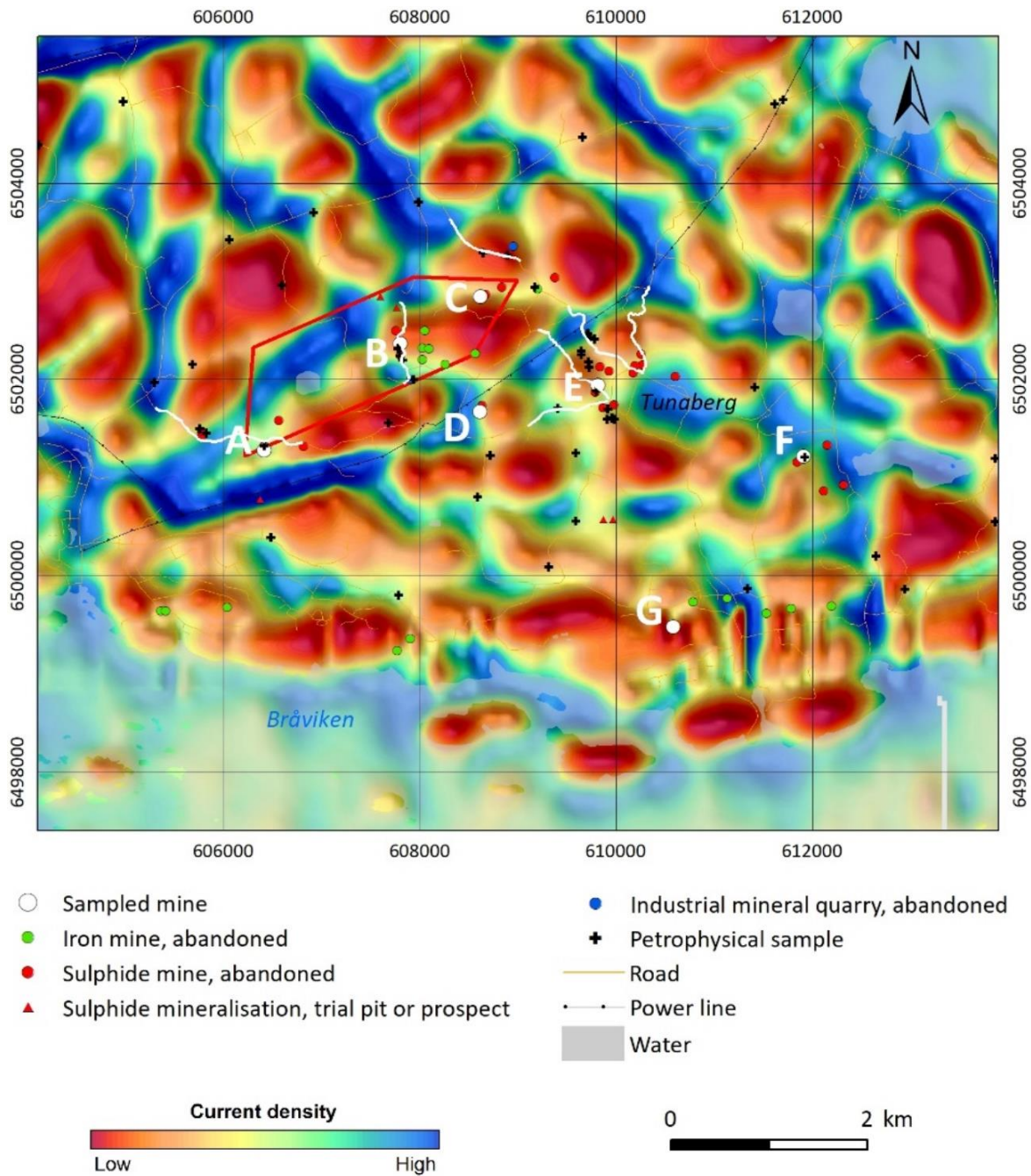


Figure 97. Map showing the current density in the ground at the investigated mines in this study along with their surroundings. The current density is derived from airborne VLF measurements from two transmitters, acquired by SGU in 1999 and 2020. White lines show profiles along which ground VLF data previously have been acquired. The red polygon delineates the area where exploration VLF measurements previously have been made. These data are now available in SGU's databases (Table 33). The investigated mine sites in this study are Mormorsgruvan (A), Kärrgruvan/Blombergstorp (B), Hultebrogruvan (C), Strömbergsgruvan (D), Tunaberg ore field (E), Skaragruvan (F), Mangruvan (G).

Table 33. Previously acquired exploration geophysical data (VLF) within the red polygon in Figure 97. These data are now available in SGU's databases.

Name of exploration area	Responsible	Geophysical method used	Year of permit
Kopparbo	Geoforum Scandinavia AB	VLF	2006–2012

Ground geophysics

During previous bedrock mapping projects at SGU, ground magnetic and VLF data have been acquired along certain profiles in the area around Tunaberg (Figs. 96 and 97). These measurements have been carried out to serve as information for modelling the bedrock geology in terms of dip and depth extent, also in conjunction with other geophysical methods like gravity data, and together with information from analysed petrophysical samples.

Two gravity surveys have been made by SGU in the area around Tunaberg. The first was in 2000, after which a network of measurement stations was achieved which had a spacing between the measurement points of 2–5 km. The second survey was carried out in 2019 when a densified network of measurements was made. During 2019, both regional measurements were made, which have a distance between the measurement stations of 1–1.5 km, along with closer spaced measurements at some key locations in the area. For example, at the Tunaberg mine the gravity measurements were made every 200–300 m in a relatively even distribution over the area. The residual gravity field over the Tunaberg area is shown in Figure 98. Approximately 2 km west of the Tunaberg mine, there are iron mineralisations which give rise to strong magnetic anomalies clearly visible in the dataset from the airborne measurements (Fig. 96). At this location, gravity measurements were carried out along a profile with 100 m station spacing, along with a densified measurement scheme in the surroundings. The resulting gravity anomalies show a strong positive anomaly, indicating denser rocks, which coincides well with the mineralisations in this area.

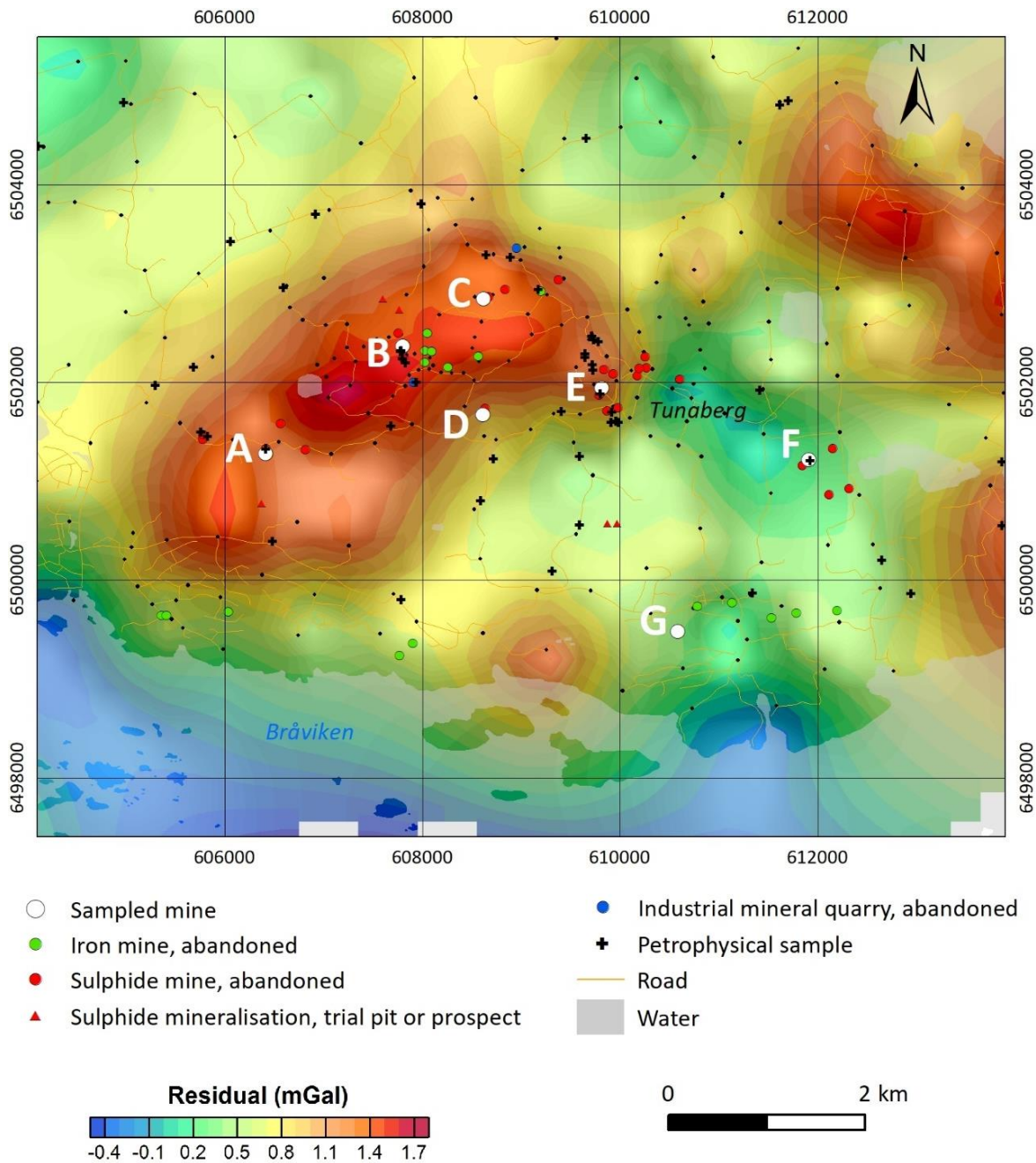


Figure 98. Map showing the residual gravity field at the investigated mines in this study along with their surroundings. The residual gravity field is expressed as the difference between the Bouguer anomaly and an analytical continuation upwards to 3 km. The small black dots represent localities for gravity measurements. The investigated mine sites in this study are Mormorsgruvan (A), Kärngruvan/Blombergstorp (B), Hultebrogruvan (C), Strömbergsgruvan (D), Tunaberg ore field (E), Skaragruvan (F), Mangruvan (G).

Waste rock

The sampling in this area differs from the other areas sampled within this project. Instead of collecting ca. 15 composite samples for each mining area, a single composite sample for each mine site was sampled. A total of eleven selected mines were sampled in the Tunaberg area (Fig. 99). The sampled mines consist of eight sulphide mines (Cu, Co), two mine site with iron oxide and one mine site with manganese mineralisation (Table 34). In general, the sampled waste rock piles were relatively small in size and to a large extent overgrown by moss and trees.

Mormorsgruvan is a small mine with scattered waste rock of different sizes in an area less than 100 square metres. The ore is described as rich in pyrrhotite with elevated nickel content, inclusions of chalcopyrite, and cobalt minerals in a metavolcanic rock (Erdman 1867). The first mining was initiated in 1559 and operations were closed down in 1850. Sampled waste rock material varies in size from 5 to 60 cm and has red weathered surfaces (Fig. 100). It consists predominantly of fine-grained metavolcanic rock, with varying degrees of magnetite dissemination and some visible sphalerite and chalcopyrite.

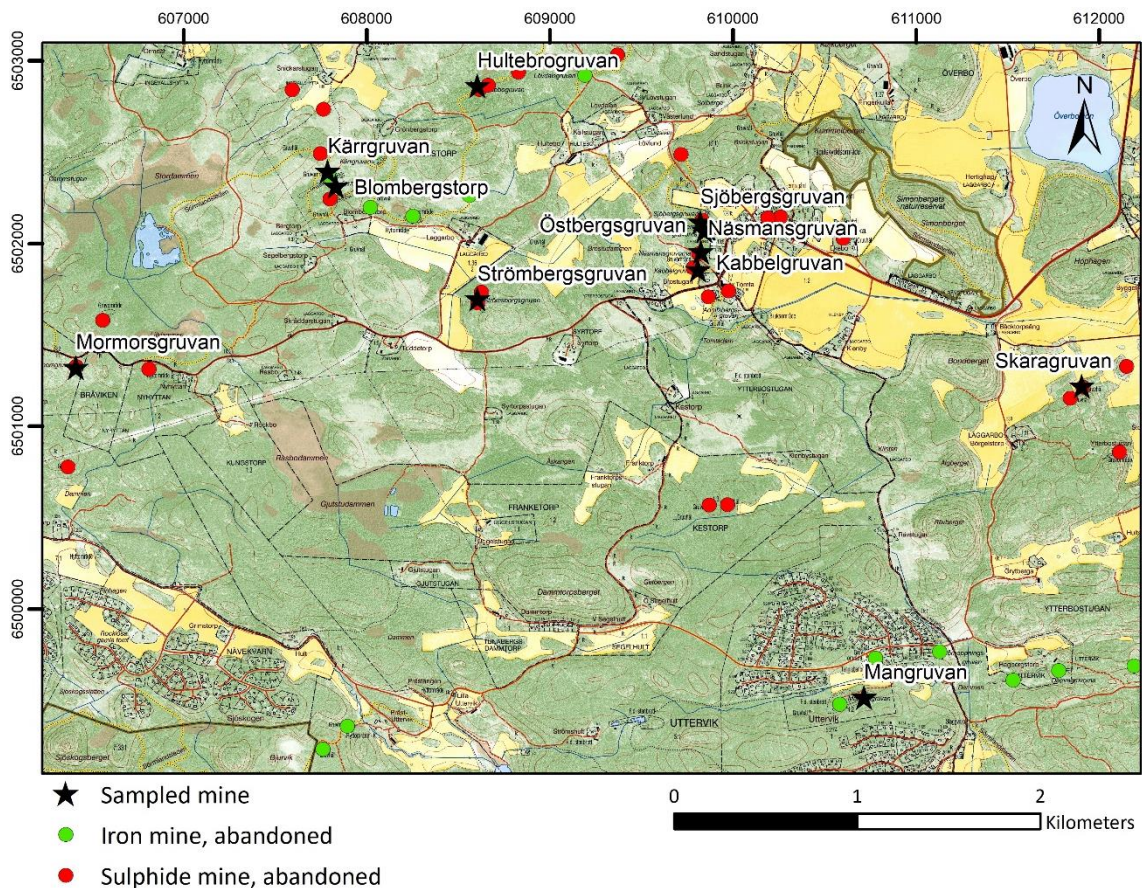


Figure 99. Overview of sampled area in Tunaberg. Black stars show the sampled mines and their names.

Tabell 34. Sampled mines in the Tunaberg area and their main commodity.

Sampled mine	Main commodity
Mormorsgruvan	Cu, Co
Kärngruvan	Fe
Blombergstorp	Fe, Cu
Strömbergsgruvan	Cu
Skaragruvan	Zn, Pb
Mangruvan	Fe, Mn
Hultebrogruvan	Cu, Zn
Sjöbergsgruvan	Cu, Co
Näsman'sgruvan	Cu, Co
Kabelgruvan	Cu, Co
Östbergsgruvan	Cu, Co



Figure 100. Waste rock material from Mormorsgruvan varies in size from 5 to 60 cm and has red weathered surfaces. Photo: Johan Camitz.

Kärrgruvan and Blombergsgruvan are two adjacent mines, mined mainly for iron oxide and copper. The mineralisation is described as skarn-hosted magnetite (Geijer & Magnusson 1944). The ore field is made up of two elongated open pits striking northeast–southwest, surrounded by a few waste rock piles with a size of a few hundred square metres each, partly overgrown by moss and trees (Fig. 101A). The waste rock material is dominated by a fine-grained metavolcanic rock, foliated, with diffuse magnetite mineralisation (Fig. 101B), and subordinately by pieces with pegmatite rich in garnet.

Skaragruvan was mined for zinc and lead. The waste rock pile is around 600 square metres and mostly well exposed (Fig. 101C). The main rock is metavolcanic rock. Part of the pile contains material rich in sphalerite (Fig. 101D).

Hultebrogruvan was mined for zinc and lead. The waste rock pile is about 150 square metres with coarse rock material partly overgrown by moss (Fig. 101E). Sphalerite is visible in some rock samples (Fig. 101F).

The Tunaberg ore field consists of several mines located on a north–south line west of Koppartorp village. Sampled mines are Sjöbergsgruvan, Östbergsgruvan, Näsmansgruvan and Kabbelgruvan. Dominating rock in the waste rock pile constitutes medium- to coarse grained dolomite with occasional amphibole skarn and sulphide mineralisation with visible chalcopyrite (Fig. 102A). These mines were mined for copper and cobalt.

Strömbergsgruvan was mined for copper. Small piles of waste rock are found. They have pieces of rock with varying particle sizes and commonly oxidised surfaces. The waste material is typically felsic metavolcanic rock locally rich in chalcopyrite. Some pieces of skarn with quartz, green amphibole, garnet and chalcopyrite were observed (Fig. 102B).

Mangruvan is an elongated waterfilled open pit where the waste rock is scattered along the sides of the mine and to a large extent overgrown by vegetation. The waste material is dominated by dark green amphibole skarn, partly rich in garnet as well as occasional magnetite mineralisation (Fig. 102C).



Figure 101. Pictures from sampled waste rock areas and rock samples. **A.** Waste rock pile from the Kärrgruvan och Blombergsgruvan area, partly overgrown by moss and trees. **B.** Rock sample from the Kärrgruvan och Blombergsgruvan area consisting of fine-grained metavolcanic rock, banded, foliated, with diffuse magnetite mineralisation. **C.** The waste rock pile in Skaragruvan is dominated by metavolcanic rock, partly rich in sphalerite. **D.** Waste rock sample from Skaragruvan, rich in sphalerite. **E.** Waste rock pile from Hultebogruvan with coarse rock material partly overgrown by moss. **F.** Visible sphalerite in rock sample from Hultebogruvan. Photo: Gunnar Rauséus.



Figure 102. Pictures from sampled waste rock areas and rock samples **A.** Example of composite samples from the Tunaberg ore field, here consisting of medium- to coarse- grained dolomite with occasional amphibole skarn and sulphide mineralisation with visible chalcopyrite. **B.** Example of rockpile material from Strömsbergsgruvan. Felsic metavolcanic rock containing skarn with quartz, green amphibole, garnet and chalcopyrite. **C.** Example of waste rock pile material from Mangruvan with dark green amphibole skarn with garnet as well as occasional magnetite mineralisation. Photos: Johan Camitz.

Results composite sampling

The result for the whole area including all the sampled mines show elevated to anomalous grades for Zn, Pb, Cu, Co, Ag, Sb, Mn and iron oxide. Elevated values for elements in the composite samples is compiled in Table 35 for the magnetite hosted skarn ores and Table 36 for composite samples from sulphide mine sites. Three mine sites show elevated values for Zn where Skaragruvan stands out with a Zn content of over 6%, 0.3% Pb, and elevated values for Ag and Sb. The content of barium is also high and is assumed to be associated with feldspar in the host rock. In addition to elevated zinc grades, Mormorsgruvan also show elevated values for nickel and iron oxide.

The four mines, sampled near Koppartorp are elevated in Cu with up to 0.3% at Kabbelgruvan and Österbergsgruvan. The cobalt contents range from 23 to 148 ppm. Österbergsgruvan also show elevated values for Pb (1,800 ppm) and Zn (844 ppm). Strömbergsgruvan shows elevated concentrations mainly for Cu, just above 0.2%. Four waste rock piles are elevated in Fe₂O₃, ranging from ca. 16 to 33%. Mangruvan contains over 8% MnO.

Table 35. Selected geochemical data for waste rock composite samples in magnetite hosted skarn ores in Tunaberg.

Sample	Mine site	Fe ₂ O ₃ %	MnO ppm	Ni ppm	As ppm	Cu ppm	Pb ppm	S %	Zn ppm
JCA220001A	Mormorsgruvan	16.85	0.58	63	459	128	136	3.66	1,315
JCA220002A	Kärrgruvan	21.3	0.83	6	2.4	66	337	0.02	440
JCA220003A	Blombergsgruvan	23.8	0.88	4	3	136	1,245	0.06	396
JCA220006A	Mangruvan/Uttergruvan	33.4	8.33	7	89.4	61	4.8	0.23	724

Table 36. Selected geochemical data for waste rock composite samples in sulphide mineralisations in Tunaberg.

Sample	Mine site	Ba ppm	Sb ppm	Ag ppm	Co ppm	Cu ppm	Pb ppm	S %	Zn ppm
JCA220004A	Strömbergsgruvan	523	0.59	4.67	6	2,310	408	0.45	395
JCA220005A	Skaragruvan	5,720	7.29	13.25	8	193	3,160	4.32	63,300
JCA220007A	Hultebrogruvan	736	1.26	0.85	5	28	1,070	0.31	4,130
JCA220008A	Sjöbergsgruvan	97	0.13	1.03	148	555	42.8	0.08	57
JCA220009A	Näsmansgruvan	15.1	2.75	1.36	23	880	44.5	0.4	41
JCA220010A	Kabbelgruvan	101.5	3.62	4.91	53	3,180	139	0.37	74
JCA220011A	Östbergsgruvan	150.5	71.7	10.3	97	2,950	1,800	0.44	844

BAGGETORP

Existing and historical data

Baggetorpsgruvan is situated 12 km southwest of the town of Finspång in Östergötland county (Fig. 2). The mining history at Baggetorp is relatively late in terms of mining history in Sweden. The tungsten mine at Baggetorp was set in production during World War II, namely in 1944, and produced until 1958 when the mine was shut down. The mining was conducted at several levels down to 150 m depth and in the later part of the mine history a mine shaft with a depth of 145 m was driven, resulting in a total depth of almost 300 m for the mining system. The total production was 0.28 Mt with an average grade of 0.2% W (SGU 2023). The documented waste rock material produced during this period was 90,000 (SGU 2023). An unknown amount of tailings covering an area of about 30,000 m² north of the mine.

The ore minerals at Baggetorp are wolframite, scheelite and in the beginning of mining even molybdenite (MoS₂) was regarded as a potential ore mineral. Genetically, wolframite is replaced and sometimes surrounded by scheelite and associated with quartz veins. Molybdenite also occurs associated with quartz veins (Gavelin 1985). The later phase of mineralisation consists of formation of pyrite, chalcopyrite and Bi-minerals according to Gavelin (1985).

The quartz veins are intensely sheared and cut by aplite and pegmatites veins, belonging to the post-Svecokarelian Småland granites, which are not affected by shearing. Gavelin (1985) concludes that the wolframite mineralisation is localized to older shear zones rather than being an end-product of the intrusion of Småland granites. This mineralisation genesis is then suggested by Gavelin (1985) to be related to the veined gneisses formed in the time interval between the emplacement of the older (synkinematic or primorogenic) granitoids and the younger post-kinematic Småland granites. This is contradicted by Wikstöm & Karis (1991) who suggest that there are strong indications that the regional deformational forces in the area very well could be contemporary with the granite intrusions, indicating that the quartz veins in Baggetorp still could be related to the intrusions of the Småland granites.

The tailings pond in Baggetorp was sampled in a SGU campaign in 2018. Five geochemical analyses are stored in the SGU database Litho geochemistry. The average concentration of W for these samples is 551 ppm with a range from 283 to 975 ppm of W.

Airborne geophysics

In this project an area has been specified for additional bedrock mapping, with the aim of improving the understanding of the geology linked to the original mineralisation, from which the waste material has been generated. A polygon showing the area identified for further geological mapping and geophysical investigations is shown as a black dashed line in Figure 103. We refer to this in subsequent text as the Baggetorp mapping area.

The earliest airborne geophysical measurements present in SGU's database around the Baggetorp mine were collected in 1979 and were produced by both SGU and LKAB. The survey collected by SGU covers the entire area shown in Figure 103, while the survey by LKAB covers an area in the southwestern corner of the map shown in Figure 103 (outside the polygon defining the Baggetorp mapping area). In 2018, SGU collected modern airborne geophysical measurements over the entire area shown in Figure 103. In all the airborne surveys, magnetic, VLF and gamma ray measurements were performed.

However, in the more recent survey, in 2018, VLF data from two different transmitters were collected as opposed to just one in the 1979 surveys. Similar acquisition parameters were utilized for the different surveys (i.e., north–south flight lines and 200 m line spacing), however, in the earlier surveys, a flight height of 30 m was used instead of 60 m in the more recent survey. A summary of the different airborne datasets which cover part, or all, of the area shown in Figure 103 is shown in Table 37.

Figure 103 shows a map of the residual magnetic field intensity in the vicinity of the Baggetorp mine (using magnetic data collected in 2018). A series of magnetic anomalies with a northeast–southwest strike can be observed, several of which, intersect the Baggetorp mapping area. In general, based on SGU's 50 000–250 000 bedrock geology maps, these anomalies can be interpreted to correlate with areas of dacite–rhyolite, granodiorite or basic rocks. These rocks likely contain higher concentrations of paramagnetic minerals when compared to the granitic rocks which in turn correlate broadly with the regions with low magnetic anomaly values.

However, in the detailed bedrock interpretation performed by LKAB in 1979 (the area around the Baggetorp mine is interpreted to consist almost exclusively of different types of granitic rocks. The interpretation by LKAB and others thereafter is that the Baggetorp mine is located within a unit of red / grey metagranite, which is surrounded by younger Smålands granites (Ohlsson 1980; Gavelin 1985). Based on this interpretation of the bedrock, it is likely that the broad magnetic anomaly at the Baggetorp site is associated with the contrast in magnetic susceptibility between the older metagranites and the younger Småland granites.

The mineralisation at Baggetorp occurs as aggregates of wolframite, scheelite and molybdenite which are somewhat irregularly distributed within a quartz vein with a northeast–southwest strike (Gavelin 1985; Wikström & Karis 1991). Other minerals which are documented within the mineralisation include magnetite, pyrite and chalcopyrite as well as native antimony and bismuth (Gavelin 1985). However, due to the scale of the deposit and the fact that much of the mineralisation has been removed prior to the airborne measurements, the mineralisation at Baggetorp is not thought to contribute significantly to the large-scale northeast–southwest striking magnetic anomaly observed in the airborne magnetic measurements (Fig. 103).

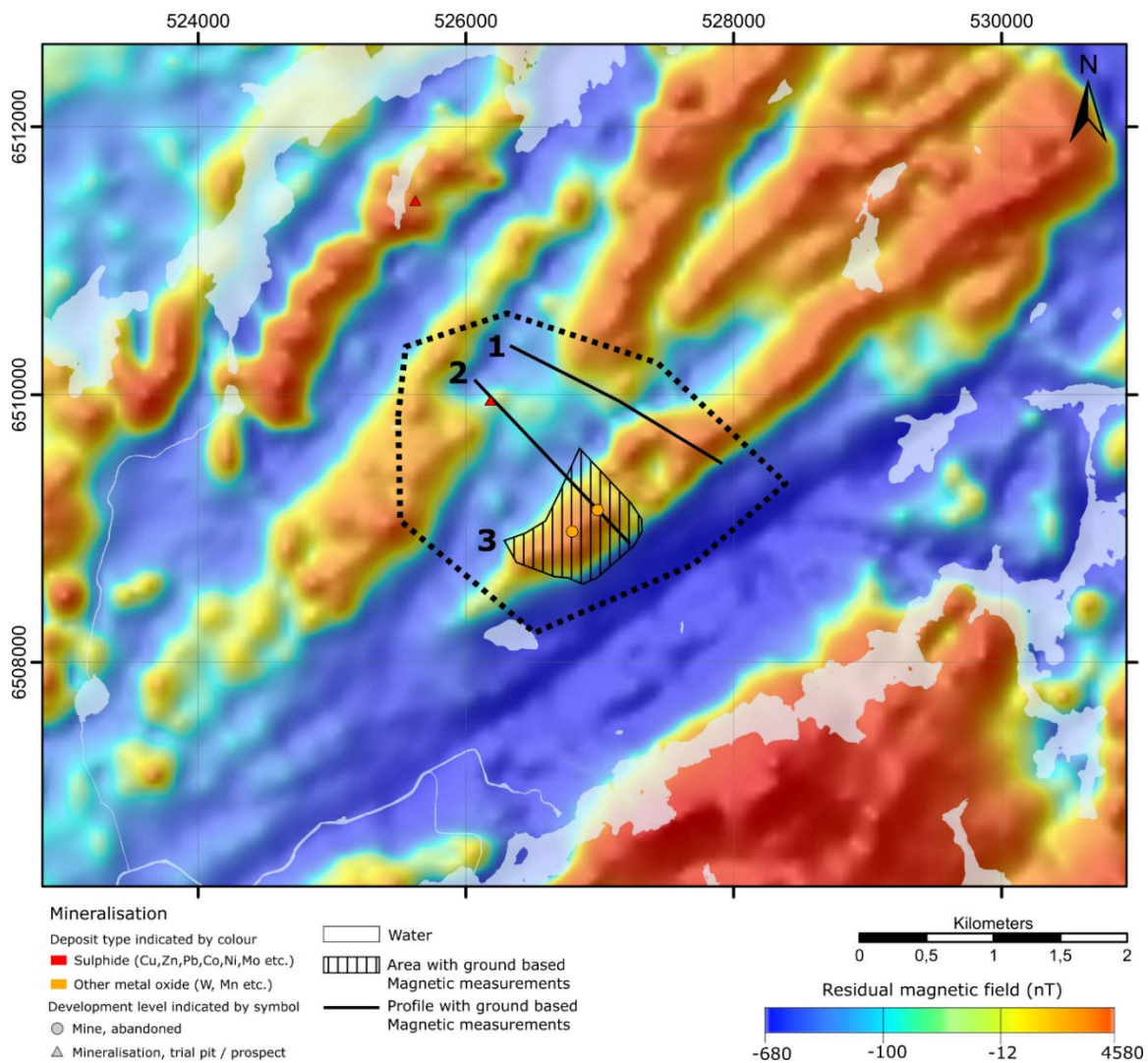


Figure 103. Map of residual magnetic field for the area around the Baggetorp mine. The Baggetorp mapping area is shown as a thick black dashed line.

Table 37. Complete list of the airborne geophysical surveys over and close to the Baggetorp mapping area (i.e., within the area shown in figure 103).

Year	Organisation	Geophysical methods used	Area	Flight direction	Flight line separation (m)	Flight altitude (m)
1979*	SGU	Magnetics, gamma spectrometry, VLF (1 transmitter)	Part of 9F	North–South (0°)	200	30
1979*	LKAB	Magnetics, gamma spectrometry, VLF (1 transmitter)	Part of 9F and 9G	North–South (0°)	200	30
2018	SGU	Magnetics, gamma spectrometry, VLF (2 transmitter)	Part of 11F, 10E, 10F, 9E, 9F, 8E and 8F	North–South (0°)	200	60

* Not used for producing maps in this report

Figure 104 shows a map of the apparent resistivity over the study area, generated using the VLF data from 2018. Several somewhat linear, low resistivity zones can be observed to intersect the Baggetorp mapping area. However, these anomalies correlate strongly with areas of low-lying land or valleys which often have streams running through them. Hence in this case, these anomalies are likely to be associated with higher soil moisture and the presence of open water in some cases. A clear, approximately east–west striking anomaly is present in the northern part of the Baggetorp mapping area which is associated with a powerline.

Ground-based electromagnetic and magnetic measurements

No ground-based electromagnetic (EM) or magnetic data are documented in the SGU archive in the vicinity of the Baggetorp mine. This is likely to be because the mine only operated between 1944 and 1957 (Wikström & Karis 1991), before the application of geophysical prospecting methods were widespread. Subsequent geophysical prospecting work performed by LKAB was focused predominantly on airborne and gravity measurements.

As part of this study additional ground based magnetic and VLF measurements were performed (Figs. 103 and 104). These were performed with the aim of improving the understanding of the mineralisation and surrounding bedrock at Baggetorp and to provide a basis for future geophysical and geological modelling efforts. Furthermore, these measurements were intended to support new bedrock mapping efforts performed as part of this project within the Baggetorp mapping area. The ground based magnetic and VLF measurements were collected using a GEM GSMV-19 instrument. Two approximately 2 km long profiles were measured across the Baggetorp mapping area, perpendicular to the regional strike with the aim of providing input for 2D geophysical modelling. For these profiles, VLF measurements were collected with frequencies of 22.2 and 23.4 kHz. These VLF measurements were taken facing an azimuth of 115°. The magnetic measurements were collected continuously at 1 second intervals. In addition, a series of profiles were collected in the area around the Baggetorp mine, with the aim of generating a detailed ground magnetic map of the area. For the survey around the Baggetorp mine, magnetic measurements were collected at 1 second intervals with a nominal profile spacing of 30 m. For the corresponding VLF measurements a profile spacing of approximately 60 m was used and measurements were taken with 22.2 kHz, facing an azimuth of 295° (Fig. 104). Some summary information about these new measurements is shown in Table 38.

Table 38. Ground-based magnetic, EM and geo-electric measurements for the area around the Baggetorp mine. Numbers correspond to the numbered polygons/lines shown in figure 103 and 104.

Polygon/Line number and name	Method	Year acquired	Responsible	Comments
1. MP21DSR0001	Magnetic	2021	SGU	One profile collected in this area
2. MP21DSR0002	Magnetic	2021	SGU	One profile collected in this area
3. MP21DSR0003 – MP21DSR0007	Magnetic	2021	SGU	Magnetic data collected over an area with approximately 30m line spacing
4. VP21DSR0001 and VP21DSR0002	VLF	2021	SGU	One profile collected in this area, two VLF frequencies (22.2 and 23.4 kHz measured)
5. VP21DSR0003 and VP21DSR0004	VLF	2021	SGU	One profile collected in this area, two VLF frequencies (22.2 and 23.4 kHz) measured
6. VP21DSR0005 – VP21DSR00010	VLF	2021	SGU	VLF data collected over an area with approximately 60m line spacing. One VLF frequency measured (22.2 kHz)

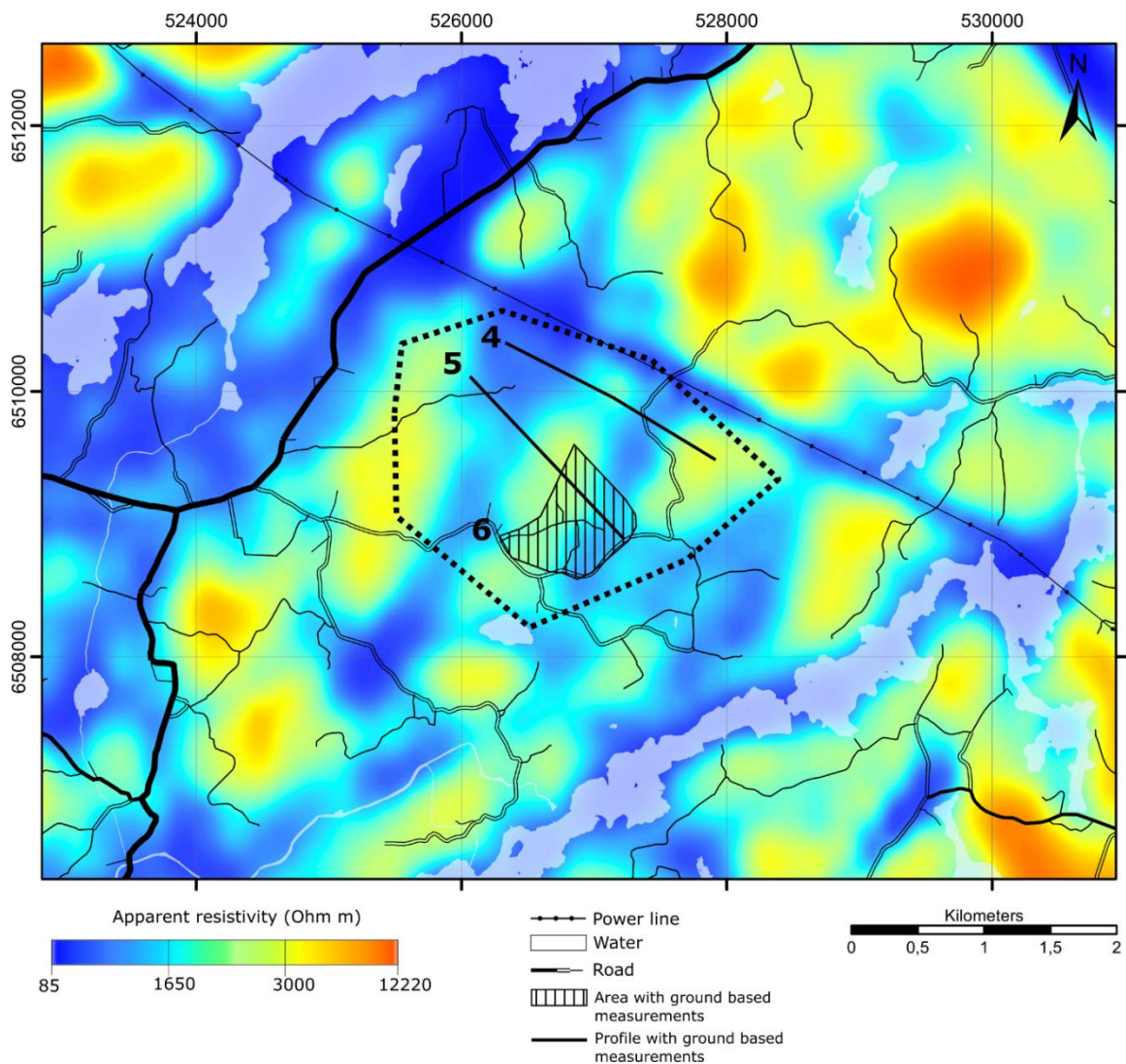


Figure 104. Map of apparent resistivity derived from airborne VLF data collected in 2018 for the area around the Baggetorp mine. The Baggetorp mapping area is shown as a thick black dashed line.

Ground-based gravity

Ground based gravity data are available for the area around the Baggetorp mine which have been collected as part of SGU's routine gravity surveying activities. These have a spacing of approximately 1 to 2 km. In addition, more tightly spaced gravity measurements were collected around the Baggetorp mine as part of LKABs exploration activities in 1983 (Andersson et al. 1984). These measurements were collected along roads and have a point spacing of approximately 200–400 m. To improve the resolution of the data and to provide a better basis for geological and geophysical modelling within the Baggetorp mapping area, 144 additional gravity measurements were collected in 2022 by SGU. Figure 105 shows a map of the residual gravity field for the area, as well as the location of the measurements. The new measurements collected in 2022 as part of this project are highlighted.

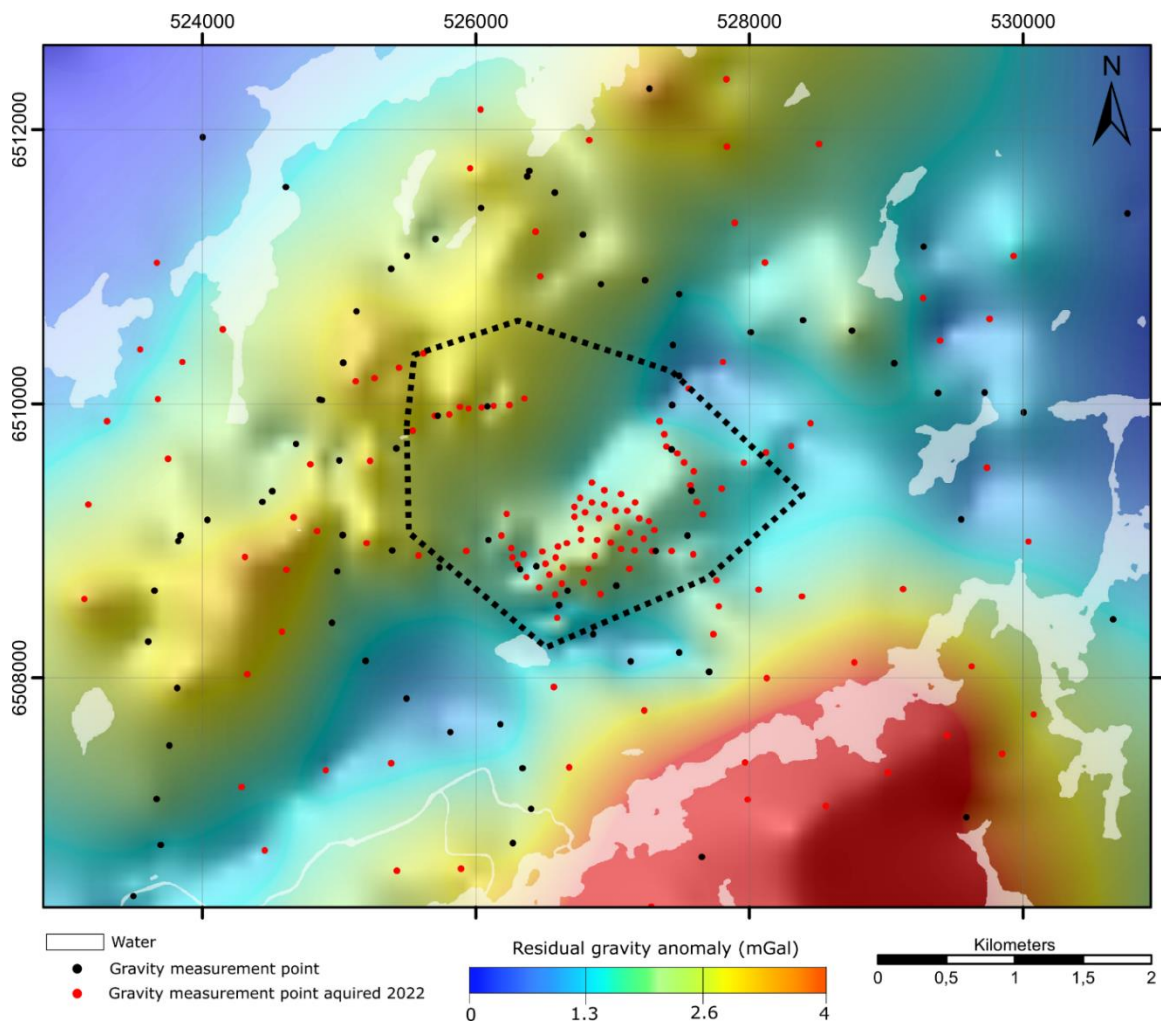


Figure 105. Map of the residual gravity anomaly around the Baggetorp mine. The Baggetorp mapping area is shown as a thick black dashed line. Gravity measurement points are shown as black and red dots.

The area around the Baggetorp mine corresponds to a small positive anomaly in the residual gravity data. This is most likely due to the contrast in density between the older metagranite which surrounds the Baggetorp mine and the younger Smålands granite. To the south of the Baggetorp mine a relatively large positive anomaly exists which is likely associated with the presence of mafic rocks. North and east of the Baggetorp mine there is a relatively large positive anomaly with a northeast–southwest strike, this is most likely to be associated with the presence of granodiorite rocks which are denser than the surrounding granitic rocks.

Petrophysical data

The map in Figure 106 shows the petrophysical data available for the area around the Baggetorp mine. Prior to this project there was only one petrophysical sample available in SGU’s database from the Baggetorp mapping area. As part of this project an additional 18 samples were taken from the different rocks around the Baggetorp mine (Fig. 106). A summary of the results from the petrophysical samples collected between 2021 and 2022 are shown in Table 39.

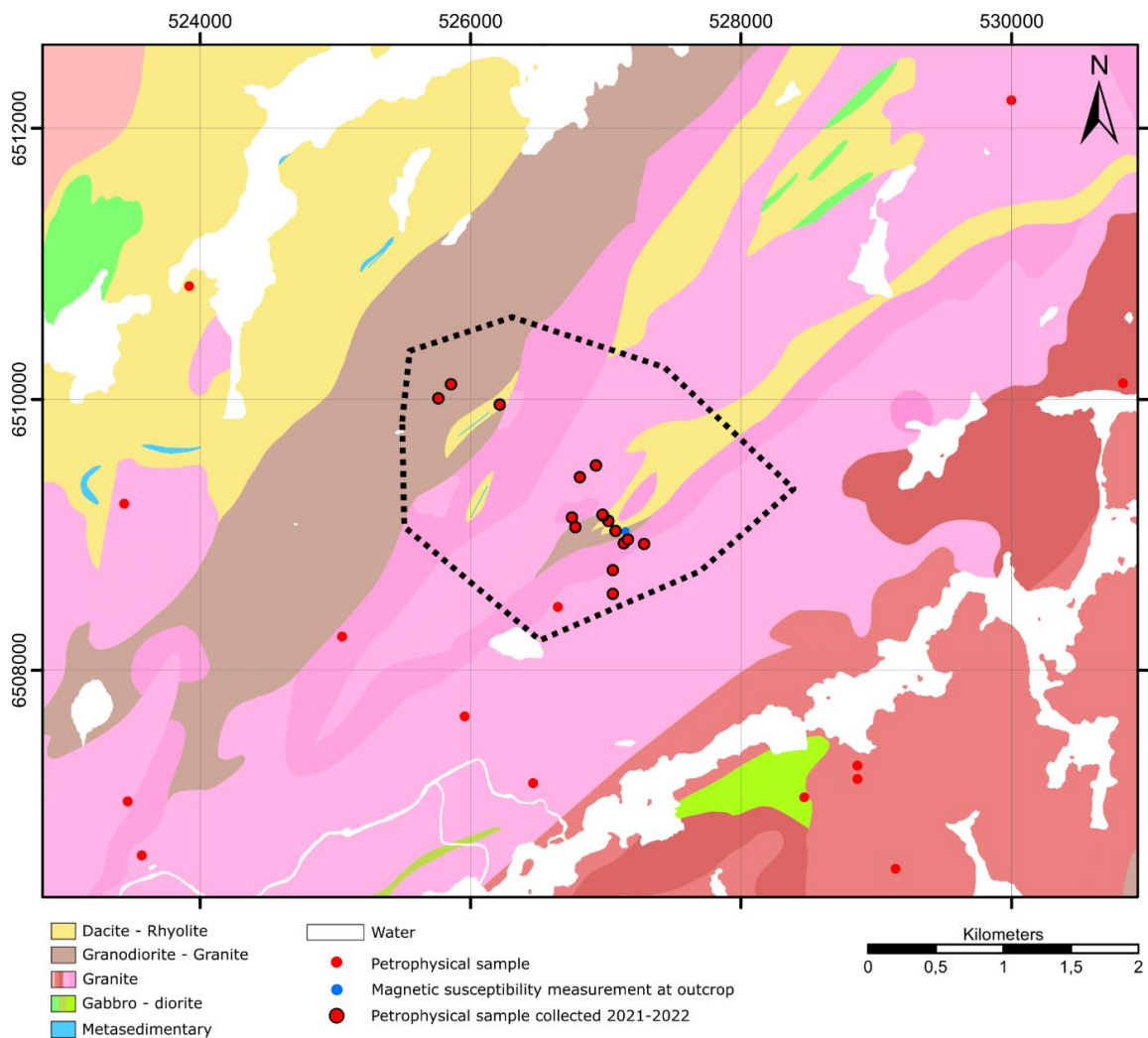


Figure 106. Map of the petrophysical data from and around the Baggetorp mine. The Baggetorp mapping area is shown as a thick black dashed line.

Based on the results from the new petrophysical data it can be observed that the coarse-grained younger granites to the south of the mine and also the granites north of the mine have relatively low magnetic susceptibilities (between $25\text{--}500 \times 10^{-5}$ SI). These can be interpreted to correspond to the younger Småland granites (Gavelin 1985). Around the Baggetorp mine the granites and granodiorites typically have higher magnetic susceptibilities of between $1,500\text{--}9,000 \times 10^{-5}$ SI. These can be interpreted to correspond to the older metamorphic plutonic rocks interpreted by Ohlsson et al. (1980) and Gavelin (1985), which exhibit a higher degree of deformation and host the Baggetorp mineralisation. The densities of these older rocks are typically higher than the surrounding Småland granites.

DSR210014A and DSR210015A are two samples taken from the Baggetorp quartz vein and associated mineralisation, respectively. The sample of the quartz vein material exhibits a relatively low-density of $2,651 \text{ kg/m}^3$ and relatively low magnetic susceptibility (compared to the surrounding gneiss granites) of 872×10^{-5} SI. Conversely, the density of the sample of metallic mineralisation has a relatively high density of $3,206 \text{ kg/m}^3$ and a magnetic susceptibility comparable to the surrounding gneiss granites of $5,538 \times 10^{-5}$ SI.

Table 39. Table summarising the petrophysical results collected as part of this project from the Baggetorp mapping area.

Sample ID	Easting (m)	Northing (m)	Description	Density (kg/m ³)	Magnetic susceptibility (10 ⁻⁵ SI)	J (mA/m)
DSR210001A	527054	6508562	Granite	2,621	539	94
DSR210002A	527055	6508736	Granite	2,677	70	113
DSR210003A	527286	6508931	Granite	2,649	25	35
DSR210004A	527021	6509100	Granite	2,669	1,555	214
DSR210004B	527021	6509100	Mafic volcanic	2,819	12,836	3,882
DSR210005A	525857	6510108	Granodiorite	2,686	157	38
DSR210006A	525764	6510004	Granodiorite	2,668	20	114
DSR210007A	526217	6509960	Sulphide mineralisation	3,182	4,277	29,387
DSR210007B	526217	6509960	Marble	2,737	1,265	92
DSR210008A	526777	6509054	Granodiorite	2,663	2,148	4,787
DSR210009A	526751	6509125	Granodiorite	2,713	1,917	294
DSR210010A	527135	6508935	Granodiorite	2,756	8,757	1,690
DSR210011A	527166	6508963	Granite	2,628	2,176	431
DSR210013A	527074	6509026	Granodiorite	2,720	31	5
DSR210014A	526983	6509137	Pegmatite / Quartz Vein	2,651	872	229
DSR210015A	526977	6509145	Mineralisation	3,206	5,538	2,446
DSR210016A	526809	6509423	Granite	2,605	26	95
JCA220044A	526929	6509512	Granite	2,632	724	138

A sample was taken to the northeast of the Baggetorp mine from what appeared to be an inclusion or fragment of a more mafic rock which appeared to exhibit layering. This rock exhibited a relatively high-density of 2,819 kg/m³ and the highest magnetic susceptibility from the collection of samples of 12,836 × 10⁻⁵ SI. This sample was taken from a fragment of brecciated mafic rock, within the older metagranite, similar to those observed by Ohlsson et al. (1980).

To the northwest of the Baggetorp mine, samples were taken from a small sulphide mineralisation as well as the surrounding marble (DSR210007A and DSR210008A, respectively). The marble and sulphide mineralisation both exhibited anomalously high densities and magnetic susceptibilities compared to the surrounding granitic rocks.

Interpretation of newly acquired data

Figure 107 shows a map of the total magnetic field intensity generated with the ground-based measurements. The magnetic map shows a somewhat complex pattern of relatively small positive anomalies across the area. However, there appears to be somewhat lower and less variable magnetic response in the north-western and south-eastern part of the surveyed area. These correspond to regions where granites with relatively low magnetic susceptibilities have been observed (for example DSR210001A-3A and DSR210016A). In the central part of the surveyed area a series of positive magnetic anomalies exist which typically have a northeast–southwest strike. The most notable of these lies in the southern part of the survey area and intersects the petrophysical samples DSR210010A and 11A. Approximately 150 m southwest of DSR210010A, this otherwise relatively coherent anomaly appears to be disrupted. On inspection of other anomalies in this area, it is possible to interpret a fault or deformation zone intersecting this point with an approximately east–west strike. In the southern part of the survey area several relatively coherent positive and negative anomalies appear to converge. This feature could potentially be interpreted as a termination or pinch out of a bedrock unit.

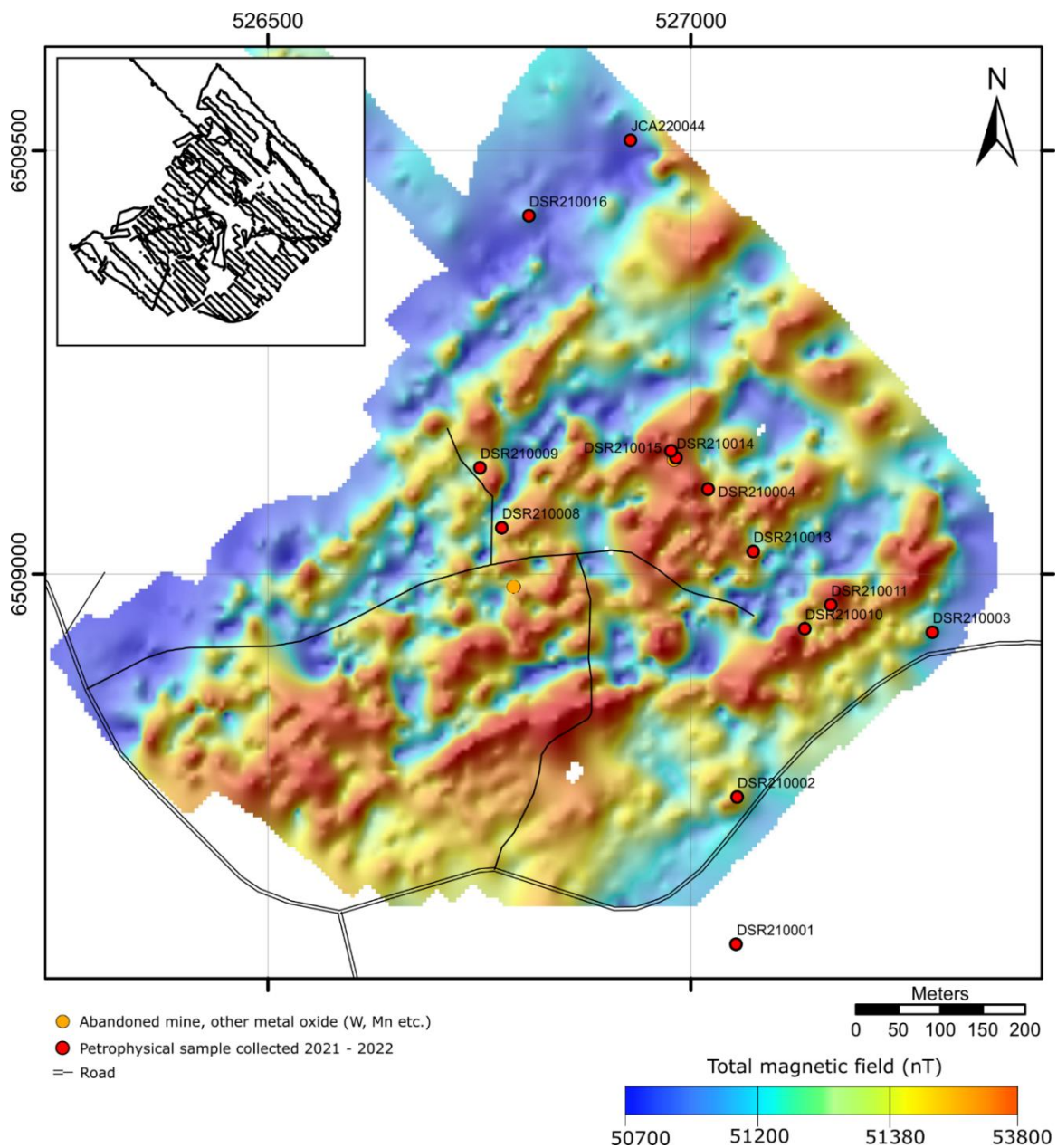


Figure 107. Map showing the total magnetic field intensity from ground measurements collected around the Baggetorp mine. Mineralisation from SGU's database as well as new petrophysical samples collected between 2021 and 2022 are shown. The inset in the top left corner shows the measurement points used to generate the map, the extent of this inset map is the same as the main map.

Figure 108 shows a potential geological interpretation of the area around the Baggetorp mine. This interpretation is modified from that of Ohlsson et al. (1980) based on the new geological observations and magnetic measurements performed in this project. In Figure 108 granites are mapped to the far southeast and northwest of the Baggetorp mine. These granites have a relatively low magnetic susceptibility and density and are interpreted to be younger Småland granites (Gavelin 1985). In the centre of the mapping area red and grey metagranite – granodiorites have been mapped, which appear to typically have higher and more variable magnetic susceptibilities. Hence, they are associated with a region of higher and more variable magnetic field values in the ground magnetic data (Fig. 108). The complex magnetic anomaly

pattern in this area is interpreted to represent heterogeneities in the concentration of paramagnetic minerals within these units. Based on the mapping of Ohlsson et al. (1980), the relatively strong magnetic anomaly in the southern part of the map appears to be associated with the contact between the red and grey metagranites. According to the description by Ohlsson et al. (1980) the red and grey metagranites are fairly similar with the exception that the grey metagranite often has a finer grain size. However, it appears that the fragments of brecciated mafic rocks which have been observed most often occur within these finer grained grey metagranites. These fragments of mafic rock, although relatively small, can have relatively high magnetic susceptibilities and hence, likely contribute to the somewhat variable anomaly pattern within this unit.

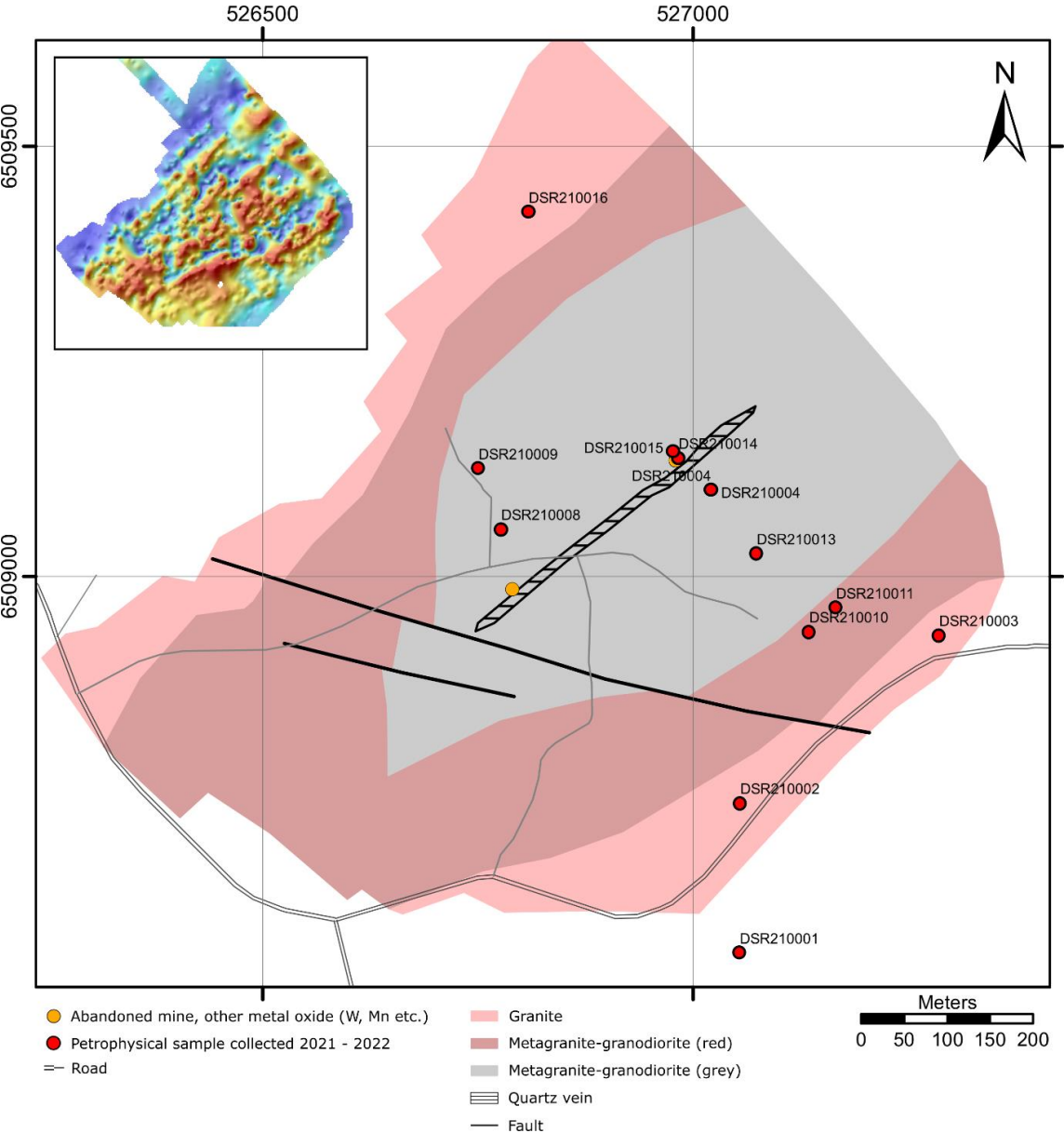


Figure 108. Map showing a modified bedrock geology map, modified from Ohlsson et al. (1980). Mineralisation from SGU’s database as well as new petrophysical samples collected between 2021 and 2022 are shown. The inset in the top left corner shows the total magnetic field from ground measurements, see Figure 107 for the colour scale, the extent of this inset map is the same as the main map.

The local density anomaly at the Baggetorp mine (Fig. 105) is interpreted to be due to the older metagranites as they typically have a higher density than the surrounding granites. The quartz vein which contains the mineralisation at Baggetorp (Gavelin 1985; Wikström & Karis 1991) is interpreted to be located within the older metagranites (Fig. 108) as mapped by Ohlsson et al. (1980). Several faults have been interpreted within the mapping area based on the magnetic measurements. However, this interpretation is somewhat supported by Ohlsson et al. (1980) who observe a fault with a similar strike in approximately the same location.

Waste rock

The waste rock deposits were sampled by a total of 15 composite samples (Fig. 109A). The sampled waste rock piles at Baggetorp are often overgrown by moss and trees which can be seen in Figure 109B. The waste rock material is dominated by greyish red to reddish grey, medium-grained granites followed by coarse-grained, quartz rich pegmatites. Sulphides such as chalcopyrite, molybdenite and pyrite were observed within a few samples. Distribution of rocks in each sample is compiled in Figure 110. Two mineralised selective samples were collected for chemical characterisation and thin section studies.



Figure 109. A. Example of different rocks included in sample JCA220022A. B. Part of the waste rock area, overgrown by moss and trees. Photos: Johan Camitz

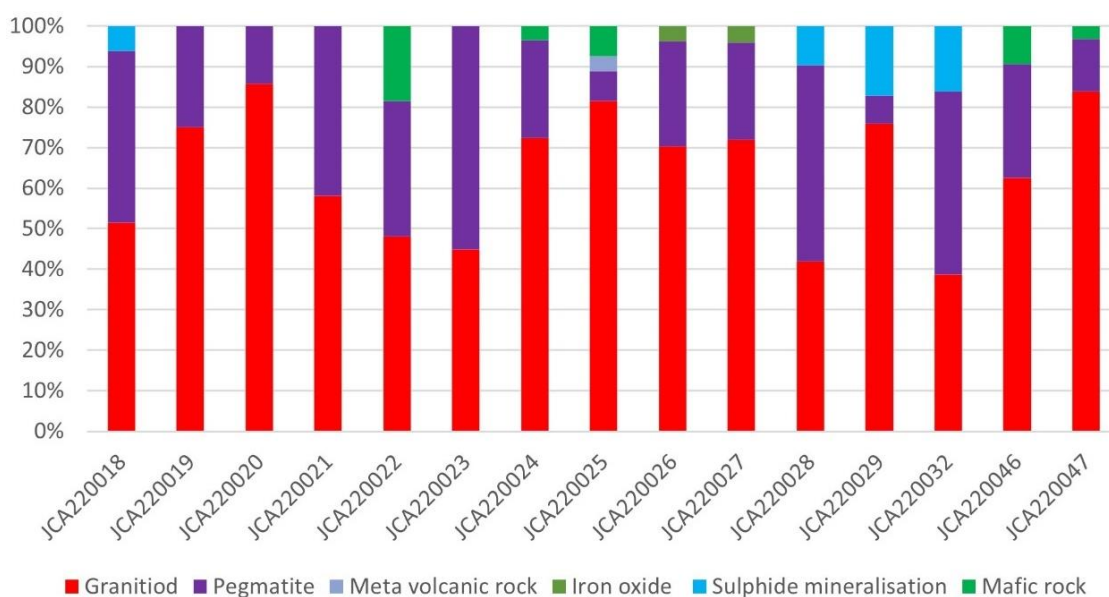


Figure 110. Distribution of rocks in composite samples from Baggetorp.

Results composite sampling

Analytical results for the composite samples show elevated concentrations for W and Mo (Table 40). The content of Mo and W show widespread concentration range with generally low content and only a few samples with elevated concentration.

Table 40. Selected geochemical data for waste rock composite samples from Baggetorp (n = 15).

	Mo ppm	W ppm
Average	113.9	342.5
Max	759	2,610
Min	3.36	3.7
Median	50.5	24.2

Results selective sampling

Two samples were selected for whole rock analysis and thin section study, JCA220018B and JCA220048A.

JCA220018B is a quartz-rich (95% SiO₂) pegmatite mineralised with a large crystal (2 cm) of wolframite (Fig. 111A). The wolframite is altered to scheelite in fractures and rims which is observed in thin section (Fig. 111B). The W concentration in this sample is 0.88%.

JCA220048A can be characterised as a foliated, hydrothermally altered volcanic rock, mineralised with abundant molybdenite, chalcopyrite and some pyrite. Figure 112 shows molybdenite, chalcopyrite and pyrite in thin section. Biotite, chlorite, sericite and small amounts of garnet are also observed within the thin section. Geochemical analyses show high content of rhenium, Re (0.95 ppm). Rhenium is one of the rarest elements in the Earth's crust with an average concentration of 1 ppb. We can also see a high alumina content in the sample (31.4% Al₂O₃) which indicates that we have a passive enrichment due to depletion of other elements during hydrothermal alteration processes. Elements with elevated concentrations are listed in Table 41.

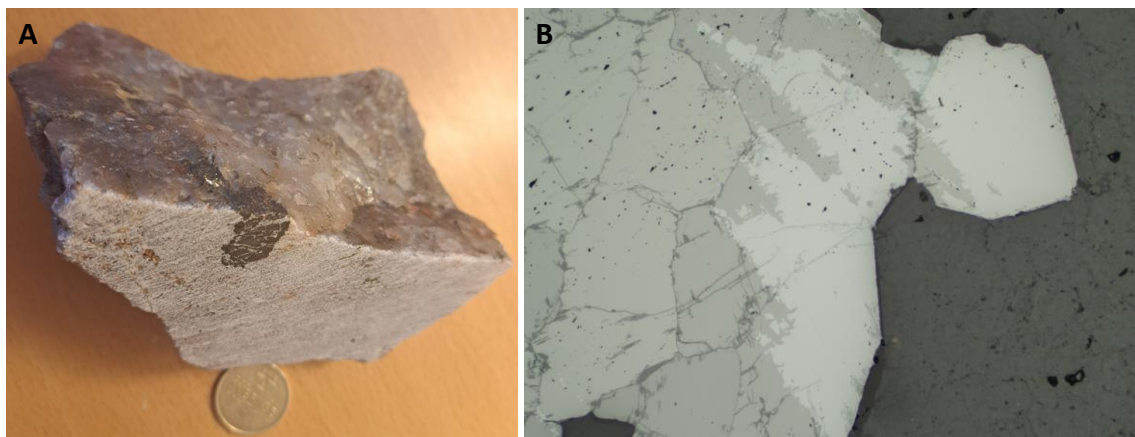


Figure 111. A. Whole rock sample JCA220018B with quartz and a dark wolframite crystal in the upper middle part of the rock. B. Thin section from JCA220018B under reflected light with wolframite (grey) altered to scheelite (light grey) and quartz (dark grey). Photos: Johan Camitz.

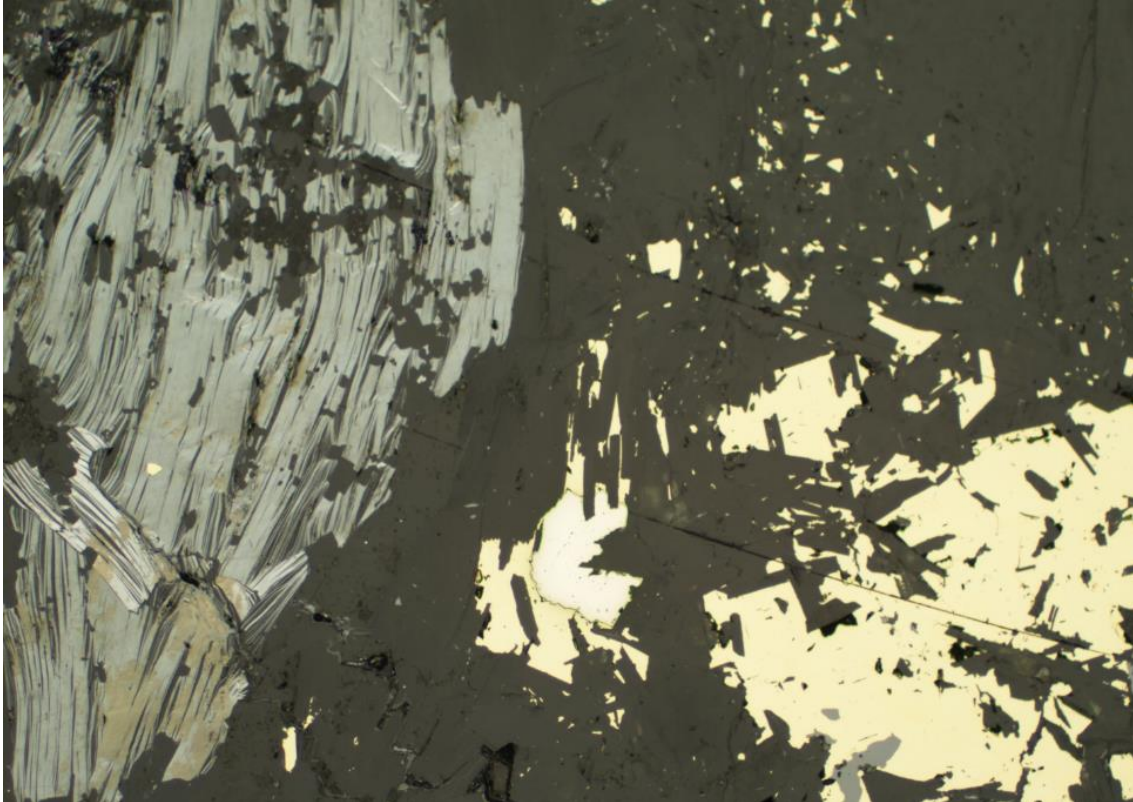


Figure 112. Thin section of JCA210048A in reflected light showing elongated crystals of molybdenite (grey), chalcopyrite (yellow) and pyrite (light yellow). Dark grey area consists of silicates. Photo: Johan Camitz.

Table 41. Selected geochemical data for selective sample JCA220048A from Baggetorp.

Element	Nb ppm	Rb ppm	Th ppm	W ppm	Bi ppm	Te ppm	Cu ppm	Mo %
	107	193	27	185	16	0.85	1,525	5.5
Element	Ga ppm	Sc ppm	Se ppm	Li ppm	Tl ppm	Re ppm	Y ppm	REE ppm
	55	35	9	190	2	0.95	183	391

Potential resource

The waste rock material in the Baggetorp is estimated to 90,000 tonnes (SGU 2023). Assuming that the average grades from composite sampling is representative for the whole waste rock pile a potential resource of about 32 tonnes of W and ca. 10 tonnes of Mo is possible.

There is no estimation of tonnage for the tailings in Baggetorp and therefore no estimation of potential resource is made. The area of the tailing pond is ca. 30,000 square metres, measured from orthophoto, and previous sampling by SGU (five surface samples) gives an average of 551 ppm of W.

REFERENCES

- Andersson, L. G., Jonuks, R., Liikanen, J., Engvall, A. & Mattsson, C., 1984: Project 3814: Finspång 1/4-31/12 1983. *Rapport No Bsg 84-348*. 57 pp.
- Ambros, M., 1983: Berggrundskartan 11F Lindesberg NO. *Sveriges geologiska undersökning Af 141*.
- Bergquist E., 1985: Beskrivning till slutkartor över delar av Riddarhytte malmfält i Skinnskattebergs kommun och socken, Västmanlands län. Bäckegrube AB. (Tillgänglig via SGU)
- Bäckström, M.; 2005: Översiktlig geokemisk undersökning av gruvavfall inom Venafältet, Askersunds kommun. Forskningscentrum Människa-Teknik-Miljö, Örebro universitet.
- Boynton W.V., 1984. Cosmochemistry of rare earth elements: meteorite studies. In P. Henderson (ed.): *Rare earth element geochemistry*. Elsevier, Amsterdam, 63–114.
- Blomberg, A. & Holm, G., 1902: Geologisk beskrifning öfver Nerike och Karlskoga Bergslag samt i Fellingsbro härad. *Sveriges geologiska undersökning Ca 2*. Afhandlingar och uppsatser i 4:0. N:o 2.
- de Campos Pereira, H., 2014: *Löslighet och transport av sällsynta jordarsmetaller i Källfallsfältets gruvandsmagasin*. Institutionen för mark och miljö, Sveriges Lantbruksuniversitet. Examensarbete 30 hp. Mars 2014.
- European Commission, 2023: *Critical raw materials*. <https://single-market-economy.ec.europa.eu/sectors/raw-materials/areas-specific-interest/critical-raw-materials_en>. Åtkommen 15 november 2023.
- Gavelin, S., 1985: The Baggetorp Tungsten Deposit Southern Sweden. Sveriges geologiska undersökning C 810. Avhandlingar och Uppsatser. Årsbok 79, Nr 4.
- Geijer, P., 1936: Norbergs Berggrund och malmfyndigheter. *Sveriges geologiska undersökning Ca 24*.
- Geijer, P., & Magnusson, N., H., 1944: De mellansvenska järnmalmernas geologi. *Sveriges geologiska undersökning Ca 35*.
- Hallberg, A. & Reginiussen, H., 2018: Slutrapportering av regeringsuppdrag: Kartläggning av innovationskritiska metaller och mineral. *Regeringsrapport 2018:05*. Sveriges geologiska undersökning. 90 s.
- Hallberg, A. & Reginiussen, H. 2020: Critical raw materials in ores, waste rock and tailings in Bergslagen. *SGU-rapport 2020:38*. Sveriges geologiska undersökning. 60 s.
- Hellström, F., Bergman, T., Hildebrand, L., Berggren, R., 2022: Malmer, industriella mineral och bergarter i Norbergs kommun, Västmanlands län. *Sveriges geologiska undersökning, Rapporter och meddelanden 151*.
- Henriques, Å., 1964: Geology and ores of the Ämmeberg district (Zinkgruvan) Sweden. *Arkiv för Mineralogi och Geologi 4*, 246 pp.
- Holstam, D., Kolitsch, U. & Andersson, U. B., 2005: Västmanlandite-(Ce)-a new lanthanide-and F-bearing sorosilicate mineral from Västmanland, Sweden: description, crystal structure, and relation to gatelite-(Ce). *European Journal of Mineralogy 17*, 129–141.
- Jonsson, E., Nysten, P., Bergman, T., Sadeghi, M., Söderhjelm, J. & Claeson, D., 2019: REE mineralisations in Sweden. In M. Sadeghi (red.): Rare earth elements distribution, mineralisation and exploration potential in Sweden, s. 20. *Sveriges geologiska undersökning, Rapporter och meddelanden 146*, 180 pp
- Jonsson, E. & Högdahl, K., 2013: New evidence for the timing of formation of Bastnäs-type REE mineralisation in Bergslagen, Sweden. In E. Jonsson et al. (eds.) *Mineral deposit research for a high-tech world*, 1724–1727.

- Lewerentz, A., Bakker, E., Hedin, P. & Leopardi, D., 2020: Ore-proximal surveys in southern Bergslagen: Vena gruvfält and Tunaberg. *SGU-rapport 2020:16*, Sveriges geologiska undersökning.
- Lundström, I., 1974: Beskrivning till berggrundskartan Nyköping SV. *Sveriges geologiska undersökning Af 109*, 123 pp.
- Ohlsson, L. G., 1980: Berggrunden runt Baggetorps Gruva. *Rapport Grb 132*. 5 pp.
- Ihre, P., 1985: Bjursjön diamantborrning. *Prap 85505*, Sveriges geologiska undersökning.
- Ihre, P. & Sädbom, S., 1986: Riddarhytte Malmfält Prospekteringsarbeten 1986. *Prap 86541*, Sveriges geologiska undersökning.
- Setterberg, J., 1839: Undersökning af ett nytt mineral, funnet uti Hvena Kobolt-grufvor uti Nerike. *Kongliga vetenskapsacademiens handlingar 27*, 188–193.
- SGI, Statens geotekniska institut, 2014: Riddarhyttan – Fördjupade undersökningar av Källfallsfältet och sjön Lien. Uppdragsrapport. Länsstyrelsen i Västmanlands län.
- SGU, 2023: Malmer och mineral – database. Bergslagen. 2023-01-15.
- SGU, 2023: *Kritiska och strategiska råvaror*. <www.sgu.se/mineralnaring/kritiska-ravaror/>. Åtkommen 15 november 2023.
- Stephens, M.B. & Jansson, N.F., 2020: Paleoproterozoic (1.9–1.8 Ga) synorogenic magmatism, sedimentation and mineralization in the Bergslagen lithotectonic unit, Svecokarelian orogen. In: M.B. Stephens & J. Bergman Weihed (eds.): Sweden: lithotectonic framework, tectonic evolution and mineral resources. *Geological Society of London Memoirs 50*, 105–206.
- Stephens, M.B., Ripa, M., Lundström, I., Persson, L., Bergman, T., Ahl, M., Wahlgren, C.-H., Persson, P.-O. & Wickström, L., 2009: Synthesis of the bedrock geology in the Bergslagen region, Fennoscandian Shield, south-central Sweden. *Sveriges geologiska undersökning Ba 58*, 259.
- Sundblad, K., 1994: A genetic reinterpretation of the Falun and Ämmeberg ore types, Bergslagen, Sweden. *Mineralium Deposita 29*, 170–179.
- Sädbom, S. & Bäckström, M., 2018: Sampling of mining waste – historical background. experiences and suggested methods. BKBAB 18–109 Rep. Bergskraft Bergslagen AB.
- Tegengren, F. R., 1924: Sveriges ädlare malmer och bergverk. *Sveriges geologiska undersökning Ca 17*.
- Wikström, A. & Karis, L., 1991: Beskrivning till berggrundskartorna Finspång NO, SO, NV, SV. *Sveriges geologiska undersökning Af 162, 163, 164, 165*. Skala 1:50 000. 218 pp.
- Zakrzewski, M. A. & Makovicky, E., 1986: Izoklakeite from Vena, Sweden, and the kobellite homologous series. *The Canadian Mineralogist 24*, 7–18.
- Zakrzewski, M.A., 1984: Jaskólskiite, a new Pb-Cu-Sb-Bi sulfosalt from the Vena Deposit, Sweden. *The Canadian Mineralogist 22*, 481–485

APPENDIX 1. SAMPLE DIGESTION AND ANALYTICAL METHODS

Analytical methods per element

Analytical method	Description ¹	Elements analysed by preferred SGU method
ME-ICP06	Fused bead, acid digestion and ICP-AES. LOI by furnace or TGA	SiO ₂ , Al ₂ O ₃ , Fe ₂ O ₃ , CaO, MgO, Na ₂ O, K ₂ O, TiO ₂ , MnO, P ₂ O ₅
ME-MES81	Lithium borate fusion, acid digestion and ICP-MS	Ba, Ce, Cr, Cs, Dy, Er, Eu, Ga, Gd, Hf, Ho, La, Lu, Nb, Nd, Pr, Rb, Sm, Sr, Ta, Tb, Th, Tm, U, V, Y, Yb, Zr, W, Sn
ME-MS41	Aqua regia digestion with ICP-MS	Bi, Hg, Sb, Se, Te, Ag , As, B, Be, Cd, Mo , Pb , Ge
ME-4ACD8	Lithium borate fusion with 4 acid digestion with ICP-MS for base metals	Co, Cu , Li, Ni, Sc, Zn
ME-MS42	Single element aqua regia analysis by ICP-MS	In, Re, Tl
PGM-ICP23	Lead oxide collection fire assay and ICP-MS analysis	Au, Pt, Pd
S-IR08	Total sulphur by induction furnace/IR	S
C-IR07	Total carbon by induction furnace/IR	C

¹Description from ALS. Bolded elements can be analysed using ore grade methodologies if concentrations exceed 10,000 ppm (Mo, Pb, Zn, Cu) or 100 ppm (Ag).